

## **INFORMATION TO USERS**

**This manuscript has been reproduced from the microfilm master. UMI films the text directly from the original or copy submitted. Thus, some thesis and dissertation copies are in typewriter face, while others may be from any type of computer printer.**

**The quality of this reproduction is dependent upon the quality of the copy submitted. Broken or indistinct print, colored or poor quality illustrations and photographs, print bleedthrough, substandard margins, and improper alignment can adversely affect reproduction.**

**In the unlikely event that the author did not send UMI a complete manuscript and there are missing pages, these will be noted. Also, if unauthorized copyright material had to be removed, a note will indicate the deletion.**

**Oversize materials (e.g., maps, drawings, charts) are reproduced by sectioning the original, beginning at the upper left-hand corner and continuing from left to right in equal sections with small overlaps.**

**Photographs included in the original manuscript have been reproduced xerographically in this copy. Higher quality 6" x 9" black and white photographic prints are available for any photographs or illustrations appearing in this copy for an additional charge. Contact UMI directly to order.**

**Bell & Howell Information and Learning  
300 North Zeeb Road, Ann Arbor, MI 48106-1346 USA  
800-521-0600**

**UMI<sup>®</sup>**



**RING-OPENING POLYMERIZATION OF  
[1]METALLOCENOPHANES:  
A ROUTE TO ORGANOMETALLIC POLYMERIC MICELLES,  
IONOMERIC POLY(FERROCENES) AND OTHER SYSTEMS OF  
INTEREST**

by

**Timothy J. Peckham**

**A thesis submitted in conformity with the requirements  
for the degree of Doctor of Philosophy  
Graduate Department of Chemistry  
University of Toronto**

**© Copyright by Timothy J. Peckham, 1998**



**National Library  
of Canada**

**Acquisitions and  
Bibliographic Services**

**395 Wellington Street  
Ottawa ON K1A 0N4  
Canada**

**Bibliothèque nationale  
du Canada**

**Acquisitions et  
services bibliographiques**

**395, rue Wellington  
Ottawa ON K1A 0N4  
Canada**

*Your file Votre référence*

*Our file Notre référence*

**The author has granted a non-exclusive licence allowing the National Library of Canada to reproduce, loan, distribute or sell copies of this thesis in microform, paper or electronic formats.**

**The author retains ownership of the copyright in this thesis. Neither the thesis nor substantial extracts from it may be printed or otherwise reproduced without the author's permission.**

**L'auteur a accordé une licence non exclusive permettant à la Bibliothèque nationale du Canada de reproduire, prêter, distribuer ou vendre des copies de cette thèse sous la forme de microfiche/film, de reproduction sur papier ou sur format électronique.**

**L'auteur conserve la propriété du droit d'auteur qui protège cette thèse. Ni la thèse ni des extraits substantiels de celle-ci ne doivent être imprimés ou autrement reproduits sans son autorisation.**

**0-612-53893-1**

**Canada**

## Abstract

Silicon-bridged [1]- and [2]ferrocenophanes with trimethylsilyl substituents on the cyclopentadienyl rings have been synthesized. The latter compound was studied by single crystal X-ray diffraction and was found to possess a larger tilt angle ( $5.4(6)^\circ$ ) than the analogous non-substituted species. No ring-opening polymerization (ROP) was observed even at elevated temperatures. The [1]ferrocenophane did polymerize readily and yielded very soluble, high molecular weight poly(ferrocenylsilane).

A series of high molecular weight poly(ferrocenylgermanes) was synthesized via the thermal ROP of germanium-bridged, [1]ferrocenophanes. Poly(ferrocenyldimethylsilane)-poly(ferrocenyldimethylgermane) random copolymers could be synthesized via ROP both thermally and in the presence of a transition metal catalyst. The thermal transition and electrochemical behaviour, and morphology of the resultant polymers were examined by differential scanning calorimetry (DSC), cyclic voltammetry and wide-angle X-ray scattering and were found to be similar to the analogous poly(ferrocenylsilanes).

The first stable phosphonium-bridged [1]ferrocenophane was synthesized and was found to undergo both thermal and transition metal-catalyzed ROP. The resultant ionomeric polymer was soluble in highly polar solvents (e.g. acetone) but displayed only limited stability. A DSC study of the glass transition temperatures of a series of methylated poly(ferrocenylphenylphosphines) of known molecular weight suggested that the molecular weight of the transition metal-catalyzed ROP product was greater than 46 000 and the thermally produced polymer was of even higher molecular weight.

The first living anionic ROP of phosphorus-bridged [1]ferrocenophanes was achieved, allowing access to poly(ferrocenylphosphine) homopolymers and block copolymers with controlled architectures. The aggregation behaviour of poly(ferrocenylphenylphosphine)-*b*-poly(dimethylsiloxane) in a non-solvent (hexane) for the poly(ferrocenylphosphine) block was examined by dynamic light scattering and by transmission electron microscopy and atomic force microscopy after solvent evaporation. The most commonly observed morphology was spheres although other morphologies were also observed. Preliminary metal coordination studies were also conducted.

Spirocyclic [1]zirconocenophanes were synthesized and found to undergo transition metal-catalyzed ROP.

***For my parents, my family and my friends.***

***"I can see clearly now the rain has gone..."***

## Acknowledgements

Well, folks, it's been a long, LONG time that I've spent here as a member of the Spongo Crew. So many people have come and gone, and now it's my turn to say goodbye. First of all, I would like to thank my supervisor, Ian "Old Bean" Manners for all the years he has shown me the value of patience and perseverance. There is no way that I would have gotten to this point without your support, imagination and advice. Much success and happiness in the future, Ian!

I have also had the privilege of working closely on a number of projects with past and present group members and now take the time to thank them for all of their help. Jason Massey, Nikki (AFM) Power and Howie Honeyman have all been fellow crew members on the good ship "Anionics" (may she sail on smoother seas in the days to come!). Paul Nguyen and Sara Bourke have also been an instrumental part of the Zr project (keep at it, Sara...solubility one of these days!). Dan Foucher, Mark Edwards and Jason Massey were a part of the Ge project which I came in to tie up. Jason is the Master of Light-Scattering ("use the force"), Mark MacLachlan has been the king of powder XRD while Alan Lough has been a god when it came to getting single crystal X-ray structures from even the smallest of samples. A special thanks as well to Prof. Morris and the 'B' Team for use of the electrochemical equipment and also Patricia Aroca-Ouellette and Tim Burrow who ran a number of crucial NMR spectra for me.

Of course, I also thank the many members of the group, past and present, who have given me their friendship and asked for nothing in return (well...maybe except for the occasional pint...). In particular, I would like to thank Yizeng Ni and Nikki Power (who also had to suffer by correcting my thesis-much appreciated!) who have occupied (though not at the same time!) the bench next to mine and have kept me company despite all my a-cursin' and a-swearin'. Best of luck always to the both of you! Oh gosh, this could go on forever...Shark, old bean, keep up the good work and thanks for the countless hours of carousing at the Bedford, Einstein's, etc...Frieder, it's only a matter of time before it'll be Prof. Jaekle...and to the many I just can't mention, here or wherever you are now, you know who you are... I owe you big time.

But there just has to be an extra special section dedicated to some very special people and here it is. Tina Fong, how can I possibly thank you enough? You have stood by me through all the sunshine and especially the storms of my life here in Hotel Lash Miller. You are certainly the best of friends. I hope the future holds much happiness and good fortune for you. Danno, I would never have gotten into this lab, started on my graduate work and even beyond to merry old England without your help, your advice and all those nights over a pint (or two..or three...or four...) talking about chemistry and life in general. Hope to keep in touch always. And, finally (yes, the acknowledgements must come to an end some time), I would like to express my deepest love and gratitude to my parents and family who have put up with me from day one (and that's saying a lot!) Without you, I would never have had the strength to get where I am today. I will never forget what you have done for me and I am in your debt forever.

## Table of Contents

<b>Chapter 1</b>	<b>Introduction</b>	<b>1</b>
1.1	Inorganic Polymer Science	1
1.2	Well-Characterized Polymers Based on Main Group Elements	2
1.3	Transition Metal-Based Polymer Science	4
1.4	Side Chain Metallocene-Containing Polymers	8
1.5	Main Chain Metallocene-Containing Polymers	14
	1.5.1 With Short Spacer Units	15
	1.5.2 With Long Spacer Units	30
1.6	Metal-Based Polymers in Catalysis	34
1.7	Block Copolymer Micelles	39
1.8	Research Objectives	45
1.9	References	49
<b>Chapter 2</b>	<b>The Synthesis and Polymerization Behaviour of Silicon-Bridged [1]- and [2]Ferrocenophanes with Sterically Demanding Trimethylsilyl Substituents Attached to the Cyclopentadienyl Rings</b>	<b>62</b>
2.1	Abstract	62
2.2	Introduction	63
2.3	Results and Discussion	65
	2.3.1 Synthesis of the Bis(trimethylsilyl)-Substituted, Silicon-Bridged [1]Ferrocenophane <b>5</b>	65
	2.3.2 Thermal ROP of the Bis(trimethylsilyl)-Substituted, Silicon-Bridged [1]Ferrocenophane <b>5</b>	67
	2.3.3 Synthesis of the Bis(trimethylsilyl)-Substituted, Disilane-Bridged [2]Ferrocenophane <b>7</b>	68
	2.3.4 X-ray Structure of <b>7</b>	69
	2.3.5 Thermal Polymerization Behaviour of the Bis(trimethylsilyl)-Substituted, Disilane-Bridged [2]Ferrocenophane <b>7</b>	78



2.4	Summary	79
2.5	Experimental Section	79
2.6	References	84
<b>Chapter 3</b>	<b>Synthesis, Characterization, and Properties of High Molecular Weight Poly(ferrocenylgermanes) and Poly(ferrocenylsilane)-Poly(ferrocenylgermane) Random Copolymers</b>	<b>87</b>
3.1	Abstract	87
3.2	Introduction	88
3.3	Results and Discussion	90
3.3.1	Synthesis and Characterization of the Germanium-Bridged [1]Ferrocenophanes <b>4c</b> and <b>6</b>	90
3.3.2	Synthesis and Characterization of the Poly(ferrocenylgermanes) <b>5c</b> and <b>7</b>	91
3.3.3	Light Scattering Measurements for <b>5a</b> in THF	92
3.3.4	Synthesis and Characterization of the Poly(ferrocenylsilane)-Poly(ferrocenylgermane) Copolymer <b>8</b>	93
3.3.5	Thermal Transition Behaviour and Polymer Morphology	96
3.3.6	Electronic and Electrochemical Properties	100
3.4	Summary	104
3.5	Experimental Section	105
3.6	References	113
<b>Chapter 4</b>	<b>Ring-Opening Polymerization of a Phosphonium-Bridged, [1]Ferrocenophane: Synthesis of an Ionomeric Poly(ferrocene)</b>	<b>116</b>
4.1	Abstract	116
4.2	Introduction	117
4.3	Results and Discussion	120
4.3.1	Attempted Transition Metal-Catalyzed ROP of [1]Ferrocenophanes <b>5a</b> , <b>6</b> and <b>7</b>	120

4.3.2	The Synthesis and Characterization of <b>10b</b>	121
4.3.3	Single Crystal X-ray Diffraction Study of <b>10b</b>	122
4.3.4	Electronic Spectrum and Electrochemical Behaviour of <b>10b</b>	128
4.3.5	Thermal ROP Behaviour of <b>10b</b>	130
4.3.6	Transition Metal-Catalyzed ROP Behaviour of <b>10b</b>	132
4.3.7	Attempted Copolymerizations of <b>10b</b> with <b>1</b> ( $ER_x = SiMe_2$ )	133
4.3.8	Methylation of Poly(ferrocenylphenylphosphine) <b>14</b> as an Alternative Route to <b>11</b>	133
4.3.9	Electronic and Electrochemical Properties of <b>11</b>	136
4.3.10	Thermal Transition Behaviour, Thermal Stability and Morphology of <b>11</b> and <b>14</b>	139
4.3.11	Molecular Weight Determination for <b>11</b>	140
4.4	Summary	143
4.5	Experimental Section	144
4.6	References	150
<b>Chapter 5</b>	<b>Living Anionic Polymerization of Phosphorus-Bridged, [1]Ferrocenophanes: A Route to Well-Defined Poly(ferrocenylphosphine) Homopolymers and Block Copolymers</b>	<b>154</b>
5.1	Abstract	154
5.2	Introduction	155
5.3	Results and Discussion	157
5.3.1	Anionic ROP of Phosphorus-Bridged, [1]Ferrocenophane <b>1</b> with <i>n</i> -BuLi	157
5.3.2	Thermal Transition Behaviour, Thermal Stability and Morphology of <b>5</b> and <b>6</b> (where $n = 100$ )	160
5.3.3	Synthesis and Characterization of the Diblock Copolymers PFP <sub>11</sub> - <i>b</i> -PDMS <sub>81</sub> ( <b>7a</b> ),	

	<b>PFP<sub>50</sub>-<i>b</i>-PDMS<sub>141</sub> (<b>7b</b>) and PFP<sub>11</sub>-<i>b</i>-PFS<sub>11</sub> (<b>8</b>)</b>	162
5.3.4	<b>Thermal Behaviour of Block Copolymers 7b and 8</b>	166
5.3.5	<b>Metal Coordination Behaviour of Block Copolymer 7 with PdCl<sub>2</sub> and Fe(CO)<sub>4</sub></b>	166
5.3.6	<b>Solution Aggregation Behaviour of Block Copolymers 7b and 12 in Hexane and Film Morphology of 7b</b>	170
5.4	<b>Summary</b>	176
5.5	<b>Experimental Section</b>	177
5.6	<b>References</b>	186
<b>Chapter 6</b>	<b>The Synthesis, Characterization and Polymerization Behaviour of Silicon-Bridged [1]-, [1][1]- and Spirocyclic Group 4 Metallocenophanes: Ring- Opening Polymerization as a Prospective Route to Polymer-Supported Ziegler-Natta Catalysts</b>	189
6.1	<b>Abstract</b>	189
6.2	<b>Introduction</b>	190
6.3	<b>Results and Discussion</b>	192
6.3.1	<b>ROP Behaviour of the Silicon-Bridged Group 4 [1]Metallocenophanes 4a and 4b</b>	192
6.3.2	<b>Synthesis of [1][1]Zirconocenophanes 7a and 7b</b>	193
6.3.3	<b>Thermal ROP Behaviour of 7a and 7b</b>	195
6.3.4	<b>Transition Metal-Catalyzed ROP Behaviour of 7a and 7b with PtCl<sub>2</sub></b>	195
6.3.5	<b>Synthesis and Characterization of the Spirocyclic, [1]Zirconocenophanes 9a and 9b</b>	196
6.3.6	<b>A Comparative Study of the Single Crystal X-ray Structures for 9a and 9b</b>	198
6.3.7	<b>Attempted Thermal and Transition Metal- Catalyzed ROP of 9a</b>	211

6.3.8	Transition Metal-Catalyzed ROP Behaviour of <b>9b</b>	212
6.3.9	Synthesis and Transition Metal-Catalyzed ROP Behaviour of <b>9c</b>	214
6.4	Summary	217
6.5	Experimental Section	218
6.6	References	227
	<b>Ciriculum Vitae</b>	<b>230</b>

## List of Tables

Table 2.1	Summary of Crystal Data and Intensity Collection Parameters for <b>7</b>	71
Table 2.2	Final Fractional Coordinates and Equivalent Isotropic Displacement Coefficients for the Non-Hydrogen Atoms of <b>7</b>	72
Table 2.3	Selected Bond Lengths for <b>7</b>	73
Table 2.4	Selected Bond Angles for <b>7</b>	75
Table 2.5	Selected Structural Data for [1]- and [2]Metallocenophanes	76
Table 3.1	Thermal Transition Data for Selected Polymers	97
Table 3.2	Electronic and Electrochemical Data for Selected Polymers and Model Systems	100
Table 4.1	Summary of Crystal Data and Intensity Collection Parameters for <b>10b</b>	124
Table 4.2	Selected Structural Parameters for <b>10b</b> and Related Phosphorus-Bridged, [1]Ferrocenophanes	125
Table 4.3	Atomic Coordinates and Equivalent Isotropic Displacement Coefficients for the Non-Hydrogen Atoms of <b>10b</b>	125
Table 4.4	Bond Lengths for <b>10b</b>	127
Table 4.5	Selected Bond Angles for <b>10b</b>	127
Table 4.6	Thermal Data for Polymer <b>11</b>	141
Table 5.1	Synthesis of Poly(ferrocenylphosphines) and Related Copolymers via the Living Anionic ROP of <b>1</b>	159
Table 6.1	Selected Structural Parameters for <b>7a</b> , <b>9a</b> , <b>9b</b> and Related Zirconocenes	201
Table 6.2	Summary of Crystal Data and Collection Parameters for <b>7a</b>	202
Table 6.3	Summary of Crystal Data and Collection Parameters for <b>9a</b>	203
Table 6.4	Summary of Crystal Data and Collection Parameters for <b>9b</b>	204
Table 6.5	Atomic Coordinates and Equivalent Isotropic Displacement Coefficients for the the Non-Hydrogen Atoms of <b>7a</b>	205
Table 6.6	Bond Lengths for <b>7a</b>	206
Table 6.7	Selected Bond Angles for <b>7a</b>	206

Table 6.8	<b>Atomic Coordinates and Equivalent Isotropic Displacement Coefficients for the the Non-Hydrogen Atoms of 9a</b>	207
Table 6.9	<b>Bond Lengths for 9a</b>	208
Table 6.10	<b>Selected Bond Angles for 9a</b>	208
Table 6.11	<b>Atomic Coordinates and Equivalent Isotropic Displacement Coefficients for the the Non-Hydrogen Atoms of 9b</b>	209
Table 6.12	<b>Bond Lengths for 9b</b>	210
Table 6.13	<b>Selected Bond Angles for 9b</b>	210

## List of Figures

Figure 1.1	The Three Major Inorganic Polymer Systems	2
Figure 1.2	Poly(cobaltocyclopentadienes) and Thermal Rearrangement Products	6
Figure 1.3	A Poly(zirconacyclopentadiene)	7
Figure 1.4	Some Other Transition Metal-Containing Polymers	8
Figure 1.5	Some Organic Polymers with Ferrocene Substituents	11
Figure 1.6	Inorganic Polymer with Ferrocene Substituents	13
Figure 1.7	Poly(ferrocenes)	17
Figure 1.8	Some Other [1]Ferrocenophanes and Poly(ferrocenes)	23
Figure 1.9	A Poly(ferrocenylsilane)-Containing Pentablock Copolymer	26
Figure 1.10	Poly(ferrocenylsilane) Homopolymers and Graft Copolymers Produced via Controlled Transition Metal-Catalyzed ROP	28
Figure 1.11	Insertion Products of a Transition Metal into the Silicon- <i>ipso</i> -Carbon Bond of a [1]Ferrocenophane	28
Figure 1.12	A Ferrocene-Containing Polyurethane Copolymer	32
Figure 1.13	Polymeric Zirconocene-Silsesquioxanes	33
Figure 1.14	Poly(ferrocenylhexylsilane)	33
Figure 1.15	Poly(ferrocenylene thienylene)	34
Figure 1.16	Polymer-Supported Hydrogenation Catalysts	36
Figure 1.17	A Dendrimer Used for Supporting Metal-Based Catalysts	37
Figure 1.18	Schematic Representations of the Three General Classes of Block Copolymer Micelles	40
Figure 1.19	Typical Mesophase Structures of Segregating Block Copolymers	41
Figure 1.20	Schematic Structure of a Large Complex Micelle Filled with Bulk Reverse Micelles	42
Figure 1.21	Cross-Sectional Drawings of the Basic Structural Components of Dendrimers and SCK's	44
Figure 2.1	Molecular Structure of <b>7</b>	70
Figure 2.2	Distortions in [1]Ferrocenophanes	77
Figure 3.1	Low Angle Laser Light Scattering Results for <b>5a</b>	93
Figure 3.2	Gel Permeation Chromatograph of <b>8</b>	94

Figure 3.3	<b><math>^{29}\text{Si}</math> NMR Spectrum of <b>8</b></b>	95
Figure 3.4	<b><math>^{13}\text{C}</math> NMR Spectrum of <b>8</b>, Methyl Region</b>	95
Figure 3.5	<b>DSC Thermogram of <b>5c</b></b>	98
Figure 3.6	<b>WAXS Pattern of <b>5c</b></b>	99
Figure 3.7	<b>Cyclic Voltammograms of <b>5c</b></b>	103
Figure 4.1	<b>Molecular Structure of <b>10b</b></b>	123
Figure 4.2	<b>Distortions in Group 8 Metallocenophanes: Defining Angles <math>\alpha</math>, <math>\beta</math>, <math>\gamma</math> and <math>\delta</math></b>	123
Figure 4.3	<b>DSC Thermogram of <b>10b</b></b>	131
Figure 4.4	<b><math>^{31}\text{P}</math> NMR Spectra of the Methylation of Polymer <b>14</b></b>	135
Figure 4.5	<b>Cyclic Voltammogram of <b>11</b> in DMF</b>	138
Figure 4.6	<b>DSC Thermogram of <b>11</b></b>	140
Figure 4.7	<b><math>T_g</math> as a Function of <math>M_n^{-2/3}</math> for <b>11</b></b>	142
Figure 5.1	<b>Graph of Number Average Molecular Weight versus the Ratio of Monomer:Initiator for <b>5</b> (runs 1 - 5)</b>	160
Figure 5.2	<b><math>^{31}\text{P}</math> NMR Spectra of <b>5</b> (runs 1 - 3, 5)</b>	161
Figure 5.3a)	<b>DSC Thermogram of <b>5</b> (<math>n = 100</math>)</b>	163
Figure 5.3b)	<b>DSC Thermogram of <b>6</b> (<math>n = 100</math>)</b>	163
Figure 5.4	<b>GPC Chromatogram of <b>7b</b></b>	164
Figure 5.5	<b>CP-MAS <math>^{31}\text{P}</math> NMR Spectrum of <b>11</b></b>	168
Figure 5.6	<b><math>^{31}\text{P}</math> NMR Spectrum of Polymer <b>12</b></b>	169
Figure 5.7	<b>IR Spectrum of <b>12</b>, CO Stretching Region</b>	170
Figure 5.8	<b>TEM Image of <b>7b</b> after Solvent Evaporation</b>	172
Figure 5.9	<b>Another TEM Image of <b>7b</b> after Solvent Evaporation</b>	172
Figure 5.10	<b>TEM Image of <b>12</b> after Solvent Evaporation</b>	173
Figure 5.11	<b>TEM Image of Film of <b>7b</b></b>	173
Figure 5.12a)	<b>AFM (Height) Image of <b>7b</b> after Solvent Evaporation</b>	174
Figure 5.12b)	<b>AFM (Phase) Image of <b>7b</b> after Solvent Evaporation</b>	174
Figure 6.1	<b>Distortions in Ansa-Zirconocenes Defining Angles <math>\alpha</math>, <math>\beta</math>, <math>\theta</math>, <math>\delta</math> and <math>\epsilon</math></b>	199
Figure 6.2	<b>Molecular Structure of <b>7a</b></b>	199
Figure 6.3	<b>Molecular Structure of <b>9a</b></b>	200
Figure 6.4	<b>Molecular Structure of <b>9b</b></b>	200
Figure 6.5	<b>CP-MAS <math>^{29}\text{Si}</math> NMR Spectrum of the Insoluble Polymer <b>11b</b></b>	213
Figure 6.6	<b>CP-MAS <math>^{13}\text{C}</math> NMR Spectrum of the Insoluble Polymer <b>11b</b></b>	213



Figure 6.7	CP-MAS $^{29}\text{Si}$ NMR Spectrum of the Insoluble Product: $\text{H}_2\text{PtCl}_6$ -catalyzed ROP of <b>9c</b>	215
Figure 6.8	CP-MAS $^{29}\text{Si}$ NMR Spectrum of the Insoluble Product: Karstedt's-catalyzed ROP of <b>9c</b>	216
Figure 6.9	CP-MAS $^{13}\text{C}$ NMR Spectrum of the Insoluble Product: Karstedt's-catalyzed ROP of <b>9c</b>	217

## List of Reactions

Reaction 1.1	Synthesis of Poly(metallynes)	5
Reaction 1.2	A More Recent Synthetic Route to Poly(metallynes)	5
Reaction 1.3	Synthesis of Poly(vinylferrocene)	9
Reaction 1.4	A Polycondensation Route to Poly(ferrocenylene)	16
Reaction 1.5	Synthesis of a Soluble Poly(ferrocenylvinylene)	17
Reaction 1.6	Synthesis of Face-to-Face Metallocenes	18
Reaction 1.7	Synthesis of Poly(ferrocenyl persulfides)	19
Reaction 1.8	Synthesis of Poly(ferrocenylsilanes) via Thermal ROP	20
Reaction 1.9	Synthesis of Poly(ferrocenylgermanes) via Thermal ROP	22
Reaction 1.10	Synthesis of Poly(ferrocenylphosphines) via Thermal ROP and Their Conversion to Poly(ferrocenylphosphine sulfides)	23
Reaction 1.11	Synthesis of Poly(ferrocenylethylenes) and Poly(ruthenocenylethylenes) via Thermal ROP	24
Reaction 1.12	Synthesis of Poly(ferrocenylsilane)-Poly(silane) Random Copolymers via Thermal ROP	25
Reaction 1.13	Random Copolymers from TROP of a Silicon-Bridged, Bis(benzene) Chromium Complex and <b>27</b> (R = R' = Me)	25
Reaction 1.14	Synthesis of Regioregular Poly(ferrocenylsilane) via Transition-Metal Catalyzed ROP	27
Reaction 1.15	Synthesis of Poly(ferrocenylethylene) via ROMP	29
Reaction 1.16	Synthesis of Poly(ferrocenylenedivinylenes) via ROMP	30
Reaction 1.17	Synthesis of Poly(ferrocenylenebutylene) via ROMP	30
Reaction 1.18	Synthesis of Some Ferrocene-Containing Polyamides	31
Reaction 1.19	Synthesis of Polysiloxane-Supported Ziegler-Natta Catalyst	38
Reaction 3.1	Synthesis of Symmetrically-Substituted Poly(ferrocenylgermanes)	89
Reaction 3.2	Synthesis of Bis(trimethylsilyl)-Substituted Poly(ferrocenyldimethylgermane) via TROP	91
Reaction 4.1	Synthesis of Poly(ferrocenes)	117
Reaction 4.2	Ring-Opening of a Phosphorus-Bridged, [1]Ferrocenophane	119
Reaction 4.3	Methylation of Polymer <b>14</b>	134

Reaction 5.1	Synthesis of Poly(ferrocenylphosphines) and Poly(ferrocenylphosphine sulfides) via Thermal ROP of <b>1</b>	157
Reaction 5.2	Synthesis of Poly(ferrocenylphosphines) and Poly(ferrocenylphosphine sulfides) via Living Anionic ROP of <b>1</b>	158
Reaction 5.3	Synthesis of Poly(ferrocenylphosphine)-Poly(siloxane) Block Copolymers	165
Reaction 5.4	Synthesis of Poly(ferrocenylphosphine)-Poly(ferrocenylsilane) Block Copolymers	165
Reaction 6.1	Synthesis of Compounds <b>7a</b> and <b>7b</b>	194
Reaction 6.2	Metathesis Reaction Between <b>7a</b> and $\text{PtCl}_2$	196

## List of Abbreviations

AFM	atomic force microscopy
APT	attached proton test
$\alpha$	ring-tilt angle
<i>b</i>	block
Bu	butyl
<i>n</i> -Bu	normal butyl
<i>t</i> -Bu	tertiary butyl
ca.	approximately
C <sub>6</sub> D <sub>6</sub>	deuterated benzene
CDCl <sub>3</sub>	deuterated chloroform
C <sub>12</sub> H <sub>25</sub> O	dodecyloxy
CH <sub>2</sub> Cl <sub>2</sub>	dichloromethane
Cl	chloro
Cp or $\eta$ -C <sub>5</sub> H <sub>5</sub>	cyclopentadienyl
CP-MAS	cross polarized-magic angle spinning
$\delta$	chemical shift in ppm, NMR
CV	cyclic voltammetry
DEPT	distortionless enhancement by polarization transfer
DLS	dynamic light scattering
DMF	dimethylformamide
DMSO	dimethylsulfoxide
DSC	differential scanning calorimetry
$\Delta E$	peak-to-peak separation value, CV
E <sub>1/2</sub>	half-wave potential
EA	elemental analysis
EHMO	extended Hückel molecular orbital
EI	electron impact
ES	electrospray
Esd	estimated standard deviation
<i>et al.</i>	and others
FAB	fast atom bombardment
fc	ferrocenediyl Fe( $\eta$ -C <sub>5</sub> H <sub>4</sub> ) <sub>2</sub>
Fc	ferrocenyl Fe( $\eta$ -C <sub>5</sub> H <sub>4</sub> )( $\eta$ -C <sub>5</sub> H <sub>5</sub> )
g	gram

GPC	gel permeation chromatography
h	hours
Hz	hertz
HOMO	highest occupied molecular orbital
IR	infrared
$I_{ox}$	anodic current
$I_{red}$	cathodic current
J	coupling constant, NMR
LALLS	low angle laser light scattering
LUMO	lowest unoccupied molecular orbital
m	multiplet
M	moles/litre or metal
Me	methyl
min	minutes
$M_n$	number average molecular weight
$M_w$	weight average molecular weight
mg	milligram
MHz	megahertz
ml	millilitre
mmol	millimole
mol	mole
mp	melting point
MS	mass spectrometry
NMR	nuclear magnetic resonance
OTf	triflate, $SO_3CF_3$
PDI	polydispersity index ( $M_w/M_n$ )
PDMS	poly(dimethylsiloxane)
PFP	poly(ferrocenylphenylphosphine)
PFS	poly(ferrocenyldimethylsilane)
Ph	phenyl
ppm	parts per million
q	quartet
R	alkyl or aryl group
ROMP	ring-opening metathesis polymerization
ROP	ring-opening polymerization
s	strong (IR), singlet (NMR)

<b>SLS</b>	<b>static light scattering</b>
<b>T<sub>c</sub></b>	<b>crystallization temperature</b>
<b>T<sub>g</sub></b>	<b>glass transition temperature</b>
<b>T<sub>m</sub></b>	<b>melting transition temperature</b>
<b>TEM</b>	<b>transmission electron microscopy</b>
<b>TGA</b>	<b>thermal gravimetric analysis</b>
<b>THF</b>	<b>tetrahydrofuran</b>
<b>TMEDA</b>	<b>tetramethylethylenediamine</b>
<b>TROP</b>	<b>thermal ring-opening polymerization</b>
<b>UV</b>	<b>ultraviolet</b>
<b>vis</b>	<b>visible</b>
<b>vs</b>	<b>very strong (IR)</b>
<b>WAXS</b>	<b>wide angle X-ray scattering</b>

# **Chapter 1 Introduction**

## **1.1 Inorganic Polymer Science**

One of the major driving forces in chemistry today is the search for new materials which exhibit properties that are not possessed by natural substances such as wood, stone and metals. During the twentieth century, polymers in particular have assumed a dominant role in our lives as plastics and similar products have occupied a niche in the modern world ranging from simple plastic shopping bags to components for automobiles and aircraft. The vast majority of these polymers are organic and thus primarily based on carbon which is partially a result of the fact that many organic monomers are derived from the petrochemical industry.

Inclusion of inorganic elements into a polymer backbone allows for the possibility of variations in oxidation states, coordination number and geometries as well as new pathways for electron delocalization. This allows for the creation of new materials with potentially interesting properties (e.g. magnetic, catalytic, optical) that are not readily achieved with organic-based polymer systems and has been one of the major driving forces behind research in this area.<sup>1-4</sup>

The area of inorganic and transition metal-containing polymers is large and thus cannot be discussed at length within the confines of this Thesis. Brief mention will be made of the three well-characterized inorganic polymer systems: polysiloxanes, polyphosphazenes and polysilanes. As the major focus of the research comprising this Thesis was on transition metal-containing polymers, these systems will be examined in greater detail as regards to synthesis, properties and, wherever possible, potential or actual applications. Emphasis will be placed on the more recent developments in this field. Relevant background material for the Thesis project in the areas of metal-based polymers in catalysis and block copolymer micelles is also discussed.

## 1.2 Well-Characterized Polymers Based on Main Group Elements

The three major classes of inorganic polymers are illustrated in Figure 1.1. Of these, polysiloxanes (1) are the most well-developed, having been intensively investigated since the 1940's and now comprise a billion dollar industry.<sup>5,6</sup> These polymers were formerly synthesized via the Rochow-Müller Process<sup>7</sup> but now are primarily made via the ring-opening polymerization (ROP) of organosiloxane trimers and tetramers using ionic initiators.

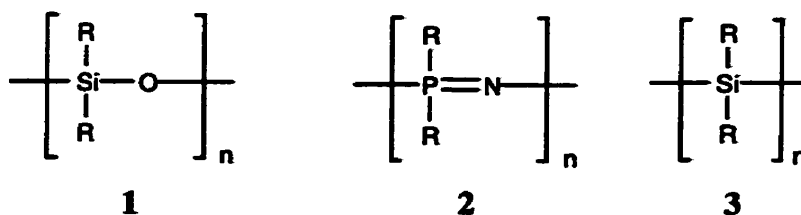


Figure 1.1 The Three Major Inorganic Polymer Systems

The flexibility of the siloxane polymer backbone has been the feature of greatest interest in the case of this polymer system and has led to some of the lowest known glass transition temperatures (e.g. for  $(\text{Me}_2\text{SiO})_n$ ,  $T_g = -123\text{ }^\circ\text{C}$ ).<sup>7</sup> A number of factors contribute to this property. Firstly, the longer Si-O bond length of 1.64 Å (cf. C-C bond length is 1.54 Å) reduces steric hindrance and intramolecular congestion. Secondly, the skeletal oxygen atoms are unencumbered by any side groups. Finally, the Si-O-Si bond angle of ca.  $143^\circ$  is more open than found for tetrahedral carbon (ca.  $110^\circ$ ) and thus torsional rotation can occur more easily.

Thousands of different materials based on polysiloxanes have been made. Other than low temperature flexibility, these polymers also possess high thermal stability (up to 300 to 350 °C) and resistance to ozone, UV light and organic oils and solvents, very high oxygen permeability, excellent biocompatibility and high hydrophobicity. The major applications of



polysiloxanes have been as low temperature rubbers, sealants, surfactants and in biomedical devices.<sup>7</sup>

In contrast to polysiloxanes, both polyphosphazenes (2) and polysilanes (3) are still in earlier stages of development although they have found a number of commercial applications.<sup>7,8</sup>

Polyphosphazenes possess highly flexible backbones, are thermally and oxidatively stable, flame retardant. They are primarily synthesized via the thermal ROP of the cyclic trimer,  $[\text{NPCl}_2]_3$ , followed by subsequent substitution of the chlorine atoms by various nucleophiles. In addition to ROP, there are several other methods including polycondensation<sup>9-11</sup> and anionic polymerization<sup>12</sup> routes. Most recently, the synthesis of poly(dichlorophosphazene) has been achieved at ambient temperature via the  $\text{PCl}_5$ -catalyzed condensation of N-silylphosphoranimine,  $\text{Cl}_3\text{P}=\text{NSiMe}_3$  which also allows for molecular weight control.<sup>13,14</sup>

Although a wide variety of polyphosphazenes have been made, applications have been limited to date to hydrocarbon-resistant devices (e.g. fuel lines, O-rings and gaskets), heat and sound-insulating rubber tubes, and flame-retardant textiles. Potential applications for these polymers as components in polymeric electrolytes for batteries, biomaterials, hydrogels and membranes are currently under investigation.<sup>7</sup>

Polysilanes have attracted a great deal of interest due to the unique electronic and optical properties resulting from delocalization of  $\sigma$  electrons along the polymer backbone. The major synthetic route to polysilanes has been the Wurtz coupling of dichlorosilanes. In attempts to circumvent the harsh nature of these reaction conditions, alternative syntheses based on dehydrocoupling<sup>15-18</sup> and anionic polymerization<sup>19,20</sup> have been used with limited success though these routes do allow for the formation of polymers with more sensitive side-groups.

Research into potential applications for these materials include their use as hole transport layers in electroluminescent devices, in microlithographic applications and as

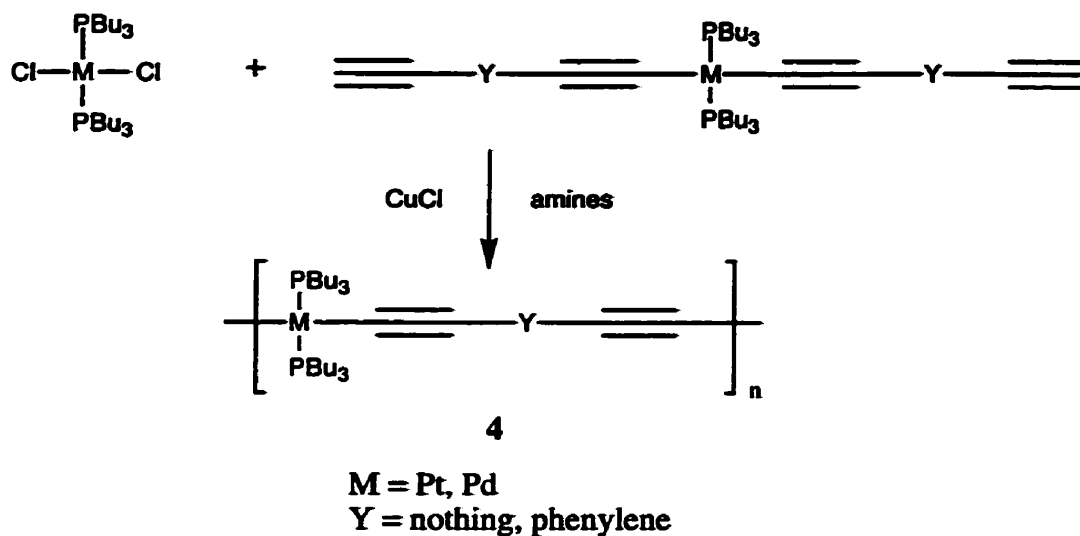
polymerization initiators.<sup>7,21-23</sup> They have also been investigated as thermal precursors to silicon carbide fibers.

### **1.3 Transition Metal-Based Polymer Science**

Complexes and solid state materials containing transition metals display a wide variety of interesting and useful redox, magnetic, optical, electrical and catalytic properties.<sup>24,25</sup> Inclusion of transition metals in a polymer, therefore, offers the potential of combining these properties with the processability commonly found for organic polymer systems.<sup>26-28</sup>

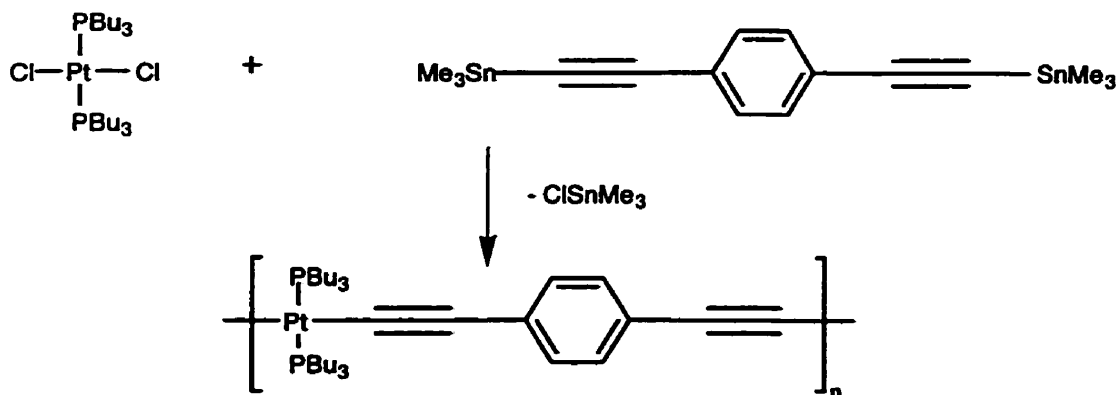
Due in part to the excellent thermal stability, interesting physical properties (e.g. redox), ease of synthesis and relatively low cost of ferrocene, extensive efforts have been made to include this moiety in a polymer both as a side chain and also a part of the polymer backbone. As ferrocene and other metallocene-containing polymers form the bulk of known transition metal-containing polymers, these will be dealt with in Sections 1.4 and 1.5. Other systems will be discussed briefly within this section.

Poly(metallynes) (e.g. 4) which are based on conjugated  $C\equiv C$  and transition metal repeat units remain one of the best characterized transition metal-containing polymers to date. These were first synthesized in 1977 (Reaction 1.1) and have a rigid-rod backbone structure.<sup>29-33</sup> Initially, only platinum or palladium could be incorporated as the transition element.



### Reaction 1.1 Synthesis of Poly(metallynes)

More recently, an improved synthetic route (Reaction 1.2) has allowed access to poly(metallynes) that incorporate other transition elements such as iron,<sup>34</sup> rhodium,<sup>35</sup> and nickel<sup>36</sup> into the polymer main chain.



### Reaction 1.2 A More Recent Synthetic Route to Poly(metallynes)

A number of interesting properties have been found for these poly(metallynes) due to their novel rigid-rod structures and their conjugated backbones, including the formation of lyotropic liquid crystalline phases and third-order nonlinear optical properties.

A rather novel class of  $\pi$ -conjugated organometallic polymers has been reported recently (Figures 1.2 and 1.3) containing metallocyclopentadiene units. These were first synthesized by Nishihara *et al* but the products were found to be insoluble.<sup>37</sup> More recently, Endo *et al.* were able to synthesize soluble polymers (e.g. 5) by incorporating flexible aliphatic spacers in the main chain. Thermal rearrangement led to the formation of the new polymer 6.<sup>38-41</sup>

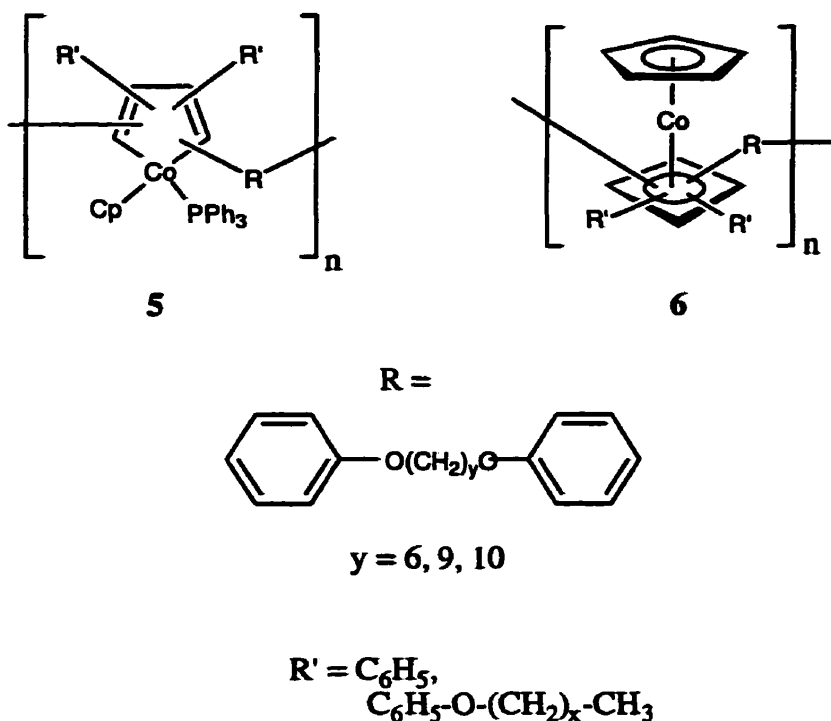
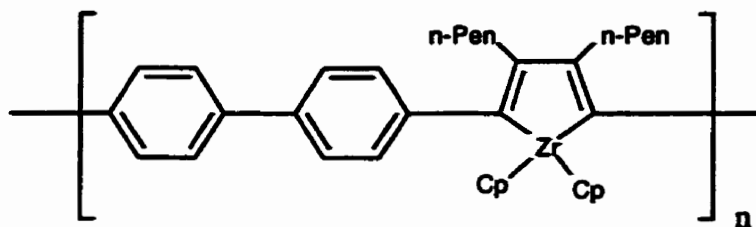


Figure 1.2 Poly(cobaltocyclopentadienes) and Thermal Rearrangement Products

Tilley *et al.* have also synthesized analogous poly(zirconacyclopentadienes) (7) via the coupling of diynes to zirconocene. These compounds were reported to possess molecular

weights ( $M_w$ ) of 37 000. Related polymers derived from zirconocene coupling with silicon-containing diynes have also been synthesized.<sup>42</sup>



7

Figure 1.3 A Poly(zirconacyclopentadiene)

Other recent examples of non-metallocene, transition metal-containing polymer systems include other rigid-rod polymers (8), polymers with metal-metal bonds in the main chain (9) and coordination polymers (10). Dendritic coordination polymers based on Ru- or Pt-polyipyridyl systems have also been reported.<sup>43-45</sup>

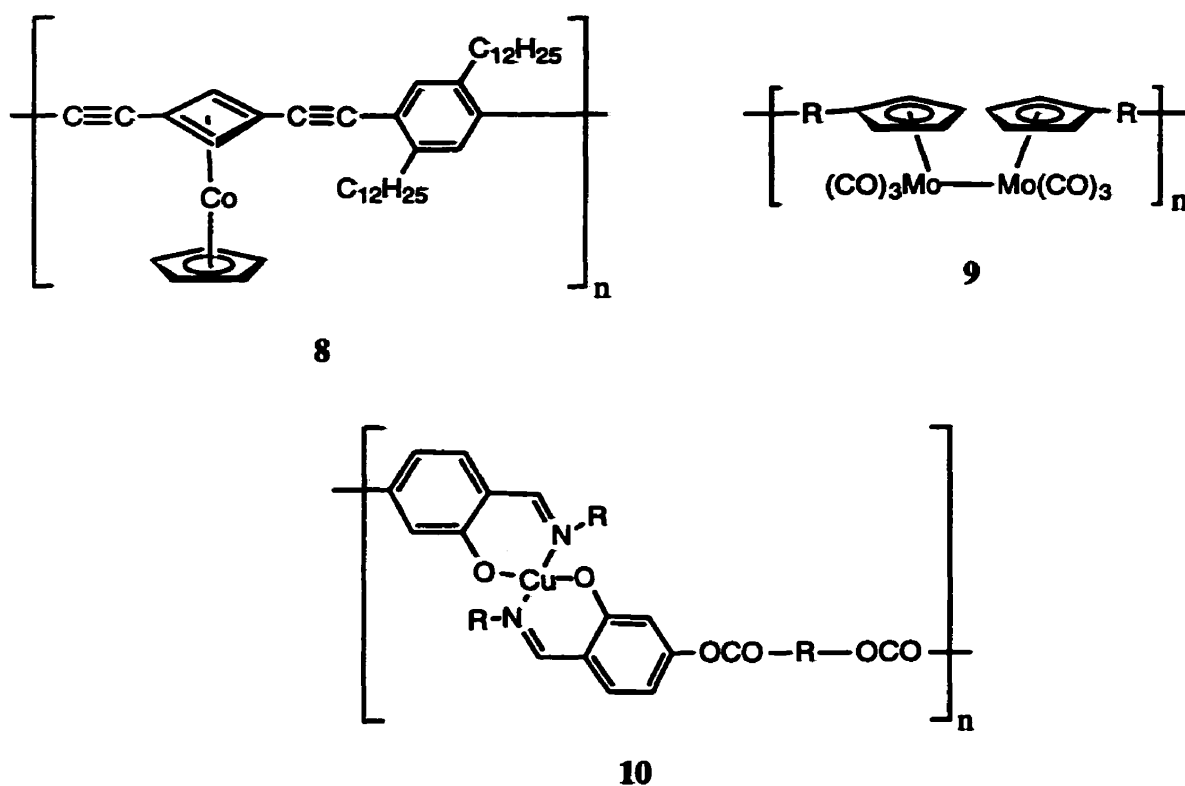
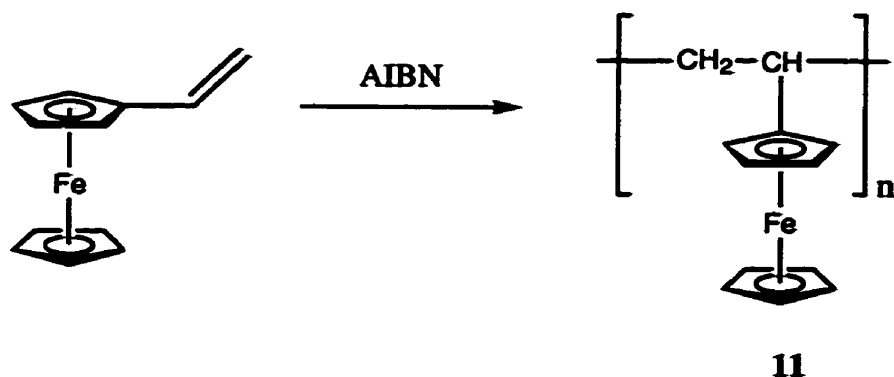


Figure 1.4 Some Other Transition Metal-Containing Polymers

#### 1.4. Side Chain Metallocene-Containing Polymers

Only a few years after the discovery of ferrocene in the early 1950's, poly(vinylferrocene) (**11**) was synthesized via radical-initiated polymerization of vinylferrocene (Reaction 1.3) with non-oxidizing initiators such as AIBN.<sup>46-52</sup> Molecular weights are generally less than 10 000 but values as high as  $M_w = 382\ 000$  (PDI = 1.33) have been reported but with multimodal weight distributions.<sup>50</sup> In subsequent years, it has also been found that cationic, Ziegler-Natta and even living anionic polymerization (at low temperatures) may be used to obtain poly(vinylferrocene).<sup>53,54</sup>



### Reaction 1.3 Synthesis of Poly(vinylferrocene)

Poly(vinylferrocene) is a yellow powder soluble in most common organic solvents. Much of the interest in poly(vinylferrocene) is due to the presence of redox active iron sites attached to the polymer chain. Cyclic voltammetry experiments<sup>55,56</sup> have revealed that the iron sites are non-interacting and only one reversible oxidation wave is observed for which the intensity of the current is directly proportional to the molecular weight of the polymer sample.<sup>55</sup> This is in contrast to polymers in which the ferrocene units are in close proximity in the polymer backbone, such as poly(ferrocenylsilanes) (see Section 1.5.1). For these materials there is evidence for communication between iron centres as shown by the presence of two reversible oxidation waves. The redox behaviour of poly(vinylferrocene) (PVFc<sup>+/0</sup>) has been utilized in the construction of a microchemical diode along with an N, N'-dibenzyl-4,4'-bipyridinium-based polymer (BPQ<sup>2+/+</sup>)<sub>n</sub> which was found to possess long switching times in comparison with conventional solid state diodes.<sup>57</sup>

Poly(vinylferrocene) is an insulator in its pristine state (i.e. when all iron centres present as Fe<sup>II</sup>) with conductivities in the region of 10<sup>-14</sup> S cm<sup>-1</sup>.<sup>58</sup> Oxidation with e.g. I<sub>2</sub> yields mixed valent systems in which both Fe<sup>II</sup> and Fe<sup>III</sup> sites are present. These materials display much higher conductivities with values within the semiconductor range (10<sup>-8</sup> to 10<sup>-7</sup> S cm<sup>-1</sup>).<sup>58</sup> Based on studies of ferrocenium and mixed-valent biferrocene compounds<sup>59,60</sup> and

Mössbauer spectroscopic analyses of vinylferrocene-containing copolymers,<sup>61,62</sup> charge has been found to be mainly localized on iron. An electron-hopping model has been suggested as the mode for electron transfer<sup>63</sup> as the all-carbon backbone of the polymer is insulating.

A variety of other organic polymers with metallocene-containing side groups have been synthesized. However, few are as well-studied as poly(vinylferrocene). A few notable, more recent examples (12 - 15) are shown in Figure 1.5

Copolymer 12 was synthesized via a random, radically-initiated copolymerization between methyl methacrylate and a ferrocene-containing methacrylate in a 95:5 ratio respectively, and was found to possess thermal properties virtually identical to those of poly(methyl methacrylate). After poling, the material was analyzed for second-order nonlinear optical properties and was found to possess a second harmonic generation efficiency approximately four times that of a quartz standard.

Ferrocene-substituted norbornenes have allowed access to polymers such as 13 via ring-opening metathesis polymerization.<sup>64,65</sup> As this is a living polymerization, block copolymers could also be made and molecular weights could be controlled from  $M_n = 5090 - 9030$  with PDI = 1.13 or less. Consistent with a polymer containing non-interacting iron sites, only one reversible oxidation wave was found in cyclic voltammetric experiments. Polymers end-capped with pyrene were found to quench the emission of the pyrene unit by a factor of 30 in comparison with 1-vinylpyrene. This was believed to be due to the presence of the neighbouring ferrocene moieties.

Well-defined poly(ethynylmetallocenes) (14)<sup>66-70</sup> with controlled molecular weights (where M = Fe, Ru) have been synthesized. The living polymers could be terminated with



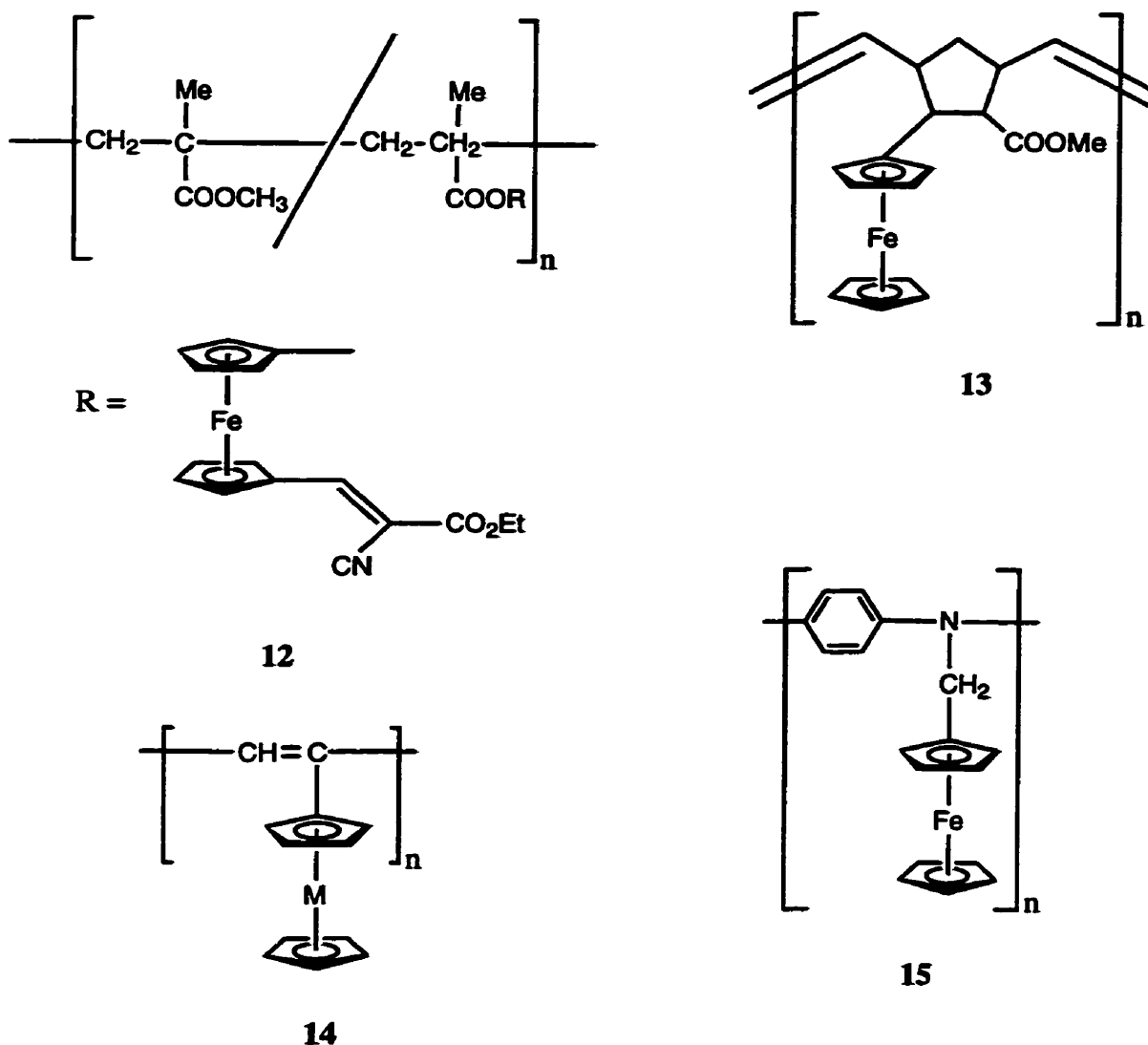


Figure 1.5 Some Organic Polymers with Ferrocene Substituents

pyridinecarboxaldehyde and the tertiary nitrogen subsequently quarternized with methyl iodide. The charged systems were found to exhibit a more intense, red-shifted absorption in the UV/visible spectrum than the corresponding uncharged systems.

Ruthenium and osmium analogues of poly(vinylferrocene) have been reported in the past but characterization was limited. They were tested as preheat shields for targets in inertial-confinement nuclear fusion.<sup>71,72</sup> Recently, a conjugated polymer with ferrocene substituents,

poly(anilinemethylferrocene) (**15**), was employed as an electrode mediator and could be used as sensor for peroxides in organic media.<sup>73</sup>

Very few example of metallocene-containing polymers with inorganic backbones exist. Not surprisingly, they are based on a poly(phosphazene) (**16 - 18**), poly(silane) (**19**) or poly(siloxane) (**20**) framework as can be seen in Figure 1.6. These will all be discussed briefly.

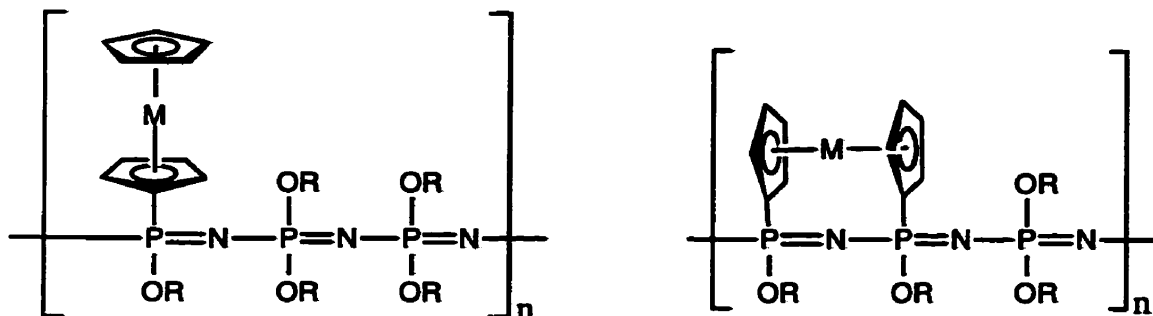
Thermal ROP of ferrocene- or ruthenocene-substituted cyclic triphosphazene monomers is a facile route to polymers **16** and **17** with molecular weights ( $M_w$ ) in excess of  $2 \times 10^6$ .<sup>74,75</sup> In general, cyclotriphosphazenes with less than three halogen substituents do not undergo thermal ring-opening polymerization. However, a range of cyclic phosphazenes without any halogen side groups have been found to polymerize provided transannular ferrocenyl substituents are present.<sup>76,77</sup> In most cases, the presence of a small amount of an initiator such as  $[NPCl_2]_3$  is necessary for polymerization to occur. X-ray crystallographic studies of several of these strained ferrocenylorganocyclotriphosphazenes have shown that the phosphazene ring is forced into a high energy, non-planar conformation.<sup>78</sup> By contrast, in most cyclotriphosphazenes, the phosphorus-nitrogen ring is virtually planar.

Polymers **16** and **17** (as well as copolymers bearing both ferrocene and ruthenocene moieties) have been partially oxidized with iodine resulting in weakly semiconducting materials. These materials have also been deposited on an electrode surface where the polymers act as electrode mediator coatings which can aid electron transfer between the electrode and redox active species in solution.<sup>79</sup>

Polyphosphazenes with ferrocenyl substituents have also been synthesized via functionalization of poly(methylphenylphosphazene) to yield the random copolymer **18**.<sup>80</sup> Substitution was not complete with a degree of substitution of 45 % and 36 % for polymers **18a** and **18b**, respectively. Molecular weights for these polymers were  $M_w = 2.0 \times 10^5$  and  $1.5 \times 10^5$  respectively (typically PDI = 1.4 – 2.0). The glass transition temperatures increased

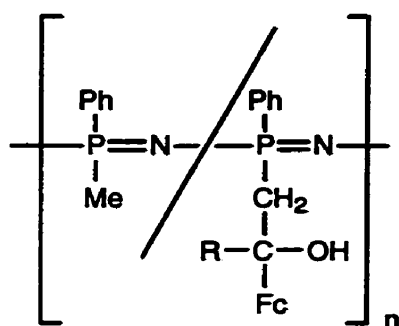
in comparison with the unsubstituted polymers with values of 92 °C and 87 °C for **18a** and **18b** respectively.

The synthesis of polysilanes bearing low loadings of ferrocene substituents (**19**) has

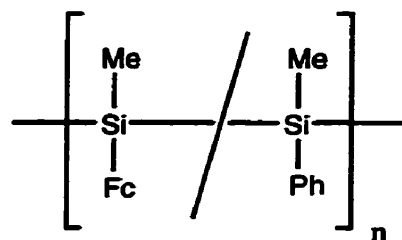


**16a** (M = Fe)  
**16b** (M = Ru)

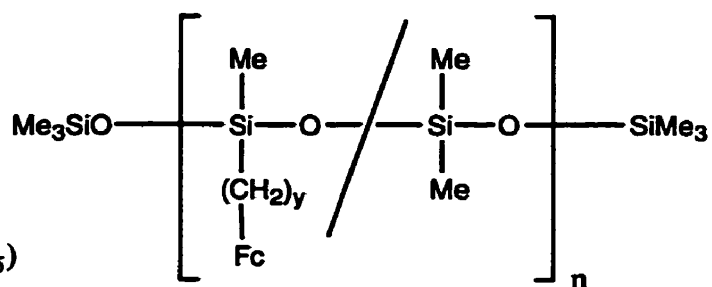
**17a** (M = Fe)  
**17b** (M = Ru)



**18a** (R = H)  
**18b** (R = Me)



**19**



$\text{Fc} = (\eta\text{-C}_5\text{H}_4)\text{Fe}(\eta\text{-C}_5\text{H}_5)$

**20**  
(y = 2 or 9)

Figure 1.6 Inorganic Polymers with Ferrocene Substituents

been reported via Wurtz coupling.<sup>81</sup> Random copolymers with weights ( $M_w$ ) up to 390 000 were isolated from mixtures of high and low molecular weight fractions. The ratio of methylphenylsilane to methylferrocenylsilane segments ranged from 6:1 to 27:1. In common with other polysilanes, these materials were photosensitive and depolymerized upon exposure to UV light. However, the copolymers did display greater stability than a corresponding sample of poly(methylphenylsilane) indicating that ferrocene moieties bound to the polymer chain provided a degree of stabilization for the polysilane backbone towards photodegradation. Cyclic voltammetry experiments<sup>82</sup> revealed two oxidation waves for the polymers. The first wave, which was reversible due to oxidation of iron sites whereas the second, irreversible oxidation at higher potential was assigned to oxidation of the polysilane backbone. No electrochemical interaction was observed between neighbouring iron sites or between iron sites and the polymer backbone.

Polysiloxane random copolymers (with molecular weights of 5000 to 10 000) with pendant ferrocene groups have recently been synthesized (**20**) via hydrosilylation of vinylferrocene or 9-ferrocenyl-1-nonene with a poly(methylhydrosiloxane)-poly(dimethylsiloxane) random copolymer. These materials were used as amperometric biosensors for the detection of glucose.<sup>83</sup> The polymers effectively mediated electron transfer between reduced glucose oxidase and a conventional carbon paste electrode. The response of the sensor to glucose was dependent upon the nature of the polymeric backbone. The optimal response was a compromise between increased polymer flexibility and decreased spacing between individual relay (i.e. ferrocene) sites.

## **1.5 Main Chain Metallocene-Containing Polymers**

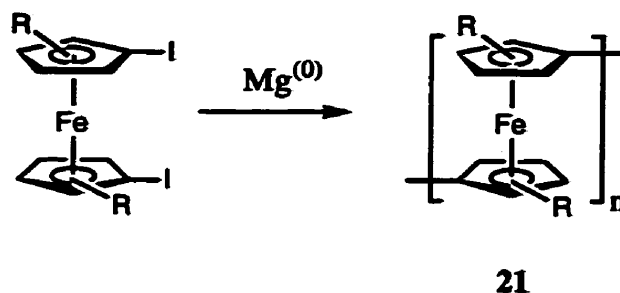
The synthesis of main chain ferrocene-containing polymers in which the metal atoms are separated by a considerable distance is relatively well developed as the extensive organic chemistry of ferrocene has allowed easy access to difunctional monomers which can be used

in controlled polycondensation reactions to yield well-defined, high molecular weight products. In contrast, well-characterized, high molecular weight materials in which the ferrocene units are in close proximity to one another are rare and, in general, cannot be obtained via polycondensation reactions since suitable reactants (e.g. dilithioferrocene) often cannot be obtained in a pure enough form for exact reaction stoichiometries.

Polymers with short spacer units and with long spacer units separating the ferrocene moieties will be dealt with separately with the concentration being on the former as this formed the major focus of this Thesis. Main chain metallocene-containing polymers other than those involving ferrocene are quite rare and will only be mentioned briefly within the appropriate sections. Some rather interesting star-shaped<sup>84-86</sup> and dendritic<sup>84,87</sup> ferrocene-containing macromolecules have also been synthesized but these will not be discussed.

### 1.5.1 With Short Spacer Units

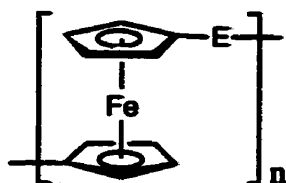
Poly(ferrocenylene)s (**21**), with no bridging units between ferrocene centres, have been synthesized with varying degrees of success since the 1960's when low molecular weight products were obtained via polycondensation of ferrocene radicals generated by thermolysis of ferrocene in the presence of peroxides.<sup>88-90</sup> However, these materials were later found to possess other linking units in the main chain such as CH<sub>2</sub> and O.<sup>60,91</sup> Other poly(condensation) routes include the reaction between 1,1'-dilithioferrocene•TMEDA with 1,1'-diiodoferrocene<sup>92</sup> ( $M_n < 4\ 000$ ) and the reaction of 1,1'-diiodoferrocene with magnesium (Reaction 1.4) (where R = H). Soluble low molecular weight materials ( $M_n = 4\ 600$ ) could be extracted from the products of Reaction 1.4 and were found to possess an appreciable degree of crystallinity.<sup>93</sup> Additionally, oxidation of these polymers with TCNQ led to materials that were delocalized at room temperature on the Mössbauer time scale (ca.  $10^{-7}$  s) and electrical conductivities of up to  $10^{-2}$  S cm<sup>-1</sup>.



#### Reaction 1.4 A Polycondensation Route to Poly(ferrocenylene)

More recently, a more soluble poly(ferrocenylene) (**21** where R = *n*-hexyl) has been made by the reaction of the dihexylfulvene dianion with  $[FeCl_2(THF)_2]$ .<sup>94</sup> Generally, the products were of low molecular weight but higher molecular weight products ( $M_n > 4\ 000$ ) were formed in low yield. In addition, when oxidized with TCNQ or TCNE, this material exhibited photoconductivity and also acted as a p-type semiconductor, as was previously noted for non-substituted ferrocenylenes.<sup>95</sup>

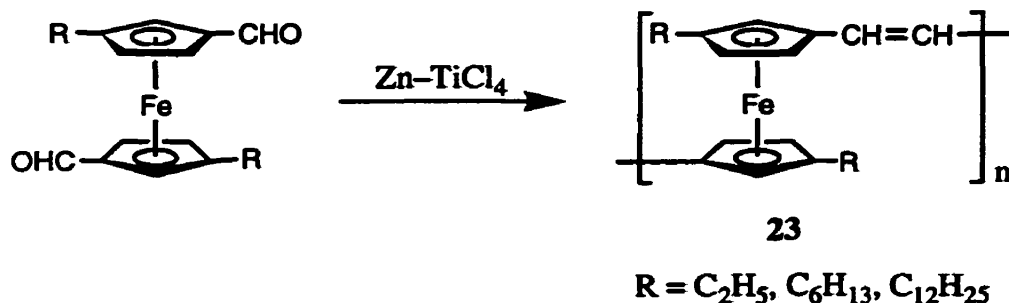
Attempts to prepare macromolecules in which the ferrocene units are separated by short spacer units (e.g. E =  $SiR_2$ ,  $CH_2$ ) (**22**) by polycondensation methods have met with limited success.<sup>96-103</sup> In general, the products were of low molecular weight ( $M_n < 10\ 000$ ) and poorly defined. For example, the first poly(ferrocenylsilanes), synthesized by the reaction of dilithioferrocene with organodichlorosilanes at ambient temperatures, were described as partially soluble, chocolate-brown materials.<sup>101</sup> In contrast, soluble, high molecular weight poly(ferrocenylsilanes) have been found to be yellow-orange materials,<sup>104,105</sup> suggesting that the earlier attempts had led to impure materials.



22

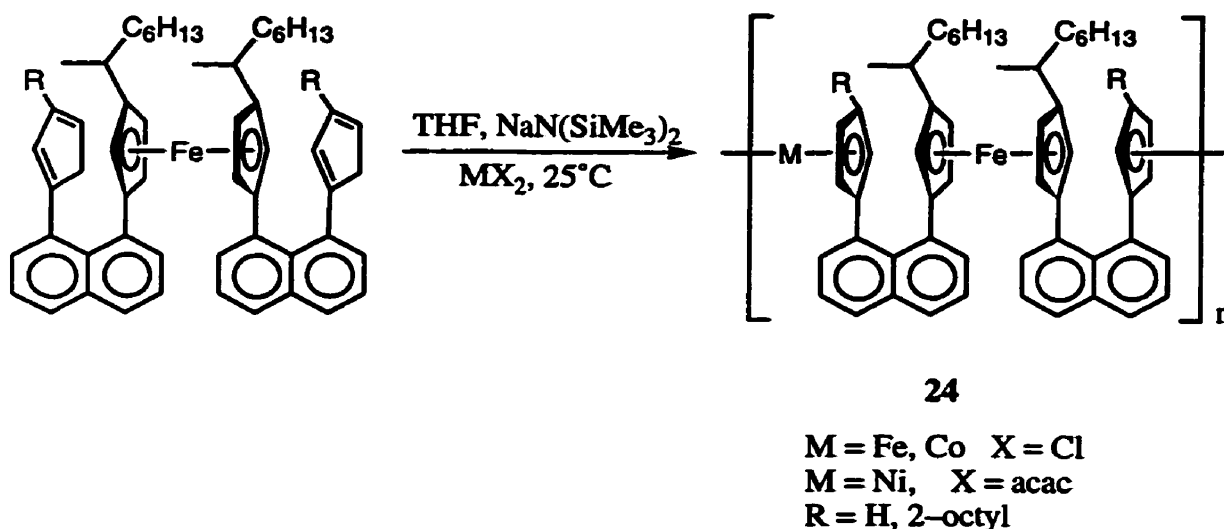
Figure 1.7 Poly(ferrocenes)

More recently, poly(ferrocenylenevinylene) derivatives (**23**) with  $M_n = 8000 - 10\,000$  (by GPC) have been synthesized<sup>106</sup> in high yields via the titanium-induced McMurry coupling reaction of the corresponding alkylferrocenyl carbaldehyde monomers (Reaction 1.5). These soluble polymers were characterized by NMR and IR which revealed the presence of *trans*-vinylene units. The UV-vis spectra of the polymers are similar to those of the monomers, indicating a fairly localized electronic structure. This is also reflected in the electrical and optical properties with values for conductivity ( $\sigma = 10^{-2} \text{ S cm}^{-1}$ ) and non-linear third-order optical susceptibility ( $\chi^{(3)} = 1 - 4 \times 10^{-12} \text{ esu}$ ) lower than those of linear conjugated polymers such as poly(1,4-phenylenevinylene) ( $\sigma = 2.5 \times 10^3 \text{ S cm}^{-1}$ , susceptibility  $\chi^{(3)} = 8 \times 10^{-12} \text{ esu}$ ).



Reaction 1.5 Synthesis of a Soluble Poly(ferrocenylenevinylene)

The very unusual and interesting face-to-face metallocene polymers (**24**) have also been prepared via polycondensation (Reaction 1.6) by Rosenblum and co-workers.<sup>107-111</sup> Purple polymers with molecular weights up to  $M_n = 18\ 000$  could be made using this route although higher molecular weight products were also present. Mixed-metal copolymers in which both Fe and Ni are present could be obtained using  $[\text{Ni}(\text{acac})_2]$  as a reagent in addition to  $\text{FeCl}_2$ , although the molecular weights were significantly lower ( $M_n < 3\ 000$ ). Structural work on well-defined oligomers suggests that the stacked metallocene units in the polymer form a helical structure. Both homopolymers and copolymers have been examined for their electrical and magnetic



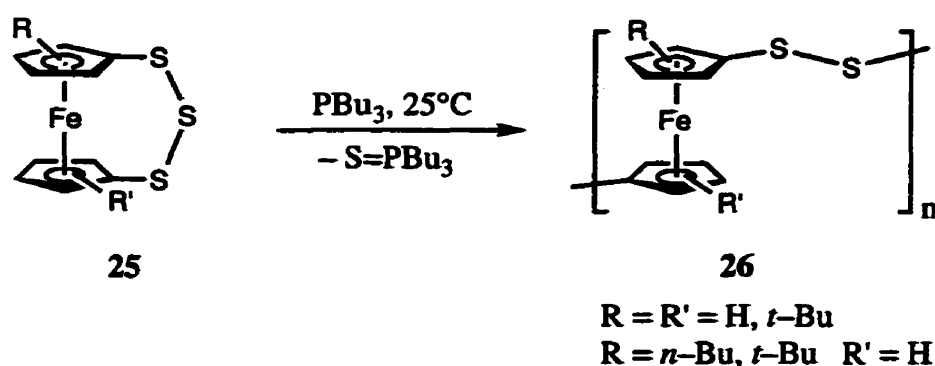
#### Reaction 1.6 Synthesis of Face-to-Face Metallocenes

behaviour. Conductivities up to  $6.7 \times 10^{-3} \text{ S cm}^{-1}$  have been found for  $\text{I}_2$ -doped materials. The bulk magnetic susceptibility was determined for the paramagnetic nickel polymer and heterometallic copolymers. In all of them the values were greater than those for the corresponding nickelocene or cobaltocene which was interpreted in terms of cooperative magnetic behavior.



ROP is an attractive route to poly(metallocenes) as it proceeds via a chain-growth mechanism which removes the requirement for the stringent stoichiometric and conversion requirements necessary to obtain high molecular weight products via polycondensation. In the last several years, ROP has been used with a great deal of success to produce soluble, well-defined, high molecular weight poly(metallocenes).

In 1992, there were two reports of ROP being used as a route to poly(metallocenes). In the first case, poly(ferrocenylene persulfides) (**26**) were synthesized by Rauchfuss and co-workers via the atom abstraction induced ROP of **25** with  $\text{PBU}_3$  (Reaction 1.7).<sup>112</sup>



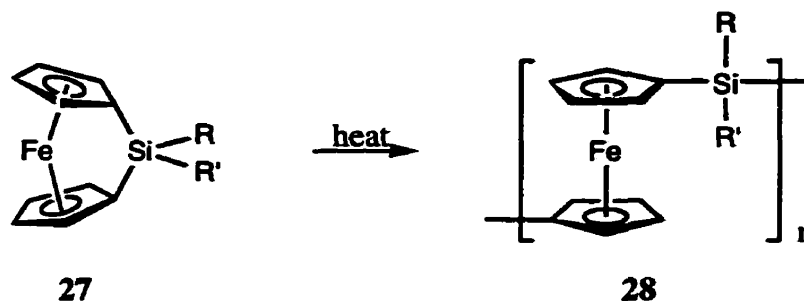
#### Reaction 1.7 Synthesis of Poly(ferrocenyl persulfides)

Soluble polymers could be obtained when  $\text{R} = n\text{-Bu}$  and molecular weights, depending upon the solvent used for the desulfurization reaction, ranged between 12 000 and 359 000 (by GPC). Copolymers from the ROP of **25** ( $\text{R} = \text{H}$ ) and **25** ( $\text{R} = n\text{-Bu}$ ) could also be made with  $M_w = 25\ 000$ . More recently, polymers with *t*-butyl substituents and network polymers ( $M_w = 50\ 000 - 1\ 000\ 000$ ) obtained via ROP of the doubly-bridged analogue of **25** ( $\text{R} = n\text{-Bu}$ ) have also been made.

Polymer **26** and related copolymers have been found to possess a number of interesting properties. The polymer backbone can be reductively cleaved and oxidatively regenerated in a reversible manner. Cyclic voltammetric studies have shown two reversible oxidation waves

with a separation of 0.31 V. The first wave is attributed to alternating iron sites and the second wave to the remaining iron sites which are more difficult to oxidize as they are sandwiched between previously oxidized iron centres.

In 1992, Manners and co-workers also reported ROP as a route to poly(ferrocenes). Thermal ROP of the silicon-bridged, [1]ferrocenophane **27** led to the formation of high molecular weight poly(ferrocenylsilane) **28**.<sup>104</sup> The driving force of this reaction is believed to be the strained nature of **27** in which the cyclopentadienyl rings are tilted with respect to one another by about 21° in contrast to the parallel rings in ferrocene. Using differential scanning calorimetry (DSC), the strain energy which is released by polymerization has been found to range from 70 - 80 kJ mol<sup>-1</sup>, depending upon the substituents present on silicon.



#### Reaction 1.8 Synthesis of Poly(ferrocenylsilanes) via Thermal ROP

A key feature that was initially noted concerning these polymers was the presence of two reversible oxidation waves in their cyclic voltammograms.<sup>104</sup> The proposed explanation is the same as has been described for the poly(ferrocenylene persulfides). Recent studies on model oligo(ferrocenylsilanes) fully support this theory.<sup>113,114</sup> The peak separations for the different polymers, which reflect the degree of interaction between the metal centers, are generally in the range  $\Delta E_{1/2} = 0.16 - 0.29$  V depending on the substituents present.<sup>104,115-117</sup> When oxidized, poly(ferrocenylsilanes) undergo a color change from amber to blue. The interesting electrochromic behavior has been studied in some detail for several polymers.<sup>117,118</sup>

Pristine high molecular weight poly(ferrocenylsilanes) are found to be insulating ( $\sigma = 10^{-14} \text{ S cm}^{-1}$ ) and when partially oxidized by  $\text{I}_2$ , the conductivities range from  $\sigma = 10^{-8} - 10^{-7} \text{ S cm}^{-1}$  up to  $2 \times 10^{-4} \text{ S cm}^{-1}$  and show electron localization on the Mössbauer spectroscopic timescale. Studies on TCNE-oxidized oligo(ferrocenylsilanes) ( $M_w = \text{c.a. } 1500$ ) have indicated the presence of electron delocalization and in some cases the presence of ferromagnetic ordering at low temperature.<sup>119</sup>

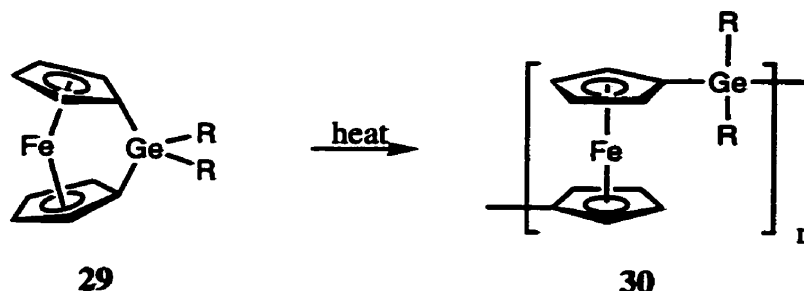
Poly(ferrocenylsilanes) such as **28** ( $R = R' = \text{Me}$ ) are thermally stable up to  $350 - 400$  °C and retain  $35 - 40$  % of their weight at  $1000$  °C, yielding ferromagnetic Fe-Si-C ceramic composites.<sup>120,121</sup> The highest ceramic yield (weight retention of  $90$  % at  $600$  °C and  $63$  % at  $1000$  °C) was obtained from the pyrolysis of the insoluble, semicrystalline poly(ferrocenyldihydrosilane) **28** ( $R = R' = \text{H}$ ).<sup>122</sup> More recently, in situ ROP of **27** ( $R = R' = \text{Me}$ ) inside the channels of mesoporous silica (MCM-41) followed by pyrolysis in a tube furnace led to the formation of interesting magnetic ceramics confined within the channels of the host material.<sup>123</sup>

Glass transitions for poly(ferrocenylsilanes) are in the range of  $-51$  to  $116$  °C (by DSC analysis) depending on the substituents present upon silicon. Symmetrically substituted derivatives often show a propensity to crystallize and have been studied by DSC, WAXS, and atomic force microscopy.<sup>124-126</sup> The morphology of many of the materials show thermal history dependence with increasing crystallinity over time.

Another, recently studied feature of poly(ferrocenylsilanes) is their tunability. Thus functional materials can be prepared via substitution reactions on polymers with Si-Cl bonds.<sup>127</sup> More recently, hydrosilylation reactions have been used with polymers containing Si-H groups to attach mesogenic groups which allows access to thermotropic side chain liquid crystalline materials.<sup>128</sup>

This ROP methodology has also been extended to other [1]- and [2]metallocenophanes. Poly(ferrocenylgermanes) (**30**) have been reported as high molecular weight ( $M_w = 10^5 - 10^6$ )

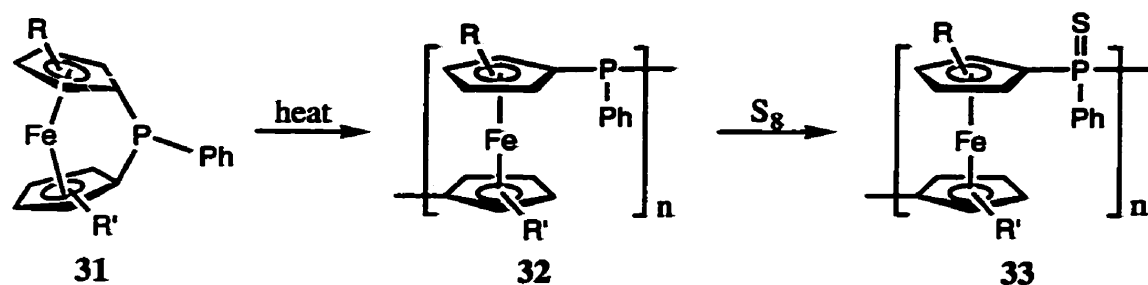
materials from the ROP of the corresponding [1]ferrocenophanes **29** at 90 °C (Equation 12).<sup>129</sup> The resulting golden–yellow polymers exhibit similar electrochemical and thermal behaviour to the analogous poly(ferrocenylsilanes) with slightly lower  $T_g$  values.<sup>118,129-132</sup>



#### Reaction 1.9 Synthesis of Poly(ferrocenylgermanes) via Thermal ROP

Poly(ferrocenylphosphines) (**32**), analogous to those previously synthesized by condensation routes,<sup>133,134</sup> have also been prepared via thermal ROP (Reaction 1.10).<sup>135</sup> Solubility increased when one of the cyclopentadienyl rings is substituted with an *n*-butyl group or both rings with SiMe<sub>3</sub> groups. Polymers **32** (R = R' = H or R = *n*-Bu, R' = H) could only be analyzed by GPC after sulfurization (yielding **33**). Sulfurization of the unsubstituted and *n*-butyl substituted polymers was carried out in order to facilitate their characterization by GPC. Those polymers with trimethylsilyl substituents on the cyclopentadienyl rings, however, could be analyzed by GPC without sulfurization. A comparison between sulfurized (**33**, R = R' = SiMe<sub>3</sub>) and unsulfurized (**32**, R = R' = SiMe<sub>3</sub>) samples of this polymer revealed essentially the same molecular weight.

Polymerization of sulfur-bridged [1]ferrocenophane (**34**) produces poly(ferrocenylsulfide) (**35**).<sup>136,137</sup> The recent synthesis of a [1]stannaferrocenophane has led, upon heating at 150 °C, to the first high molecular weight poly(ferrocenylstannane) ( $M_w = 1.3 \times 10^5$ , PDI = 1.6). The polymer **36** also possess significant interactions between iron atoms as shown by cyclic voltammetry ( $\Delta E_{1/2} = 0.24$  V).<sup>138</sup> Very recently, the first example



Reaction 1.10 Synthesis of Poly(ferrocenylphosphines) via Thermal ROP and Their Conversion to Poly(ferrocenylphosphine sulfides)

of a boron-bridged [1]ferrocenophane (37), with the highest tilt angle to date of  $32.4(2)^\circ$ , has been synthesized and also been found to polymerize.<sup>139</sup>

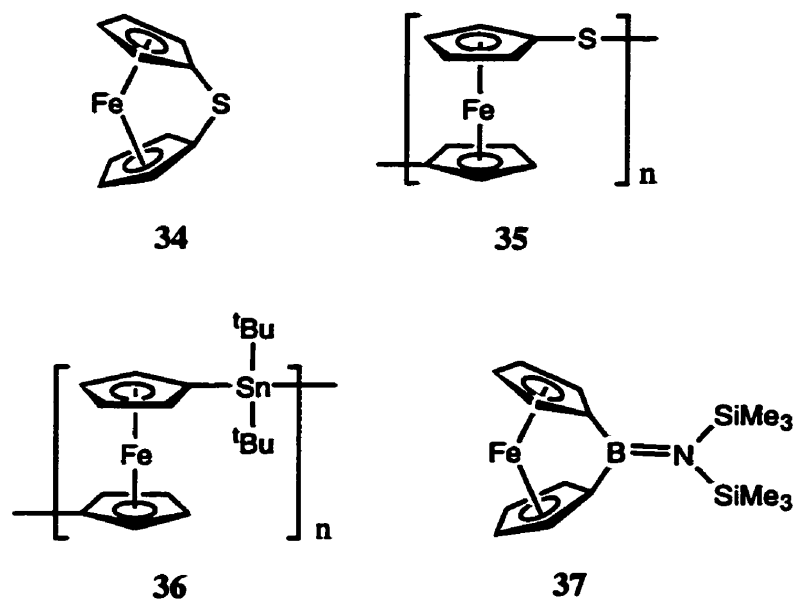
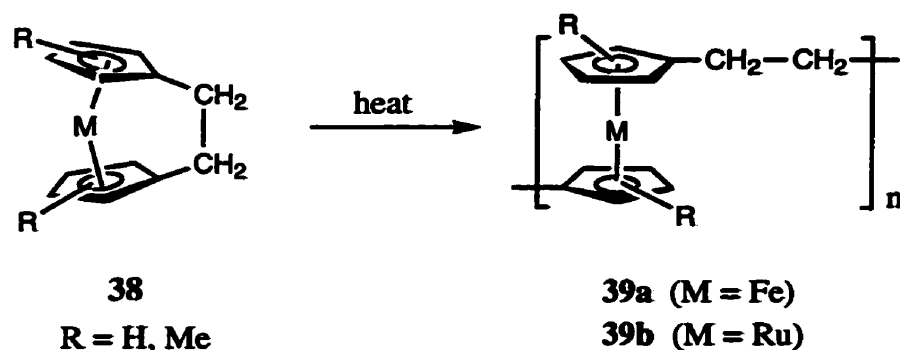


Figure 1.8 Some Other [1]Ferrocenophanes and Poly(ferrocenes)

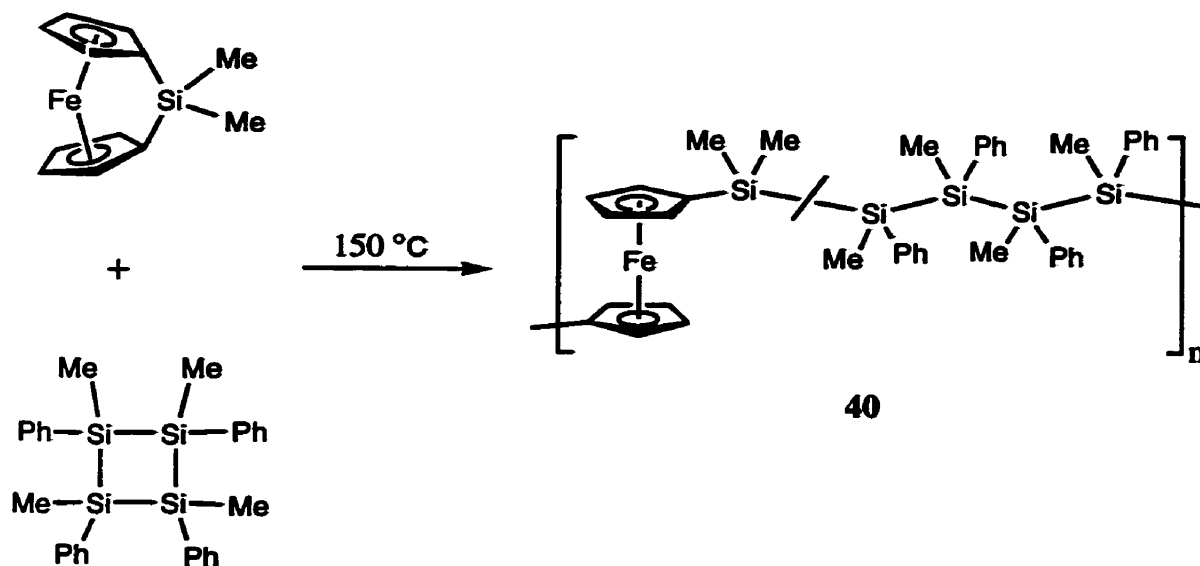
Hydrocarbon-bridged [2]ferrocenophanes (38) were found to undergo ROP at  $300^\circ\text{C}$ , providing the first reported poly(ferrocenylethylenes) (39a).<sup>140</sup> The polymers were insoluble

if  $R = H$ , but readily soluble when  $R = Me$ . In the latter case, a bimodal weight distribution was found, with an oligomeric fraction ( $M_w = 4800$ ) and a high molecular weight fraction ( $M_w = 8.1 \times 10^4$ ). Due to the more insulating hydrocarbon bridge, only slight electronic communication is observed by cyclic voltammetry (peak separation of  $\Delta E_{1/2} = 90$  mV). Cooperative magnetic behavior, however, is observed in oxidized materials at low temperature.<sup>141</sup> The analogous [2]ruthenocenophanes, which possess greater ring-tilt angles, undergo ROP at lower temperatures (220 °C) to yield poly(ruthenocenylethylenes) (**39b**) although their electrochemistry is significantly different.<sup>142</sup>



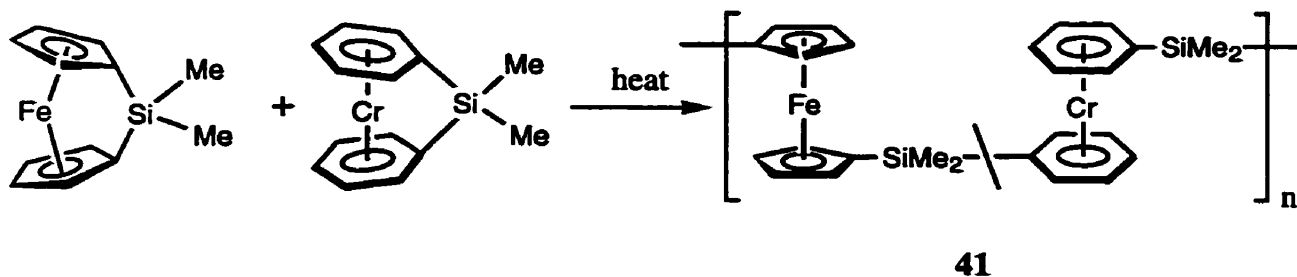
### Reaction 1.11 Synthesis of Poly(ferrocenylethylenes) and Poly(ruthenocenylethylenes) via Thermal ROP

The use of thermal ROP also allows access to novel random copolymers. The first examples, poly(ferrocenylsilane)-*co*-poly(silane) materials (**40**), were reported in early 1995.<sup>143</sup> These materials are particularly interesting since they contain ferrocene moieties linked by  $\sigma$ -delocalized oligosilane segments and these are inaccessible via thermal ROP of ferrocenophanes with oligosilanes bridges, as they are insufficiently strained.<sup>144</sup> The polymers are photosensitive and the polysilane segments can be cleaved with UV light. Interesting charge transport properties have also been found for these materials.<sup>145</sup>



**Reaction 1.12 Synthesis of Poly(ferrocenylsilane)-Poly(silane) Random Copolymers via Thermal ROP**

A range of other copolymers derived from different [1]ferrocenophanes<sup>122 130</sup> as well as [1]ferrocenophanes and silicon-bridged bis(benzene)chromium complexes<sup>146</sup> (**41**, Reaction 1.13) have subsequently been reported.



**Reaction 1.13 Random Copolymers from TROP of a Silicon-Bridged, Bis(benzene)-Chromium Complex and 27 (R = R' = Me)**

In 1994, the first anionic ROP reactions for [1]ferrocenophanes (**27** where  $R = R' = \text{Me}$ ) resulted in the formation of oligomers.<sup>113</sup> Using extremely pure monomer and stringent reaction conditions, the anionic ROP of **27** ( $R = R' = \text{Me}$ ) was shown to be living.<sup>147</sup> Poly(ferrocenylsilanes) with controlled molecular weights (depending upon the initial monomer to initiator ratio) up to  $M_w = \text{c.a. } 80\,000$  and with very narrow polydispersities ( $\text{PDI} = 1.05 - 1.10$ ) were formed. Due to the living nature of the reaction, diblock and multiblock copolymers (such as **42**) using [1]silaferrocenophanes and hexamethylcyclotrisiloxane and/or styrene have been obtained.<sup>148</sup>

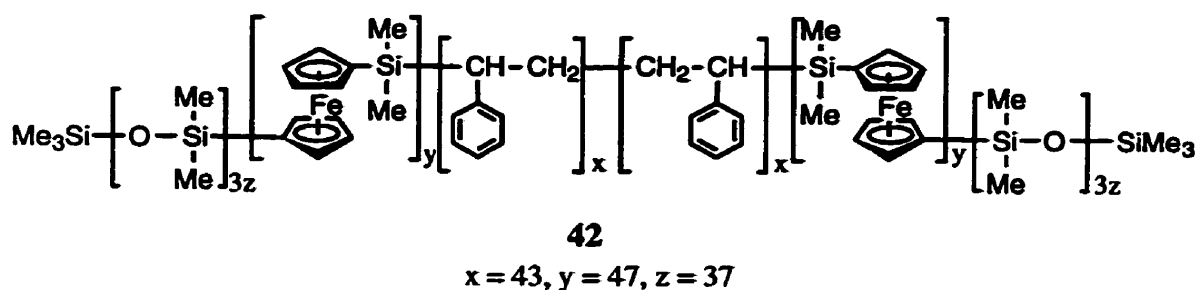


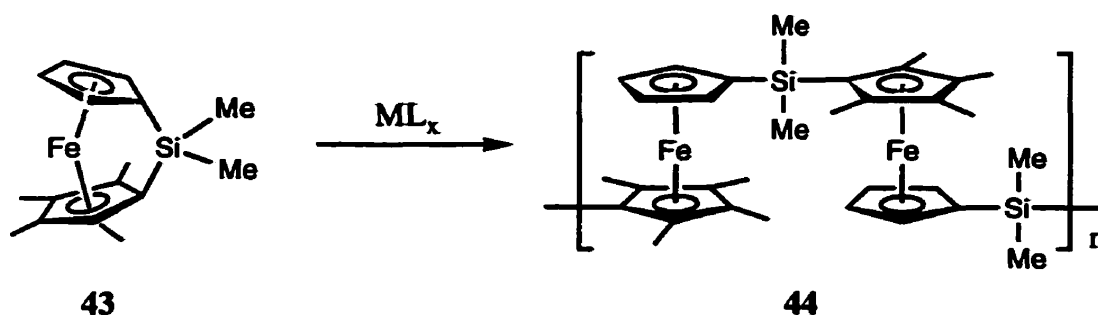
Figure 1.9 A Poly(ferrocenylsilane)-Containing Pentablock Copolymer

A mild ROP route to poly(metallocenes) from metallocenophanes using transition metal catalysts was reported in 1995. Manners *et al.* reported that a series of  $\text{Rh}^{\text{I}}$ ,  $\text{Pd}^{\text{II}}$ , and  $\text{Pt}^{\text{II}}$  complexes catalyzed the ROP of **27** ( $R = R' = \text{Me}$ ) at room temperature to yield high molecular weight poly(ferrocenylsilanes) ( $M_n = \text{c.a. } 10^5$ ).<sup>149</sup> Slightly later, Tanaka *et al.* independently reported transition metal catalyzed ROP reactions using mainly  $\text{Pd}^0$  and  $\text{Pt}^0$  catalysts.<sup>150</sup> A major advantage of these transition metal catalyzed processes is that, unlike anionic polymerization, ambient temperature polymerization is possible without the need for an extremely pure monomer. Copolymerization of silicon- and germanium-bridged [1]ferrocenophanes is possible and affords random copolymers.<sup>130,150</sup> Random copolymerization of silicon-bridged [1]ferrocenophanes with cyclocarbosilanes is also possible yielding novel poly(ferrocenylsilane)-poly(carbosilane) random copolymers.<sup>151</sup> Transition



metal-catalyzed ROP is especially advantageous in the case of [1]ferrocenophanes with halogen substituents at silicon as thermal ROP proceeds at higher temperatures than normal ( $> 250\text{ }^{\circ}\text{C}$ ).<sup>127</sup>

Moreover, recent work<sup>152</sup> has shown that unsymmetrically Cp-methylated species such as **43** yield regioregular poly(ferrocenylsilanes) (**44**) via transition metal catalysts as a result of exclusive Cp<sup>H</sup>-Si bond cleavage. In contrast, thermal ROP yields more random structures arising from cleavage of both Cp<sup>H</sup>-Si and Cp<sup>Me</sup>-Si bonds.<sup>153</sup>



**Reaction 1.14 Synthesis of Regioregular Poly(ferrocenylsilane) via Transition Metal-Catalyzed ROP**

Furthermore, molecular weight control in the range  $M_n = 10^3 - 10^5$  is also possible by the addition of  $\text{Et}_3\text{SiH}$  which leads to the isolation of end-capped polymers **45**. The use of poly(methylhydrosiloxane) as the source of Si-H bonds allows access to novel graft copolymers **46**.<sup>152</sup>

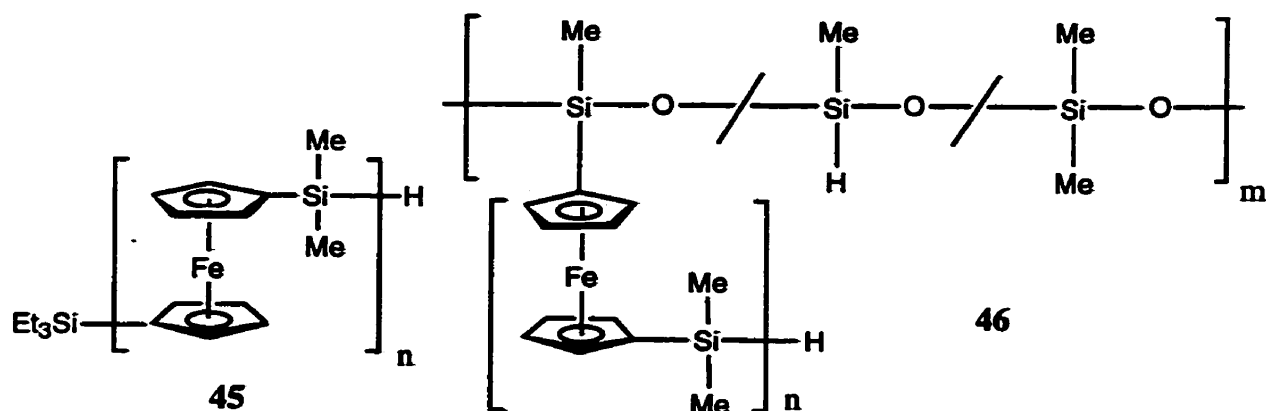


Figure 1.10 Poly(ferrocenylsilane) Homopolymers and Graft Copolymers Produced via Controlled Transition Metal-Catalyzed ROP

Recent work has also focused on understanding the mechanism of the transition metal-catalyzed ROP reactions. A logical first step in the polymerizations is insertion of the transition metal into the strained Cp-carbon-bridging element bond in the ferrocenophane. Very recently Sheridan, Manners and co-workers reported the first examples of this type of insertion product, **47** and **48**.<sup>154,155</sup>

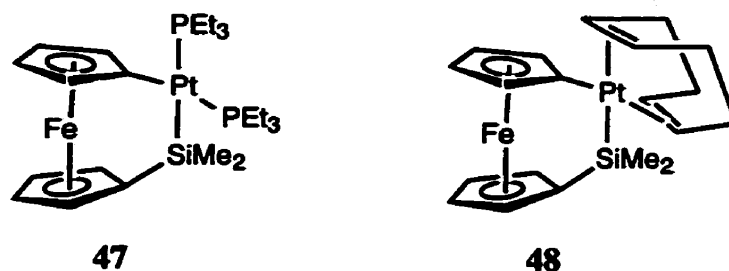
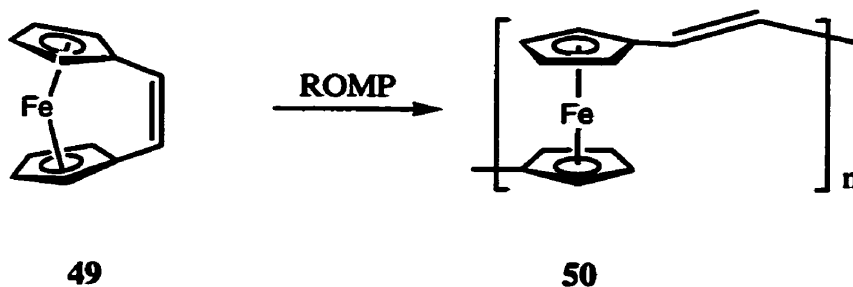


Figure 1.11 Insertion Products of a Transition Metal into the Silicon - ipso-Carbon Bond of a [1]Ferrocenophane

The [2]platinasiliferrocenophane **47** does not react further with [1]siliferrocenophane **27** (R = R' = Me). However, if the phosphine groups are replaced by more weakly bound

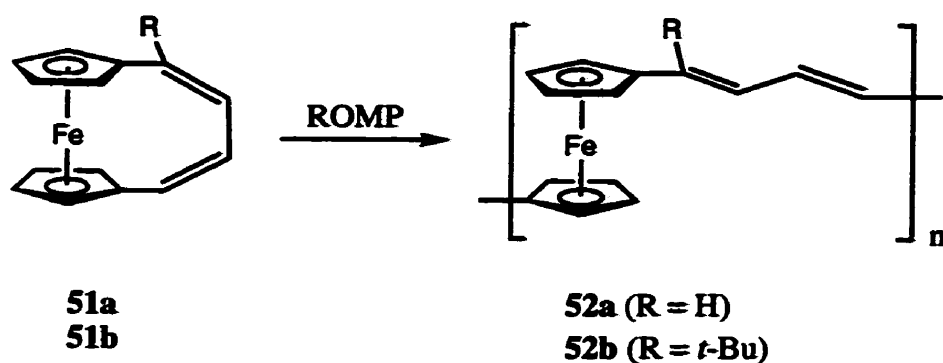
substituents as in **48**, synthesized via the reaction of **27** ( $R = R' = \text{Me}$ ) with  $\text{Pt}(1,5\text{-cod})_2$ , this species does function as a ROP catalyst.<sup>155</sup> Moreover, the ROP is inhibited by the presence of added 1,5-cod supporting labile ligand dissociation as a key step in the transition metal-catalyzed ROP mechanism.

Recently, the synthesis and ring-opening metathesis polymerization (ROMP) behaviour of the strained ethene-bridged [1]ferrocenophane **49** has been reported by Tilley *et al.*<sup>156</sup> The resultant polymer (**50**) was found to be an insoluble, orange powder which exhibited conductivity of  $10^{-3} \text{ S cm}^{-1}$  upon doping with  $\text{I}_2$ . A partially soluble random copolymer was synthesized by the ROMP of a mixture of **49** and norbornene. Values of  $M_w = 1710$  to 21 000 were observed with higher values for increasing amounts of norbornene.

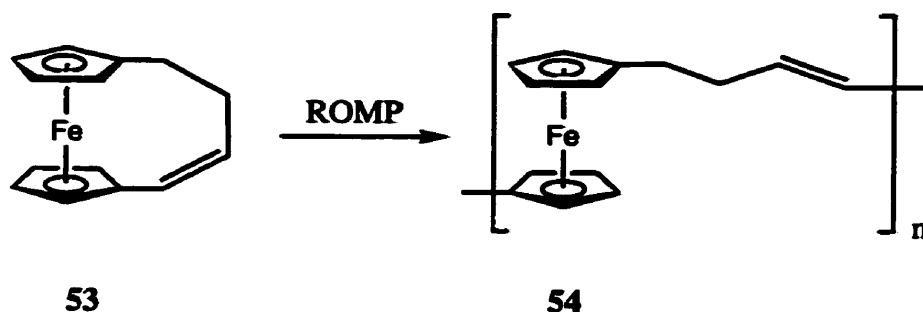


#### Reaction 1.15 Synthesis of Poly(ferrocenylethene) via ROMP

ROMP has also been used by Grubbs *et al.* on [4]ferrocenophanes **51a** and **53** to yield poly(ferrocenyldivinylene) (**52a**) and poly(ferrocenylenebutylene) (**54**) respectively.<sup>157</sup> Polymer **52a** was found to be insoluble although the copolymerization of **51a** with *sec*-butylcyclooctatetraene yielded a more soluble product with  $M_w$  up to 24 400 (PDI = 2.1).



**Reaction 1.16 Synthesis of Poly(ferrocenylendivinylenes) via ROMP**



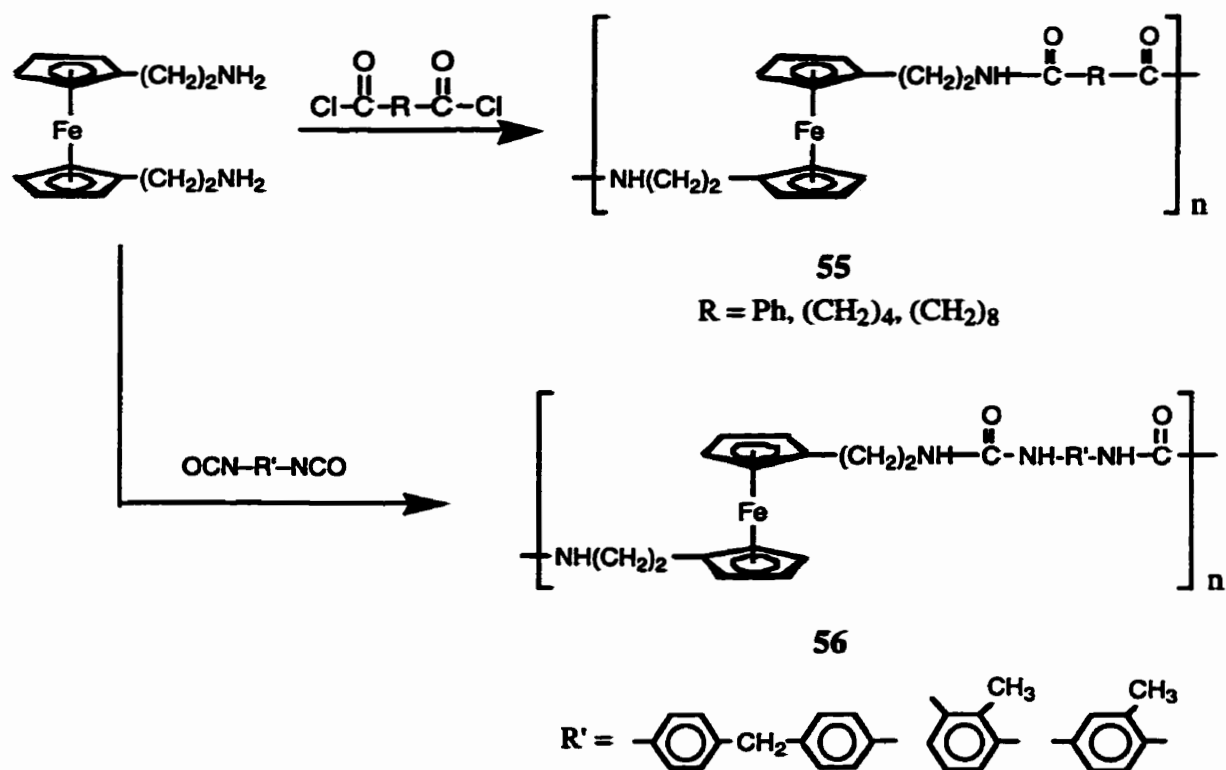
**Reaction 1.17 Synthesis of Poly(ferrocenylenebutylene) via ROMP**

Very recently, a soluble polymer (**52b**) was obtained from ROMP of **51b** by Lee *et al.* with molecular weights ( $M_w$ ) ranging up to 320 000.<sup>158</sup>

### 1.5.2 With Long Spacer Units

The organic chemistry of ferrocene has for many years allowed researchers to synthesize polymers with ferrocene in the main chain when the interspacing units are long. However, as this area is rather large and did not form part of the research conducted for this Thesis, this section will deal with only a few recent examples.

The synthesis of elastomeric polyamides (**55**,  $M_n = 10\,000 - 18\,000$ ) in high yields from 1,1'-bis( $\beta$ -aminoethyl)ferrocene and diacid chlorides (Reaction 1.15) has been reported.<sup>159</sup> Polyureas (**56**), polyesters and polyurethanes have also been synthesized but possessed much lower molecular weights. These materials were characterized by scanning electron microscopy, X-ray and IR analyses. The use of ferrocenes in which the active center is separated by at least two methylene units was crucial in order to reduce steric effects and the instability found previously in polymers of  $\alpha$ -functionalized ferrocene due to the  $\alpha$ -ferrocenyl carbonium ion stability.<sup>160</sup>



#### Reaction 1.18 Synthesis of Some Ferrocene-Containing Polyamides

Wright *et al.*<sup>161</sup> have utilized Knoevenagel condensations to prepare new non-linear optical (NLO) ferrocene-containing polymers for second harmonic generation (SHG) applications. The recent use of ferrocenes in this area is based on their large hyperpolarizability

values<sup>162</sup> combined with their thermal and photochemical stability which make them desirable candidates for NLO materials. Thus, they synthesized a polyurethane copolymer (**57**) in moderate yields from a ferrocene derivative in which side reactions are minimized. The polymer was fully characterized and possessed a value of  $M_n = 7600$  although no  $T_g$  was found using DSC.<sup>161</sup> Contrary to previous results with perfectly oriented organometallic polymers,<sup>163</sup> due to its random orientation in a head to tail sense, it displays SHG activity at 150 °C by corona poling with reasonable stability for the SHG signal.

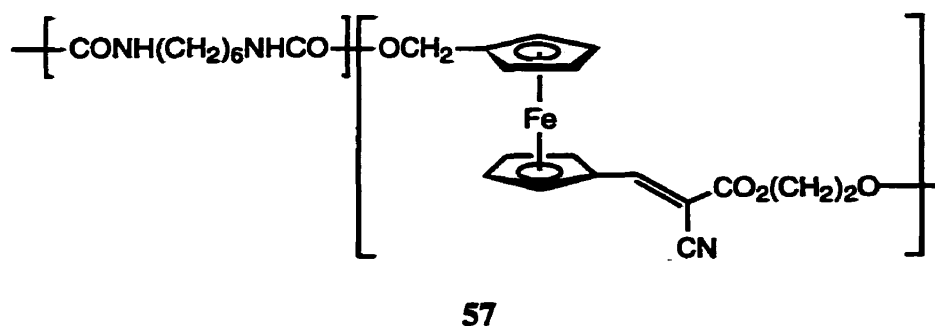


Figure 1.12 A Ferrocene-Containing Polyurethane Copolymer

The synthesis of novel polymeric zirconocene–silsesquioxanes (**58**) has been reported by Lichtenhan and Haddad.<sup>164,165</sup> The condensation of zirconocene derivatives with polyhedral silsesquioxanes led to amorphous polymers in high yields ( $\approx 90\%$ ) that were characterized by NMR spectroscopy and elemental analysis. These high molecular weight ( $M_n = 14\,000$ ) materials exhibited very high thermal stability ( $T_{dec} = 474 - 515\text{ °C}$ ) and stability to both air and hydrolysis in the case of **58a**.

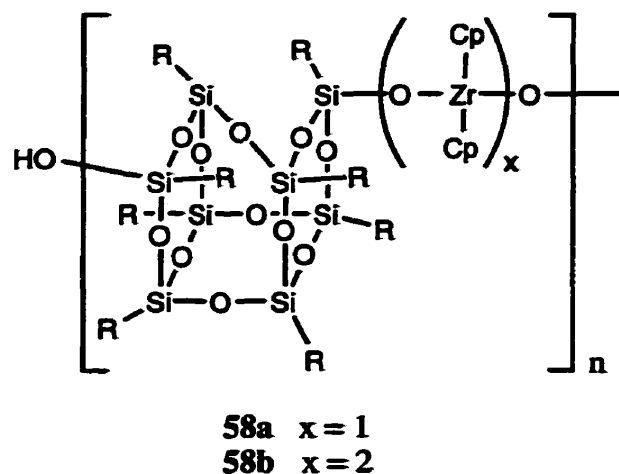
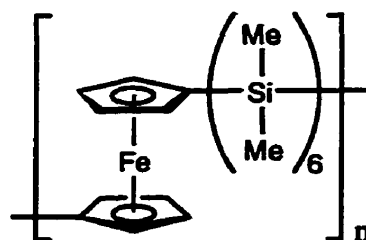


Figure 1.13 Polymeric Zirconocene-Silsesquioxanes

Also poly(ferrocenylhexasilane) (**59**) has been synthesized in an attempt to obtain polymers in which ferrocenes are joined to  $\sigma$ -delocalized polysilane segments in a regular alternating structure.<sup>166</sup> The condensation of dilithioferrocene and 1,6-dichlorodecamethylhexasilane gave a soluble, well-characterized polymer showing monomodal molecular weight distribution by GPC ( $M_w \approx 3500$ ). After doping, conductivity values ( $\sigma = 3 \times 10^{-5} \text{ S cm}^{-1}$ ) were three orders of magnitude higher than octadecasilane which appear to indicate that conjugation between ferrocenediyl and hexasilanediyl units contribute to the conductivity, although the values are lower than for the corresponding poly(1,1'-ferrocenylenes).<sup>167</sup>



**59**

Figure 1.14 Poly(ferrocenylhexasilane)

Thiophene units have been also used as spacer units in order to obtain conjugated polymers.<sup>119</sup> The reaction of a di-zinc ferrocene derivative with a dibromotrithiophene afforded poly(ferrocenylene thienylene) (**60**) with moderate molecular weight ( $M_n \approx 4500$ ) which was characterized by NMR spectrometry and elemental analysis. Studies on doped materials with  $\text{SbCl}_6^-$ ,  $\text{BF}_4^-$  and  $\text{TCNQ}^-$  counteranions showed the presence of weak antiferromagnetic interactions.

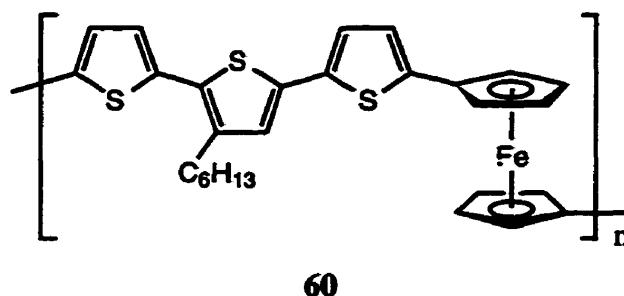


Figure 1.15 Poly(ferrocenylene thienylene)

## 1.6 Metal-Based Polymers in Catalysis

One of the major driving forces in research on organometallic compounds has been their use in catalysis. Several major reactions (e.g. Ziegler-Natta catalysis, Wacker process, olefin hydrogenation) have been made possible or at least facilitated by the use of organometallic compounds.<sup>168</sup> In general, industry favours heterogeneous catalysts which are robust, reusable and easy to separate from the final products. The difficulty arises from the fact that the nature of the active catalytic site is often unclear with heterogeneous systems and often there are many different types of catalytic centres which can lead to the formation of different products. Homogeneous catalysts, on the other hand, are much easier to study and



can be tuned in such a way that the nature of the final product(s) can be controlled. Unfortunately, it can be difficult to recover small molecule homogeneous catalysts leading to problems with effectively short catalyst lifetimes (and associated expense) and impurities in the final products. One possible route to combine the advantages of both homogeneous and heterogeneous catalysts is to bind the small molecule homogeneous catalyst to a support. Examples of possible supports include inorganic materials such as silica and  $\text{MgCl}_2$  and also polymers. Only the latter will be covered here and, as the area is quite large, only a few notable examples will be discussed.

In one sense, polymer-supported catalysts have always been with us. Enzymes, in which catalytic sites are enclosed within a protein framework, are incredibly selective and efficient polymer-supported catalysts.<sup>169</sup> One early example of a man-made, polymer-supported catalyst was the attachment of Wilkinson's catalyst to a polystyrene backbone (61) through donor ligands.<sup>170</sup> The catalytic activity of this species was reported to be average in comparison to regular catalysts and unfortunately suffered from loss of catalyst due to leaching of the metal centres from the polymer backbone. A more recent example of a polymer-supported hydrogenation catalyst is the methacrylate copolymer 62.<sup>171</sup> In this case, the N donor ligands are used to bind  $\text{Pd}(\text{OAc})_2$  or  $\text{RhCl}_3 \cdot x\text{H}_2\text{O}$  and then treatment with  $\text{NaBH}_4$  to activate the metal species. Again, catalytic activities were found to be lower than in the case for the homogeneous species but recovery of the catalyst was reported to be almost quantitative.

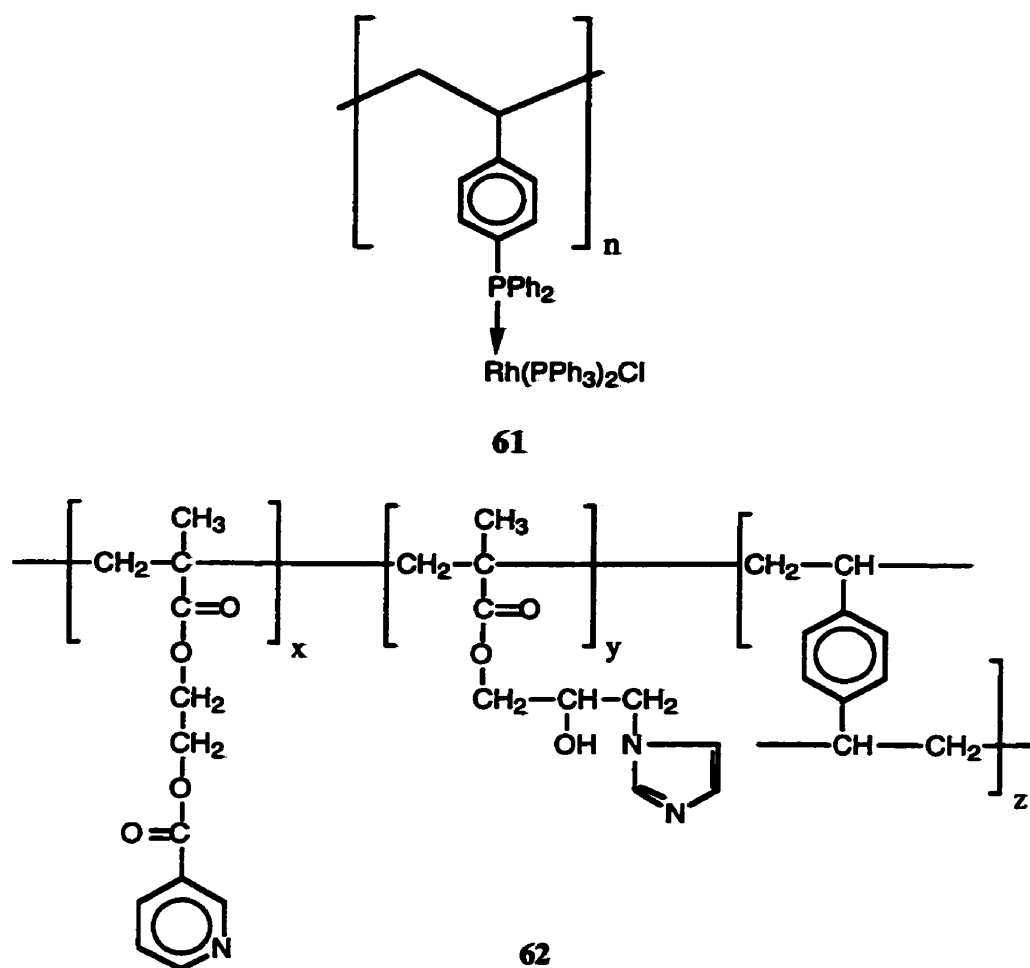
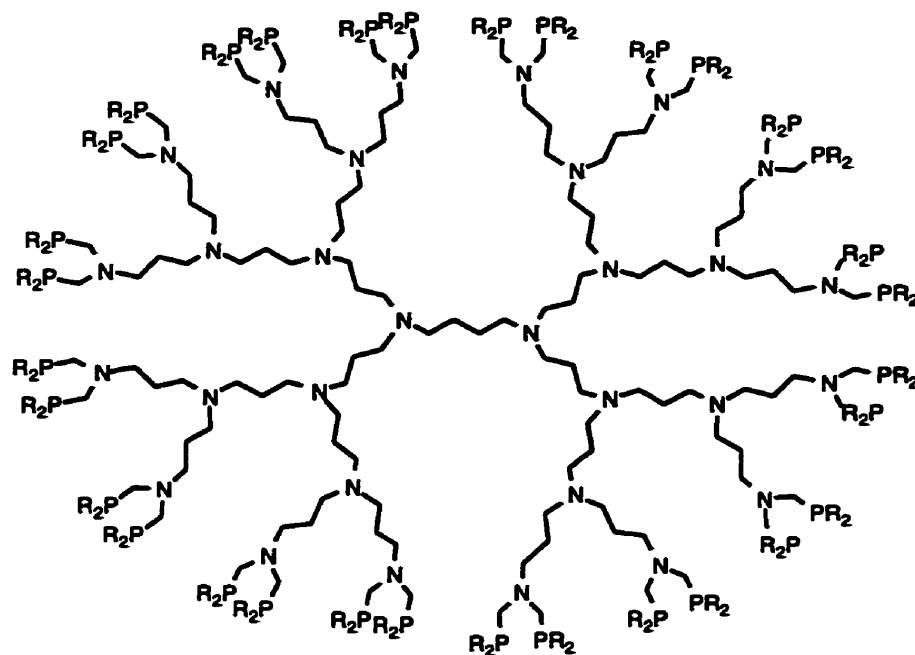


Figure 1.16 Polymer-Supported Hydrogenation Catalysts

Dendrimers have also recently been used as catalyst supports. A silane dendrimer with 12 arylnickel (II)-bearing termini was used to catalyze the addition of  $\text{CCl}_4$  to methyl methacrylate although no description was given for product-catalyst separation.<sup>172</sup> Other examples include dendrimer-supported Ti alkoxides for the addition of  $\text{Et}_2\text{Zn}$  to benzaldehyde<sup>173</sup> and the electrochemical reduction of  $\text{CO}_2$  to  $\text{CO}$  using a dendrimer with Pd-bearing triphosphane units.<sup>174</sup> A more recent example is the functionalization of a polyamino dendrimer with phosphine groups resulting in 63 and followed by reaction with metal complexes such as  $[\text{PdCl}_2(\text{PhCN})_2]$ ,  $[\text{Pd}(\text{CH}_3)_2(\text{TMEDA})]$ ,  $[\text{Ir}(\text{cod})_2][\text{BF}_4]$  or

$[\text{Rh}(\text{cod})_2][\text{BF}_4]$ .<sup>175</sup> The Pd-bearing dendrimers were found to be effective catalysts for the Heck reaction, displaying a significantly higher catalytic activity than the corresponding monomeric species. The Rh-bearing dendrimer was tested as a hydroformylation catalyst and displayed similar activity to the monomeric species.



63

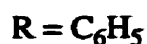
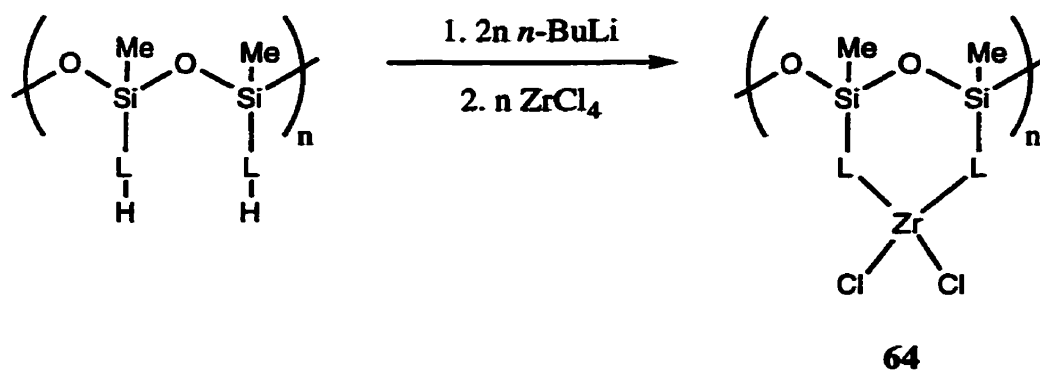


Figure 1.17 A Dendrimer Used for Supporting Metal-Based Catalysts

A very recent example of a polymer supported catalyst was described in a preliminary report and involves the immobilization of a Lewis acid,  $\text{Sc}(\text{OTf})_3$ , by microencapsulation near the surface of a polystyrene support which was formed into small beads.<sup>176</sup> These catalysts were shown to be remarkably versatile for a number of reactions catalyzed by Lewis acids, easy to recover by simple filtration and could be used repeatedly without any apparent loss of catalytic activity.

Attaching metallocene-based catalysts to polymer supports is an area of potential interest. Specialty polyolefins (e.g. poly(ethylene)-*r*-(1-hexene) copolymer) are now being manufactured by industry in growing amounts and these products can only be obtained by the use of metallocene catalysts.<sup>168,177-179</sup> Again, as is common with the use of homogeneous catalysts in other reactions, these processes suffer from catalyst impurities remaining in the final product. There have been a number of reports of "classical" Ziegler-Natta catalysts (e.g.  $\text{TiCl}_4/\text{AlR}_3$ ) being attached to a polymer<sup>180</sup> but only recently has research begun into using metallocene-based species instead.<sup>181-183</sup> One example involved attaching suitable ligands (e.g.  $\text{L} = \text{cyclopentadienyl, indenyl}$ ) to a polysiloxane backbone and then reacting these with a suitable metal species to produce the catalytic precursors (**64**).<sup>182,183</sup> The activities of these catalysts were described as intermediate to those of the homogeneous metallocenes and those attached to inorganic supports such as  $\text{SiO}_2$  or  $\text{Al}_2\text{O}_3$  for producing poly(ethylene) and poly(propylene). The broad molecular weight distributions of the products suggested that the active catalytic species formed by these supported zirconocenes were not uniform.<sup>183</sup>



#### Reaction 1.19 Synthesis of a Polysiloxane-Supported Ziegler-Natta Catalyst

Research in the area of polymer-supported catalysts is on-going as efforts are made to design supported catalysts for particular reactions. However, many problems still remain and the goal

of achieving well-defined, highly-active and stable (i.e. no leaching of the catalytic metal) polymer-supported catalysts remains yet to be realized.

## 1.7 Block Copolymer Micelles

Amphiphilic block copolymers, which can display similar solution behaviour to surfactants, have also been investigated as possible supports for catalysts. The amphiphilic nature of surfactants has been known for many years as well as their ability to stabilize the interfaces of incompatible solvents (e.g. the oil-water interface). A number of mesophase structures have been observed for surfactants in solution.<sup>184</sup> However, these phases are rarely stable as dynamic exchange processes result in rapid interconversion. Amphiphilic block copolymers, too, have been found to form micellular-like aggregates in solution (Figure 1.18) due to the solubility differences of the constituent blocks and form phase-separated structures in the solid state (Figure 1.19). In contrast to classical surfactants, however, block copolymers can be adjusted such that any interface between incompatible substances can be stabilized.<sup>184</sup> Additional stability of a block copolymer micelle may be imparted by crosslinking either the corona or the core of the micelle. The potential uses of block copolymer micellular-like aggregates range from stabilizers for drugs and metal colloids to mini-reactors.<sup>184</sup>

The most commonly observed morphology for block copolymer micelles is the sphere. However, more unusual shapes such as cylinders and vesicles have been observed.<sup>185-187</sup> Eisenberg *et al.*<sup>87</sup> studied the morphological behaviour of polystyrene-*b*-poly(acrylic acid) and varied the length of the poly(acrylic acid) block. By altering the ratio of polystyrene:poly(acrylic acid) over the range of 200:21 to 200:4, they were able to indirectly observe six different morphologies in aqueous solution (for which the polystyrene block was incompatible), including spheres, rods, lamellae and even vesicles by depositing the solutions onto suitable grids, staining with

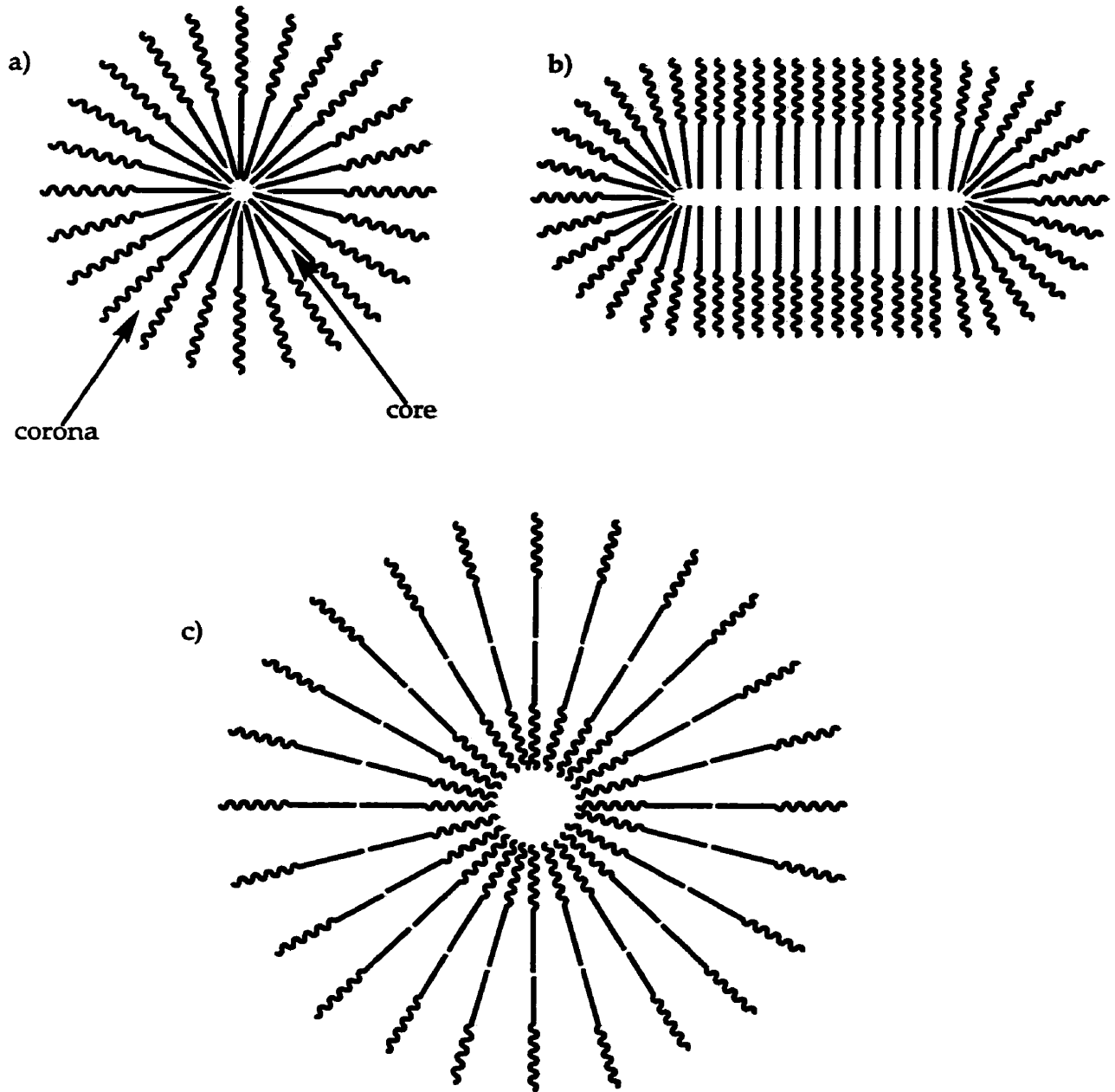


**Figure 1.18 Schematic Representations of the Three General Classes of Block Copolymer Micelles: a) Spherical, b) Cylindrical and c) Vesicular**

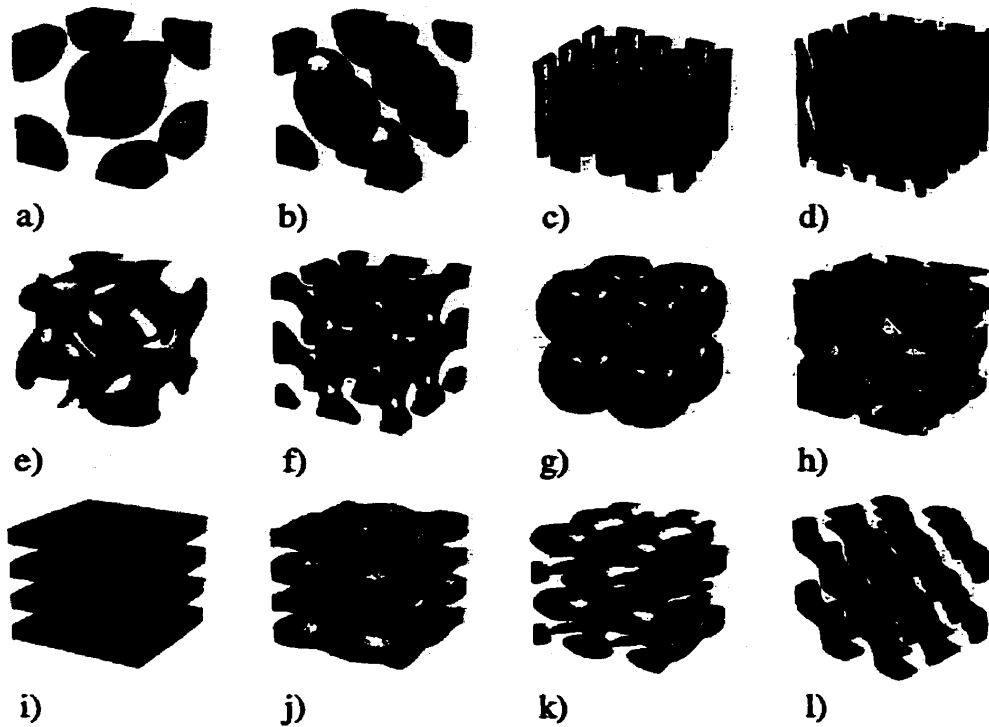


**Figure 1.19** Typical Mesophase Structures of Segregating Block Copolymers:  
 a) body-centred cubic packing of disperse spheres; b) face-centered cubic packing of disperse spheres; c) hexagonal structure; d) undulated cylinders with tetragonal packing; e) gyroid phase; f) bicontinuous double-diamond structure; g)  $Im3m$  phase; h)  $L_3$  phase (spongelike structure); i) planar lamellar structure; j) undulated lamellae with tetragonal symmetry; k) tetragonally perforated lamellae; l) hexagonally perforated lamellae with rhombohedral symmetry<sup>184</sup>

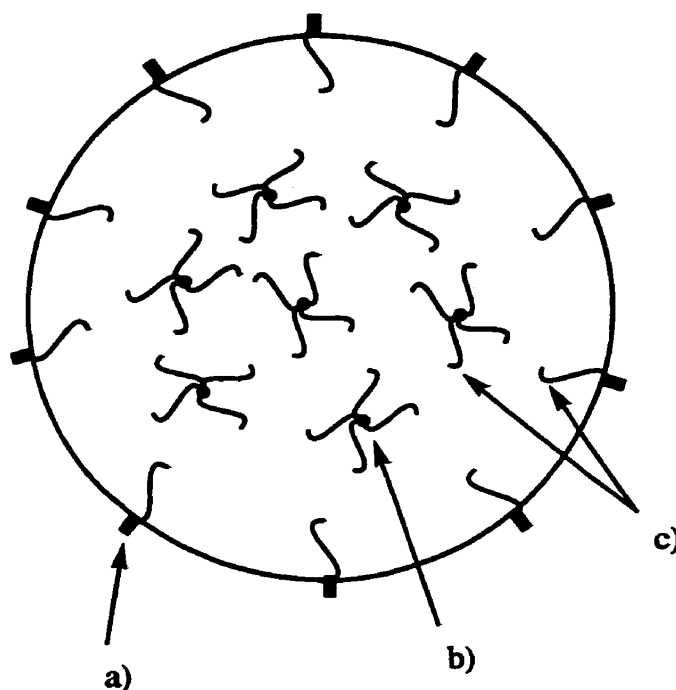


**Figure 1.20** Schematic structure of large complex micelle filled with bulk reverse micelles where a) poly(acrylic acid) chain in corona, b) core of reverse micelle (poly(acrylic acid) chains and c) polystyrene chains

CsOH, allowing the water to evaporate and then observing the samples by transmission electron microscopy (TEM). An unusual morphology formed by these "crew-cut" micelles (so called because of the short length of the chains forming the corona in comparison to those forming the core) involved micrometer-sized spheres whose cores were filled with reverse micelle-like aggregates (see Figure 1.20).

Vesicles formed by block copolymers have also been observed by Liu *et al.* using polyisoprene-*b*-poly(2-cinnamoyl ethyl methacrylate) in which there was an equal number of units in each block.<sup>188</sup> In contrast to the polymer system used by Eisenberg, this polymer was found to form vesicles in organic solution (THF/hexanes mixture). The block copolymers were first dissolved in THF and then hexanes (in which the poly(2-cinnamoyl ethyl methacrylate) block is insoluble) was added. Analysis by TEM was accomplished by spraying



the samples onto suitable grids and then staining with OsO<sub>4</sub>. The size of the vesicle was found to be dependant upon the original THF:hexanes ratio and a comparison between crosslinked<sup>189</sup> and uncrosslinked samples found few differences suggesting that the morphologies observed were also present in solution and had not undergone a transition upon evaporation of the solvent. In general, the vesicles were found to be spherical. However, on water surfaces, the vesicles were found to form hexagonal unit cells in a "honeycomb" pattern with varying cell size. As there was no evidence for deformation upon drying or in the TEM chamber, it was thought that deformation of the vesicles from spheres had occurred on the water surface.

As described earlier, additional stability may be imparted to polymeric micelles by crosslinking the chains in either the core or the corona. When the corona is crosslinked, the micelles are termed shell-crosslinked knedels (SCK's).<sup>190</sup> These species resemble dendrimers in that they have a spherical shape, a large number of peripheral functionalities with limited mobility and a core-shell structure (see Figure 1.21). Work by Wooley *et al.* on SCK's has involved using systems such as polystyrene-*b*-poly(4-vinylpyridine).<sup>191</sup> Quarternization of the pyridine units with *p*-chloromethylstyrene allowed for formation of micelles in water (a non-solvent for polystyrene) and then introduction of a radical initiator resulted in crosslinking of the *p*-chloromethylstyrene units attached to the poly(4-vinylpyridine) block. Variation of the block lengths has allowed the formation of SCK's with diameters ranging from 5 to 200 nm.<sup>192</sup> Despite the crosslinked nature of the shell of these SCK's, they have been shown to be permeable to medium-sized hydrophobic organic molecules such as pyrene.

Antonietti *et al.* in 1997 reported the preparation of Pd colloids in block copolymer micelles and subsequently studied their ability to catalyze the Heck reaction.<sup>193</sup> The polymer system used was polystyrene-*b*-poly-4-vinylpyridine. The synthesis of the colloids involved mixing the block copolymer with Pd(OAc)<sub>2</sub> in a solvent (e.g. toluene) in which the poly-4-vinylpyridine block was insoluble. Reduction of Pd(II) to Pd(0) was accomplished by using Li[BEt<sub>3</sub>H]. A large number of small Pd colloids (ca. 10 - 1000) were formed in each micelle

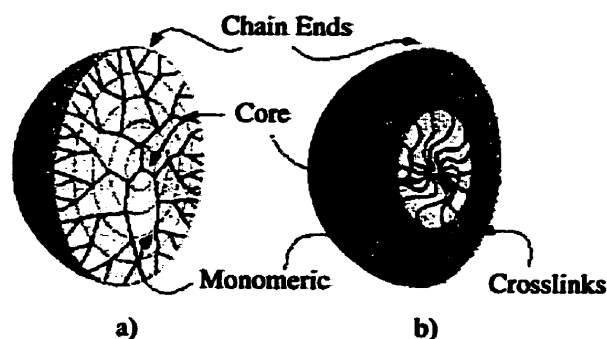


Figure 1.21 Cross-Sectional Drawings of the Basic Structural Components of  
a) Dendrimers and b) SCK's<sup>190</sup>

core as determined by TEM.<sup>194,195</sup> The catalytic activity for the Heck reaction of the Pd colloids was comparable to that of classical low molecular weight Pd complexes but the stability of the micellized-catalysts was found to be much higher with catalytic activity remaining even after 50 000 turn-over cycles.

A very recent example of an unusual block copolymer aggregate was reported by Jenekhe *et al.* in 1998.<sup>196</sup> In this case, poly(phenylquinoline)-*b*-polystyrene was found to self-organize into micrometer-scale spherical, vesicular, cylindrical and lamellar aggregates (in which the poly(phenylquinoline) formed the corona and the polystyrene formed the core of the micelles) from solution. The spherical and cylindrical aggregates were found to have extremely large hollow cavities with diameters as large as 30  $\mu\text{m}$ , larger than bacteria.<sup>197</sup> When the block copolymers were allowed to form aggregates in the presence of fullerenes ( $\text{C}_{60}$  and  $\text{C}_{70}$ ), spherical aggregates were found to form with aggregation numbers in excess of  $10^9$  and each aggregate allowed the solubilization of over  $10^{10}$  fullerene molecules.

Very recently, Manners, Winnik *et al.* reported the first example of micelles being formed by an organometallic-inorganic block copolymer.<sup>198</sup> Poly(ferrocenyldimethylsilane)-*b*-poly(dimethylsiloxane) was found to micellize in hexanes. Measurements by static laser light scattering indicated an aggregation number of approximately 2000. Preparation of the samples

for TEM similar to the way used by Liu *et al.* (see earlier) but without staining (the presence of Fe sites within the poly(ferrocenylsilane) block was sufficient for contrast) indicated that the block copolymers had formed wormlike micelles that appeared to be flexible and on average were about 440 nm long with a thickness of ca. 20 nm.

## 1.8 Research Objectives

The research in this Thesis covers two different polymer systems: poly(ferrocenes) with a variety of different bridging elements between ferrocene moieties and poly(carbosilanes) with zirconocene substituents. The general goals were to study some of the properties of known poly(ferrocenes), to find routes to both new and well-defined organometallic polymers and to synthesize metallocene-containing polymers that could potentially act as catalyst supports.

The objectives for my PhD work were:

- 1) To further explore the use of ROP as a route to poly(ferrocenes) and specifically to
  - i) determine the effects of sterically-demanding substituents upon the ROP behaviour of silicon-bridged, [1]- and [2]ferrocenophanes and the properties of any resultant polymers
  - ii) study the properties of a series of symmetrically-substituted poly(ferrocenylgermanes)
  - iii) investigate the thermal and transition metal-catalyzed ROP behaviour of tetra-coordinate, phosphorus-bridged [1]ferrocenophanes.

- 2) To develop living anionic ROP of phosphorus-bridged [1]ferrocenophanes as a route to more well-defined poly(ferrocenylphosphines), to synthesize poly(ferrocenylphosphine) block copolymers, to determine whether these block copolymers formed micellular-like aggregates and to conduct preliminary metal coordination studies.
- 3) To develop polymer-supported, Ziegler-Natta catalytic precursors via ROP

Aspects of the projects detailed in this Thesis were carried out in collaboration with other researchers within and external to the group. The actual breakdown of these collaborations is provided as follows on a chapter by chapter basis.

In Chapter Two, the initial syntheses of **5** and **6** were performed by Dr. Dan Foucher. The synthesis of **7** was carried out by myself. The single crystal X-ray structure of **7** was solved by Dr. Alan Lough.  $^{29}\text{Si}$  NMR data were obtained by Nick Plavac. Mass spectra were obtained by Dr. Alex Young. Elemental analyses were carried out by the Canadian Microanalytical Service. All other analyses were performed by myself.

In Chapter Three, the synthesis and characterization (NMR, GPC where appropriate) of compounds **4a**, **b** and **d**, **5a**, **b** and **d**, **6**, **7** and **8** (by thermal ROP) were carried out by Dr. Dan Foucher and Dr. Mark Edwards. Compounds **8** (by transition metal-catalyzed ROP), **10c** and **11** were synthesized by myself.  $^{29}\text{Si}$  NMR data were obtained by Nick Plavac. Elemental analyses were carried out by either the Canadian Microanalytical Services Ltd. or Quantitative Technologies Inc. Mass spectra were run by Dr. Alex Young. WAXS patterns were obtained by Dr. Srebri Petrov with the exception of **8** which was obtained by Mark MacLachlan. Low angle laser light scattering studies were carried out by Jason Massey. All other analyses including NMR, GPC, UV/visible, DSC and cyclic voltammetry were carried out by myself.

In Chapter Four, all syntheses were carried out by myself. The single crystal X-ray structure of **9b** was solved by Dr. Alan Lough. The 400 MHz  $^1\text{H}$  NMR data were obtained by Karen Temple. Elemental analyses were obtained by Quantitative Technologies Inc. WAXS

patterns were obtained by Mark MacLachlan. Dynamic light scattering studies were carried out by Jason Massey. Electrospray mass spectra were obtained by Doreen Wan. All other analyses including NMR, UV/visible, DSC, TGA and cyclic voltammetry were carried out by myself.

In Chapter Five, the initial anionic ROP studies were done by Dr. Charles Honeyman. Subsequent anionic ROP reactions were carried out by Jason Massey and myself. All other reactions were carried out by myself.  $^{29}\text{Si}$  NMR data were obtained by Nick Plavac. Solid state NMR spectra were obtained by Dr. Patricia Aroca-Ouellete and Dr. Tim Burrows. WAXS patterns were obtained by Mark MacLachlan. TEM, DLS and SLS studies were carried out by Jason Massey. AFM studies were carried out by Nicole Power. All other analyses including NMR and GPC were carried out by myself.

In Chapter Six, all reactions and NMR characterization were carried out by Dr. Paul Nguyen and myself, except **9c** and **11c** which I alone synthesized and **12** which was synthesized by Sara Bourke. The single crystal X-ray structures of **7a** and **9a** were solved by Dr. Arnold Rheingold and Louise Liable-Sands and that of **9b** by Dr. Alan Lough. 400 MHz NMR data were obtained by either Dr. Paul Nguyen or Sara Bourke. Solid state NMR spectra were obtained by Dr. Patricia Aroca-Ouellete and Dr. Tim Burrows. Mass spectra were run by Dr. Alex Young. All other analyses were carried out by myself.

In keeping with the policy of our research group, each Thesis chapter is essentially self-contained and is in the form of a publication that is intended for the open, peer-reviewed scientific literature. In the case of each Chapter, the first draft was written by myself.

Portions of this thesis have been published previously:

Chapter One: Figures 1.20 and 1.22 were reproduced with permission respectively from *Angew. Chem. Int. Ed. Engl.* **1997**, *36*, 911 and *Chem. Eur. J.* **1997**, *3*, 1397.

**Chapter Two: All text and figures were reproduced with permission from  
*Can J. Chem.* 1995, 73, 2069.**

**Chapter Three All text and figures were reproduced with permission from  
*Macromolecules* 1996, 29, 2396.**

**Chapter Five Initial results were reported in *Chem. Commun.* 1996, 2589.**

## 1.9 References

- (1) *Inorganic and Organometallic Polymers with Special Properties*; Laine, R. M., Ed.; Kluwer Academic Publishers: London, 1992; Vol. 206.
- (2) (a) Pittman, C. U.; Carraher, C. E.; Reynolds, J. R. in *Encyclopedia of Polymer Science and Engineering*; Eds. Mark, H. F.; Bikales, N. M.; Overberger, C. G.; Menges, G.; Wiley: New York, 1989; Vol. 10; p. 541. (b) Sheats J. E.; Carraher, C. E.; Pittman, C. U.; Zeldin M., Currell B.; *Inorganic and Metal-Containing Polymeric Materials*; Plenum: New York, 1989. (c) Gonsalves K. E.; Rausch M. D. in *Inorganic and Organometallic Polymers. ACS Symposium Series 360*; Eds. Zeldin, M.; Wynne, K.; Allcock, H. R. American Chemical Society: Washington, DC. 1988. (d) Allcock, H. R. *Adv. Mater.* **1994**, *6*, 106. (e) Manners, I. *Chem. Br.* **1996**, *32*, 46. (f) Foucher, D.A.; Ziembinski, R.; Rulkens, R.; Nelson, J.; Manners, I. In *Inorganic and Organometallic Polymers II*; P. Wisian-Neilson, H. R. Allcock and K.J. Wynne, Ed.; American Chemical Society: Washington, D. C., 1994; Vol. ACS Symposium Series 572; pp 442-455.
- (3) a) Fyfe, H. B.; Melkuz, M.; Zargarian, D.; Taylor, N. J.; Marder, T. B. *J. Chem. Soc., Chem. Commun.* **1991**, 188. b) Wright, M. E.; Sigman, M. S. *Macromolecules* **1992**, *25*, 6055. (c) Davies, S. J.; Johnson, B. F. G.; Khan, M. S.; Lewis, J.; *J. Chem. Soc., Chem. Commun.* **1991**, 187. (d) Tenhaeff, S. C.; Tyler, D. R. *J. Chem. Soc., Chem. Commun.* **1989**, 1459. (e) Manners, I. *J. Chem. Soc., Ann. Rep. Prog. Chem. A.* **1991**, 77. (f) Neuse, E. W.; Bednarik, L. *Macromolecules* **1979**, *12*, 187. (g) Sturge, K. C.; Hunter, A. D.; McDonald, R.; Santarsiero, B. D. *Organometallics* **1992**, *11*, 3056. (h) Gonsalves, K.; Zhan-ru, L.; Rausch, M. D. *J. Am. Chem. Soc.* **1984**, *106*, 3862. (i) Katz, T. J.; Sudhakar, A.; Teasley, M. F.; Gilbert, A. M.; Geiger, W. E.; Robben, M. P.; Wuensch, M.; Ward, M. D. *J. Am. Chem. Soc.* **1993**, *115*, 3182. (j) Nugent, H. M.; Rosenblum, M. *J. Am. Chem. Soc.* **1993**, *115*, 3848. (k) Patterson, W. J.; McManus, S. P.; Pittman, C. U. *J. Polym. Sci.: Poly. Chem. Ed.* **1974**, *12*, 837.

- (4) Manners, I. *Angew. Chem. Int. Ed. Engl.* **1996**, *35*, 1602.
- (5) *Silicon-Based Polymer Science*; Ziegler, J. M.; Fearon, F. W. G., Eds.; American Chemical Society: Washington, D.C., 1990.
- (6) *Siloxane Polymers*; Semlyen, J. A.; Clarson, S. J., Eds.; Prentice Hall: Englewood Cliffs, N. J., 1991.
- (7) Mark, J. E.; Allcock, H. R.; West, R. *Inorganic Polymers*; Prentice Hall: Englewood Cliffs, NJ, 1992, .
- (8) Allcock, H. R. *Phosphorus-Nitrogen Compounds*; Academic: New York, 1972, .
- (9) Neilson, R. H.; Wisian-Neilson, P. *Chem. Rev.* **1988**, *88*, 541.
- (10) D'Halluin, G.; de Jager, R. *Bull. Soc. Chim. Belg.* **1989**, *98*, 653.
- (11) D'Halluin, G.; de Jager, R.; Chambrette, J. P.; Potin, P. *Macromolecules* **1992**, *25*, 1254.
- (12) Montague, R. A.; Matyjaszewski, K. *J. Am. Chem. Soc.* **1990**, *112*, 6721.
- (13) Honeyman, C. H.; Manners, I.; Morrissey, C.; Allcock, H. R. *J. Am. Chem. Soc.* **1995**, *117*, 7035.
- (14) Allcock, H. R.; Nelson, J. M.; Reeves, S. D.; Honeyman, C. H.; Manners, I. *Macromolecules* **1997**, *30*, 50.
- (15) a) Aitken, C. T.; Harrod, J. F.; Samuel, E. *J. Organomet. Chem.* **1985**, *279*, C11. b) Aitken, C. T.; Harrod, J. F.; Samuel, E. *J. Am. Chem. Soc.* **1986**, *108*, 4059.
- (16) Tilley, T. D. *Acc. Chem. Res.* **1993**, *26*, 22.
- (17) Scarlete, M.; Brienne, S.; Butler, I. S.; Harrod, J. F. *Chem. Mater.* **1994**, *6*, 977.
- (18) Hsio, Y.; Waymouth, R. M. *J. Am. Chem. Soc.* **1994**, *116*, 9779.
- (19) a) Cypryk, M.; Gupta, Y.; Matyjaszeski, K. *J. Am. Chem. Soc.* **1991**, *113*, 1046. b) Fossum, E.; Matyjaszeski, K. *Macromolecules*, **1995**, *28*, 1618.
- (20) Sakamoto, K.; Obata, K.; Hirata, H.; Nakajima, M.; Sakurai, H. *J. Am. Chem. Soc.* **1989**, *111*, 7641.



- (21) Suzuki, H.; Meyer, H.; Simmerer, J.; Yang, J.; Haarer, D. *Adv. Mater.* **1993**, *5*, 743.
- (22) West, R. *J. Organomet. Chem.* **1986**, *300*, 327.
- (23) Miller, R. D.; Michl, J. *Chem. Rev.* **1989**, *89*, 1359.
- (24) a) *Inorganic Materials*; Bruce, D. W., O'Hare, D.; Wiley: Toronto, 1992. b) *Extended Linear Chain Compounds, Vols. 1 -3*, Millers, J.S.; Plenum: New York, 1982. c) Ingham, S. L.; Long, N. J. *Angew. Chem. Int. Ed.* **1994**, *33*, 1752. d) Oriol, L.; Serrano, J. L. *Adv. Mater.* **1995**, *7*, 348.
- (25) a) Connelly, N. G.; Geiger, W. E. *Adv. Organomet. Chem.* **1984**, *23*, 1. b) Connelly, N.G.; Geiger, W. E. *Adv. Organomet. Chem.* **1985**, *24*, 87.
- (26) Sheats, J. E.; Carraher, C. E.; Pittman, C. U. *Metal Containing Polymer Systems*; Plenum: Toronto, 1985, .
- (27) Pittman, C. U., Jr.; Carraher, C. E.; Reynolds, J. R. In *Encycl. Polym. Sci. Eng.* **1987**; Vol. 10; pp 541.
- (28) Manners, I. *Chem. Br.* **1996**, *32*, 46.
- (29) Sonogashira, S.; Takahashi, S.; Hagihara, N. *Macromolecules* **1977**, *10*, 879.
- (30) Takahasi, S.; Morimoto, H.; Murata, E.; Kataoka, S.; Sonogashira, K.; Hagihara, N. *Polymer Science: Polymer Chem. Ed.* **1982**, *20*, 565.
- (31) Hagihara, N.; Sonogashira, K.; Takahashi, S. *Adv. Polym. Sci.* **1981**, *41*, 149.
- (32) Abe, A.; Kimura, N.; Tabata, S. *Macromolecules* **1991**, *14*, 6238.
- (33) Chisholm, M. *Angew. Chem. Int. Ed. Engl.* **1991**, *30*, 673.
- (34) Johnson, B. F. G.; Kakkar, A. K.; Khan, M. S.; Lewis, J. J. *Organomet. Chem.* **1991**, *409*, C12.
- (35) Fyfe, H. B.; Mlekuz, M.; Zargarian, D.; Taylor, N. J.; Marder, T. B. *J. Chem. Soc., Chem. Commun.* **1991**, 188.
- (36) Sturge, K. C.; Hunter, A. D.; McDonald, R.; Santarsiero, B. D. *Organometallics* **1992**, *11*, 3056.

- (37) Ohkubo, A.; Aramaki, A.; Nishihara, H. *Chem. Lett.* **1993**, 271.
- (38) Tomita, I.; Nishio, A.; Igarashi, T.; Endo, T. *Polym. Bull.* **1993**, *30*, 179.
- (39) Tomita, I.; Nishio, A.; Endo, T. *Macromolecules* **1994**, *27*, 7009.
- (40) Tomita, I.; Hishio, A.; Endo, T. *Macromolecules* **1995**, *28*, 3042.
- (41) Rozhanskii, I.; Tomita, I.; Endo, T. *Macromolecules* **1996**, *29*, 1934.
- (42) Mao, S. H.; Tilley, T. D. *J. Am. Chem. Soc.* **1995**, *117*, 5365.
- (43) Achar, S.; Puddephatt, R. J. *Angew. Chem. Int. Ed. Engl.* **1994**, *33*, 847.
- (44) Serroni, S.; Denti, G.; Campagna, S.; Juris, A.; Ciano, M.; Balzani, V. *Angew. Chem. Int. Ed. Engl.* **1992**, *31*, 1493.
- (45) Newkome, G. R.; Cardullo, F.; Constable, E. C.; Moorefield, C. N.; Cargill Thompson, A. M. W. *J. Chem. Soc., Chem. Commun.* **1993**, 925.
- (46) Arimoto, F. S.; Haven, A. C. *J. Am. Chem. Soc.* **1955**, *77*, 6295.
- (47) Pittmann, C. U., Jr.; Voges, R. L.; Elder, J. *Polym. Lett.* **1971**, *9*, 191.
- (48) Pittmann, C. U., Jr. *J. Polym. Sci. Part A-1* **1971**, *9*, 3175.
- (49) Lai, J. C.; Rounsefell, T.; Pittmann, C. U., Jr. *J. Polym. Sci. Part A-1* **1971**, *9*, 651.
- (50) Sasaki, Y.; Walker, L. L.; Hurst, E. L.; Pittmann, C. U., Jr. *J. Polym. Sci. Polym. Chem. Ed.* **1973**, *11*, 1213.
- (51) George, M. J.; Hayes, G. F. *J. Polym. Sci. Polym. Chem. Ed.* **1975**, *13*, 1049.
- (52) George, M. H.; Hayes, G. F. *J. Polym. Sci. Polym. Chem. Ed.* **1976**, *14*, 475.
- (53) Aso, C.; Kunitake, T.; Nakashima, T. *Makromol. Chem.* **1969**, *124*, 232.
- (54) Nuyken, O.; Burkhardt, V.; Pöhlmann, T.; Herberhold, M. *Makromol. Chem., Macromol. Symp.* **1991**, *44*, 195.
- (55) Smith, T. W.; Kuder, J. E.; Wychick, D. *J. Polym. Sci. Polym. Chem. Ed.* **1976**, *14*, 2433.
- (56) Flanagan, J. B.; Margel, S.; Bard, A. J.; Anson, F. C. *J. Am. Chem. Soc.* **1978**, *100*, 4248.

- (57) Kittlesen, G. P.; White, H. S.; Wrighton, M. S. *J. Am. Chem. Soc.* **1985**, *107*, 7373.
- (58) Cowan, D. O.; Park, J.; Pittman, C. U., Jr.; Sasaki, Y.; Mukherjee, T. K.; Diamond, N. A. *J. Am. Chem. Soc.* **1972**, *94*, 5110.
- (59) Cowan, D. O.; Kaufman, F. *J. Am. Chem. Soc.* **1970**, *92*, 219.
- (60) Bilow, N.; Landis, A. L.; Rosenberg, H. *J. Polym. Sci. Part A-1* **1969**, *7*, 2719.
- (61) Pittmann, C. U., Jr.; Lai, J. C.; Vanderpool, D. P.; Good, M.; Prados, R. *Macromolecules* **1970**, *3*, 105.
- (62) Pittmann, C. U., Jr.; Lai, J. C.; Vanderpool, D. P.; Good, M.; Prados, R. In *Polymer Characterization: Interdisciplinary Approaches*; C. D. Craver, Ed.; Plenum Publishing Corp.: New York, 1971; pp 97 .
- (63) Cowan, D. O.; Park, J.; Pittmann, C. U., Jr.; Sasaki, Y.; Mukherjee, T. K.; Diamond, N. A. *J. Am. Chem. Soc.* **1972**, *94*, 5110.
- (64) Albagli, D.; Bazan, G.; Wrighton, M. S.; Schrock, R. R. *J. Am. Chem. Soc.* **1992**, *114*, 4150.
- (65) Albagli, D.; Bazan, G. C.; Schrock, R. R.; Wrighton, M. S. *J. Phys. Chem.* **1993**, *97*, 10211.
- (66) Nakashima, T.; Kunitake, T. *Makromol. Chem.* **1971**, *157*, 73.
- (67) Pittmann, C. U., Jr.; Sasaki, Y.; Grube, P. L. *J. Macromol. Sci., Chem.* **1974**, *A8* (5), 923.
- (68) Simionescu, C.; Lixandru, T.; Mazilu, I.; Tataru, L. *Makromol. Chem.* **1971**, *147*, 69.
- (69) Simionescu, C.; Lixandru, T.; Negulescu, I.; Mazilu, I.; Tataru, L. *Makromol. Chem.* **1973**, *163*, 59.
- (70) Buchmeiser, M.; Schrock, R. R. *Macromolecules* **1995**, *28*, 6642.

- (71) Sheats, J. E.; Hessel, F.; Tsarouhas, L.; Podejko, K. G.; Porter, T.; Kool, L. B.; Nolan, R. L., Jr. In *Metal-containing Polymer Systems*; J. E. Sheats, C. E. Carraher, Jr. and C. U. Pittmann, Jr., Eds.; Plenum Publishing Corp.: New York, 1985; pp 83 .
- (72) Sheats, J. E.; Hessel, F.; Tsarouhas, L.; Podejko, K. G.; Porter, T.; Kool, L. B.; Nolan, R. L. In *New and Unusual Monomers and Polymers*; B. M. Culbertson and C. U. Pittmann, Jr., Eds.; Plenum Publishing Corp.: New York, 1983; pp 83 .
- (73) Wang, C.-L.; Mulcandani, A. *Anal. Chem.* **1995**, *67*, 1109.
- (74) Allcock, H. R.; Riding, G. H.; Lavin, K. D. *Macromolecules* **1985**, *18*, 1340.
- (75) Allcock, H. R.; Riding, G. H.; Lavin, K. D. *Macromolecules* **1987**, *20*, 6.
- (76) Manners, I.; Riding, G. H.; Dodge, J. A.; Allcock, H. R. *J. Am. Chem. Soc.* **1989**, *111*, 3067.
- (77) Allcock, H. R.; Dodge, J. A.; Manners, I.; Riding, G. H. *J. Am. Chem. Soc.* **1991**, *113*, 9596.
- (78) Allcock, H. R.; Dodge, J. A.; Manners, I.; Parvez, M.; Riding, G. H.; Visscher, K. B. *Organometallics* **1991**, *10*, 3098.
- (79) Saraceno, R. A.; Riding, G. H.; Allcock, H. R.; Ewing, A. G. *J. Am. Chem. Soc.* **1988**, *110*, 7254.
- (80) Wisian-Neilson, P.; Ford, R. R. *Macromolecules* **1989**, *22*, 72.
- (81) Pannell, K. H.; Rozell, J. M.; Ziegler, J. M. *Macromolecules* **1988**, *21*, 276.
- (82) Diaz, A.; Seymour, M.; Pannell, K. H.; Rozell, J. M. *J. Electrochem. Soc.* **1990**, *137*, 503.
- (83) Hale, P. D.; Boguslavsky, L. I.; Inagaki, T.; Karan, H. I.; Lee, H. S.; Skotheim, T. A. *Anal. Chem.* **1991**, *63*, 677.
- (84) Fillaut, J.-L.; Linares, J.; Astruc, D. *Angew. Chem. Int. Ed. Engl.* **1994**, *33*, 2460.
- (85) Jutzi, P.; Batz, C.; Neumann, B.; Stammler, H.-G. *Angew. Chem., Int. Ed. Engl.* **1996**, *35*, 2118.

- (86) Casado, C. M.; Cuadrado, I.; Morán, M.; Alonso, B.; Lobete, F.; Losada, J. *Organometallics* **1995**, *14*, 2618.
- (87) Alonso, B.; Morán, M.; Casado, C. M.; Lobete, F.; Losada, J.; Cuadrado, I. *Chem. Mater.* **1995**, *7*, 1440.
- (88) Korshak, V. V.; Sosin, S. L.; Alekseeva, V. P. *Akad. Nauk SSR* **1960**, *132*, 360.
- (89) Korshak, V. V.; Sosin, S. L.; Alekseeva, V. P. *Vysokomol. Soedin.* **1961**, *3*, 1332.
- (90) Nesmenayov, A. N.; Korshak, V. V.; Voevodskii, N. S.; Kochetkova, S. L.; Sosin, S. L.; Materikova, R. B.; Bolotnikova, T. N.; M., C. V.; Bazhin, N. M. *Dokl. Akad. Nauk SSSR* **1961**, *137*, 1370.
- (91) Rosenberg, H.; Neuse, E. W. *J. Organomet. Chem.* **1966**, *76*.
- (92) Neuse, E. W.; Bednarik, L. *Macromolecules* **1979**, *12*, 187.
- (93) Yamamoto, T.; Sanechika, K.; Yamamoto, A.; Katada, M.; Motoyama, I.; Sano, H. *Inorg. Chim. Acta* **1983**, *73*, 75.
- (94) Hirao, T.; Kurashina, M.; Aramaki, K.; Nishihara, H. *J. Chem. Soc., Dalton Trans.* **1996**, 2929.
- (95) Oyama, N.; Takizawa, Y.; Matsuda, H.; Yakamoto, T.; Sanechika, K. *Denkikagaku* **1988**, *56*, 781.
- (96) Neuse, E. W.; Rosenberg, H. *J. Macromol. Sci. – Revs. Macromol. Chem.* **1970**, *C4*, 1.
- (97) Greber, G.; Hallensleben, M. L. *Makromol. Chem.* **1966**, *92*, 137.
- (98) Patterson, W. J.; McManus, S. P.; Pittman, C. U., Jr. *J. Polym. Sci. Polym. Chem.* **1974**, *12*, 837.
- (99) Fellman, J. D.; Garrou, P. E.; Withers, H. P.; Seyferth, D.; Traficante, D. D. *Organometallics* **1983**, *2*, 818.
- (100) Rosenberg, H.; Rausch, M. D. U.S. Patent 3,060,215 **1962**
- (101) Rosenberg, H. U.S. Patent 3,426,053 **1969**

- (102) Osborne, A. G.; Whitelely, R. H.; Meads, R. E. *J. Organomet. Chem.* **1980**, *193*, 345.
- (103) Seyferth, D.; Withers, H. P. *Organometallics* **1982**, *1*, 1275.
- (104) Foucher, D. A.; Tang, B.-Z.; Manners, I. *J. Am. Chem. Soc.* **1992**, *114*, 6246.
- (105) Foucher, D. A.; Ziembinski, R.; Tang, B.-Z.; Macdonald, P. M.; Massey, J.; Jaeger, C. R.; Vancso, G. J.; Manners, I. *Macromolecules* **1993**, *26*, 2878.
- (106) Itoh, T.; Saitoh, H.; Iwatsuki, S. *J. Polym. Sci. Polym. Chem.* **1995**, *33*, 1589.
- (107) Nugent, H. M.; Rosenblum, M.; Klemarczyk, P. *J. Am. Chem. Soc.* **1993**, *115*, 3848.
- (108) Rosenblum, M.; Nugent, H. M.; Jang, K.-S.; Labes, M. M.; Cahalane, W.; Klemarczyk, P.; Reiff, W. M. *Macromolecules* **1995**, *28*, 6330.
- (109) Foxman, B. M.; Rosenblum, M.; Sokolov, V.; Khrushchova, N. *Organometallics* **1993**, *12*, 4805.
- (110) Foxman, B. M.; Gronbeck, D. A.; Rosenblum, M. *J. Organomet. Chem.* **1991**, *413*, 287.
- (111) Rosenblum, M. *Adv. Mater.* **1994**, *6*, 159.
- (112) Brandt, P. F.; Rauchfuss, T. B. *J. Am. Chem. Soc.* **1992**, *114*, 1926.
- (113) Rulkens, R.; Lough, A. J.; Manners, I. *J. Am. Chem. Soc.* **1994**, *116*, 797.
- (114) Rulkens, R.; Lough, A. J.; Manners, I.; Lovelace, S. R.; Grant, C.; Geiger, W. E. *J. Am. Chem. Soc.* **1996**, *118*, 12683.
- (115) Foucher, D. A.; Ziembinski, R.; Petersen, R.; Pudelski, J.; Edwards, M.; Ni, Y.; Massey, J.; Jaeger, C. R.; Vancso, G. J.; Manners, I. *Macromolecules* **1994**, *27*, 3992.
- (116) Foucher, D. A.; Honeyman, C. H.; Nelson, J. M.; Tang, B.-Z.; Manners, I. *Angew. Chem.* **1993**, *105*, 1843.
- (117) Nguyen, M. T.; Diaz, A. F.; Dement'ev, V. V.; Pannell, K. H. *Chem. Mater.* **1993**, *5*, 1389.

- (118) Foucher, D. A.; Ziembinski, R.; Rulkens, R.; Nelson, J. M.; Manners, I. In *Inorganic and Organometallic Polymers II*; P. A. Wisian-Nielson, H. R.; Wynne, K. J., Eds, Ed. American Chemical Society: Washington, DC, 1994, ; Vol. ACS Symposium Series 572; pp 449.
- (119) Hmyene, M.; Yassar, A.; Escorne, M.; Percheron-Guegan, A.; Garnier, F. *Adv. Mater.* **1994**, *6*, 564.
- (120) Tang, B.-Z.; Petersen, R.; Foucher, D. A.; Lough, A. J.; Coombs, N.; Sodhi, R.; Manners, I. *J. Chem. Soc., Chem. Commun.* **1993**, 523.
- (121) Petersen, R.; Foucher, D. A.; Tang, B.-Z.; Lough, A. J.; Raju, N. P.; Greedan, J. E.; Manners, I. *Chem. Mater.* **1995**, *7*, 2045.
- (122) Pudelski, J. K.; Rulkens, R.; Foucher, D. A.; Lough, A. J.; Macdonald, P. M.; Manners, I. *Macromolecules* **1995**, *28*, 7301.
- (123) MacLachlan, M. J.; Aroca, P.; Coombs, N.; Manners, I.; Ozin, G. A. *Adv. Mater.* **1998**, *10*, 144.
- (124) Rasburn, J.; Petersen, R.; Jahr, T.; Rulkens, R.; Manners, I.; Vancso, G. J. *Chem. Mater.* **1995**, *7*, 871.
- (125) Nguyen, P.; Lough, A. J.; Manners, I. *Macromol. Rapid Commun.* **1997**, *18*, 953.
- (126) Nguyen, P.; Stojcevic, G.; Kulbaba, K.; MacLachlan, M.; Liu, X.-H.; Lough, A. J.; Manners, I. *Macromolecules* **1998**, submitted for publication.
- (127) Zechel, D. L.; Hultsch, K. C.; Rulkens, R.; Balaishtis, D.; Ni, Y.; Pudelski, J. P.; Lough, A. J.; Manners, I. *Organometallics* **1996**, *15*, 1972.
- (128) Liu, X.-H.; Bruce, D. W.; Manners, I. *J. Organomet. Chem.* **1997**, *548*, 49.
- (129) Foucher, D. A.; Manners, I. *Makromol. Chem., Rapid Commun.* **1993**, *14*, 63.
- (130) Peckham, T. J.; Massey, J. A.; Edwards, M.; Manners, I.; Foucher, D. A. *Macromolecules* **1996**, *17*, 2396.
- (131) Foucher, D. A.; Edwards, M.; Burrow, R. A.; Lough, A. J.; Manners, I. *Organometallics* **1994**, *13*, 4959.

- (132) Kapoor, R. N.; Crawford, G. M.; Mahmoud, J.; Dement'ev, V. V.; Nguyen, M. T.; Diaz, A. F.; Pannell, K. H. *Organometallics* **1995**, *14*, 4944.
- (133) Pittman, C. U., Jr. *J. Poly. Sci., Polym. Chem. Ed.* **1967**, *5*, 2927.
- (134) Withers, H. P.; Seyferth, D.; Fellman, J. D.; Garrou, P. E.; Martin, S. *Organometallics* **1982**, *1*, 1283.
- (135) Honeyman, C. H.; Foucher, D. A.; Dahmen, F. Y.; Rulkens, R.; Lough, A. J.; Manners, I. *Organometallics* **1995**, *14*, 5503.
- (136) Pudelski, J. K.; Gates, D. P.; Rulkens, R.; Lough, A. J.; Manners, I. *Angew. Chem., Int. Ed. Engl.* **1995**, *34*, 1506.
- (137) Insoluble poly(ferrocenylene sulfide) was obtained early by condensation routes. See: Chien, J. C. W.; Gooding, R. D.; Lillya, C. P. *Polym. Mater. Sci. Eng.* **1983**, *49*, 107.
- (138) Rulkens, R.; Lough, A. J.; Manners, I. *Angew. Chem., Int. Ed. Engl.* **1996**, *35*, 1805.
- (139) Braunschweig, H.; Dirk, R.; Müller, M.; Nguyen, P.; Resendes, R.; Gates, D. P.; Manners, I. *Angew. Chem. Int. Ed. Engl.* **1997**, *36*, 2338.
- (140) Nelson, J. M.; Rengel, H.; Manners, I. *J. Am. Chem. Soc.* **1993**, *115*, 7035.
- (141) Nelson, J. M.; Rengel, H.; Petersen, R.; Nguyen, P.; Manners, I.; Raju, N. P.; Greedan, J. E.; Barlow, S.; O'Hare, D. *Chem. Eur. J.* **1997**, *3*, 573.
- (142) Nelson, J. M.; Lough, A. J.; Manners, I. *Angew. Chem., Int. Ed. Engl.* **1994**, *33*, 989.
- (143) Fossum, E.; Matyjaszewski, K.; Rulkens, R.; Manners, I. *Macromolecules* **1995**, *28*, 401.
- (144) Finckh, W.; Tang, B.-Z.; Foucher, D. A.; Zamble, D. B.; Ziemienski, R.; Lough, A.; Manners, I. *Organometallics* **1993**, *12*, 823.
- (145) Rulkens, R.; Resendes, R.; Verma, A.; Manners, I.; Murti, K.; Fossum, E.; Miller, P.; Matyjaszewski, K. *Macromolecules* **1997**, *30*, 8165.



- (146) Hultzsch, K. C.; Nelson, J. M.; Lough, A. J.; Manners, I. *Organometallics* **1995**, *14*, 5496.
- (147) Rulkens, R.; Ni, Y. Z.; Manners, I. *J. Am. Chem. Soc.* **1994**, *116*, 12121.
- (148) Ni, Y. Z.; Rulkens, R.; Manners, I. *J. Am. Chem. Soc.* **1996**, *118*, 4102.
- (149) Ni, Y. Z.; Rulkens, R.; Pudelski, J. K.; Manners, I. *Makromol. Chem. Rapid Communications* **1995**, *16*, 637.
- (150) Reddy, N. P.; Yamasita, H.; Tanaka, M. *J. Chem. Soc. Chem. Commun.* **1995**, 2263.
- (151) Sheridan, J. B.; Gómez Elipe, P.; Manners, I. *Makromol. Chem. Rapid Commun.* **1996**, *17*, 319.
- (152) Gómez-Elipe, P.; Macdonald, P.; Manners, I. *Angew. Chem. Int. Ed. Engl.* **1997**, *36*, 762.
- (153) Pudelski, J. K.; Manners, I. *J. Am. Chem. Soc.* **1995**, *117*, 7265.
- (154) Sheridan, B. S.; Lough, A. J.; Manners, I. *Organometallics* **1996**, *15*, 2195.
- (155) Sheridan, J. B.; Temple, K.; Lough, A. J.; Manners, I. *J. Chem. Soc., Dalton Trans.* **1997**, 711.
- (156) Buretea, M. A.; Tilley, T. D. *Organometallics* **1997**, *16*, 1507.
- (157) Stanton, C. E.; Lee, T. R.; Grubbs, R. H.; Lewis, N. S.; Pudelski, J. K.; Callstrom, M. R.; Erickson, M. S.; McLaughlin, M. L. *Macromolecules* **1995**, *28*, 8713.
- (158) Heo, R. W.; Somoza, F. B.; Lee, T. R. *J. Am. Chem. Soc.* **1998**, *120*, 1621.
- (159) Gonsalves, K.; Zhan-ru, L.; Rausch, M. D. *J. Am. Chem. Soc.* **1984**, *106*, 3862.
- (160) Pittman, C. U.; Rausch, M. D. *Pure Appl. Chem.* **1986**, *58*, 617.
- (161) Wright, M. E.; Toplikar, E. G.; Lackritz, H. S.; Kerney, J. T. *Macromolecules* **1994**, *27*, 3016.
- (162) Marder, S. R.; Perry, J. W.; Tiemann, B. G.; Schaefer, W. P. *Organometallics* **1991**, *10*, 1896.
- (163) Wright, M. E.; Toplikar, E. G. *Macromolecules* **1992**, *25*, 6050.

- (164) Lichtenhan, J. D. *Comments Inorg. Chem.* **1995**, *17*, 115.
- (165) Haddad, T. S.; Lichtenhan, J. D. *J. Inorg. Organomet. Polym.* **1995**, *5*, 237.
- (166) Tanaka, M.; Hayashi, T. *Bull. Chem. Soc. Jpn.* **1993**, *66*, 334.
- (167) Sanechika, K.; Yakamoto, T.; Yamamoto, A. *Polymer J.* **1981**, *13*, 255.
- (168) Herrmann, W. A.; Cornils, B. *Angew. Chem. Int. Ed. Engl.* **1997**, *36*, 1048.
- (169) Kirby, A. J. *Angew. Chem. Int. Ed. Engl.* **1996**, *35*, 707.
- (170) Grubbs, R. H.; Kroll, L. C. *J. Am. Chem. Soc.* **1971**, *93*, 3062.
- (171) Selvaraj, P. C.; Mahadevan, V. *J. Polym. Sci. A: Polym. Chem.* **1997**, *35*, 105.
- (172) Knapen, J. W. J.; van der Made, A. W.; de Wilde, J. C.; van Leeuwen, P. W. N. M.; Wijkens, P.; Grove, D. M.; van Koten, G. *Nature* **1994**, *372*, 659.
- (173) Seeback, D.; Marti, R. E.; Hintermann, T. *Helv. Chim. Acta.* **1996**, *79*, 1710.
- (174) Miedaner, A.; Curtis, C. J.; Barkley, R. M.; DuBois, D. L. *Inorg. Chem.* **1994**, *33*, 5482.
- (175) Reetz, M. T.; Lohmer, G.; Schwickardi, R. *Angew. Chem. Int. Ed. Engl.* **1997**, *36*, 1526.
- (176) Kobayashi, S.; Nagayama, S. *J. Am. Chem. Soc.* **1998**, *120*, 2985.
- (177) Thayer, A. M. In *Chem. Eng. News*; 1995; pp 15.
- (178) Hamielec, A. E.; Soares, J. P. *Prog. Polym. Sci.* **1996**, *21*, 651.
- (179) Kaminsky, W. *Macromol. Chem. Phys.* **1996**, *197*, 3907.
- (180) For a more recent example, see: Sun, L.; Hsu, C. C.; Bacon, D. W. *J. Polym. Sci. Polym. Chem.* **1994**, *32*, 2127.
- (181) Jüngling, S.; Koltzenburg, S.; Mülhaupt, R. *J. Polym. Sci. Polym. Chem.* **1997**, *35*, 1.
- (182) Soga, K.; Arai, T.; Hoang, B. T.; Uozumi, T. *Macromol. Rapid Commun.* **1995**, *16*, 905.
- (183) Arai, T.; Ban, H. T.; Uozumi, T.; Soga, K. *J. Polym. Sci. Polym. Chem.* **1998**, *36*, 412.

- (184) Antonietti, M.; Göltner, C. *Angew. Chem. Int. Ed. Engl.* **1997**, *36*, 911.
- (185) Antonietti, M.; Heinz, S.; Schimdt, M.; Rosenauer, C. *Macromolecules* **1994**, *27*, 3276.
- (186) Tao, J.; Stewart, S.; Liu, G.; Yang, M. *Macromolecules* **1997**, *30*, 2738.
- (187) Zhang, L.; Eisenberg, A. *Science* **1995**, *268*, 1728.
- (188) Ding, J.; Liu, G. *Macromolecules* **1997**, *30*, 655.
- (189) Liu and co-workers previously reported that star polymers and nanospheres could be obtained from the same block copolymer system by crosslinking the poly(2-cinnamoyl ethyl methacrylate) core with UV light. See: Guo, A.; Liu, G.; Tao, J. *Macromolecules*, **1996**, *29*, 2487.
- (190) Wooley, K. L. *Chem. Eur. J.* **1997**, *3*, 1397.
- (191) Thurmond II, K. B.; Kowalewski, H. T.; Wooley, K. L. *J. Am. Chem. Soc.* **1996**, *118*, 7239.
- (192) Thurmond II, K. B.; Kowalewski, H. T.; Wooley, K. L. *J. Am. Chem. Soc.* **1997**, *119*, 6656.
- (193) Klingelhöfer, S.; Heitz, W.; Greiner, A.; Oestreich, S.; Förster, S.; Antonietti, M. *J. Am. Chem. Soc.* **1997**, *119*, 10116.
- (194) Antonietti, M.; Weinz, E.; Bronstein, L.; Seregina, M. *Adv. Mater.* **1995**, *7*, 1000.
- (195) Serigina, M.; Bronstein, L.; Platonova, O. A.; Chernyshov, D. M.; Valetsky, P. M.; Weinz, E.; Hartmann, J.; Antonietti, M. *Chem. Mater.* **1997**, *9*, 923.
- (196) Jenekhe, S.; Chen, X. L. *Science* **1998**, *279*, 1903.
- (197) Zurer, P. *Chem. Eng. News* **1998**, *76*, 8.
- (198) Massey, J. A.; Power, K. N.; Manners, I.; Winnik, M. A. *J. Am. Chem. Soc.* **1998**,
- Manuscript accepted for publication.

## Chapter 2 The Synthesis and Polymerization Behaviour of Silicon-Bridged [1]- and [2]Ferrocenophanes with Sterically Demanding Trimethylsilyl Substituents Attached to the Cyclopentadienyl Rings

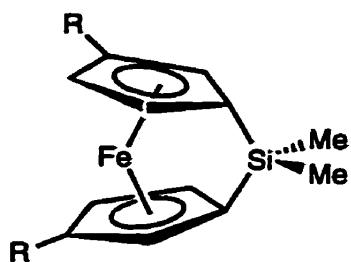
### 2.1 Abstract

The silicon-bridged [1]ferrocenophane  $\text{Fe}(\eta\text{-C}_5\text{H}_3\text{SiMe}_3)_2(\text{SiMe}_2)$  (**5**) was synthesized via the reaction of  $\text{Li}_2[\text{Fe}(\eta\text{-C}_5\text{H}_3\text{SiMe}_3)_2] \cdot \text{TMEDA}$  (TMEDA = tetramethylethylenediamine) with  $\text{Me}_2\text{SiCl}_2$  in hexanes. The disilane-bridged [2]ferrocenophane  $\text{Fe}(\eta\text{-C}_5\text{H}_3\text{SiMe}_3)_2(\text{Si}_2\text{Me}_4)$  (**7**) was prepared using a similar route from the disilane  $\text{ClMe}_2\text{SiSiMe}_2\text{Cl}$ . Despite the presence of sterically demanding  $\text{SiMe}_3$  substituents on the cyclopentadienyl rings, compound **5** was found to undergo thermal ring-opening polymerization at 170 °C to produce very soluble, high molecular weight poly(ferrocenylsilane), **6** with  $M_w = 1.4 \times 10^5$ ,  $M_n = 8.4 \times 10^4$ . However, the [2]ferrocenophane **7** was found to be resistant to thermal ring-opening polymerization even at 350 °C and decomposed above 380 °C. A single crystal X-ray diffraction study of **7** revealed that the steric interactions between the bulky  $\text{SiMe}_3$  groups are relieved by a significant twisting of the disilane bridge with respect to the plane defined by the centroids of the cyclopentadienyl ligands and the metal atom. The angle between the planes of the cyclopentadienyl rings in **7** was found to be  $5.4(6)^\circ$ , slightly greater than that in the non-silylated analogue  $\text{Fe}(\eta\text{-C}_5\text{H}_4)_2(\text{Si}_2\text{Me}_4)$  (**4a**) ( $4.19(2)^\circ$ ), and dramatically less than the corresponding tilt-angle of the strained, polymerizable silicon-bridged, [1]ferrocenophane  $\text{Fe}(\eta\text{-C}_5\text{H}_4)_2(\text{SiMe}_2)$  (**1**) ( $20.8(5)^\circ$ ). The length of the Si-Si bond in **7** ( $2.342(3)\text{Å}$ ) was found to be close to the sum of the covalent radii ( $2.34\text{ Å}$ ). Crystals of **7** are monoclinic, space group  $C2/c$ , with  $a = 23.689(3)\text{ Å}$ ,  $b = 11.174(1)\text{ Å}$ ,  $c = 31.027(3)\text{ Å}$ ,  $\beta = 109.16(1)^\circ$ ,  $V = 7758(2)\text{Å}^3$ , and  $Z = 12$ .

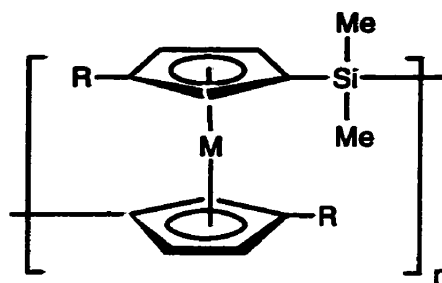
## 2.2 Introduction

High polymers in which transition metals are incorporated directly into the main chain are attractive synthetic targets due to their unusual physical and chemical properties. Such materials are expected to possess an interesting and potentially useful range of electronic, magnetic and optical characteristics which are not readily achieved using traditional organic polymers.<sup>1-4</sup> However, for the most part, progress in this area has been limited by the synthetic challenge of obtaining high molecular weight, well-defined polymers.<sup>4</sup>

In 1992, we reported the synthesis of soluble, high molecular weight poly(ferrocenylsilanes) (**2**) via the thermal ring-opening polymerization (ROP) of silicon-bridged, [1]ferrocenophanes (**1**).<sup>5</sup> More recently, we have demonstrated that living ROP can also be achieved in solution at room temperature in the presence of anionic initiators.<sup>6</sup> This has provided access to poly(ferrocenylsilanes) with controlled molecular weights as well as block copolymers.<sup>7</sup> In addition, random copolymers are accessible via thermal copolymerization of different monomers.<sup>8</sup> We have also shown that ROP is catalyzed in solution by certain transition metal complexes<sup>9</sup> and that the ROP route can be extended to other strained [n]metallocenophanes; thus, polymers such as poly(ferrocenylgermanes) and poly(ferrocenylethylenes) have been prepared from germanium-bridged [1]ferrocenophanes and hydrocarbon-bridged [2]ferrocenophanes, respectively.<sup>10-17</sup> Crystallographic studies have revealed that these polymerizable monomers possess ring-tilted structures in which the planes of the cyclopentadienyl ligands are tilted by angles of up to 31°. <sup>17</sup> By contrast, in ferrocene the cyclopentadienyl rings are planar. The apparent strain in these highly ring-tilted molecules is believed to provide the driving force for their facile thermal ROP.

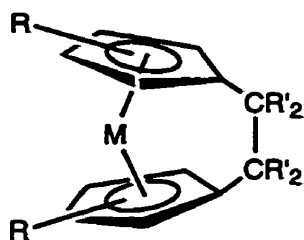


**1a** R = H  
**1b** R = SiMe<sub>3</sub>

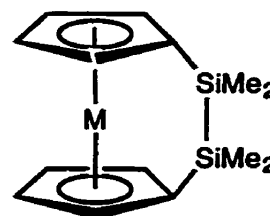


**2a** R = H  
**2b** R = SiMe<sub>3</sub>

Although the ROP strategy has been successfully applied to [2]metallocenophanes with a hydrocarbon-bridge (**3a - c**), the analogues **4a** and **4b** with a disilane-bridge possess only modest tilt angles (**4a** 4.19(2)<sup>o</sup> **4b** 7.8(5)<sup>o</sup>) and are resistant to ROP, presumably as a result of their significantly less strained structures.<sup>13,18</sup>



**3a** M = Fe, R = H, R' = H  
**3b** M = Fe, R = Me, R' = H  
**3c** M = Ru, R = H, R' = H  
**3d** M = Fe, R = H, R' = Me



**4a** M = Fe  
**4b** M = Ru

The rationale behind the work in this chapter is described in the following lines. Firstly, it is known that the presence of sterically demanding substituents generally hinders the formation of high molecular weight polymers via ROP. For example, Rauchfuss and coworkers have reported that the desulfurization of [3]trithiaferrocenophanes with phosphines yields polymers with ferrocene and disulfido units in the backbone.<sup>19</sup> The molecular weights of the polymers formed when an *n*-butyl substituent is present on the cyclopentadienyl rings

( $M_n = \text{ca } 100,000$ ) are much higher than when bulkier *t*-butyl substituents are attached ( $M_n = \text{ca } 3,000$ ). It was therefore of interest to examine if significantly lower molecular weight products would be generated by the ROP of [1]ferrocenophanes incorporating bulky substituents. Isolation of low molecular weight poly(ferrocenylsilanes) would allow end-group analysis and might yield useful information on the thermal ROP mechanism. Secondly, we felt that polymerization of disilane-bridged [2]ferrocenophanes might even be facilitated if sterically-demanding substituents, such as trimethylsilyl groups, were present on the cyclopentadienyl rings. Thus, the preference for these bulky substituents to minimize steric interactions with one another might provide an additional driving force for ROP. Thirdly, we have previously shown that a trans zig-zag conformation is likely for the high polymer **2** in ordered regions in the solid state.<sup>20</sup> The presence of bulky trimethylsilyl substituents might be expected to impart unusual conformational properties to the macromolecules both in the solid state and solution which would influence the interactions between the transition metal centers which dominate the electrochemical behaviour.<sup>4</sup>

In this chapter, we describe our studies on the influence of trimethylsilyl groups on the thermal polymerization behaviour of silicon-bridged, [1]- and [2]ferrocenophanes.

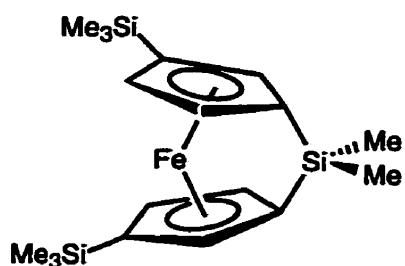
## 2.3 Results and Discussion

### 2.3.1 Synthesis of the Bis(trimethylsilyl)-Substituted, Silicon-Bridged [1]Ferrocenophane **5**.

The dilithiation of bis(trimethylsilyl)ferrocene has been previously shown to be regio- and stereoselective by Silver and coworkers.<sup>21</sup> Thus, reaction of this species with *n*-BuLi•TMEDA (TMEDA = tetramethylethylenediamine) followed by Ph<sub>2</sub>PCl yielded 1,1'-bis(diphenylphosphino)-3,3'-bis(trimethylsilyl)ferrocene. This regio- and stereoselectivity was

viewed to be attractive as the formation of more well-defined ferrocenophane monomers and corresponding polymers rather than mixtures of isomers would be anticipated.

The silicon-bridged [1]ferrocenophane **5** was prepared via the reaction of the dilithium salt  $\text{Li}_2[\text{Fe}(\eta\text{-C}_5\text{H}_3\text{SiMe}_3)_2]\cdot\text{TMEDA}$  with dichlorodimethylsilane.<sup>22</sup> The synthesis and isolation of the dilithium salt was achieved by reacting dilithioferrocene with 2 equivalents of chlorotrimethylsilane, purification of the bis(trimethylsilyl)ferrocene by vacuum distillation, deprotonation of the product with 2 equivalents of *n*-BuLi in the presence of TMEDA, followed by recrystallization from hexanes at  $-78\text{ }^\circ\text{C}$ . The final product (**5**) was purified by vacuum distillation ( $80\text{ }^\circ\text{C}$ ,  $0.005\text{ mmHg}$ ) as a red-orange liquid.



**5**

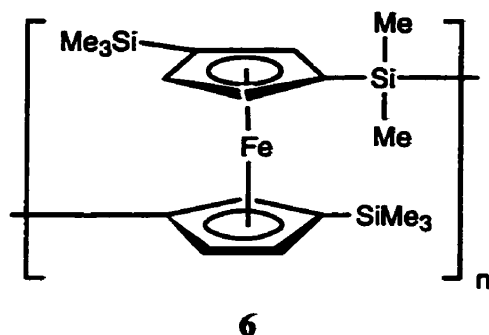
The purified silicon-bridged [1]ferrocenophane **5** was characterized by  $^1\text{H}$ ,  $^{13}\text{C}$  and  $^{29}\text{Si}$  NMR as well as mass spectrometry and the data were consistent with the assigned 1,1'-3,3'-substituted structure. In particular, the  $^{13}\text{C}$  NMR chemical shift of the ipso carbons of the cyclopentadienyl groups attached to the  $\text{SiMe}_2$  bridge ( $36.9\text{ ppm}$ ) showed the characteristic upfield shift compared to the other cyclopentadienyl carbons.<sup>22</sup> This upfield shift is a well-established trend for strained, ring-tilted main group element-bridged [1]ferrocenophanes and is probably indicative of increased  $\text{sp}^3$  character for the ipso carbon bonded to the bridging silicon in comparison with ipso carbons in unbridged, substituted ferrocenes.<sup>22,23</sup> Interestingly, all the other cyclopentadienyl  $^{13}\text{C}$  NMR resonances are located further downfield than the resonances reported for other symmetrically substituted, silicon-bridged



[1]ferrocenophanes (e.g. **1**). The  $^1\text{H}$  NMR revealed two pseudo quartets and a pseudo triplet in the cyclopentadienyl region, characteristic of an  $\text{A}_2\text{B}_2\text{C}_2$  spin system. The  $^{29}\text{Si}$  NMR spectrum of **5** showed two singlet resonances at - 3.3 and - 5.4 ppm of relative intensity 1 : 2 which were assigned to the  $\text{SiMe}_2$  bridge and the two equivalent trimethylsilyl groups, respectively. The mass spectrum of **5** showed a molecular ion at  $m/e$  386 as the most abundant peak.

### 2.3.2 Thermal ROP of the Bis(trimethylsilyl)-Substituted, Silicon-Bridged [1]Ferrocenophane **5**

When **5** was heated in an evacuated Pyrex tube for 3 h at 170 °C the tube contents became more viscous and then immobile. The poly(ferrocenylsilane) **6**, a red-orange powder, was isolated by dissolution in THF followed by precipitation into methanol. GPC analysis revealed that the polymer was of high molecular weight ( $M_w = 140\ 000$ ) with a relatively narrow weight distribution ( $M_w/M_n = 1.7$ ). The results of multinuclear NMR studies were consistent with the

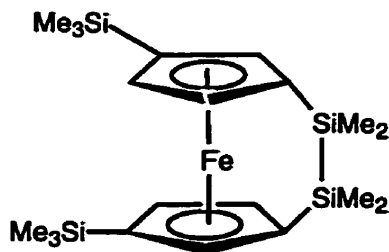


assigned structure. A single, broad  $^1\text{H}$  NMR resonance was found in the cyclopentadienyl region. In addition, broad resonances for the protons from the bridging  $\text{SiMe}_2$  and pendant  $\text{SiMe}_3$  groups were observed. The  $^{29}\text{Si}$  NMR spectrum for **6** revealed two broad resonances (-5.9 ppm,  $\text{SiMe}_2$ ; -2.5 ppm,  $\text{SiMe}_3$ ) that are found upfield with respect to the monomer **5**.

The  $^{13}\text{C}$  NMR resonance attributable to the ( $\text{C}_{\text{ipso}}\text{-SiMe}_2$ ) ipso carbons was shifted to a more conventional region associated with cyclopentadienyl carbons in unbridged, substituted ferrocenes compared to that in **5**. This indicated that the strain of the ring-tilted monomer **5** was relieved by ROP to yield polymer **6** in which the cyclopentadienyl ligands were approximately parallel. The polymer formed air-stable, amber, free-standing, brittle films which were cast from a solution of **6** in toluene via slow solvent evaporation. The polymer was shown to be extremely soluble, even in non-polar solvents such as hexanes.

### 2.3.3 Synthesis of the Bis(trimethylsilyl)-Substituted, Disilane-Bridged [2]Ferrocenophane **7**

The disilane-bridged [2]ferrocenophane **7** was synthesized in a similar manner to the [1]ferrocenophane **5** by employing 1,2-dichloro-1,1,2,2-tetramethyldisilane in the place of dichlorodimethylsilane. Compound **7** was isolated by vacuum distillation (120 °C, 0.05 mmHg) as reddish-orange crystals of low melting point. Multinuclear NMR studies were



**7**

consistent with the assigned structure. The  $^{29}\text{Si}$  NMR spectrum revealed two resonances: one corresponding to the  $\text{SiMe}_3$  substituents (- 9.7 ppm) and the other to the bridging  $\text{SiMe}_2$  groups (- 4.0 ppm). In sharp contrast to **5**, the  $^{13}\text{C}$  NMR resonances associated with the cyclopentadienyl carbons bonded to the bridging disilane unit occur at 76.0 ppm. This is

consistent with a much less tilted and strained structure for **7** in comparison to **5**. One interesting feature of the  $^1\text{H}$  NMR of **7** was the presence of *three* resonances in the region for methyl groups bonded to silicon. The resonance at 0.28 ppm (singlet, 18 H) was attributed to the protons in the two  $\text{SiMe}_3$  groups. The other two resonances (multiplets at 0.45 ppm and 0.25 ppm, 6 H for each) were assigned to inequivalent methyl groups bonded to the bridging silicons. In addition, two resonances were detected in the methyl region of the  $^{13}\text{C}$  NMR spectrum of **7**. This situation was in contrast with that for the [1]ferrocenophane **5** in which the methyl substituents at the bridging silicon atom were found to be equivalent. In order to examine in detail the effects the bulky  $\text{SiMe}_3$  groups would have on the structure of the disilane-bridged [2]ferrocenophane **4a**,<sup>13</sup> compound **7** was studied by single crystal X-ray diffraction.

#### 2.3.4 X-ray Structure of **7**

Reddish-orange, X-ray diffraction quality crystals of **7** were isolated from a vacuum distillation. Figure 2.1 shows two alternative views of **7** (molecule B).

A summary of cell constants and data collection parameters is included in Table 2.1 and the fractional coordinates and important bond lengths and angles are listed in Tables 2.2 and 2.3.

A summary of important structural features is presented in Table 2.4.

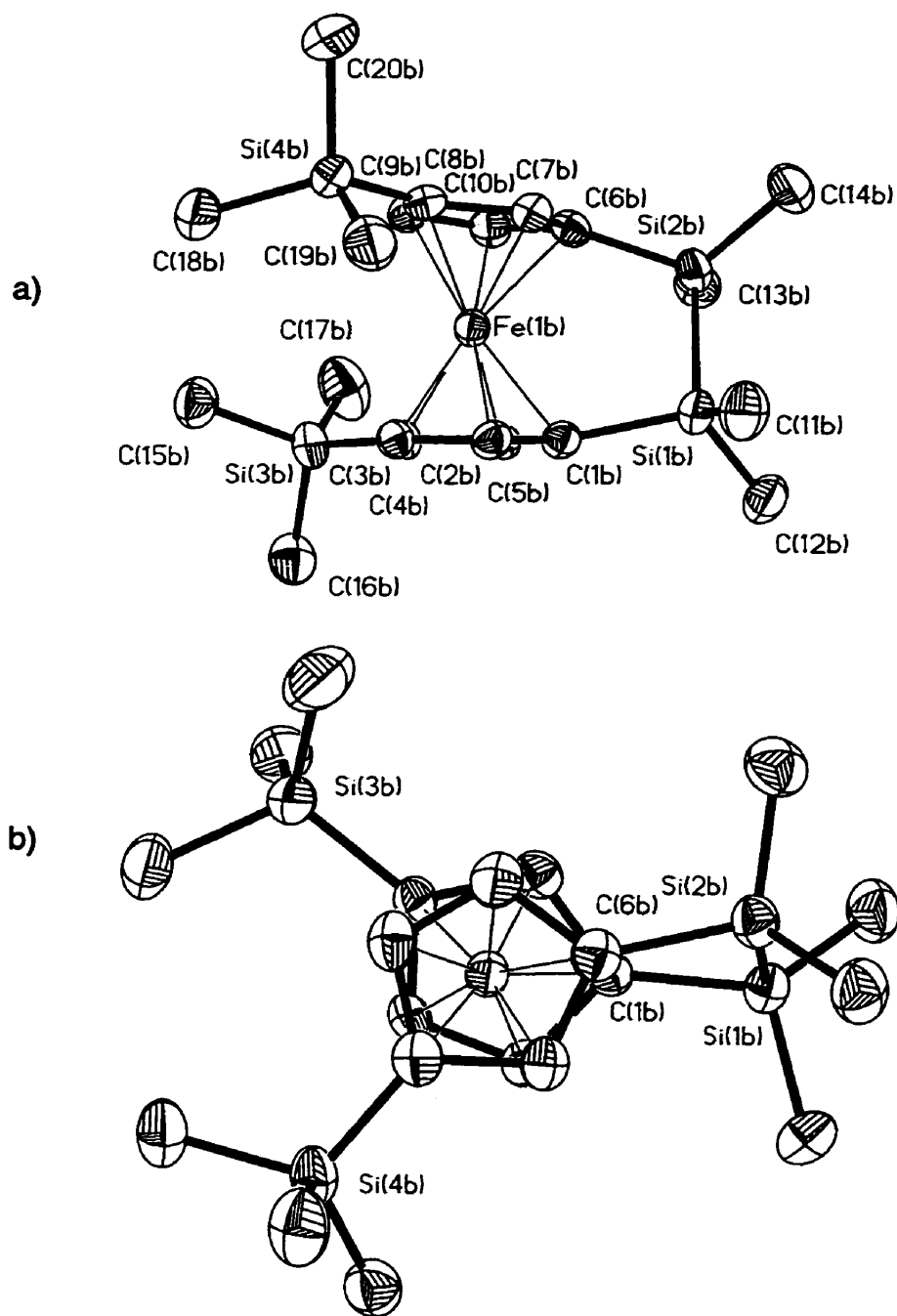


Figure 2.1 (a) Molecular Structure of 7 (molecule B) (vibrational ellipsoids at the 25 % probability level). (b) Alternate view of 7 (vibrational ellipsoids at the 25 % probability level).

Table 2.1 Summary of Crystal Data and Intensity Collection Parameters for 7

empirical formula	$C_{20}H_{36}FeSi_4$
$M_r$	444.7
cryst class	monoclinic
space group	$C2/c$
$a$ , Å	23.689(3)
$b$ , Å	11.174(1)
$c$ , Å	31.027(3)
$\beta$ , deg	109.16(1)
$V$ , Å <sup>3</sup>	7758(2)
$Z$	12
$D_{calc}$ , g cm <sup>-3</sup>	1.142
$\mu(Mo, K\alpha)$ , cm <sup>-1</sup>	7.71
$F(000)$	2856
$\omega$ -scan width, deg	$0.37 + 0.68 \tan \theta$
range $2\theta$ collcd, deg	4.1 to 52.0
total no. of rflns	8246
no. of unique rflns	7605
$R_{int}$	0.024
no. of obsd data used [ $I > 3 \sigma(I)$ ]	2694
weighting $g$	0.0006
$R$	0.0399
$R_w$	0.0460
GOF	1.17

Table 2.2 Final Fractional Atomic Coordinates ( $\times 10^4$ ) and Equivalent Isotropic Displacement Coefficients ( $\text{\AA}^2 \times 10^3$ ) for the Non-Hydrogen Atoms of 7

	x	y	z	U (eq) <sup>a</sup>
Fe(1A)	0.5000	0.1079(1)	0.2500	0.046(1)
Si(1A)	0.5498(1)	-0.1688(1)	0.2737(1)	0.054(1)
Si(2A)	0.5099(1)	0.2970(2)	0.3442(1)	0.082(1)
C(1A)	0.5625(2)	-0.0073(5)	0.2910(2)	0.053(3)
C(2A)	0.5314(2)	0.0552(5)	0.3168(2)	0.057(3)
C(3A)	0.5391(3)	0.1819(5)	0.3140(2)	0.060(3)
C(4A)	0.5762(2)	0.1962(5)	0.2858(2)	0.064(3)
C(5A)	0.5900(2)	0.0826(5)	0.2723(2)	0.057(3)
C(6A)	0.5642(3)	-0.2617(5)	0.3264(2)	0.080(3)
C(7A)	0.6010(3)	-0.2142(5)	0.2419(2)	0.079(3)
C(8A)	0.4452(3)	0.2366(6)	0.3580(3)	0.116(4)
C(9A)	0.4855(4)	0.4332(5)	0.3093(3)	0.126(5)
C(10A)	0.5722(3)	0.3342(7)	0.3972(2)	0.129(5)
Fe(1B)	0.1769(0)	0.1682(1)	0.0961(0)	0.055(1)
Si(1B)	0.2136(1)	-0.1140(2)	0.0926(1)	0.070(1)
Si(2B)	0.2560(1)	0.0040(2)	0.0486(1)	0.074(1)
Si(3B)	0.0230(1)	0.2458(2)	0.0559(1)	0.077(1)
Si(4B)	0.2518(1)	0.3942(2)	0.1732(1)	0.078(1)
C(1B)	0.1574(3)	-0.0087(5)	0.1015(2)	0.057(3)
C(2B)	0.1098(3)	0.0504(5)	0.0672(2)	0.062(3)
C(3B)	0.0867(3)	0.1484(5)	0.0860(2)	0.061(3)
C(4B)	0.1206(3)	0.1479(5)	0.1334(2)	0.060(3)
C(5B)	0.1632(3)	0.0538(5)	0.1432(2)	0.059(3)
C(6B)	0.2441(3)	0.1576(6)	0.0684(2)	0.065(3)
C(7B)	0.2664(3)	0.1979(6)	0.1144(2)	0.068(3)
C(8B)	0.2371(3)	0.3071(6)	0.1201(2)	0.071(3)
C(9B)	0.1957(3)	0.3327(6)	0.0752(3)	0.075(3)
C(10B)	0.2003(3)	0.2433(6)	0.0443(2)	0.075(3)

C(11B)	0.2678(3)	-0.1509(6)	0.1498(2)	0.099(4)
C(12B)	0.1779(3)	-0.2555(5)	0.0655(2)	0.098(4)
C(13B)	0.2129(3)	-0.0098(7)	-0.0137(2)	0.101(4)
C(14B)	0.3375(3)	-0.0222(6)	0.0593(3)	0.104(4)
C(15B)	0.0268(3)	0.3873(6)	0.0869(3)	0.107(4)
C(16B)	-0.0471(3)	0.1670(6)	0.0540(2)	0.106(5)
C(17B)	0.0219(3)	0.2753(8)	-0.0019(2)	0.152(5)
C(18B)	0.1872(3)	0.4911(6)	0.1706(3)	0.103(4)
C(19B)	0.2681(3)	0.2917(6)	0.2226(2)	0.096(4)
C(20B)	0.3178(3)	0.4922(6)	0.1793(3)	0.120(4)

<sup>a</sup> Equivalent isotropic U defined as one third of the trace of the orthogonalized  $U_{ij}$  tensor

Table 2.3 Selected Bond Lengths (Å) for 7 (Molecule B)

(Estimated Standard Deviations (Esd's) Are in Parentheses)

Fe(1A)-C(3A)	2.069(5)	Fe(1A)-C(2A)	2.045(5)
Fe(1A)-C(1A)	2.057(5)	Fe(1A)-C(5A)	2.033(5)
Fe(1A)-C(4A)	2.037(5)	Fe(1A)-C(3C)	2.069(5)
Fe(1A)-C(2C)	2.045(5)	Fe(1A)-C(1C)	2.057(5)
Fe(1A)-C(5C)	2.033(5)	Fe(1A)-C(4C)	2.037(5)
Si(1A)-C(1A)	1.878(6)	Si(1A)-C(6A)	1.872(6)
Si(1A)-C(7A)	1.868(7)	Si(1A)-Si(1C)	2.334(3)
Si(2A)-C(3A)	1.853(7)	Si(2A)-C(8A)	1.849(8)
Si(2A)-C(9A)	1.847(7)	Si(2A)-C(10A)	1.860(6)
C(3A)-C(2A)	1.434(8)	C(3A)-C(4A)	1.438(10)
C(2A)-C(1A)	1.434(9)	C(1A)-C(5A)	1.420(9)
C(5A)-C(4A)	1.409(8)	Fe(1B)-C(1B)	2.050(6)
Fe(1B)-C(2B)	2.034(6)	Fe(1B)-C(3B)	2.068(6)
Fe(1B)-C(4B)	2.046(7)	Fe(1B)-C(5B)	2.047(6)
Fe(1B)-C(6B)	2.046(8)	Fe(1B)-C(7B)	2.034(6)

Fe(1B)-C(8B)	2.072(6)	Fe(1B)-C(9B)	2.046(7)
Fe(1B)-C(10B)	2.050(8)	Si(1B)-Si(2B)	2.349(3)
Si(1B)-C(1B)	1.863(7)	Si(1B)-C(11B)	1.862(6)
Si(1B)-C(12B)	1.860(6)	Si(1B)-C(6B)	1.876(7)
Si(2B)-C(13B)	1.873(6)	Si(2B)-C(14B)	1.870(6)
Si(3B)-C(3B)	1.846(6)	Si(3B)-C(15B)	1.838(7)
Si(3B)-C(16B)	1.863(7)	Si(3B)-C(17B)	1.815(8)
Si(4B)-C(8B)	1.846(7)	Si(4B)-C(18B)	1.855(7)
Si(4B)-C(19B)	1.849(7)	Si(4B)-C(20B)	1.866(7)
C(1B)-C(2B)	1.434(7)	C(1B)-C(5B)	1.436(9)
C(2B)-C(3B)	1.429(9)	C(3B)-C(4B)	1.427(8)
C(4B)-C(5B)	1.421(8)	C(6B)-C(7B)	1.422(9)
C(6B)-C(10B)	1.438(9)	C(7B)-C(8B)	1.443(9)
C(8B)-C(9B)	1.445(9)	C(9B)-C(10B)	1.405(10)

---



**Table 2.4 Selected Bond Angles (°) for 7 (Molecule B)  
(Estimated Standard Deviations (Esd's) Are in Parentheses)**

C(1A)-Si(1A)-C(7)	109.9(3)	C(1A)-Si(1A)-C(6A)	108.5(3)
C(1A)-Si(1A)-Si(1C)	102.4(2)	C(6A)-Si(1A)-C(7A)	110.3(3)
C(7A)-Si(1A)-Si(1C)	111.3(2)	C(6A)-Si(1A)-Si(1C)	114.1(2)
C(3A)-Si(2A)-C(9A)	111.9(3)	C(3A)-Si(2A)-C(8A)	109.7(3)
C(3A)-Si(2A)-C(10A)	106.4(3)	C(3A)-Si(2A)-C(9A)	108.2(4)
C(9A)-Si(2A)-C(10A)	109.8(3)	C(8A)-Si(2A)-C(10A)	110.8(4)
C(9A)-Si(2A)-C(10A)	112.6(2)	Si(2B)-Si(1B)-C(1B)	101.2(2)
Si(2B)-Si(1B)-C(11B)	115.6(3)	C(1B)-Si(1B)-C(11B)	107.6(3)
Si(2B)-Si(1B)-C(12B)	108.2(3)	C(1B)-Si(1B)-C(12B)	111.3(3)
C(11B)-Si(1B)-Si(12B)	111.2(2)	Si(1B)-Si(2B)-C(6B)	100.6(3)
Si(1B)-Si(2B)-C(13B)	115.0(3)	C(6B)-Si(2B)-C(13B)	108.9(3)
Si(1B)-Si(2B)-C(14B)	110.6(3)	C(6B)-Si(2B)-C(14B)	110.0(3)
C(13B)-Si(2B)-C(14B)	108.0(3)	C(3B)-Si(3B)-C(15B)	110.6(3)
C(3B)-Si(3B)-C(16B)	110.5(4)	C(15B)-Si(3B)-C(16B)	108.2(3)
C(3B)-Si(3B)-C(17B)	109.4(3)	C(15B)-Si(3B)-C(17B)	110.1(4)
C(16B)-Si(3B)-C(17B)	109.9(3)	C(8B)-Si(4B)-C(18B)	110.9(3)
C(8B)-Si(4B)-C(19B)	107.8(4)	C(18B)-Si(4B)-C(19B)	110.1(4)
C(8B)-Si(4B)-C(20B)	109.9(3)	C(18B)-Si(4B)-C(20B)	108.3(3)
C(19B)-Si(4B)-C(20B)	127.2(4)	Si(1B)-C(1B)-C(2B)	127.4(5)
Si(3B)-C(3B)-C(2B)	127.8(5)	Si(1B)-C(1B)-C(5B)	125.3(4)
Si(4B)-C(8B)-C(7B)	126.7(5)	Si(4B)-C(8B)-C(9B)	128.8(5)

Table 2.5 Selected Structural Data for [1]- and [2]Metallocenophanes

	<b>1</b>	<b>3d</b>	<b>4a</b>	<b>7<sup>d</sup></b>	<b>4b</b>
Si-Si distance Å			2.3535(9)	2.334(3) 2.349(3)	2.370(2)
M displacement, <sup>a</sup> Å	0.2164(11)	0.432(12)	0.027(3)	0.069(5) 0.071(5)	0.092(6)
ring tilt, $\alpha$ , deg	20.8(5)	23(1)	4.19(2)	4.8(6) 5.9(6)	7.8(5)
$\beta$ , <sup>b</sup> deg	37.0(6)	10.8(10)	10.8(3)	12.7(4) 12.0(4) 12.6(4)	12.4(3)
twist, <sup>c</sup> deg		8.9(13)	8.4(4)	18.3(8) 22.9(8)	0.2(5)
Cp-Fe-Cp, $\delta$ , deg	167.74(8)	163.4(6)	176.48(3)	175.2(3) 175.1(3)	174.2(2)
ref.	13	24	13	this work	18

<sup>a</sup>The displacement of the metal atom from the line joining the two centroids of the cyclopentadienyl rings. <sup>b</sup>The angle(s) between the planes of the cyclopentadienyl ligands and the C(Cp)-E bonds (where E = bridging atom). <sup>c</sup>The angle(s) between the plane defined by the centroids of the cyclopentadienyl ligands and the metal atom and the E-E bond (where E = bridging atom). <sup>d</sup>The first line represents the value for molecule A and the second line is for molecule B.

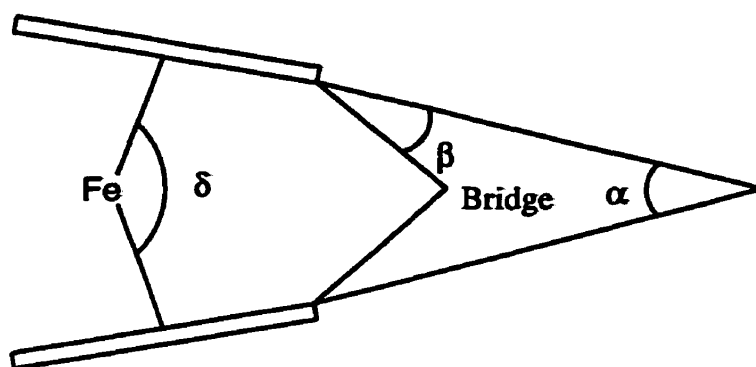


Figure 2.2 Distortions in [1]Ferrocenophanes

Compound **7** crystallizes in space group  $C2/c$  with  $Z = 12$ . Hence there are two independent molecules in the structure. One of these molecules (molecule A) has two-fold crystallographic symmetry with the Fe atom on a special position. The presence of a  $C2$  axis leads to the inequivalent methyl groups on the bridging silicon atoms. All bond lengths and angles quoted within the text for **7** are for molecule B. Molecules A and B were not found to possess significantly different geometrical parameters with the exception of the C(ipso)-Si-Si-C(ipso) torsion angle.

A comparison of the structural features of **7** with those of the strained monomer **1**<sup>13</sup> and the relatively strain-free **4a**<sup>13</sup> is informative and suggests that **7** is relatively unstrained. The dihedral angle between the planes of the cyclopentadienyl rings is  $5.9(6)^\circ$ , only slightly greater than for **4a** ( $4.19(2)^\circ$ ) and is dramatically smaller than for **1** ( $20.8(5)^\circ$ ). Also, the angle  $\beta$  between the plane of the cyclopentadienyl rings and the bridging silicon-ipso carbon bond is  $12.6(4)^\circ$  compared to  $10.8(3)^\circ$  for **4a**. The corresponding value in **1** is much greater ( $37.0(6)^\circ$ ) and suggests significantly less strain in both **7** and **4a**. The twist angle for **7** ( $22.9(8)^\circ$ ) is significantly greater than in **4a** ( $8.4(4)^\circ$ ) and is attributable to the unfavourable steric interactions between the two  $\text{SiMe}_3$  groups. The twist angle for **4a** is comparable to the corresponding angle in **3d**<sup>24</sup> ( $8.9(13)^\circ$ ) whereas virtually no twisting occurs with the disilane-

bridged [2]ruthenocenophane **4b**<sup>18</sup> (0.2(5)°). The twisting of the bridge in **7** as well as the bulkiness of the SiMe<sub>3</sub> groups, also results in a significantly increased staggering of the cyclopentadienyl rings such that the stagger angle of 17.7(8)° is much greater than those found in either **4a** (6.0(1)°) or **4b** (rings are virtually eclipsed, 0.6(7)°). The larger Ru atom of **4b** leads to an elongated Si-Si bond (2.370(2)Å) in comparison to **7** in which the Si-Si bond length (2.349(3) Å) is similar to that found for **4a** (2.3535(9)Å) and close to the average for a typical Si-Si bond length (2.34 Å).

### 2.3.5 Thermal Polymerization Behaviour of the Bis(trimethylsilyl)-substituted, Disilane-Bridged [2]Ferrocenophane **7**

In contrast to the [1]ferrocenophane **5**, when the [2]ferrocenophane **7** was heated in a sealed, evacuated tube at 350 °C for 24 h, no increase in melt viscosity was observed. Furthermore, analysis of the contents of the tube by <sup>1</sup>H NMR revealed only the presence of **7** and no high molecular weight material ( $M_w > 1000$ ) was detected by GPC. Similarly, a sample of compound **7** was heated from 380 to 420 °C over a span of about two hours and another sample heated at about 160 °C over a span of 20 h in the presence of the anionic initiator, potassium trimethylsilanoate, K[OSiMe<sub>3</sub>].<sup>25</sup> In both cases, no oligomeric or polymeric material could be detected by either GPC or mass spectrometry. <sup>1</sup>H NMR for the sample heated in the presence of K[OSiMe<sub>3</sub>] revealed only the presence of unreacted **7** whereas <sup>1</sup>H NMR of the sample heated over the range of 380 to 420 °C showed both the presence of unreacted **7** and very broad resonances in both the cyclopentadienyl region and the SiMe region which were assigned to unidentified decomposition products.

## 2.4 Summary

The introduction of sterically-demanding trimethylsilyl substituents to the cyclopentadienyl rings does not significantly affect the polymerizability of silicon-bridged [1]ferrocenophanes. A high molecular weight poly(ferrocenylsilane) was still formed via the ROP of **5** at elevated temperatures. The presence of these bulky ligands has some significant effects on the structure of disilane-bridged [2]ferrocenophane with an increase in both the tilt-angle and the degree of twisting of the disilane bridge. However, these distortions were found to be insufficient to allow ROP, and **7** was found to be stable to 380 °C.

We are now studying the properties of the poly(ferrocenylsilane) **6** and related polymers with bulky side groups in detail. Our results will be reported in the near future.

## 2.5 Experimental Section

All chemicals unless otherwise noted were purchased from Aldrich Chemicals Co. 1,2-dichloro-1,1,2,2,-tetramethyldisilane<sup>26</sup> and dilithioferrocene<sup>27</sup> were synthesized using literature methods. All silanes were distilled and stored under nitrogen. Ferrocene was purified via Soxhlet extraction using hexanes. All syntheses were carried out under an atmosphere of prepurified nitrogen using either standard Schlenk techniques or an inert-atmosphere drybox (Vacuum Atmospheres). Solvents used in these syntheses were dried by standard methods, distilled and stored under nitrogen.

200 or 400 MHz <sup>1</sup>H NMR spectra were recorded on a Varian Gemini 200 and a Varian XL 400 spectrometer respectively. 100.5 MHz <sup>13</sup>C NMR and 79.5 MHz <sup>29</sup>Si NMR were recorded on the Varian XL 400 spectrometer. The <sup>29</sup>Si NMR data were acquired in a proton-decoupled mode using a DEPT pulse sequence with <sup>2</sup>J<sub>Si-H</sub> = 6.7 Hz. The <sup>13</sup>C NMR data were acquired in a proton decoupled mode using an APT pulse sequence. Mass spectra were obtained with the use of a VG 70-250S mass spectrometer operating in an electron impact (EI)

mode. Elemental analyses were performed by the Canadian Microanalytical Service Ltd., Delta, B.C., Canada.

Molecular weights were estimated by gel permeation chromatography (GPC) using a Water Associates liquid chromatograph equipped with a 510 HPLC pump, U6K injector, ultrastyrigel columns with a pore size between  $10^3$  to  $10^5$  Angstroms, and a Waters 410 differential refractometer. A flow rate of 1.0 mL/min was used and samples were dissolved in a solution of 0.1 % tetra-*n*-butylammonium bromide in THF. Polystyrene standards were used for calibration purposes.

**Synthesis of Dilithio-1,1'-bis(trimethylsilyl)ferrocene•TMEDA.** The synthesis of dilithio-1,1'-bis(trimethylsilyl)ferrocene was a modification of a literature method.<sup>21,28</sup>

Dilithioferrocene•TMEDA (25.0 g, 79.6 mmol) was suspended in 180 ml of freshly distilled diethyl ether. Chlorotrimethylsilane (20.1 ml, 159.2 mmol) was added dropwise to the above solution with stirring at 0 °C using an ice-water bath. The reaction mixture was allowed to warm up to room temperature and stir overnight. Unreacted dilithioferrocene was separated from the reaction mixture by cannulation of the solution through a filter frit. The solvent was removed under high vacuum before subliming to remove any ferrocene. The resultant bright red oil was further purified by distillation under high vacuum (80 °C, 0.05 mm Hg). Yield of 1, 1'-bis(trimethylsilyl)ferrocene: 19.8 g (75 %).

The distilled 1,1'-bis(trimethylsilyl)ferrocene was then dissolved in 100 mL of freshly distilled hexanes. Butyllithium in hexanes (75 mL, 181.2 mmol) and TMEDA (14.0 mL, 120 mmol) were added dropwise to the solution at room temperature with stirring. The solution was stir overnight. The product was precipitated from hexanes at -78 °C as a reddish-orange solid which was isolated by cannulation of the suspension onto a filter frit at -78 °C. Yield (based on 1,1'-bis(trimethylsilyl)ferrocene): 7.1 g (26 %).

**Synthesis of 1,1'-Bis(trimethylsilyl)ferrocenyldimethylsilane (5).** Dilithio-1,1'-bis(trimethylsilyl)ferrocene•TMEDA (2.00 g, 4.37 mmol) was suspended in 100 mL of freshly distilled hexanes and cooled down to -78 °C. To this stirred suspension was added 0.6 mL (4.95 mmol) of freshly distilled dichlorodimethylsilane. The mixture was allowed to warm up to room temperature and stir overnight. This solution was filtered through a filter frit and the solvent removed under high vacuum. The moisture sensitive product was then isolated as a red-orange liquid by high vacuum distillation (88 °C, 0.005 mmHg). Yield: 0.95 g (56 %). For **5**:  $^{29}\text{Si}$  NMR ( $\text{C}_6\text{D}_6$ )  $\delta = -3.3$  ppm (s, SiMe<sub>2</sub>, 1 Si), -5.4 ppm (s, SiMe<sub>3</sub>, 2 Si);  $^{13}\text{C}$  NMR ( $\text{C}_6\text{D}_6$ )  $\delta = 82.9$  ppm ( $\eta\text{-C}_5\text{H}_3$ ), 82.7 ppm ( $\eta\text{-C}_5\text{H}_3$ , C-SiMe<sub>3</sub>), 80.4 ppm ( $\eta\text{-C}_5\text{H}_3$ ), 77.4 ppm ( $\eta\text{-C}_5\text{H}_3$ ), 36.9 ppm ( $\eta\text{-C}_5\text{H}_3$ , C-Si), 0.34 ppm (-SiMe<sub>3</sub>), -3.0 ppm (-SiMe<sub>2</sub>) ppm;  $^1\text{H}$  NMR ( $\text{C}_6\text{D}_6$ )  $\delta = 4.39$  ppm (m, 2 H, Cp), 4.13 ppm (m, 2 H, Cp), 4.03 ppm (m, 2 H, Cp), 0.40 ppm (s, 6H, SiMe<sub>2</sub>), 0.24 ppm (s, 18 H, SiMe<sub>3</sub>); MS (EI, 70 eV) m/e (%) 386 (100, M<sup>+</sup>), 371 (26, M<sup>+</sup> - CH<sub>3</sub>), 357 (5, M<sup>+</sup> - CH<sub>3</sub>, - CH<sub>2</sub>);

**Thermal Ring-Opening Polymerization of 5** A 0.35 g (0.91 mmol) sample of **5** was sealed in an evacuated Pyrex glass tube and heated at 170 °C for 3 h. The resultant polymer **6** was dissolved in THF and precipitated dropwise into methanol. The polymer was isolated as a red-orange powder. Yield: 0.19 g (54%). For **6**:  $^{29}\text{Si}$  NMR ( $\text{C}_6\text{D}_6$ )  $\delta = -5.9$  ppm (br s, SiMe<sub>2</sub>, 1 Si), -2.5 ppm (s, SiMe<sub>3</sub>, 2 Si);  $^{13}\text{C}$  NMR ( $\text{C}_6\text{D}_6$ )  $\delta = 79.5$  ppm (Cp), 77.0 ppm (Cp), 76.2 (Cp), 76.2 ppm (br s, Cp, C-Si), 74.7 ppm (Cp), 1.1 ppm (-SiMe<sub>3</sub>), 0.25 ppm (-SiMe<sub>2</sub>);  $^1\text{H}$  NMR ( $\text{C}_6\text{D}_6$ )  $\delta = 4.30$  ppm (br s, 6 H, Cp), 0.75 ppm (br s, 6H, SiMe<sub>2</sub>), 0.32 ppm (br s, 18 H, SiMe<sub>3</sub>). Anal. Calcd: C 55.9, H 7.8, Found: C 55.2, H 7.6: GPC:  $M_w = 1.4 \times 10^5$ ,  $M_n = 8.4 \times 10^4$ , polydispersity ( $M_w/M_n$ ) = 1.7.

**Synthesis of 1,1'-Bis(trimethylsilyl)ferrocenyldi-(1,1,2,2)-tetramethyldisilane (7)** Dilithio-1,1'-bis(trimethylsilyl)ferrocene•TMEDA (1.65 g, 3.60 mmol) was dissolved in 80 mL of freshly distilled hexanes and cooled to -78°C in a dry ice acetone slurry. 1,2-

dichloro-1,1,2,2-tetramethyldisilane (0.7 mL, 3.74 mmol) was added dropwise with stirring. The reaction mixture was allowed to warm up to room temperature and stir overnight. The solution was then filtered through a filter frit and the solvent removed under high vacuum. The product **7** was isolated as a red-orange liquid by high vacuum distillation (120 °C, 0.05 mm Hg). Yield: 0.75 g (47 %). For **7**:  $^{29}\text{Si}$  NMR ( $\text{CDCl}_3$ )  $\delta = -4.0$  ppm ( $\text{SiMe}_2$ ),  $-9.7$  ppm ( $\text{SiMe}_3$ );  $^{13}\text{C}$  NMR ( $\text{CDCl}_3$ )  $\delta = 78.3$  ppm (Cp),  $77.4$  ppm (Cp),  $76.8$  ppm (ipso C,  $-\text{SiMe}_3$ ),  $76.0$  ppm (ipso C,  $-\text{SiMe}_2-$ ),  $75.4$  (Cp)  $0.1$  ( $\text{SiMe}_3$ ),  $-0.1$  ( $\text{SiMe}_2$ ),  $-3.8$  ( $\text{SiMe}_2$ ) ppm;  $^1\text{H}$  NMR ( $\text{CDCl}_3$ )  $\delta = 4.6$  ppm (m, 2H, Cp),  $4.5$  ppm (m, 2H, Cp),  $4.0$  ppm (m, 2H, Cp),  $0.45$  ppm (s, 6H,  $-\text{SiMe}_2-$ ),  $0.28$  ppm (s, 18 H,  $\text{SiMe}_3-$ ),  $0.25$  ppm (s, 6H,  $-\text{SiMe}_2-$ ); MS (EI, 70 eV)  $m/e$  (rel intensity) = 444 (100,  $\text{M}^+$ ), 429 (18,  $\text{M}^+ - \text{Me}$ ), 386 (6,  $\text{M}^+ - \text{SiMe}_2$ ), 371 (15,  $\text{M}^+ - \text{SiMe}_3$ ). Anal. Calcd: C, 54.1; H, 8.1; Found: C, 53.8; H, 8.2.

**Attempted Thermal ROP of 7** A 0.10 g (0.22 mmol) sample of **7** was sealed in an evacuated Pyrex glass tube and heated at 350 °C for 24 hours. A second sample (0.22 g, 0.50 mmol) was sealed in an evacuated Pyrex glass tube and heated at (i) 380 °C for 30 minutes, (ii) 390 °C for 30 minutes, (iii) 400 °C for 30 minutes, (iv) 410 °C for 30 minutes and (v) 420 °C for 30 minutes. A third sample (0.30 g, 0.68 mmol) was sealed in an evacuated Pyrex glass tube in the presence of a trace amount of  $\text{K}[\text{OSiMe}_3]$  and heated at 140 °C for 2 hours and 160 °C for 14 hours and then at 180 °C for 2 hours. All samples were dissolved in THF and precipitated dropwise into methanol. Subsequent analysis of the first two samples revealed only **7** ( $^1\text{H}$  NMR) and small molecules (GPC). The third sample was a dark reddish-brown viscous liquid that was mostly soluble in THF (the insoluble product was a black precipitate). Analysis by  $^1\text{H}$  NMR showed only **7** and unidentified products (broad resonances from 4.0 to 4.4 ppm (cyclopentadienyl region) and 0.0 to 0.4 ppm (Si-Me region)). Analysis by GPC and mass spectrometry revealed only small molecules.



**X-ray Structure Determination Technique.** Intensity data were collected on an Enraf-Nonius CAD4 diffractometer at low temperature (185 K) using graphite monochromated Mo  $K\alpha$  radiation,  $\lambda = 0.71073 \text{ \AA}$ . The  $\omega$  scan technique was used with variable scan speeds. The intensities of three standard reflections which were measured every 2 h indicated no decay. The data were corrected for Lorentz and polarization effects and also for absorption (using psi-scan data). The structures were solved by direct methods.<sup>29</sup> Non-hydrogen atoms were refined with anisotropic thermal parameters by full-matrix least squares to minimize  $\sum w(F_o - F_c)^2$ , where  $w^{-1} = \sigma_2^2(F_o) + g(F_o)^2$ . The hydrogen atoms were included in calculated positions with C-H = 0.96  $\text{\AA}$ . Crystal data, data collection, and least squares parameters are listed in Table 1. All calculations were performed and structural diagrams created using SHELXTL PC<sup>29</sup> on a 486 personal computer.

## 2.6 References

- (1) (a) Pittman, C. U.; Carraher, C. E.; Reynolds, J. R. in *Encyclopedia of Polymer Science and Engineering*; Eds. Mark, H. F.; Bikales, N. M.; Overberger, C. G.; Menges, G.; Wiley: New York, 1989; Vol. 10; p. 541. (b) Sheats J. E.; Carraher, C. E.; Pittman, C. U.; Zeldin M., Currell B.; *Inorganic and Metal-Containing Polymeric Materials*; Plenum: New York, 1989. (c) Gonsalves K. E.; Rausch M. D. in *Inorganic and Organometallic Polymers. ACS Symposium Series 360*; Eds. Zeldin, M.; Wynne, K.; Allcock, H. R. American Chemical Society: Washington, DC. 1988. (d) Allcock, H. R. *Adv. Mater.*, **1994**, *6*, 106.
- (2) a) Fyfe, H. B.; Melkuz, M.; Zargarian, D.; Taylor, N. J.; Marder, T. B. *J. Chem. Soc., Chem. Commun.*, **1991**, 188. b) Wright, M. E.; Sigman, M. S. *Macromolecules*, **1992**, *25*, 6055. (c) Davies, S. J.; Johnson, B. F. G.; Khan, M. S.; Lewis, J.; *J. Chem. Soc., Chem. Commun.*, **1991**, 187. (d) Tenhaeff, S. C.; Tyler, D. R. *J. Chem. Soc., Chem. Commun.*, **1989**, 1459. (e) Manners, I. *J. Chem. Soc., Ann. Rep. Prog. Chem. A.*, **1991**, 77. (f) Neuse, E. W.; Bednarik, L. *Macromolecules*, **1979**, *12*, 187. (g) Sturge, K. C.; Hunter, A. D.; McDonald, R.; Santarsiero, B. D. *Organometallics*, **1992**, *11*, 3056. (h) Gonsalves, K.; Zhan-ru, L.; Rausch, M. D. *J. Am. Chem. Soc.*, **1984**, *106*, 3862. (i) Katz, T. J.; Sudhakar, A.; Teasley, M. F.; Gilbert, A. M.; Geiger, W. E.; Robben, M. P.; Wuensch, M.; Ward, M. D. *J. Am. Chem. Soc.*, **1993**, *115*, 3182. (j) Nugent, H. M.; Rosenblum, M. *J. Am. Chem. Soc.*, **1993**, *115*, 3848. (k) Patterson, W. J.; McManus, S. P.; Pittman, C. U. *J. Polym. Sci.: Poly. Chem. Ed.*, **1974**, *12*, 837.
- (3) Brandt, P. F.; Rauchfuss, T. B. *J. Am. Chem. Soc.* **1992**, *114*, 1926.
- (4) Manners, I. *Adv. Organomet. Chem.* **1995**, *37*, 131.
- (5) Foucher, D. A.; Tang, B.-Z.; Manners, I. *J. Am. Chem. Soc.* **1992**, *114*, 6246.
- (6) Rulkens, R.; Lough, A. J.; Manners, I. *J. Am. Chem. Soc.* **1994**, *116*, 797.
- (7) Rulkens, R.; Ni, Y.; Manners, I. *J. Am. Chem. Soc.* **1994**, *116*, 12121.

- (8) a) Fossum, E.; Matyjaszewski, K.; Rulkens, R.; Manners, I. *Macromolecules* **1995**, *28*, 401. b) Pudelski, J. K.; Rulkens, R.; Foucher, D. A.; Lough, A. J.; Macdonald, P. M.; Manners, I. *Macromolecules* **1995**, *28*, 7301.
- (9) Ni, Y. Z.; Rulkens, R.; Pudelski, J. K.; Manners, I. *Makromol. Chem. Rapid Communications* **1995**, *16*, 637.
- (10) Foucher, D. A.; Manners, I. *Makromol. Chem., Rapid Commun.* **1993**, *14*, 63.
- (11) Foucher, D. A.; Ziembinski, R.; Tang, B. Z.; Macdonald, P. M.; Massey, J.; Jaeger, R.; Vancso, G. V.; Manners, I. *Macromolecules* **1993**, *26*, 2878.
- (12) Foucher, D. A.; Honeyman, C. H.; Nelson, J. M.; Tang, B.-Z.; Manners, I. *Angew. Chem., Int. Ed. Engl.* **1993**, *32*, 1709.
- (13) Finckh, W.; Tang, B.-Z.; Foucher, D. F.; Zamble, D. B.; Ziembinski, R.; Lough, A.; Manners, I. *Organometallics* **1993**, *12*, 823.
- (14) Foucher, D. A.; Ziembinski, R.; Petersen, R.; Pudelski, J.; Edwards, M.; Ni, Y.; Massey, J.; Jaeger, C. R.; Vancso, G. J.; Manners, I. *Macromolecules* **1994**, *27*, 3992.
- (15) Foucher, D. A.; Edwards, M.; Burrow, R. A.; Lough, A. J.; Manners, I. *Organometallics* **1994**, *13*, 4959.
- (16) Pudelski, J. K.; Foucher, D. A.; Honeyman, C. H.; Lough, A. J.; Manners, I.; Barlow, S.; O'Hare, D. *Organometallics* **1995**, in press.
- (17) Pudelski, J.; Gates, D. P.; Rulkens, R.; Lough, A.; Manners, I. *Angew. Chem., Int. Ed. Engl.* **1995**, *34*, 1506.
- (18) Nelson, J. M.; Lough, A. J.; Manners, I. *Organometallics* **1994**, *13*, 3703.
- (19) Compton, D. L.; Rauchfuss, T. B. *Organometallics* **1994**, *13*, 4367.
- (20) Rasburn, J.; Petersen, R. J.; Jahr, T.; Rulkens, R.; Manners, I.; Vancso, G. J. *Chem. Mater.* **1995**, *7*, 871.
- (21) Brown, R. A.; Houlton, A.; Roberts, R. M. G.; Silver, J.; Frompton, C. S. *Polyhedron* **1992**, *11*, 2611.
- (22) Osborne, A. G.; Whiteley, R. H.; Meads, R. E. *J. Organomet. Chem.* **1980**, *193*, 345.

- (23) Seyferth, D.; Withers, H. P. *J. Organomet. Chem.* **1980**, *185*, C1.
- (24) Burke-Laing, M.; Trueblood, K. N. *Acta Crystallogr.* **1965**, *19*, 373.
- (25) Anionic ROP has been used successfully for a number of silicon-containing ring systems. See, for example: ref. 6; M. Cypryk, M. Gupta, and K. Matyjaszewski. *J. Am. Chem. Soc.* **113**, 1046 (1991).
- (26) Sakurai, H.; Tominaga, K.; Wantanabe, T.; Kumada, M. *Tetrahedron Lett.* **1966**, 5493.
- (27) Bishop, J. J.; Davison, A.; Katcher, M. L.; Lichtenberg, D. W.; Merrill, R. E.; Smart, J. *C. J. Organomet. Chem.* **1971**, *27*, 241.
- (28) Rausch, M. D.; Ciapenelli, D. J. *J. Organomet. Chem.* **1967**, *10*, 127.
- (29) Sheldrick, G. M. SHELXTL-PC, Siemens Analytical X-ray Instruments Inc., Madison, Wisconsin, USA, 1990.

# Chapter 3 Synthesis, Characterization, and Properties of High Molecular Weight Poly(ferrocenylgermanes) and Poly(ferrocenyldimethylsilane)-Poly(ferrocenylgermane) Random Copolymers

## 3.1 Abstract

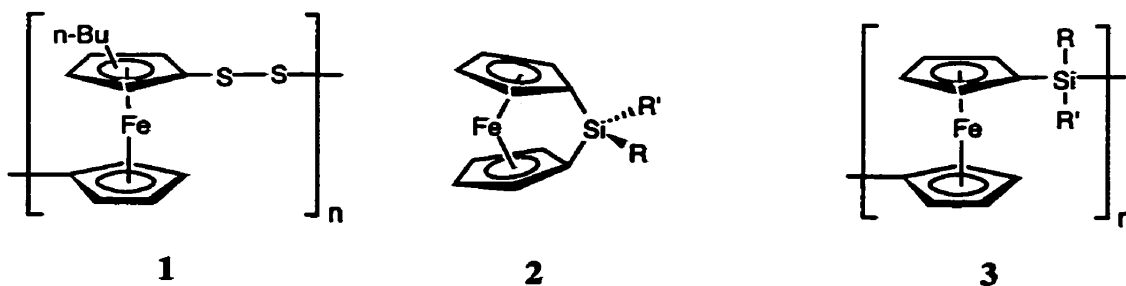
A series of high molecular weight poly(ferrocenylgermanes)  $[\text{Fe}(\eta\text{-C}_5\text{H}_3\text{X})_2\text{GeR}_2]_n$ , **5a - d** ( $\text{X} = \text{H}$ ; **a**,  $\text{R} = \text{Me}$ ; **b**,  $\text{R} = \text{Et}$ ; **c**,  $\text{R} = n\text{-Bu}$ ; **d**,  $\text{R} = \text{Ph}$ ) and **7** ( $\text{X} = \text{SiMe}_3$ ,  $\text{R} = \text{Me}$ ) were synthesized via the thermal ring-opening polymerization of the corresponding germanium-bridged [1]ferrocenophanes (**4a - d**, **6**). Poly(ferrocenyldimethylsilane)-poly(ferrocenyldimethylgermane) random copolymer **8** was obtained by the thermal and transition metal-catalyzed ring-opening polymerization of a mixture of the [1]germaferrocenophane  $[\text{Fe}(\eta\text{-C}_5\text{H}_4)_2\text{GeMe}_2]$  **4a** and the corresponding [1]silaferrocenophane  $[\text{Fe}(\eta\text{-C}_5\text{H}_4)_2\text{SiMe}_2]$ , **2** ( $\text{R} = \text{R}' = \text{Me}$ ). The molecular weights for the homo- and copolymers were estimated by gel permeation chromatography in THF versus polystyrene standards and were found to be in the range of  $M_w = 5.0 \times 10^4$  to  $2.0 \times 10^6$  and with polydispersities in the range of  $M_w/M_n = 1.2$  to  $2.4$ . A low angle laser light scattering study of **5a** in THF gave an absolute value of  $M_w$  of  $3.3 \times 10^6$  which was significantly greater than the GPC estimate ( $M_w = 8.2 \times 10^5$ ). Polymer thermal transition behaviour and morphology were investigated by differential scanning calorimetry (DSC) and wide-angle X-ray scattering (WAXS). Glass transitions ( $T_g$ ) for the polymers were in the range of  $-7^\circ\text{C}$  to  $+128^\circ\text{C}$  and were found to be strongly dependent on the size and nature of the substituents attached to germanium and the substitution of the cyclopentadienyl rings. The semicrystalline nature of the poly(ferrocenyldialkylgermanes) **5a - c** and the copolymer **8** was apparent from the appearance of several fairly sharp diffraction peaks in the WAXS profiles of these polymers and the presence of melt transitions ( $T_m$ ) in the DSC thermograms. In contrast, polymers **5d**

and **7** were found to be amorphous. Cyclic voltammetry of the polymers showed the presence of two oxidation waves, which is consistent with the presence of redox coupling arising from significant interactions between the iron centers. UV/visible spectra of polymers **5a - c**, **7** and **8** were measured in THF in the 350 - 800 nm range and were found to be consistent with an essentially localized electronic structure for the polymer backbone.

### 3.2 Introduction

High molecular weight transition metal-based polymers have received considerable recent attention.<sup>1-5</sup> These materials are expected to possess a range of attractive and useful attributes such as high thermal stability, tunable redox characteristics, and possibly novel magnetic and charge transport properties which are often difficult or impossible to achieve in organic polymers.

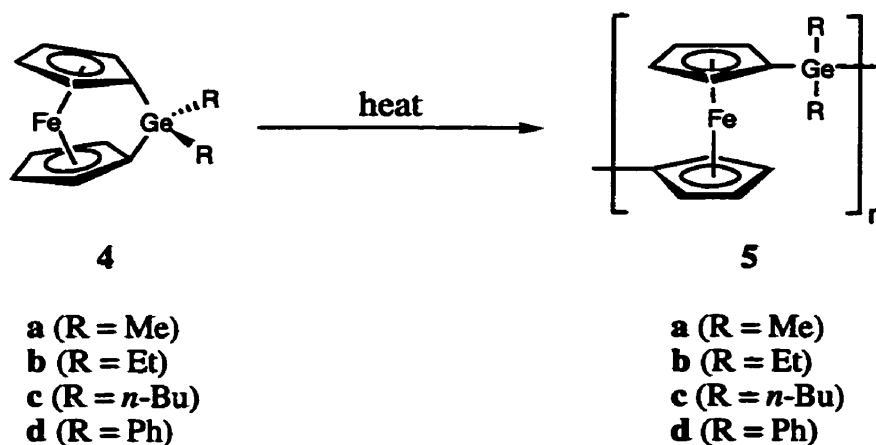
In 1992, ring-opening polymerization (ROP) was first reported as a method for successfully obtaining high molecular weight polymers with ferrocene in the main chain. A novel atom abstraction route was used by Rauchfuss *et al.*<sup>3,6</sup> to prepare poly(ferrocenylpersulfides) (**1**) from [3]trithiaferrocenophanes, while we described the use of thermal ring-opening polymerization (TROP) of strained, ring-tilted silicon-bridged [1]ferrocenophanes (**2**) to obtain high molecular weight, poly(ferrocenylsilanes) **3**.<sup>7</sup>



We have since employed a similar TROP methodology to prepare high molecular

weight polymers from other strained [1]- and [2]ferrocenophanes.<sup>8-14</sup> In addition, random copolymers are accessible via thermal copolymerization of **2** ( $R = R' = \text{Me}$ ) with different silicon-bridged ferrocenophane monomers, with the cyclotetrasilane  $[\text{SiMePh}]_4$ , or with silicon-bridged bis(arene)chromium complexes ([1]silachromaarenophanes).<sup>15-17</sup> We have also found that living ROP of silicon-bridged [1]ferrocenophanes can also be achieved in solution at room temperature in the presence of anionic initiators.<sup>18</sup> This has provided access to poly(ferrocenylsilanes) with controlled molecular weights as well as block copolymers.<sup>19</sup> More recently, we have reported the ROP of [1]silaferrocenophanes in solution at room temperature using transition metal catalysts.<sup>20</sup>

As part of our efforts to extend the scope of the ROP route to poly(metallocenes) we have previously reported the synthesis of a series of germanium-bridged [1]ferrocenophanes (**4a**, **b** and **d**) and their thermal ROP to yield poly(ferrocenylgermanes) (**5a**, **b** and **d**).<sup>8,9</sup> In this chapter as a follow-up to this work and our brief previous reports<sup>21</sup> of the electrochemistry and thermal transition behavior of these poly(ferrocenylgermanes), we report the full details of our studies of the properties of these and some other related new materials.



Reaction 3.1 Synthesis of Symmetrically-Substituted, Poly(ferrocenylgermanes)

### 3.3 Results and Discussion

#### 3.3.1 Synthesis and Characterization of the Germanium-Bridged

##### [1]Ferrocenophanes **4c** and **6**.

The synthesis and structural characterization of monomers **4a**, **4b**, and **4d** and their respective polymers **5a**, **5b**, and **5d** have been reported previously.<sup>9</sup> The preparation of these monomers was achieved using the method previously described by Osborne and co-workers.<sup>22</sup> The new germanium-bridged [1]ferrocenophane **4c** was similarly prepared by the reaction of *n*-Bu<sub>2</sub>GeCl<sub>2</sub> and dilithioferrocene•TMEDA in Et<sub>2</sub>O at -78 °C. The product was isolated as orange-red, moisture-sensitive crystals.

The synthesis of 3,3'-bis(trimethylsilyl)-1,1'-dimethyl-[1]germaferrocenophane (**6**) was accomplished by using a modification<sup>11,23</sup> of the method outlined by Silver and co-workers to prepare regio- and stereospecifically substituted bis(trimethylsilyl)ferrocenes.<sup>24</sup> First, dilithio-1,1'-bis(trimethylsilyl)ferrocene•TMEDA was prepared by addition of 2 equivalents of Me<sub>3</sub>SiCl at -78 °C to dilithioferrocene•TMEDA in Et<sub>2</sub>O followed by metallation of the isolated 1,1'-bis(trimethylsilyl)ferrocene with 2 equivalents of BuLi and 2 equivalents of TMEDA. Addition of Me<sub>2</sub>GeCl<sub>2</sub> to dilithio-1,1'-bis(trimethylsilyl)ferrocene•TMEDA in hexanes at -78 °C and subsequent warming to room temperature resulted in the formation of **6** which was isolated as a dark red liquid by vacuum distillation.

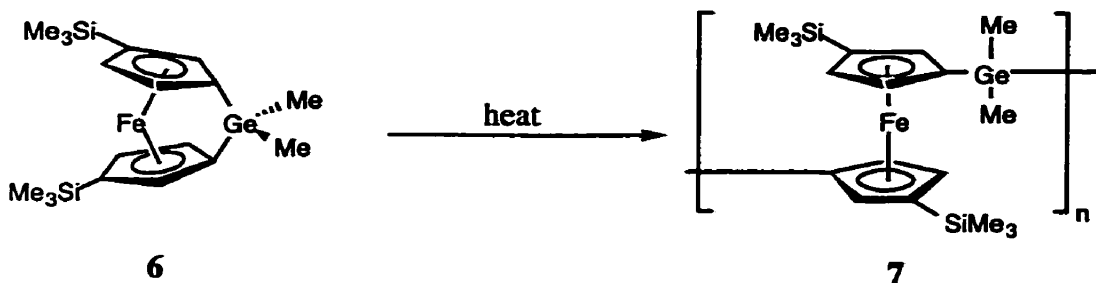
Characterization of the new monomers **4c** and **6** was achieved by <sup>1</sup>H and <sup>13</sup>C NMR spectroscopy, and by mass spectrometry which provided data consistent with the assigned structures. As has been found with other silicon- and germanium-bridged [1]ferrocenophanes, the cyclopentadienyl bridging C<sub>ipso</sub> signals were shifted significantly upfield by ca. 30 - 40 ppm compared to the other Cp carbons which resonated at ca. 76 - 82 ppm. This is indicative of significant strain and distortion from a planar geometry at the cyclopentadienyl ipso carbon attached to the bridge in these molecules. In the case of **4c**, there was also a relatively large



separation (ca. 0.4 ppm) between the  $^1\text{H}$  NMR signals for the cyclopentadienyl protons  $\alpha$  and  $\beta$  in comparison to unbridged, substituted ferrocenes in which separations of  $\approx 0.2$  ppm are found. The  $^1\text{H}$  NMR spectrum of **6** revealed two pseudo quartets and a pseudo triplet in the cyclopentadienyl region, characteristic of an  $\text{A}_2\text{B}_2\text{C}_2$  spin system. A similar pattern was observed with the analogous silicon-bridged [1]ferrocenophane.<sup>23</sup>

### 3.3.2 Synthesis and Characterization of the Poly(ferrocenylgermanes) **5c** and **7**.

Polymer **5c** was obtained by heating **4c** at  $180^\circ\text{C}$  for 2 h in a sealed, evacuated Pyrex tube. The polymer was purified by dissolution in THF and precipitation into methanol, and was then dried under high vacuum to give a yellow fibrous material. The temperature required for this ROP was significantly higher than was found for the ROP of either **4a** or **4b** ( $90^\circ\text{C}$ ) but less than that of **4d** ( $230^\circ\text{C}$ ). Polymer **7** was obtained from the distillation residue of **6** and was purified in a manner similar to **5c**.



Reaction 3.2 Synthesis of Bis(trimethylsilyl)-Substituted Poly(ferrocenyldimethylgermane) via TROP

The polymers were found to be of high molecular weight with  $M_w = 5.0 \times 10^4$  ( $M_w/M_n = 1.4$ ) for **5c** and  $5.8 \times 10^4$  ( $M_w/M_n = 2.1$ ) for **7** by GPC in THF using polystyrene standards.  $^1\text{H}$

and  $^{13}\text{C}$  NMR and elemental analysis data were consistent with the assigned structures. In the case of **5c**, the downfield position of the Cp  $\text{C}_{\text{ipso}}$   $^{13}\text{C}$  NMR resonance (73.6 ppm) relative to that for the monomer (33.0 ppm) illustrates the relief of strain on ring-opening these germanium-bridged [1]ferrocenophanes. Similar changes in the chemical shift have been found for the Cp  $\text{C}_{\text{ipso}}$  resonances in the analogous silicon compounds.<sup>25</sup> For **7**, the  $^{13}\text{C}$  NMR spectrum showed five broad peaks in the cyclopentadienyl region and these could not be specifically assigned. The  $^1\text{H}$  NMR spectra also showed two broad peaks in the cyclopentadienyl region for **5c** and three broad peaks for **7**. In both cases, the separation between these signals was considerably less than had been observed in the respective monomers.

### 3.3.3 Light Scattering Measurements for **5a** in THF

In order to investigate the solution properties of poly(ferrocenylgermanes) and to provide an absolute determination of molecular weight, low-angle laser light scattering (LALLS) studies were carried out on THF solutions of polymer **5a** which was selected as a representative example.

Results of LALLS measurements for the polymer **5a** are shown in Figure 3.1 as a function of the solution concentration. The value of  $M_w$  was determined from the fitted intercept of the straight line in Figure 3.1 with the y-axis, and  $M_w = 3.3 \times 10^6$  g/mol was obtained. To our knowledge this is the highest absolute molecular weight ever reported for a polymer containing a transition metal in the main chain. There is a difference between the absolute  $M_w$  obtained from LALLS and that obtained from GPC measurements,  $M_w = 8.2 \times 10^5$  g/mol. GPC is a size-exclusion chromatographic technique and requires calibration with sharp fractions of known molecular weight to determine  $M_w$ . Often a calibration curve for polystyrene is utilized even for polymers with very different structures. In this case, the molecular weight value obtained by GPC is a relative, but useful quantity called the

"polystyrene effective molecular weight". An absolute value for  $M_w$  can be obtained by GPC if the universal calibration technique is used<sup>26</sup> or if the column is calibrated with the polymer being studied. GPC separation is based on the effective hydrodynamic size, where the effective hydrodynamic size of a polystyrene random coil of a given  $M_w$  in a given solvent is not expected to be the same as a coil of a different polymer under the same conditions. Thus GPC underestimates the molecular weight of polymer **5a** due to the differences in the coil sizes if polystyrene column calibration is used. This was also found to be the case for poly(ferrocenylsilanes) studied by LALLS.

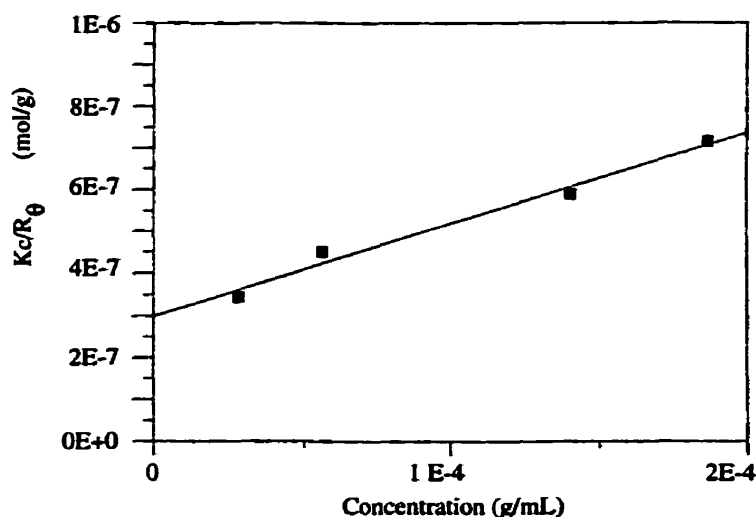


Figure 3.1 Low-Angle Laser Light Scattering Results for **5a**.

### 3.3.4 Synthesis and Characterization of the Poly(ferrocenylsilane)-Poly(ferrocenylgermane) Copolymer, **8**.

Thermal and transition-metal catalyzed copolymerization reactions between the [1]germaferrocenophane **4a** and [1]silaferrocenophane **2** ( $R = R' = \text{Me}$ ) were also attempted. For the thermal reaction these two monomers were viewed as promising candidates for

copolymerization because they homopolymerize at similarly low temperatures (**4a** at 90 °C, **2** (R = R' = Me) at 125 °C), to give THF soluble polymeric products. When an approximately 1:2 mole ratio of the monomers **4a** and **2** (R = R' = Me) was heated at 90 °C for 10 min, the contents of the tube became viscous, and then immobile. The relatively low polymerization temperature, which is coincident with the ROP temperature of **4a**, suggests that ring-opened germanium species may have initiated the polymerization of the mixture. The products dissolved in THF and polymer **8** was then precipitated from hexanes as a fibrous, bright yellow material. GPC analysis revealed that the product was a high molecular weight polymer ( $M_w = 3.2 \times 10^5$ ;  $M_n = 2.1 \times 10^5$ ) with a monomodal weight distribution (Figure 3.2) which suggested the formation of a copolymer rather than a mixture of two homopolymers.

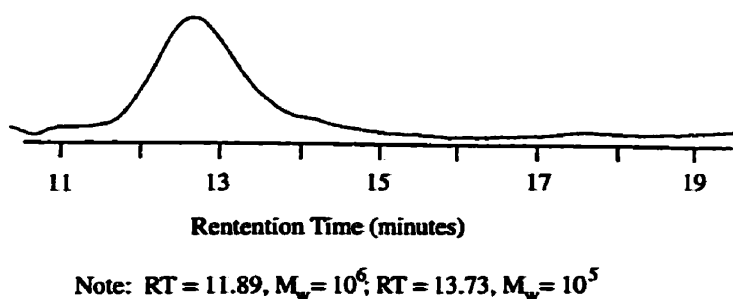


Figure 3.2 Gel Permeation Chromatograph of **8** (produced via thermal ROP)

Transition metal-catalyzed ROP of a mixture of **4a** and **2** (R = R' = Me) with 5 mol % of  $\text{PtCl}_2$  in  $\text{C}_6\text{D}_6$  also yielded a similar, amber polymeric material with a monomodal molecular weight distribution by GPC. Analysis of polymer products of the thermal and transition metal-catalyzed reactions by NMR confirmed that they possess the random copolymer structure **8**. For example,  $^{29}\text{Si}$  NMR showed the presence of 3 resonances (Figure 3.3) assigned to Si environments neighboring two fcSi, two fcGe or both fcSi and fcGe monomer units (fc =  $\text{Fe}(\eta\text{-C}_5\text{H}_4)_2$ ). Similarly, new resonances were apparent in the  $^{13}\text{C}$  NMR spectrum of **8** which are not present in the spectra of the corresponding homopolymers **3a** and **5a**. This is

illustrated for the  $\text{SiMe}_2$  (at ca - 0.4 ppm) and  $\text{GeMe}_2$  (at ca - 1.1 ppm) regions in Figure 3.4 where the presence of three resonances again arises from the presence of three possible permutations of neighbouring monomer units.

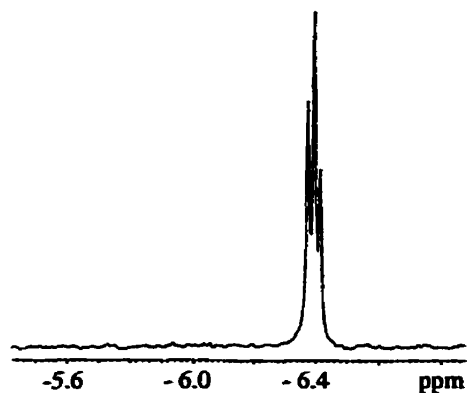


Figure 3.3  $^{29}\text{Si}$  NMR (79.5 MHz) Spectrum of **8** (produced via transition metal-catalyzed ROP) in  $\text{C}_6\text{D}_6$

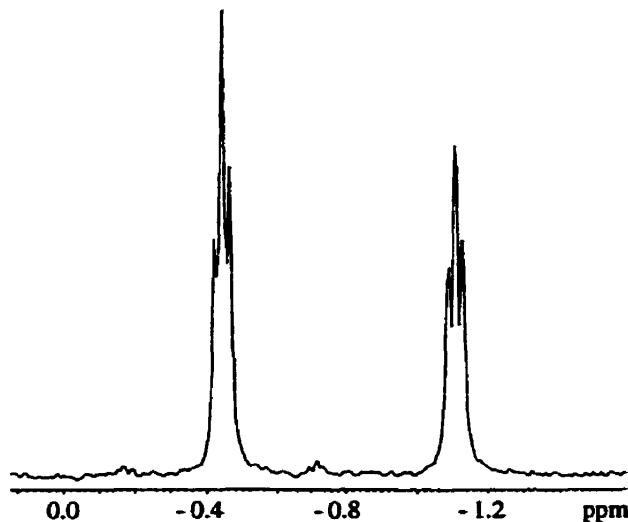
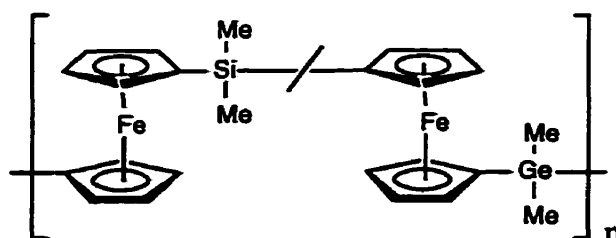


Figure 3.4  $^{13}\text{C}$  NMR (100.5 MHz) Spectrum of **8** (produced via transition metal-catalyzed ROP) in  $\text{C}_6\text{D}_6$ , Methyl region

Further evidence for copolymerization was provided by analysis of the oligomeric residues recovered from the initial precipitation of the polymer. This was found to contain hexane soluble cyclic oligomeric species which were identified by mass spectrometry. In addition to peaks that were assigned to homo-silane and germane cyclic oligomers, molecular ions were detected which corresponded to large ferrocene-containing rings with one or two bridging Si and two bridging Ge atoms ( $1\text{Si}, 2\text{Ge } M^+ = 818\text{ m/e}$ ,  $2\text{Si}, 2\text{Ge } M^+ = 1060\text{ m/e}$ ). Pyrolysis-mass spectrometry analysis of the polymer **8** led to the detection of similar species and also supported a random copolymer structure.

**8**

### 3.3.5 Thermal Transition Behaviour and Polymer Morphology.

The thermal transition behaviour of **5a - d**, **7** and **8** was studied by DSC. The glass and melt transitions for the alkyl and aryl poly(ferrocenylgermanes) (**5a - d**, **7**) and the poly(ferrocenylsilane)-poly(ferrocenylgermane) copolymer (**8**) are reported in Table 3.1.

For the poly(ferrocenyldialkylgermanes), lower glass transition temperatures were observed upon increasing the length of the substituent attached to germanium. A similar trend was previously observed for the analogous poly(ferrocenyldialkylsilanes).<sup>27</sup> Interestingly, the  $T_g$  for **8** ( $30\text{ }^\circ\text{C}$ ) falls in between those of the two homopolymers ( $33\text{ }^\circ\text{C}$  for **3a** and  $28\text{ }^\circ\text{C}$  for **5a**). The presence of bulky trimethylsilyl substituents on the cyclopentadienyl rings is expected to cause a decrease in the conformational flexibility which explains the high  $T_g$  value ( $128\text{ }^\circ\text{C}$ ) detected for **7**. Similarly, increasing the number of methyl substituents on the

cyclopentadienyl rings of poly(ferrocenyldimethylsilane) leads to higher  $T_g$  values.<sup>28</sup> The high  $T_g$  (114 °C) for **5d** in comparison to **5a** is probably a consequence of the more rigid and bulky phenyl substituents at germanium. High glass transitions have also been detected for a

Table 3.1 Thermal Transition Data for Selected Polymers.

Polymer	$M_w$	$M_n$	$T_g$ (°C)	$T_m$ (°C)	Reference
<b>3a</b>	$5.2 \times 10^5$	$3.4 \times 10^5$	33	120	27
<b>5a</b>	$2.0 \times 10^6$	$8.5 \times 10^5$	28	125	this work
<b>5b</b>	$1.0 \times 10^6$	$8.1 \times 10^5$	12	79	this work
<b>5c</b>	$5.0 \times 10^4$	$3.5 \times 10^4$	-7	74, 111	this work
<b>5d</b>	$1.0 \times 10^6$	$8.2 \times 10^5$	114	-	this work
<b>7</b>	$5.8 \times 10^4$	$2.7 \times 10^4$	128	-	this work
<b>8</b>	$3.2 \times 10^5$	$2.1 \times 10^5$	30	81, 117	this work
<b>9</b>	$1.4 \times 10^5$	$8.4 \times 10^4$	128	-	this work

series of unsymmetrically substituted poly(ferrocenylsilanes) bearing aryl substituents attached to silicon,<sup>29</sup> as well as for organic polymers where ferrocenyl groups have been introduced into the side chain structure.<sup>30</sup>

DSC melt transitions were detected for polymers **5a - c** and **8**, and their values are listed in Table 3.1. In all cases, samples which were annealed for 36 h at 60 °C showed considerably more intense melt endotherms (ie higher degrees of crystallinity) in comparison to the unannealed polymers. In the case of **5c** (Figure 3.5), two well-separated melt transitions were observed in the first DSC scan at 74 °C and 111 °C. A subsequent DSC run on the same sample showed only a single melt transition at 111 °C. Two distinct melt transitions were observed during the first DSC scan for the copolymer **8** at 81°C and 117 °C while no melt

transitions were seen on subsequent runs. No obvious melt transitions were observed in the case of polymers **5d** or **7**, consistent with the results for the poly(ferrocenylsilanes) with the same substituents.<sup>27,31</sup>

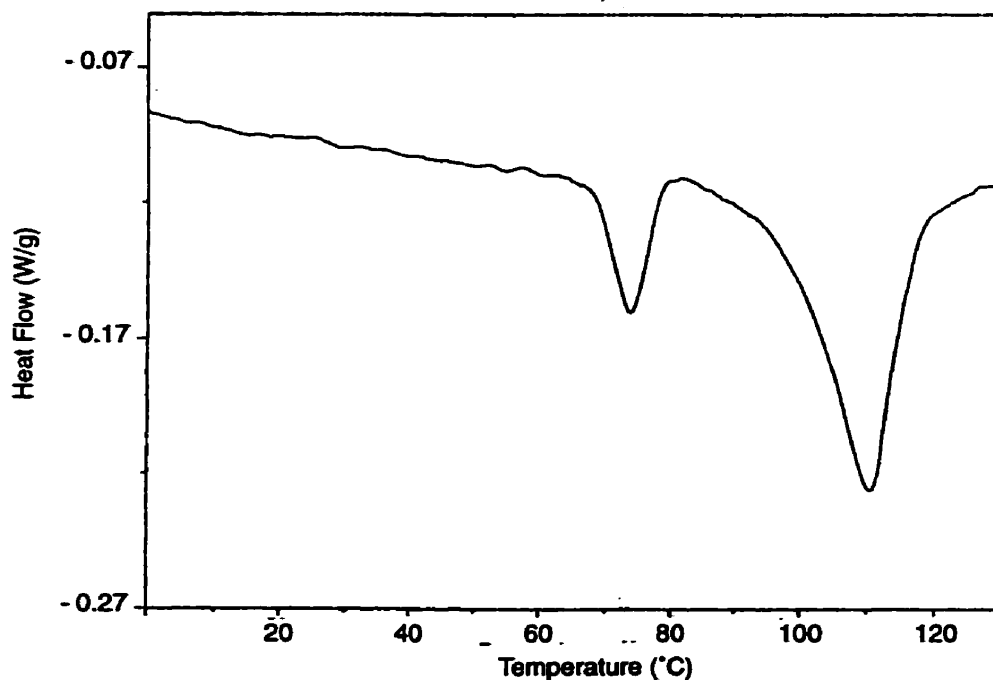


Figure 3.5 DSC Thermogram of **5c** (first scan)

Further morphological information on the polymers was provided by wide angle X-ray scattering (WAXS). The WAXS patterns for the poly(ferrocenylgermanes) also revealed significant structural ordering for **5a - c** as well as for the copolymer **8**. The di-*n*-butyl substituted polymer **5c** (Figure 3.6) displayed highly ordered and crystalline features with several strong diffraction peaks in contrast to **7** which showed only a single broad amorphous halo.



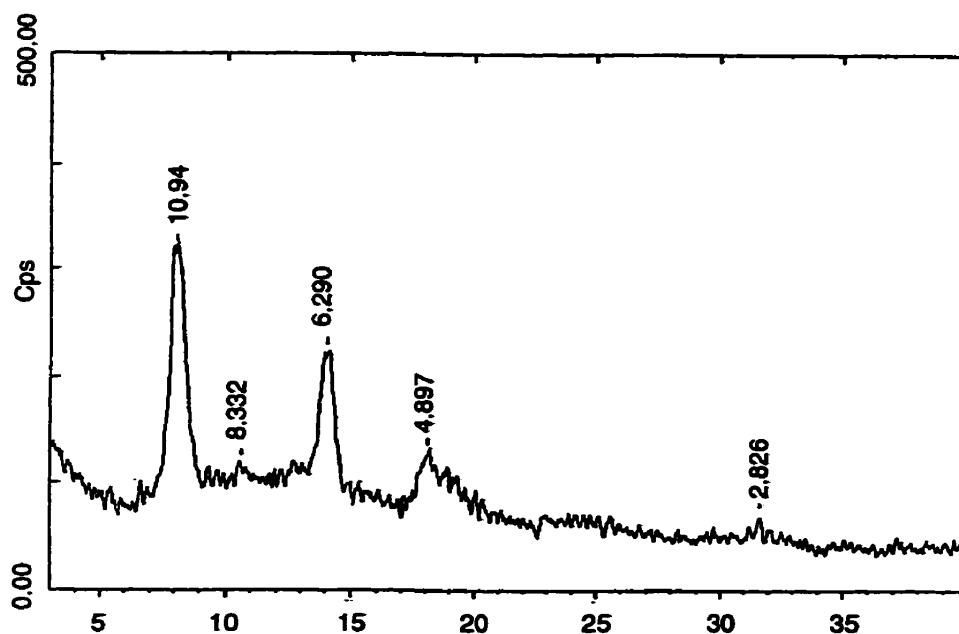


Figure 3.6 WAXS Pattern of **5c**

The maximum d-spacings for **5a** at 6.58 Å and **5c** at 10.94 Å are in accordance with the increasing size of the substituent attached to germanium. This was also observed for the analogous poly(ferrocenylsilanes) **3a** and **3c**, where the maximum d-spacings are 6.34 Å and 11.06 Å respectively.<sup>32</sup> Although less crystalline than either **5a** or **5c**, **5d** showed three resolved but broad peaks with a maximum d-spacing of 8.11 Å. This value is intermediate to those for **5a** and **5c** and thus also appears to be a function of the side group size. The amorphous character of **7** may be related to the irregular structure of the polymer backbone as a consequence of the bulky trimethylsilyl substituents. A single sharp diffraction peak superimposed upon an amorphous halo in the WAXS pattern for the copolymer **8** with a d-spacing of 6.37 Å is similar to the value found for the silicon homopolymer **3a** (6.34 Å).

### 3.3.6 Electronic and Electrochemical Properties

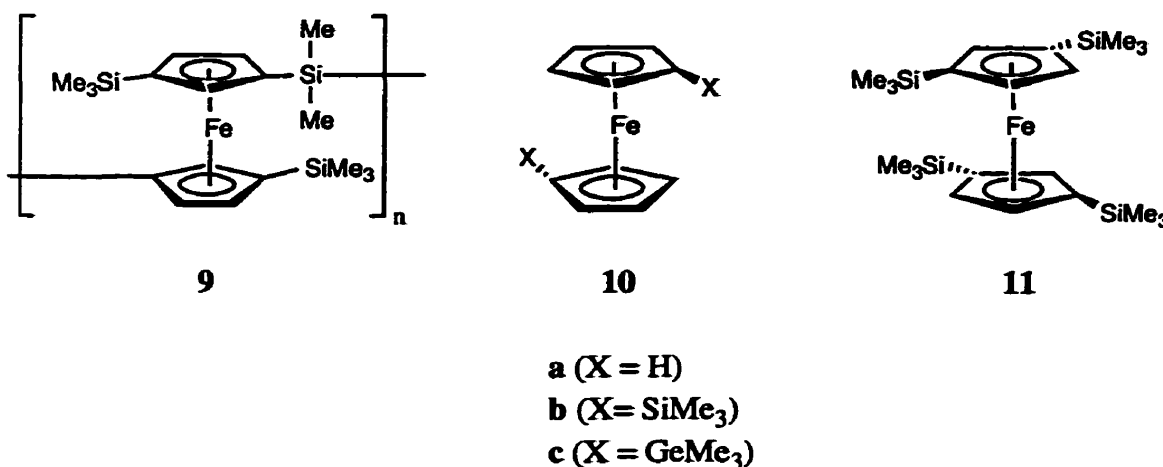
In order to obtain information concerning the electronic structure of these polymers, UV/visible spectra in the 350 to 800 nm region were obtained for solutions of **5a - c**, **7** and **8** in THF. The  $\lambda_{\text{max}}$  values for the bands in the visible region are reported for these polymers, poly(ferrocenylsilane) **9** (the Si-analogue of polymer **7**) and several small molecule models **10a - 10c** and **11** are listed in Table 3.2.

Table 3.2 Electronic and Electrochemical Data for Selected Polymers and Model Systems

Polymer	$^1E_{1/2}$ (V)	$^2E_{1/2}$ (V)	$\Delta E$ (V)	$\lambda_{\text{max}}$ (nm)	$\epsilon$ (L mol <sup>-1</sup> cm <sup>-1</sup> )	Reference
<b>3</b> (R = R' = Me)	-0.04	0.17	0.21	442	230	7
<b>5a</b>	-0.06	0.12	0.18	448	179	10, this work
<b>5b</b>	-0.09	0.18	0.27	448	188	this work
<b>5c</b>	-0.03	0.23	0.26	448	125	this work
<b>7</b>	-0.04	0.14, 0.19	0.18, 0.23	474	228	this work
<b>8</b>	-0.01	0.16	0.17	446	189	this work
<b>9</b>	0.00	0.25	0.25	476	215	this work
<b>10a</b>	0.00	-	-	440	90	25
<b>10b</b>	0.05	-	-	448	132	this work
<b>10c</b>	-0.03	-	-	444	160	this work
<b>11</b>	-0.01	-	-	484	187	this work

By analogy with UV/visible spectral assignments for ferrocene (**10a**), the lowest energy

absorption in the visible region for poly(ferrocenylgermanes) can be considered to arise from HOMO-LUMO electronic transitions which are essentially d-d in character.<sup>5</sup> All of the poly(ferrocenylgermanes) show weak bands with  $\lambda_{\max} = 448$  nm, with the exception of **7** where the transition occurs 474 nm. The values for **5a - c** are similar to those for ferrocene ( $\lambda_{\max} = 440$  nm) and bis(trimethylgermylferrocene) **11c** ( $\lambda_{\max} = 444$  nm). As found with poly(ferrocenylsilanes), the lack of formation of a band structure is indicative of an essentially localized electronic structure for the backbone of these polymers.<sup>5</sup>



The  $\lambda_{\max}$  value for the copolymer **8** is close to the corresponding value for the homopolymer **5a**. The significantly lower energy transition for the trimethylsilyl-substituted polymer **7** compared to those for **5a - 5c** is interesting. The poly(ferrocenylsilane) analogue of **7**, polymer **9**, possesses a similarly red-shifted transition ( $\lambda_{\max} = 476$  nm) relative to polymer **3a**. In order to examine the effect of the introduction of additional trimethylsilyl groups at the small molecule level we have compared the UV/vis spectrum of bis(trimethylsilyl)ferrocene **10b** ( $\lambda_{\max} = 448$  nm) with that of tetrakis(trimethylsilyl)ferrocene **11**. For the latter species  $\lambda_{\max} = 484$  nm and so the cause of the bathochromic shift of polymer **7** relative to **5a** and polymer **9** relative to **3a** also operates in small molecule models of the polymer repeat units. Perhaps significantly, a single crystal X-ray study of compound **11** by Okuda et al.<sup>33</sup> has revealed that the cyclopentadienyl rings are tilted with respect to one another (tilt angle = 6 °)

due to the steric interactions between the bulky trimethylsilyl substituents. In contrast, ferrocene and its disubstituted derivatives possess cyclopentadienyl rings which are parallel (or almost parallel) to one another.<sup>34</sup> It therefore seems possible that the red-shifted band for **11** and perhaps that for the polymers **7** and **9** is related to a weakening of the iron-cyclopentadienyl bond which decreases the HOMO-LUMO energy difference and leads to a consequent increase in  $\lambda_{\text{max}}$ . An alternative explanation provided by EHMO calculations on some [1]ferrocenophanes has suggested that the red-shift seen with increasing tilt angle is due at least in part to the loss of degeneracy for and a lowering in energy of the LUMO orbitals.<sup>35</sup> We have also found that poly(ferrocenylsilanes) with methylated cyclopentadienyl rings show similar bathochromic shifts for the lowest energy visible absorption band<sup>27</sup> and further work aimed at investigating this phenomenon in more detail in these and related materials with substituted cyclopentadienyl rings is in progress.

Cyclic voltammetry experiments were performed on compounds **5a - c**, **7** and **8** and the half-wave potentials ( $^1E_{1/2}$  and  $^2E_{1/2}$ ) and the peak-to-peak separation values ( $\Delta E$ ) are reported in Table 2. The shapes of the cyclic voltammograms for several of these polymers are significantly modified by electrode adsorption effects. As was previously found for a series of symmetrically and unsymmetrically substituted poly(ferrocenylsilanes),<sup>27,29</sup> the cyclic voltammograms in  $\text{CH}_2\text{Cl}_2$  show two reversible redox waves corresponding to oxidation of essentially half the iron centers with the first wave and subsequent oxidation of the remaining iron centers with the second wave, as shown in Figure 3.7 for **5c**. The peak-to-peak separation values or redox couplings ( $\Delta E$ ) of the first and second oxidation waves for these polymers fall in the range between 0.17 V and 0.27 V and provides a useful measure of the interaction between the skeletal transition metal centres.

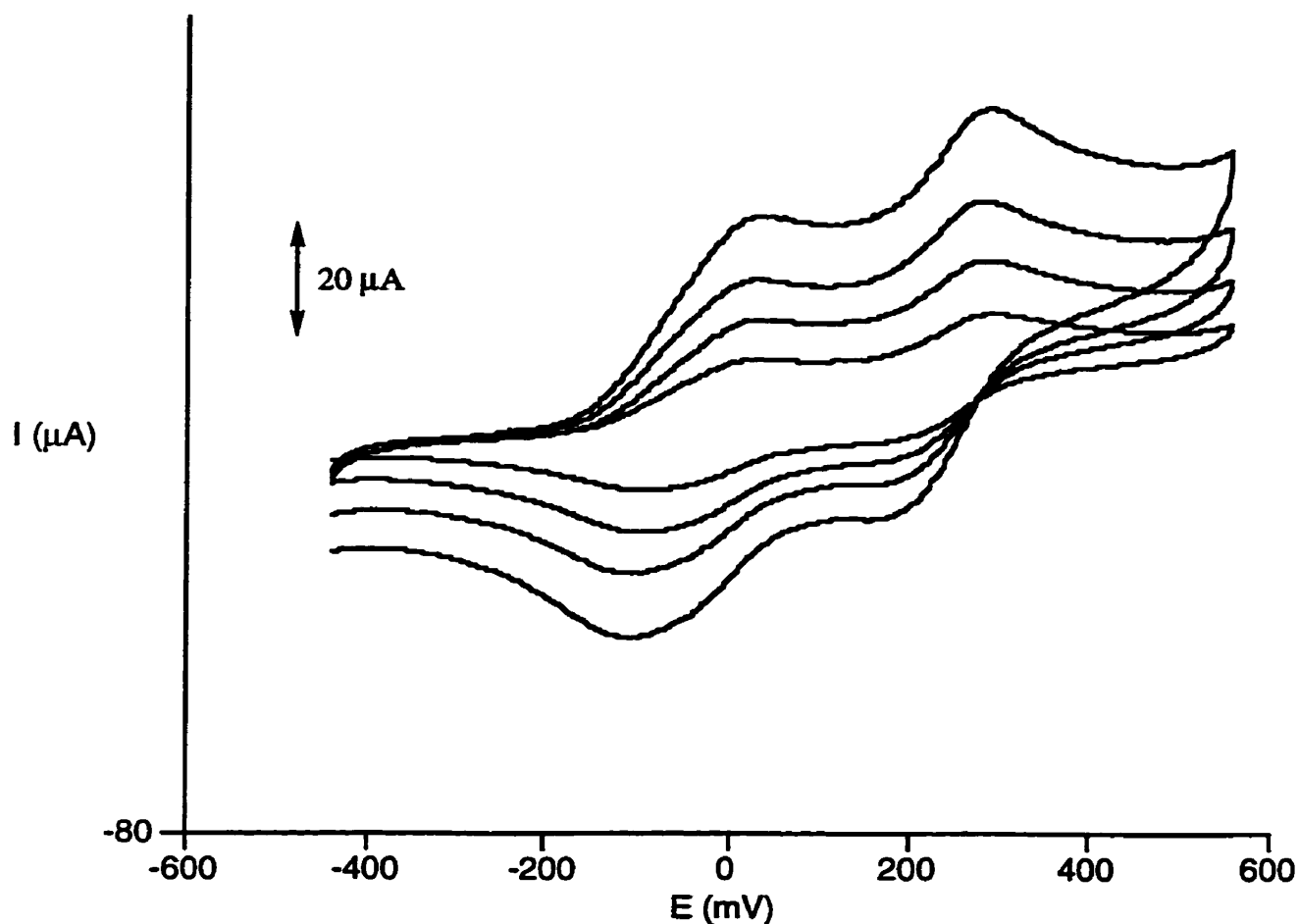


Figure 3.7 Cyclic Voltammograms of a  $5 \times 10^{-3}$  M  $\text{CH}_2\text{Cl}_2$  Solution of **5c** at Scan Rates of 100, 250, 500 and 1000 mV/s at 25 °C. (The x-axis is referenced to the ferrocene/ferrocenium ion couple at  $E = 0.0$  mV)

A comparison of the  $\Delta E$  values for a series of group 14 bridged poly(ferrocenes),  $[\text{Fe}(\eta\text{-C}_5\text{H}_4)_2\text{X}(n\text{-Bu})_2]_n$   $\{\text{X}(\Delta E) = \text{Si} (0.29 \text{ V}), \text{Ge} (0.26 \text{ V}), \text{Sn} (0.24 \text{ V})\}$ , reveals a decreasing electronic interaction between neighbouring iron centers with the increasing size of the bridging atom.<sup>10</sup> The cyclic voltammogram for the copolymer **8** is essentially the same as those for the two homopolymers **3a** and **5a**. Additional peaks were observed in the higher potential reduction wave for **7** which might be related to conformational effects as the polymer backbone

is particularly rigid in this case.

### 3.4 Summary

A series of symmetrically substituted poly(ferrocenylgermanes) have been prepared via the ring-opening polymerization of strained, germanium-bridged [1]ferrocenophanes. In addition, a poly(ferrocenylsilane)-poly(ferrocenylgermane) random copolymer has been synthesized. Glass transition temperatures of the polymers were found to be dependent upon the size of the substituents upon germanium as well as those attached to the cyclopentadienyl rings. The poly(ferrocenylgermanes) **5a - c** and the copolymer **8** were found to be semicrystalline according to the WAXS analysis and the presence of melting transitions in the DSC thermograms. In contrast, polymers **5d** and **7** were found to be amorphous. Cyclic voltammetry of polymers **5a - c** and **7** showed two oxidation waves, consistent with significant electronic interactions between iron centers. Similar behaviour was previously found for the poly(ferrocenylsilanes).<sup>5</sup> No distinguishable features, such as additional peaks in the cyclic voltammograms, were found for the cyclic voltammetric behaviour of the random copolymer **8**. The solution UV/visible spectra of polymers **5a - c** were similar to those of ferrocene and the analogous poly(ferrocenylsilanes). The HOMO-LUMO transition in the UV/visible spectrum of polymer **7**, which has bulky trimethylsilyl substituents on the cyclopentadienyl rings, is considerably red-shifted relative to that for the other poly(ferrocenylgermanes) and may be a consequence of weaker Fe-cyclopentadienyl bonding arising from unfavorable steric interactions between the SiMe<sub>3</sub> substituents or, alternatively, a loss of degeneracy for and a lowering in energy of the LUMO orbitals.

### 3.5 Experimental Section

**Materials.** Ferrocene, 1.6 M butyllithium in hexanes and tetramethylethylenediamine (TMEDA) were purchased from Aldrich. Dimethyldichlorogermane, diethyldichlorogermane, di(*n*-butyl)dichlorogermane and diphenyldichlorogermane and trimethylchlorogermane were purchased from Gelest and were distilled prior to use. The synthesis of dilithio-1,1'-bis(trimethylsilyl)ferrocene•TMEDA has been reported elsewhere.<sup>11,23,24</sup> Compounds **10b**, **10c** and **11** were synthesized using modifications of literature procedures.<sup>24</sup>

**Equipment.** All reactions and manipulations were carried out under an atmosphere of prepurified nitrogen using either Schlenk techniques or an inert-atmosphere glovebox (Vacuum Atmospheres), except for the polymers for which manipulations were carried out in air. Solvents were dried by standard methods, distilled, and stored under nitrogen over activated molecular sieves. 200 or 400 MHz <sup>1</sup>H NMR spectra and 50.3 or 100.5 MHz <sup>13</sup>C NMR spectra were recorded either on a Varian Gemini 200 or Varian Unity 400 spectrometer. Mass spectra were obtained with the use of a VG 70-250S mass spectrometer operating in either an Electron Impact (EI) or Fast Atom Bombardment (FAB) mode. Molecular weights were estimated by gel permeation chromatography (GPC) using a Waters Associates liquid chromatograph equipped with a Model 510 HPLC pump, a Model U6K injector, Ultrastyrigel columns with pore sizes of 10<sup>3</sup> to 10<sup>5</sup> Å and a differential refractometer. A flow rate of 1.0 mL/min was used, and the eluent was a solution of 0.1 % tetra-*n*-butylammonium bromide in THF. Polystyrene standards purchased from American Polymer Standards were used for calibration purposes. Retention time (min.)/M<sub>w</sub>/PDI: 11.89/1.75 x 10<sup>6</sup>/1.06, 12.06/6.00 x 10<sup>5</sup>/1.10, 12.78/2.00 x 10<sup>5</sup>/1.06, 13.54/1.11 x 10<sup>5</sup>/1.06, 14.19/6.30 x 10<sup>4</sup>/1.03, 15.55/2.00 x 10<sup>4</sup>/1.10, 16.72/9.00 x 10<sup>3</sup>/1.04, 17.6/4.00 x 10<sup>3</sup>/1.10, 19.24/1.00 x 10<sup>3</sup>/1.10. Static light scattering experiments were carried out by utilizing the low-angle laser light scattering (LALLS) technique, using a Chromatix KMX-6 instrument at a wavelength of 632.8 nm, and a

scattering angle of 6-7°. Measurements were carried out at room temperature (23 °C) using a metal cell 4.93 mm in length. Each solution was filtered twice through a Gelman Science arcodisk filter with a 0.2 micrometer average pore size before injection into the sample cell. The value of the refractive index increment,  $dn/dc$  of the polymer solutions was obtained by using a Chromatix KMX-16 differential refractometer operating at a wavelength of 632.8 nm. The instrument was calibrated with NaCl solutions.

Glass transition temperatures and melting points were obtained with an E.I. DuPont 910 differential scanning calorimeter operating at a heating rate of 10 °C per minute under N<sub>2</sub>. UV/vis spectra were recorded in anhydrous THF on a Hewlett-Packard 6452A diode array instrument using a 1 cm cell. Elemental analyses were performed by either Canadian Microanalytical Services, Delta, B.C., Canada or Quantitative Technologies Inc., Whitehouse, NJ.

Electrochemical experiments were carried out using a PAR model 273 potentiostat with a Pt working electrode, a W secondary electrode, and an Ag wire reference electrode in a Luggin capillary. Polymer solutions were  $1 \times 10^{-3}$  M in CH<sub>2</sub>Cl<sub>2</sub> with 0.1 M [Bu<sub>4</sub>N][PF<sub>6</sub>] as a supporting electrolyte. Peak currents were found to be proportional to the square root of the scan rate over the range studied (25 mVs<sup>-1</sup> to 1000 mVs<sup>-1</sup>) which indicated that charge transfer is similar to a semi-infinite linear diffusion process.

Powder X-ray diffraction studies were performed by Dr. Srebri Petrov from the Powder X-ray Diffraction Service at the University of Toronto. Powder diffraction data were obtained on a Siemens D5000 diffractometer using Ni filtered CuK $\alpha$  ( $\lambda = 1.54178$  Å) radiation. The samples were scanned at step widths of 0.02 ° with 1.0 s per step in the range of 3 to 40 ° 2 $\theta$ . Samples were prepared by spreading the finely ground polymer on grooved glass slides.

**Synthesis of [1]Di(*n*-butyl)germaferrocenophane 4c.** To dilithioferrocene•TMEDA (1.00 g, 3.62 mmol) in ether (100 ml) at -78 °C was added neat *n*-Bu<sub>2</sub>GeCl<sub>2</sub> (1.22 g, 5.62 mmol). The reaction mixture was slowly allowed to warm to -10 °C over 3 h. The solvent



was then removed while maintaining the temperature at  $-10\text{ }^{\circ}\text{C}$ . Residual TMEDA was then removed under vacuum ( $25\text{ }^{\circ}\text{C}$ ,  $0.005\text{ mm Hg}$ ). LiCl was removed by dissolution of the product in hexanes and filtration through a frit. The product was then recrystallized from hexanes to yield orange-red crystals. Yield  $0.41\text{ g}$  ( $31\%$ ).

For monomer **4c**:  $\text{Fe}(\eta\text{-C}_5\text{H}_4)_2\text{Ge}(n\text{-Bu})_2$  Orange-red crystals:  $^{13}\text{C}$  NMR ( $\text{C}_6\text{D}_6$ )  $\delta = 76.8$  (Cp),  $76.4$  (Cp),  $30.0$  (Ge-Cp<sub>ipso</sub>),  $27.3$  ( $\text{CH}_2\text{CH}_2\text{CH}_2\text{CH}_3$ ),  $26.4$  ( $\text{CH}_2\text{CH}_2\text{CH}_2\text{CH}_3$ ),  $14.0$  ( $\text{CH}_2\text{CH}_2\text{CH}_2\text{CH}_3$ ),  $13.5$  ( $\text{CH}_2\text{CH}_2\text{CH}_2\text{CH}_3$ ) ppm;  $^1\text{H}$  NMR ( $\text{C}_6\text{D}_6$ )  $\delta = 4.41$  (pseudo tr., 4 H, Cp),  $4.11$  (pseudo tr., 4 H, Cp),  $1.60$  (t, 4H,  $\text{CH}_2\text{CH}_2\text{CH}_2\text{CH}_3$ ),  $1.27$  (m, 8 H,  $\text{CH}_2\text{CH}_2\text{CH}_2\text{CH}_3$ ), (t, 6 H,  $\text{CH}_2\text{CH}_2\text{CH}_2\text{CH}_3$ ) ppm; MS (EI,  $70\text{ eV}$ )  $m/e$  (%)  $372$  ( $63$ ,  $\text{M}^+$ ),  $315$  ( $21$ ,  $\text{M}^+ - \text{C}_4\text{H}_9$ ),  $259$  ( $100$ ,  $\text{M}^+ - \text{C}_4\text{H}_9 - \text{C}_4\text{H}_8$ ).

**Characterization Data for the Poly(ferrocenylgermanes) 5a - b, d.** The synthesis and characterization of **4a - b, d** and the corresponding polymers (**5a - b, d**) have been reported previously.<sup>9</sup> The NMR characterization data for **5a** is repeated here for comparison purposes with respect to the copolymer **8**. The molecular weight data for the polymer samples studied in this work are also given. The molecular weights of the polymers formed in the thermal polymerization reactions were found to vary slightly from experiment to experiment as reported previously for **4a**.<sup>8,9</sup> In general, the molecular weights were higher with higher purity monomer and the polymerization times were found to be dependent on the temperature used.

For polymer **5a**:  $[\text{Fe}(\eta\text{-C}_5\text{H}_4)_2\text{GeMe}_2]_n$  Yellow fibrous powder:  $^{13}\text{C}$  NMR (in  $\text{C}_6\text{D}_6$ )  $\delta = 74.6$  (Cp<sub>ipso</sub>),  $72.9$  (Cp),  $71.0$  (Cp),  $-1.1$  ppm (GeMe<sub>2</sub>).  $^1\text{H}$  NMR (in  $\text{C}_6\text{D}_6$ )  $\delta = 4.25$  (pseudo tr.,  $^3J_{\text{HH}} = 1.6\text{ Hz}$ , 4H, Cp),  $4.11$  (pseudo tr.,  $^3J_{\text{HH}} = 1.6\text{ Hz}$ , 4H, Cp), and  $0.64$  (s, 6H, GeMe<sub>2</sub>) ppm. GPC: Sample for light scattering study  $M_w = 8.2 \times 10^5$ ,  $M_n = 2.9 \times 10^5$  polydispersity ( $M_w/M_n$ ) = 2.8; Sample for all other studies  $M_w = 2.0 \times 10^6$ ,  $M_n = 8.5 \times 10^5$  polydispersity ( $M_w/M_n$ ) = 2.4; LALLS:  $M_w = 3.3 \times 10^6$ ; WAXS:  $d = 6.58\text{ \AA}$ .

For polymer **5b**:  $[\text{Fe}(\eta\text{-C}_5\text{H}_4)_2\text{GeEt}_2]_n$  Yellow fibrous powder: GPC:  $M_w = 1.0 \times 10^6$ ,  $M_n = 8.1 \times 10^5$  polydispersity ( $M_w/M_n$ ) = 1.3; WAXS:  $d = 6.68 \text{ \AA}$ .

For polymer **5d**:  $[\text{Fe}(\eta\text{-C}_5\text{H}_4)_2\text{GePh}_2]_n$  Yellow powder: GPC:  $M_w = 1.0 \times 10^6$ ;  $M_n = 8.2 \times 10^5$  polydispersity ( $M_w/M_n$ ) = 1.2; WAXS:  $d = 8.11, 4.72, 3.10 \text{ \AA}$ .

**Synthesis of the Poly(ferrocenyldi(*n*-butyl)germane) 5c.** A sample of **4c** (0.50 g, 13.2 mmol) was sealed in an evacuated, Pyrex tube and heated at 180 °C for 2 h. The polymer was then dissolved in THF and precipitated by dropwise addition to methanol. Yield: 0.27 g (54 %).

For polymer **5c**:  $[\text{Fe}(\eta\text{-C}_5\text{H}_4)_2\text{Ge}(n\text{-Bu})_2]_n$  Yellow fibrous powder:  $^{13}\text{C}$  NMR (in  $\text{C}_6\text{D}_6$ )  $\delta = 73.6$  (Ge-Cp<sub>ipso</sub>), 73.4 (Cp), 71.2 (Cp), 28.3 ( $\text{CH}_2\text{CH}_2\text{CH}_2\text{CH}_3$ ), 27.1 ( $\text{CH}_2\text{CH}_2\text{CH}_2\text{CH}_3$ ), 15.5 ( $\text{CH}_2\text{CH}_2\text{CH}_2\text{CH}_3$ ), 14.2 ( $\text{CH}_2\text{CH}_2\text{CH}_2\text{CH}_3$ );  $^1\text{H}$  NMR (in  $\text{C}_6\text{D}_6$ )  $\delta = 4.36$  (s br, 4H, Cp), 4.21 (s br, 4H, Cp), 1.71 (m br, 4H,  $\text{CH}_2\text{CH}_2\text{CH}_2\text{CH}_3$ ), 1.54 (m br, 4H,  $\text{CH}_2\text{CH}_2\text{CH}_2\text{CH}_3$ ), 1.35 (m br, 4H,  $\text{CH}_2\text{CH}_2\text{CH}_2\text{CH}_3$ ), 1.05 (m br, 6H,  $\text{CH}_2\text{CH}_2\text{CH}_2\text{CH}_3$ ) ppm. Anal. Calcd: C 58.30, H 7.07 Found: C 57.75, H 7.15. GPC:  $M_w = 5.0 \times 10^4$ ,  $M_n = 3.5 \times 10^4$  polydispersity ( $M_w/M_n$ ) = 1.4; WAXS:  $d = 10.94, 6.29, 4.90, 2.83 \text{ \AA}$ .

**Synthesis of the Trimethylsilylated [1]Germaferrocenophane 6 and the Isolation of the Poly(ferrocenylgermane) 7.** Freshly distilled  $\text{Me}_2\text{GeCl}_2$  (0.94 mL, 8.1 mmol) was added dropwise to a stirred solution of dilithio-1,1'-bis(trimethylsilyl)ferrocene•TMEDA (3.69 g, 8.1 mmol) in 300 mL of hexanes at -78 °C. The product was filtered to remove LiCl and then purified by vacuum distillation (150 °C, 0.05 mmHg). Yield of **6** after distillation: 1.20 g (35 %). The distillation residue was dissolved in THF and filtered. The filtrate was then precipitated dropwise into methanol to yield **7** (1.82

g).

For monomer **6**:  $\text{Fe}(\eta\text{-C}_5\text{H}_3\text{SiMe}_3)_2\text{GeMe}_2$ , Red liquid:  $^{29}\text{Si}$  NMR ( $\text{CDCl}_3$ )  $\delta = -4.1$  (s,  $\text{SiMe}_3$ , 2 Si) ppm;  $^{13}\text{C}$  NMR ( $\text{CDCl}_3$ )  $\delta = 81.9$  ( $\eta\text{-C}_5\text{H}_3$ , C- $\text{SiMe}_3$ ), 81.8 ( $\eta\text{-C}_5\text{H}_3$ ), 80.3 ( $\eta\text{-C}_5\text{H}_3$ ), 77.2 ( $\eta\text{-C}_5\text{H}_3$ ), 33.4 (Cp C-Si), 0.13 (- $\text{SiMe}_3$ ), - 2.9 (- $\text{GeMe}_2$ ) ppm;  $^1\text{H}$  NMR ( $\text{CDCl}_3$ )  $\delta = 4.3$  (two ps. q, 4 H, Cp), 4.0 (ps. tr, 2 H, Cp), 0.71 (s, 6H,  $\text{GeMe}_2$ ), 0.21 (s, 18 H,  $\text{SiMe}_3$ ) ppm; MS (EI, 70 eV)  $m/e$  (%) 432 (100,  $\text{M}^+$ ), 417 (38,  $\text{M}^+ - \text{CH}_3$ ), 403 (12,  $\text{M}^+ - \text{CH}_3$ , -  $\text{CH}_2$ ).

For polymer **7**:  $[\text{Fe}(\eta\text{-C}_5\text{H}_3\text{SiMe}_3)_2\text{GeMe}_2]_n$  Red-orange powder:  $^{29}\text{Si}$  NMR ( $\text{C}_6\text{D}_6$ )  $\delta = -2.6$  (br s,  $\text{SiMe}_3$ , 2 Si) ppm;  $^{13}\text{C}$  NMR ( $\text{C}_6\text{D}_6$ )  $\delta = 78.1$  (br s, Cp), 77.9 (br s, Cp), 75.3 (br s, Cp), 74.9 (br s, Cp), 74.3 (Cp), 1.1 (- $\text{GeMe}_2$ ), 0.8 (- $\text{SiMe}_3$ ) ppm;  $^1\text{H}$  NMR ( $\text{C}_6\text{D}_6$ )  $\delta = 4.03$  (br s, 2 H, Cp), 3.95 (br s, 2 H, Cp), 3.47 (s, 2 H, Cp), 0.75 (br s, 6 H,  $\text{GeMe}_2$ ), 0.17 (br s, 18 H,  $\text{SiMe}_3$ ) ppm; Anal. Calcd: C 50.0, H 6.99, Found: C 50.7, H 6.91: GPC:  $M_w = 5.8 \times 10^4$ ,  $M_n = 2.7 \times 10^4$ , polydispersity ( $M_w/M_n$ ) = 2.1; WAXS:  $d = 9.55 \text{ \AA}$ .

### Low Angle Laser Light Scattering Measurements for **5a**

Static light scattering experiments in the low angle regime were used to determine the weight average molecular weight  $M_w$  and the second virial coefficient  $A_2$  of a sample of **5a**. The values of  $M_w$  were obtained from the Rayleigh-Debye relationship, in the limit of low scattering angles,  $\theta$ :<sup>36</sup>

$$Kc/R_\theta = 1/M_w + 2A_2c \quad (1)$$

where  $c$  is the concentration of the polymer,  $R_\theta$  is the measured Rayleigh ratio,  $A_2$  is the second virial coefficient, and  $K$  is an optical constant defined as:

$$K = [4\pi^2 n^2 / (N_0 \lambda_0^4)] (dn/dc)^2 \quad (2)$$

where  $n$  is the refractive index of the solvent,  $\lambda_0$  is the wavelength of the laser light in vacuum,  $N_0$  is the Avogadro number, and  $dn/dc$  is the refractive index increment of the polymer solution. Refractive index increment measurements were performed at five different concentrations in THF at 23 °C and a value of  $dn/dc = (0.1674 \pm 0.0001)$  ml/g was obtained.

#### **Transition Metal Catalyzed Polymerization of 4a.**

To a  $C_6D_6$  solution of **4a** (0.10 g, 0.35 mmol) was added 0.05 equiv. of  $PtCl_2$ . The solution was allowed to stir over 4 h at 25 °C by which time the polymerization was judged to be > 90 % complete by  $^1H$  NMR. The solvent was removed under high vacuum. The polymer was redissolved in THF and precipitated into hexanes. Yield: 0.092 g (92 %). The  $^1H$  NMR data was consistent with the assigned structure.<sup>9</sup> GPC:  $M_w = 3.2 \times 10^5$ ,  $M_n = 1.4 \times 10^5$  polydispersity ( $M_w/M_n$ ) = 2.4.

#### **Synthesis of the Copolymer 8.**

**a) By Thermal Copolymerization of 4a and 1** A 1:2 mole ratio of the two solid monomers **4a** (0.14 g, 0.49 mmol, mp 90 °C) and **2** ( $R = R' = Me$ ) (0.28 g, 1.17 mmol, mp 78 °C) was sealed in an evacuated, Pyrex tube and heated at 90 °C for 10 min. The contents of the tube were then dissolved in THF, filtered and precipitated dropwise into hexanes to yield **8**. Yield: 0.35 g (83 %). GPC: monomodal,  $M_w = 3.2 \times 10^5$ ,  $M_n = 2.1 \times 10^5$  polydispersity ( $M_w/M_n$ ) = 1.5.

#### **b) By Transition Metal-Catalyzed Copolymerization of 4a and 1**

To a  $C_6D_6$  solution of **1** (46 mg, 0.19 mmol) and **4a** (50 mg, 0.17 mmol) in a 5 mm NMR tube was added 0.05 mol % of  $PtCl_2$ . The contents of the tube were shaken and  $^1H$  NMR spectra were taken every 30 min over a period of 3 h. The polymerization at this point was found to be 69 % complete. After a total of 10 h, the reaction was found to be > 90 %

complete. All  $^1\text{H}$  NMR spectra were consistent with literature values for the presence of only **2** ( $\text{R} = \text{R}' = \text{Me}$ ), **4a** and **8** and the rates of depletion of **2** ( $\text{R} = \text{R}' = \text{Me}$ ) and **8** were found to be the same within the limits of  $^1\text{H}$  NMR integration..<sup>9,25</sup> The solvent was removed under high vacuum. The polymer was then redissolved in THF and precipitated into hexanes. Yield: 0.085 g (89 %). GPC: monomodal,  $M_w = 3.6 \times 10^5$ ,  $M_n = 1.2 \times 10^5$  polydispersity ( $M_w/M_n$ ) = 3.0.

The characterization data for **8** formed by thermal ROP and by transition metal-catalyzed ROP showed the copolymers to be identical except for a higher proportion of  $\text{SiMe}_2$  groups in the thermally-generated copolymer due to the composition of the monomer mixture.

For copolymer **8**: Yellow fibrous powder:  $^{29}\text{Si}$  NMR ( $\text{C}_6\text{D}_6$ )  $\delta = -6.38, -6.40, -6.41$  ( $\text{SiMe}_2$ ) ppm;  $^{13}\text{C}$  NMR (in  $\text{C}_6\text{D}_6$ )  $\delta = 74.59, 74.57, 74.53, 74.50$  ( $\text{Ge-Cp}_{\text{ipso}}$ ), 73.64, 73.59 ( $\text{Si-Cp}$ ), 72.93, 72.87 ( $\text{Ge-Cp}$ ), 71.86, 71.84, 71.80 ( $\text{Si-Cp}_{\text{ipso}}$ ), 71.77, 71.61 ( $\text{Si-Cp}$ ), 71.18, 71.01 ( $\text{Ge-Cp}$ ), -0.42, -0.44, -0.47 ( $\text{SiMe}_2$ ), -1.09, -1.11, -1.13 ( $\text{GeMe}_2$ ) ppm.  $^1\text{H}$  NMR (in  $\text{C}_6\text{D}_6$ )  $\delta = 4.26$  (s, 4H, Cp), 4.10 (s, 4H, Cp), and 0.64 (s, 6H,  $\text{GeMe}_2$ ), 0.55 (s, 6H,  $\text{SiMe}_2$ ) ppm. MS of hexanes soluble extract of the product formed by the TROP of **2** ( $\text{R} = \text{R}' = \text{Me}$ ) and **4a**.  $m/e < 1300$  (relative intensity) 1152 (33,  $\text{Ge}_4$ ), 1060 (17,  $\text{Si}_2\text{Ge}$ ), 818 (17,  $\text{SiGe}$ ), 576 (33,  $\text{Ge}_2$ ), 484 (100,  $\text{Si}_2$ ). Pyrolysis-mass spectrometry (in situ), (errors of up to 2  $m/e$  are likely above  $m/e$  1000)  $m/e$  1720 ( $\text{Ge}_6$ ), 1674 ( $\text{SiGe}_5$ ), 1584 ( $\text{Si}_3\text{Ge}_3$ ), 1542 ( $\text{Si}_4\text{Ge}_2$ ), 1496 ( $\text{Si}_5\text{Ge}$ ), 1432 ( $\text{Si}_5$ ), 1388 ( $\text{SiGe}_4$ ), 1343 ( $\text{Si}_2\text{Ge}_3$ ), 1299 ( $\text{Si}_3\text{Ge}_2$ ), 1255 ( $\text{Si}_4\text{Ge}$ ), 1209 ( $\text{Si}_5$ ), 1145 ( $\text{Ge}_4$ ), 1101 ( $\text{SiGe}_3$ ), 1057 ( $\text{Si}_2\text{Ge}_2$ ), 1013 ( $\text{Si}_3\text{Ge}$ ), 967 ( $\text{Si}_4$ ), 859 ( $\text{Ge}_3$ ), 815 ( $\text{SiGe}_2$ ), 771 ( $\text{Si}_2\text{Ge}$ ), 725 ( $\text{Si}_3$ ), 573 ( $\text{Ge}_2$ ), 483 ( $\text{Si}_2$ ), 287 ( $\text{Ge}$ ), 242 ( $\text{Si}$ ). Note  $\text{Si} = \{\text{Fe}(\eta\text{-C}_5\text{H}_4)_2\text{SiMe}_2\}$  and  $\text{Ge} = \{\text{Fe}(\eta\text{-C}_5\text{H}_4)_2\text{GeMe}_2\}$ ; WAXS:  $d = 6.37 \text{ \AA}$ .

**Synthesis of the Model Compound 10c.** Freshly distilled  $\text{Me}_3\text{GeCl}$  (1.0 mL, 8.2 mmol) was added to a suspension of dilithioferrocene•TMEDA (1.00 g, 3.62 mmol) in ether (100 ml) at  $-78 \text{ }^\circ\text{C}$ . The reaction mixture was allowed to warm up to room temperature and stir

overnight. The solvent was removed under high vacuum. The product was dissolved in hexanes and filtered through a frit. The hexanes were removed under high vacuum and any residual ferrocene or TMEDA were removed by leaving the product under high vacuum overnight. The product was purified by vacuum distillation (0.005 mm Hg, 83 °C) Yield 0.84 g (77 %). For **10c**:  $^{13}\text{C}$  NMR ( $\text{C}_6\text{D}_6$ )  $\delta = 74.8$  (Ge-Cp<sub>ipso</sub>), 72.4 (Cp), 70.7 (Cp), -0.7 (GeMe<sub>3</sub>) ppm;  $^1\text{H}$  NMR ( $\text{C}_6\text{D}_6$ )  $\delta = 4.20$  (m, 4H, Cp), 4.01 (m, 4H, Cp), 0.35 (s, 18 H, GeMe<sub>3</sub>) ppm. Low resolution MS (EI, 70 eV) m/e (%) 420 (100, M<sup>+</sup>), 405 (30, M<sup>+</sup> - CH<sub>3</sub>); 288 (68, M<sup>+</sup> - GeMe<sub>3</sub>, - Me) High resolution MS  $\text{C}_{16}\text{H}_{26}^{74}\text{Ge}_2^{56}\text{Fe}$  calcd 421.9822, found 421.9807 .

### 3.6 References

- (1) (a) Pittman, C. U.; Carraher, C. E.; Reynolds, J. R. in *Encyclopedia of Polymer Science and Engineering*; Eds. Mark, H. F.; Bikales, N. M.; Overberger, C. G.; Menges, G.; Wiley: New York, 1989; Vol. 10; p. 541. (b) Sheats J. E.; Carraher, C. E.; Pittman, C. U.; Zeldin M., Currell B.; *Inorganic and Metal-Containing Polymeric Materials*; Plenum: New York, 1989. (c) Gonsalves K. E.; Rausch M. D. in *Inorganic and Organometallic Polymers. ACS Symposium Series 360*; Eds. Zeldin, M.; Wynne, K.; Allcock, H. R. American Chemical Society: Washington, DC. 1988. (d) Allcock, H. R. *Adv. Mater.*, **1994**, *6*, 106.
- (2) a) Fyfe, H. B.; Melkuz, M.; Zargarian, D.; Taylor, N. J.; Marder, T. B. *J. Chem. Soc., Chem. Commun.*, **1991**, 188. b) Wright, M. E.; Sigman, M. S. *Macromolecules*, **1992**, *25*, 6055. (c) Davies, S. J.; Johnson, B. F. G.; Khan, M. S.; Lewis, J.; *J. Chem. Soc., Chem. Commun.*, **1991**, 187. (d) Tenhaeff, S. C.; Tyler, D. R. *J. Chem. Soc., Chem. Commun.*, **1989**, 1459. (e) Manners, I. *J. Chem. Soc., Ann. Rep. Prog. Chem. A.*, **1991**, 77. (f) Neuse, E. W.; Bednarik, L. *Macromolecules*, **1979**, *12*, 187. (g) Sturge, K. C.; Hunter, A. D.; McDonald, R.; Santarsiero, B. D. *Organometallics*, **1992**, *11*, 3056. (h) Gonsalves, K.; Zhan-ru, L.; Rausch, M. D. *J. Am. Chem. Soc.*, **1984**, *106*, 3862. (i) Katz, T. J.; Sudhakar, A.; Teasley, M. F.; Gilbert, A. M.; Geiger, W. E.; Robben, M. P.; Wuensch, M.; Ward, M. D. *J. Am. Chem. Soc.*, **1993**, *115*, 3182. (j) Nugent, H. M.; Rosenblum, M. *J. Am. Chem. Soc.*, **1993**, *115*, 3848. (k) Patterson, W. J.; McManus, S. P.; Pittman, C. U. *J. Polym. Sci.: Poly. Chem. Ed.*, **1974**, *12*, 837.
- (3) Brandt, P. F.; Rauchfuss, T. B. *J. Am. Chem. Soc.* **1992**, *114*, 1926.
- (4) Manners, I. *Adv. Mater.* **1994**, *6*, 68.
- (5) Manners, I. *Adv. Organomet. Chem.* **1995**, *37*, 131.
- (6) Compton, D. L.; Rauchfuss, T. B. *Organometallics* **1994**, *13*, 4367.
- (7) Foucher, D. A.; Tang, B.-Z.; Manners, I. *J. Am. Chem. Soc.* **1992**, *114*, 6246.
- (8) Foucher, D. A.; Manners, I. *Makromol. Chem., Rapid Commun.* **1993**, *14*, 63.

- (9) Foucher, D. A.; Edwards, M.; Burrow, R. A.; Lough, A. J.; Manners, I. *Organometallics* **1994**, *13*, 4959.
- (10) Foucher, D. A.; Honeyman, C. H.; Nelson, J. M.; Tang, B.-Z.; Manners, I. *Angew. Chem., Int. Ed. Engl.* **1993**, *32*, 1709.
- (11) Honeyman, C. H.; Foucher, D. A.; Dahmen, F. Y.; Rulkens, R.; Lough, A. J.; Manners, I. *Organometallics* **1995**, *14*, 5503.
- (12) Pudelski, J.; Gates, D. P.; Rulkens, R.; Lough, A.; Manners, I. *Angew. Chem., Int. Ed. Engl.* **1995**, *34*, 1506.
- (13) Nelson, J. M.; Rengel, H.; Manners, I. *J. Am. Chem. Soc.* **1993**, *115*, 7035.
- (14) Nelson, J. M.; Lough, A. J.; Manners, I. *Angew. Chem., Int. Ed. Engl.* **1994**, *33*, 989.
- (15) Pudelski, J. K.; Rulkens, R.; Foucher, D. A.; Lough, A. J.; MacDonald, P. M.; Manners, I. *Macromolecules* **1995**, *28*, 7301.
- (16) Fossum, E.; Matyjaszewski, K.; Rulkens, R.; Manners, I. *Macromolecules* **1995**, *28*, 401.
- (17) Hultsch, K. C.; Nelson, J. M.; Lough, A. J.; Manners, I. *Organometallics* **1995**, *14*, 5496.
- (18) Rulkens, R.; Lough, A. J.; Manners, I. *J. Am. Chem. Soc.* **1994**, *116*, 797.
- (19) Rulkens, R.; Ni, Y.; Manners, I. *J. Am. Chem. Soc.* **1994**, *116*, 12121.
- (20) Ni, Y.; Rulkens, R.; Pudelski, J. K.; Manners, I. *Makromol. Chem., Rapid Commun.* **1995**, *14*, 637.
- (21) A preliminary account of some of the work reported in this paper has been published; see refs. 8 & 9
- (22) Osborne, A. G.; Whiteley, R. H.; Meads, R. E. *J. Organomet. Chem.* **1980**, *193*, 345.
- (23) Peckham, T. J.; Foucher, D. A.; Lough, A. J.; Manners, I. *Can. J. Chem.* **1995**, *73*, 2069.



- (24) Brown, R. A.; Houlton, A.; Roberts, R. M. G.; Silver, J.; Frompton, C. S. *Polyhedron* **1992**, *11*, 2611.
- (25) Finckh, W.; Tang, B.-Z.; Foucher, D. F.; Zamble, D. B.; Ziembinski, R.; Lough, A.; Manners, I. *Organometallics* **1993**, *12*, 823.
- (26) Grubisic, Z.; Rempp, P.; Benoit, H. *J. Polym. Sci.* **1967**, *B5*, 753.
- (27) Foucher, D. A.; Ziembinski, R.; Tang, B. Z.; Macdonald, P. M.; Massey, J.; Jaeger, R.; Vancso, G. V.; Manners, I. *Macromolecules* **1993**, *26*, 2878.
- (28) Pudelski, J. K.; Foucher, D. A.; Macdonald, P. M.; Honeyman, C. H.; Manners, I. *Macromolecules* **1995**, *29*, 1894.
- (29) Foucher, D.; Ziembinski, R.; Petersen, R.; Pudelski, J.; Edwards, M.; Ni, Y.; Massey, J.; Jaeger, C. R.; Vancso, G. J.; Manners, I. *Macromolecules* **1994**, *27*, 3992.
- (30) Pittman, C. U.; Lai, J. C.; Vanderpool, D. P.; Good, M.; Prado, R. *Macromolecules* **1970**, *3*, 746.
- (31) Foucher, D. A.; Ziembinski, R.; Rulkens, R.; Nelson, J.; Manners, I. In *Inorganic and Organometallic Polymers II*; P. Wisian-Neilson, H. R. Allcock and K. J. Wynne, Eds.; American Chemical Society: Washington, D. C., 1994; Vol. ACS Symposium Series 572; pp 442.
- (32) Nguyen, M. T.; Diaz, A. F.; Dement'ev, V. V.; Pannell, K. H. *Chem Mater.* **1993**, *5*, 1389.
- (33) Okuda, J.; Herdtweck, E. *J. Organomet. Chem.* **1989**, *373*, 99.
- (34) Foucher, D. A.; Nelson, J. M.; Honeyman, C. H.; Lough, A. J.; Manners, I. *Acta Cryst. C.* **1995**, *C51*, 1795.
- (35) Rulkens, R.; Gates, D. P.; Balaishis, D.; Pudelski, J. K.; McIntosh, D. F.; Lough, A. J.; Manners, I. *J. Am. Chem. Soc.* **1997**, *119*, 10976.
- (36) Kerker, M. *The Scattering of Light and Other Electromagnetic Radiation*; Academic Press: San Diego, 1969, .

## Chapter 4 Ring-Opening Polymerization of a Phosphonium-Bridged, [1]Ferrocenophane: Synthesis and Properties of an Ionomeric Poly(ferrocene)

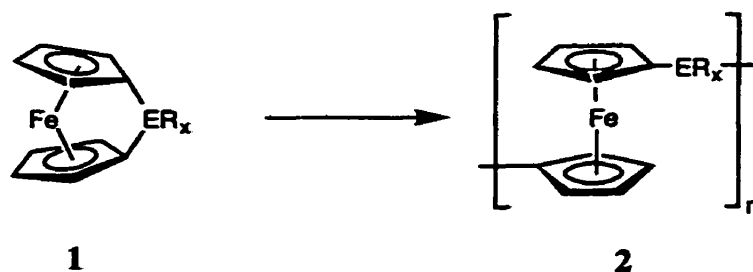
### 4.1 Abstract

A stable phosphonium-bridged, [1]ferrocenophane  $[\text{Fe}(\eta\text{-C}_5\text{H}_4)_2\text{PPhMe}][\text{OTf}]$  (**10b**) was synthesized by the reaction of the phosphorus-bridged [1]ferrocenophane  $\text{Fe}(\eta\text{-C}_5\text{H}_4)_2\text{PPh}$  (**3a**) with methyl triflate (MeOTf). A single crystal X-ray diffraction study of **10b** revealed an angle of  $24.4(5)^\circ$  between the planes of the cyclopentadienyl rings, less than the respective angle ( $26.7^\circ$ ) for **3a**. Compound **10b** and a number of other tetra-coordinate, phosphorus-bridged [1]ferrocenophanes,  $\text{Fe}(\eta\text{-C}_5\text{H}_4)_2\text{P(S)Ph}$  (**5a**),  $\text{Fe}(\eta\text{-C}_5\text{H}_4)_2\text{P}[\text{Fe}(\text{CO})_4]\text{Ph}$  (**6**) and  $[\text{Fe}(\eta\text{-C}_5\text{H}_4)_2\text{FpPh}][\text{PF}_6]$  (**7**), (where  $\text{Fp} = (\eta\text{-C}_5\text{H}_5)\text{Fe}(\text{CO})_2$ ) were tested for their ring-opening polymerization (ROP) behaviour. Only compound **10b** was found to undergo ROP which took place both thermally and in the presence of a transition metal catalyst ( $\text{PtCl}_2$ ). The resultant ionomeric polymer  $\{[\text{Fe}(\eta\text{-C}_5\text{H}_4)_2\text{PPhMe}][\text{OTf}]\}_n$  (**11**) was found to be soluble in methanol, dimethylformamide (DMF), dimethylsulfoxide (DMSO) and acetone but displayed only limited stability in these solvents. The polymer was found to possess a glass transition temperature of  $176^\circ\text{C}$  and was thermally stable to weight loss up to ca.  $400^\circ\text{C}$ . Analysis by wide angle X-ray scattering (WAXS) revealed that the polymer was amorphous. A study on the partial to full methylation of the polymer  $[\text{Fe}(\eta\text{-C}_5\text{H}_4)_2\text{PPh}]_n$  (**14**) gave results that were consistent with the results of the ROP of **10b**. Dynamic light scattering studies on polymer **11** produced via thermal ROP and transition metal-catalyzed ROP gave hydrodynamic radii in the range of 30 - 45 nm which suggested that the compounds were polymeric rather than oligomeric in nature. Based on the glass transition temperatures for a series of samples of polymer **11** of known molecular weight with varying number of repeat units (from 20 to 100), the molecular

weight ( $M_n$ ) of the transition metal-catalyzed ROP product was greater than 46 000 (ca. 100 repeat units) and the molecular weight of the thermally produced polymer was of even higher.

## 4.2 Introduction

Transition metal-containing polymers remain an area of active research due to the potential for obtaining materials with possibly useful physical or catalytic properties that are not easily obtainable with most organic polymer systems.<sup>1-3</sup> We have previously shown that ring-opening polymerization (ROP) of strained [1]ferrocenophanes (**1**) represents a general route to high molecular weight poly(ferrocenes) (**2**).<sup>4-11</sup> The polymerization behaviour of the silicon-bridged monomers (**1**,  $ER_x = SiRR'$ ) is particularly well-developed with a variety of possible substituents at silicon,<sup>5,12-14</sup> and thermal, anionic<sup>15</sup> and transition metal-catalyzed<sup>16</sup> ROP routes to the interesting polymers **2** ( $ER_x = SiRR'$ ) are all known.

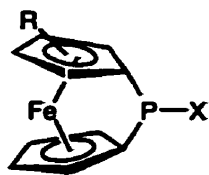


E = Si, Ge, Sn, S, B, etc.

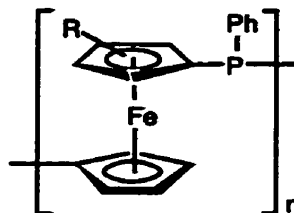
### Reaction 4.1 Synthesis of Poly(ferrocenes)

The ROP behaviour of phosphorus-bridged [1]ferrocenophanes (**3a**) has also been studied. Thus, thermal ROP of **3a** - **3b** to afford polymers **4a** - **4b** was reported by our group in 1995.<sup>10</sup> More recently, we have also reported that high molecular weight

poly(ferrocenylphosphines) and related block copolymers can be obtained via living anionic ROP of **3a**.<sup>17,18</sup> To date, no transition metal-catalyzed routes have been found as all known catalysts simply coordinate to the P(III) centre of **3a** without leading to ROP.

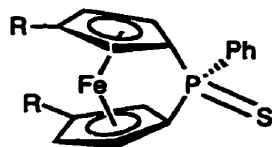


**3a** (R = H, X = Ph)  
**b** (R = *n*-Bu, X = Ph)  
**c** (R = H, X = Cl)

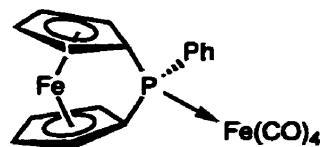


**4a** (R = H)  
**b** (R = *n*-Bu)

The interesting chemistry of compound **3a** has been explored by a number of groups, particularly by Seyferth *et al.* who were able to coordinate a number of different moieties to the phosphorus, including sulfur to give (**5a**) and Fe(CO)<sub>4</sub> moieties to give (**6**).<sup>19</sup>

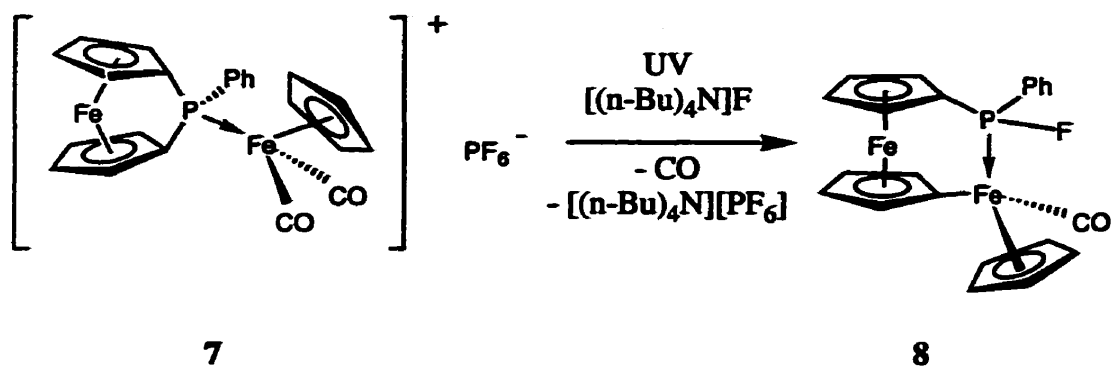


**5a** (R = H)  
**b** (R = SiMe<sub>3</sub>)



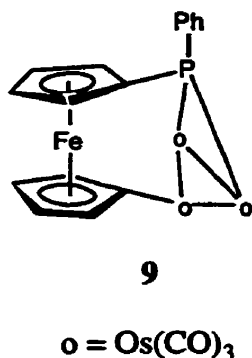
**6**

Nakazawa, Miyoshi *et al.* found that upon coordination of Fe( $\eta^5$ -C<sub>5</sub>H<sub>5</sub>)(CO)<sub>2</sub> to the bridging phosphorus atom (to give **7**), irradiation with UV light led to ring-opening and formation of **8** in the presence of [(*n*-Bu)<sub>4</sub>N]F with the concomitant loss of CO and formation of [(*n*-Bu)<sub>4</sub>N][PF<sub>6</sub>]. The formation of polymer, however, was not reported.<sup>20</sup>



#### Reaction 4.2 Ring-Opening of a Phosphorus-Bridged, [1]Ferrocenophane

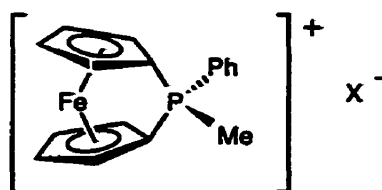
Ring-opening of 3a in the presence of a transition metal has also been reported by Cullen *et al.*<sup>21</sup> This involved the thermal reaction (125 °C) of 3a with  $\text{Os}_3(\text{CO})_{12}$  which resulted in the major product,  $\text{Os}_3(\text{CO})_9[\mu_3\text{-(C}_5\text{H}_4\text{PPh)Fe(C}_5\text{H}_4)]$  (9), as well as a number of other minor products. It is unclear as to whether the transition metal actually facilitated the ring-opening as the reaction conditions (refluxing octane) could have easily led to thermal ring-opening as the thermal ROP is known to occur at similar temperatures (ca. 130 °C).



Another potentially interesting tetra-coordinate, phosphorus-bridged, [1]ferrocenophane, 10a, was described by Seyferth *et al.*<sup>19</sup>. This compound was synthesized by the reaction of 3a with MeI. Although the compound was characterized by  $^{31}\text{P}$  and  $^1\text{H}$

NMR, no crystals suitable for X-ray analysis could be grown and the compound was reported to be unstable in solution.

We now wish to report on our studies of the ROP behaviour, particularly by transition metal catalysts, of several tetra-coordinate, phosphorus-bridged, [1]ferrocenophanes (**5**, **6**, **7**) as well as our preparation of **10b**, a more stable analogue of **10a** with a triflate counterion and our ROP studies on this species.



**10a** (X = I)  
**b** (X = OTf)

### 4.3 Results and Discussion

#### 4.3.1 Attempted Transition Metal Catalyzed ROP of [1]Ferrocenophanes **5a**, **6** and **7**

Although thermal ROP of phosphorus-bridged [1]ferrocenophanes has been reported previously by our group, only bis(trimethylsilyl)sulfide and low molecular weight material could be isolated from an otherwise insoluble product from the thermal ROP for **5b**.<sup>10</sup> In light of this evidence, it was thought that an attempt to thermally ROP **5a** would lead to the formation of H<sub>2</sub>S, a possible safety hazard. As expected, no formation of polymer was observed on attempted transition metal-catalyzed polymerization in solution using either Pt(II) (PtCl<sub>2</sub>) or Pt(0) (Karstedt's catalyst) initiators.

Similarly, the thermal ROPs of **6** and **7** were avoided due to the possibility for the release of CO. Transition metal-catalyzed experiments with both PtCl<sub>2</sub> and Karstedt's

catalyst also did not lead to the formation of polymer in the case of either compound. We then decided to investigate the ROP behaviour of phosphonium-bridged, [1]ferrocenophanes.

#### 4.3.2 The Synthesis and Characterization of 10b

As mentioned above, Seyferth reported that the treatment of **3a** with MeI led to the formation of **10a** which was reported to be unstable in solution.<sup>19</sup> In light of the sensitivity of **3a** to nucleophiles, we attempted to synthesize a derivative of **10a** with a less active counteranion.

Our choice of methyl triflate as a methylating reagent proved to be successful. Compound **10b** was isolated in high yield and characterized by <sup>1</sup>H, <sup>13</sup>C, <sup>19</sup>F and <sup>31</sup>P NMR as well as elemental analysis, which were all consistent with the proposed structure. The compound was also found to be stable in solution under N<sub>2</sub> and could be isolated as dark red microcrystals suitable for single crystal X-ray analysis by recrystallization from a THF/CH<sub>2</sub>Cl<sub>2</sub> mixture. Additionally, the compound was found to be stable to air and moisture in the solid state but decomposed slowly over several hours in solution.

An examination of the NMR data revealed some interesting features. The <sup>1</sup>H NMR spectrum of **10b** has four distinct resonances due to four inequivalent cyclopentadienyl (Cp) protons. This is in contrast to the corresponding spectrum of **3a** in which only three resonances are seen in the Cp region. The phenyl region for **10b** is also more distinct than that for **3a** and, in addition, displays a coupling pattern consistent with a monosubstituted benzene ring attached to a phosphonium centre. Perhaps most revealing in the <sup>1</sup>H NMR spectrum is the doublet at 2.66 ppm due to a methyl group attached directly to phosphorus (<sup>2</sup>J<sub>PH</sub> = 13.9 Hz). The resonance at 37.5 ppm in the <sup>31</sup>P NMR spectrum is in agreement with a tetra-substituted phosphorus centre (cf. resonance for **3a** is at 13 ppm) and almost the same shift (37 ppm) found for **10a**<sup>19</sup>. The data provided by the <sup>13</sup>C NMR spectrum is similarly

consistent with the structure proposed for **10b**, especially the upfield shifted ipso carbons of the cyclopentadienyl rings as has been commonly seen in the strained [1]ferrocenophanes.

#### 4.3.3 Single Crystal X-ray Diffraction Study of **10b**

Crystals of **10b** suitable for a single crystal X-ray diffraction study were obtained from a THF/CH<sub>2</sub>Cl<sub>2</sub> mixture at -30 °C. Only very small crystals of the sample (0.18 x 0.04 x 0.03 mm) were available for data collection. Data were collected on a Nonius Kappa-CCD using graphite monochromated MoK $\alpha$  radiation ( $\lambda = 0.71073$  Å). 180 frames, of 1° rotations of phi, were exposed for 90 seconds each. There were no measureable data higher than 21° in  $\theta$ . The data were integrated and scaled using the DENZO package.<sup>22</sup> The structures were solved and refined using the SHELXTL\PC package.<sup>23</sup> Refinement was by full-matrix least-squares on F<sup>2</sup> using all data (negative intensities included). The weighing scheme was  $w = 1/[\sigma^2(F_o^2) + (0.0699)^2 + 25.07P]$  where  $P = (F_o^2 + 2F_c^2)/3$ . Hydrogen atoms were included in calculated positions. A view of the molecular structure is shown in Figure 4.1. Table 4.2 gives selected structural data for **10b** as well as for related phosphorus-bridged [1]ferrocenophanes. The angles  $\alpha$ ,  $\beta$ ,  $\theta$  and  $\delta$  are defined in Figure 4.2. The summary of the crystal data and collection parameters is found in Table 4.1. Tables of the fractional coordinates, bond lengths and selected angles are found in Tables 4.3 - 4.5 respectively.

The single crystal X-ray diffraction study agrees with the structure assigned to **10b**. Disordered CH<sub>2</sub>Cl<sub>2</sub> molecules were found to be included within the unit cell. However, no significant interaction was found between the ferrocenophane moiety and either CH<sub>2</sub>Cl<sub>2</sub> or the triflate counterion. In comparison to other phosphorus-bridged, [1]ferrocenophanes, **10b** possesses the smallest tilt angle yet known for such a species (24.4(5)°). This value is even smaller than for the phosphorus(V)-bridged species **5b** (25.3(3)°). Perhaps most interesting to note is that the very short Fe-P distance of 2.577(3) Å, shorter than even for **5b** (2.688 (2) Å). This may indicate that there is a greater iron-phosphorus interaction occurring in this compound than in previous examples of phosphorus-bridged, [1]ferrocenophanes.



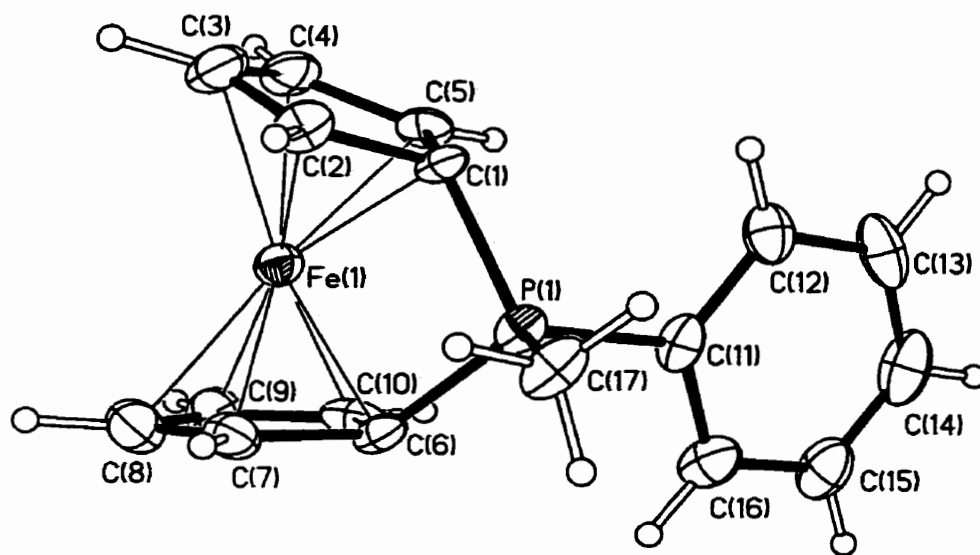


**Figure 4.1** Molecular Structure of **10b** (vibrational ellipsoids at 25 % probability level)

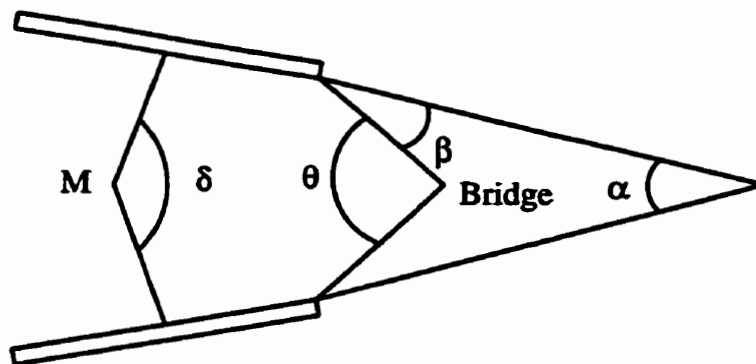


**Figure 4.2** Distortions in Group 8 Metallocenophanes:  
Defining Angles  $\alpha$ ,  $\beta$ ,  $\gamma$  and  $\delta$

**Table 4.1. Summary of Crystal Data and Intensity Collection  
Parameters for 10b**

empirical formula	$C_{18.5}H_{16}ClF_3FeO_3PS$
formula weight	497.64
wavelength (Å)	0.71073
crystal system	monoclinic
space group	$C2/c$
a (Å)	23.380(1)
b (Å)	13.339(1)
c (Å)	12.715(1)
$\alpha$ (deg)	90
$\beta$ (deg)	91.79(1)
$\gamma$ (deg)	90
V (Å <sup>3</sup> )	3963.4(14)
Z	8
$\rho$ (calculated) (g cm <sup>-3</sup> )	1.668
absorption coefficient (mm <sup>-1</sup> )	1.127
F(000)	2016
crystal size (mm)	0.18 x 0.04 x 0.03
$\theta$ range for data collection (deg)	2.40 to 20.90
reflections collected	7331
independent reflections	2052 ( $R_{int} = 0.1013$ )
data/restraints/parameters	2052/0/268
goodness-of-fit on $F^2$	1.077
final R indices [ $I > 2\sigma(I)$ ]	$R1 = 0.0569$ , $wR2 = 0.1421$
R indices (all data)	$R1 = 0.1023$ , $wR2 = 0.1640$
extinction coefficient	0.0007(2)
largest diff. peak and hole (eÅ <sup>-3</sup> )	0.510 and -0.411

**Table 4.2. Selected Structural Parameters for 10b and Related Phosphorus-Bridged, [1]Ferrocenophanes, With Esd's in Parentheses (Where Available)**

	Compound				
	3a	3b	3c	5b	10b
Fe-P dist (Å)	2.774(3)	2.784(2)	2.715(6)	2.688(2)	2.577(3)
Fe displacement (Å)		0.291(7)	0.277(8)	0.259(2)	0.232(9)
P-C (C <sub>p</sub> <sub>ipso</sub> ) (av) (Å)	1.842(13)	1.857(8)	1.841(20)	1.812(5)	1.772(10)
ring tilt $\alpha$ (deg)	26.7	27.0(6)	27.5(6)	25.3(3)	24.4(5)
$\beta$ (av) (deg)	32.5	32.0(3)	31.9(7)	35.0(4)	37.9(4)
$\theta$ (av) (deg)	90.6(3)	95.7(4)	90.1(7)	95.0(2)	99.8(4)
$\delta$ (av) (deg)	159.8	159.5(3)	160.4(6)	161.8(2)	163.6(4)
ref.	24	10	10	10	this work

**Table 4.3 Atomic Coordinates ( $\times 10^4$ ) and Equivalent Isotropic Displacement Coefficients ( $\text{Å}^2 \times 10^3$ ) for the Non-Hydrogen Atoms of 10b with Esd's in Parentheses**

	x	y	z	U(eq)
Fe(1)	-1267(1)	-2663(1)	10328(1)	36(1)
P(1)	-1292(1)	-4063(2)	8930(2)	34(1)
C(1)	-1380(4)	-2753(6)	8781(7)	33(2)
C(2)	-896(4)	-2130(7)	9032(7)	41(3)
C(3)	-1095(5)	-1320(7)	9599(8)	51(3)
C(4)	-1680(5)	-1407(7)	9740(8)	49(3)
C(5)	-1871(4)	-2287(7)	9227(7)	37(2)
C(6)	-1176(4)	-4130(6)	10316(7)	33(2)
C(7)	-666(4)	-3648(7)	10783(8)	44(3)
C(8)	-820(5)	-3139(8)	11679(9)	57(3)

C(9)	-1415(5)	-3227(8)	11828(8)	55(3)
C(10)	-1634(4)	-3822(7)	11007(8)	45(3)
C(11)	-1943(4)	-4681(7)	8549(8)	37(3)
C(12)	-2275(4)	-4320(8)	7723(8)	49(3)
C(13)	-2782(5)	-4835(10)	7443(9)	65(3)
C(14)	-2929(5)	-5670(10)	7980(11)	66(4)
C(15)	-2594(5)	-6014(8)	8783(10)	59(3)
C(16)	-2101(4)	-5526(7)	9096(8)	50(3)
C(17)	-696(4)	-4517(7)	8256(8)	48(3)
C(1S)	-4100(6)	-3133(11)	5169(11)	73(4)
O(2)	-3545(3)	-1987(5)	3982(6)	68(2)
S(1)	-4112(1)	-2078(2)	4325(3)	54(1)
F(1)	-4609(4)	-3306(7)	5536(7)	133(4)
F(2)	-3728(5)	-3001(9)	5958(8)	163(4)
F(3)	-3932(4)	-3924(6)	4759(8)	142(4)
O(1)	-4281(4)	-1336(7)	4993(10)	134(4)
O(3)	-4536(4)	-2334(8)	3547(8)	126(4)
C(2S)	-5000	-5365(15)	7500	169(13)
Cl(1)	-4392(2)	-4677(3)	7707(4)	126(2)

---

Table 4.4 Bond Lengths (Å) for **10b** with Esd's in Parentheses

Fe(1)-C(6)	1.968(8)	Fe(1)-C(10)	1.979(9)
Fe(1)-C(1)	1.979(9)	Fe(1)-C(7)	1.997(9)
Fe(1)-C(2)	2.015(9)	Fe(1)-C(5)	2.020(9)
Fe(1)-C(3)	2.062(9)	Fe(1)-C(4)	2.062(9)
Fe(1)-C(8)	2.083(11)	Fe(1)-C(9)	2.090(10)
Fe(1)-P(1)	2.577(3)	P(1)-C(17)	1.765(9)
P(1)-C(6)	1.768(9)	P(1)-C(6)	1.777(9)
P(1)-C(11)	1.785(9)	C(1)-C(2)	1.432(12)
C(1)-C(5)	1.437(12)	C(2)-C(3)	1.388(13)
C(3)-C(4)	1.389(13)	C(4)-C(5)	1.409(13)
C(6)-C(10)	1.465(12)	C(6)-C(7)	1.465(12)
C(7)-C(8)	1.384(13)	C(8)-C(9)	1.414(14)
C(9)-C(10)	1.395(13)	C(11)-C(12)	1.374(13)
C(11)-C(16)	1.380(13)	C(12)-C(13)	1.405(14)
C(13)-C(14)	1.36(2)	C(14)-C(15)	1.35(2)
C(15)-C(16)	1.372(13)	C(1S)-F(3)	1.246(14)
C(1S)-F(1)	1.311(13)	C(1S)-F(2)	1.319(14)
C(1S)-S(1)	1.770(13)	O(2)-S(1)	1.413(7)
S(1)-O(1)	1.371(9)	S(1)-O(3)	1.420(9)
C(2S)-Cl(1)	1.706(12)	C(2S)-Cl(1) #1	1.706(12)

Table 4.5 Selected Bond Angles for **10b** with Esd's in Parentheses

C(1)-P(1)-C(6)	99.8(4)	C(2)-C(1)-P(1)	117.4(7)
C(1)-P(1)-C(11)	109.4(4)	C(5)-C(1)-P(1)	118.5(6)
C(6)-P(1)-C(11)	110.4(4)	C(2)-C(1)-C(5)	107.2(8)
C(17)-P(1)-C(1)	112.2(4)	C(2)-C(3)-C(4)	110.5(9)
C(17)-P(1)-C(6)	111.5(4)	C(3)-C(2)-C(1)	106.9(8)
C(17)-P(1)-C(11)	112.9(4)		

This is not particularly surprising as the electrophilicity of the phosphorus atom in **10b** is probably greater than in any of the other examples and thus possibly a stronger dative bond from the relatively electron-rich iron atom exists in this situation. This may be partially responsible for the large  $\beta$  angle for this compound (37.9(4) °). However, it should also be noted that the ipso Cp carbon-phosphorus bond length is also shorter in **10b** (1.772(10) Å) than in the other examples. This might also at least be partially responsible for the shorter Fe-P distance as well as the larger  $\beta$  angle.

In comparison to other phosphonium compounds, the geometry and bond lengths in the case of **10b** are fairly typical with expected values in the area of 1.78 Å – 1.83 Å for P-C(sp<sup>2</sup>) and bond angles of 107 to 114°. The P-C(sp<sup>3</sup>) bond length (1.765(9) Å) is somewhat shorter than the expected value (1.80 Å) and the  $\theta$  angle of 99.8(4)° is also smaller than expected for a phosphonium compound although it is a larger angle than found for other phosphorus-bridged, [1]ferrocenophanes. These results may be the effect of the strained nature of this compound. In the case of the  $\theta$  angle, this is probably due to the combined effect of the shorter P-C (Cp-ipso) bond lengths and the possible dative interaction between iron and phosphorus.

#### 4.3.4 Electronic Spectrum and Electrochemical Behaviour of **10b**

The electronic structure of **10b** was examined by UV/vis spectroscopy. The band II  $\lambda_{\text{max}}$  value of 484 nm (in THF; the value in DMF is the same) is significantly blue shifted in comparison to the value of 498 nm (in hexanes) for **3a**. Both values are much higher than was found for ferrocene (440 nm in hexanes). This red shift has been observed previously in other strained, [1]ferrocenophanes and has been at least partially attributed to the tilting of the cyclopentadienyl rings from the planarity of ferrocene and unstrained, bridged ferrocenophanes. EHMO calculations on silicon- and sulfur-bridged, [1]ferrocenophanes as well as ferrocene in which the rings are tilted by the same angle (31.05°) as for the sulfur-

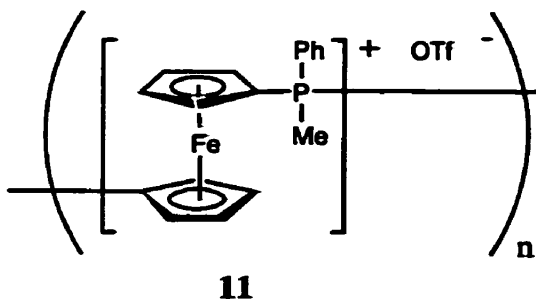
bridged, [1]ferrocenophane illustrate that the HOMO-LUMO gap grows smaller as the tilt angle is increased due to a lowering of the LUMO energy level.<sup>26,27</sup> The smaller tilt angle of **10b** ( $24.4(5)^\circ$ ) in comparison to **3a** ( $26.7^\circ$ ) would appear to agree with these calculations. However, it should also be noted that the iron-phosphorus distance in **10b** ( $2.577(3)$  Å) is significantly shorter than in **3a** ( $2.774(3)$  Å) and there may be also some degree of iron-phosphorus interaction which is influencing the size of the HOMO-LUMO gap in addition to the difference in tilt angle. Some evidence for a dative iron-bridging element bond in ferrocenophanes has been provided in the past by  $^{57}\text{Fe}$  Mössbauer spectroscopy.<sup>26</sup>

Cyclic voltammetry was used to examine the electrochemical behaviour of **10b**. Analysis (in  $\text{CH}_2\text{Cl}_2$ ) revealed one irreversible oxidation wave at ( $E_{\text{p(ox)}}$ )  $+0.72$  V (vs. ferrocene) at a scan rate of  $250$  mV/s. For comparison, the  $E_{1/2}$  value for **1** ( $\text{ER}_x = \text{SiMe}_2$ ) is only  $0.00$  V. This suggests that the phosphonium centre exhibits a strong electron-withdrawing effect on the iron centre. The value of  $+0.72$  V also represents the highest oxidation potential found to date for a [1]ferrocenophane. Measurements were also carried out in DMF. Again, there was only one irreversible wave ( $E_{\text{p(ox)}} = +0.26$  V vs. ferrocene) at a scan rate of  $250$  mV  $\text{s}^{-1}$  with the smaller difference oxidation potential versus ferrocene probably attributable to the donating nature of the solvent (DMF). In contrast to the scan carried out in  $\text{CH}_2\text{Cl}_2$  in which no other compound could be observed other than that for **10b**, the second scan of the solution of **10b** in DMF revealed that one or more uncharacterized products had been formed during the first scan which then subsequently underwent two partially reversible oxidation waves at  $-0.41$  V and  $-0.10$  V (the wave due to **10b** was still visible) at a scan rate of  $250$  mV  $\text{s}^{-1}$ .  $^{31}\text{P}$  NMR and  $^1\text{H}$  NMR analyses of the solution before and after the cyclic voltammetric experiment indicated the presence of only **10b**. These results, as expected, indicated that the compounds formed during the experiment are formed only in the vicinity of the electrode and not in the bulk solution in which **10b** is relatively stable.

### 4.3.5 Thermal ROP Behaviour of 10b

The thermal ROP behaviour of **10b** was first examined by heating a sample under  $N_2$  using a DSC (see Figure 4.3). No melting endotherm was observed. However, a strong exotherm was seen to occur at an onset temperature of  $145\text{ }^\circ\text{C}$  upon heating and no further thermal behaviour was seen during the cooling cycle. The energy of this exotherm (enthalpy of polymerization) was found to be  $61\pm 5\text{ kJ mol}^{-1}$ . By comparison, the enthalpy of polymerization for **3a** was found to be  $68\pm 5\text{ kJ mol}^{-1}$ .

This behaviour led us to believe that thermal ROP of **10b** had taken place leading to formation of **11**.





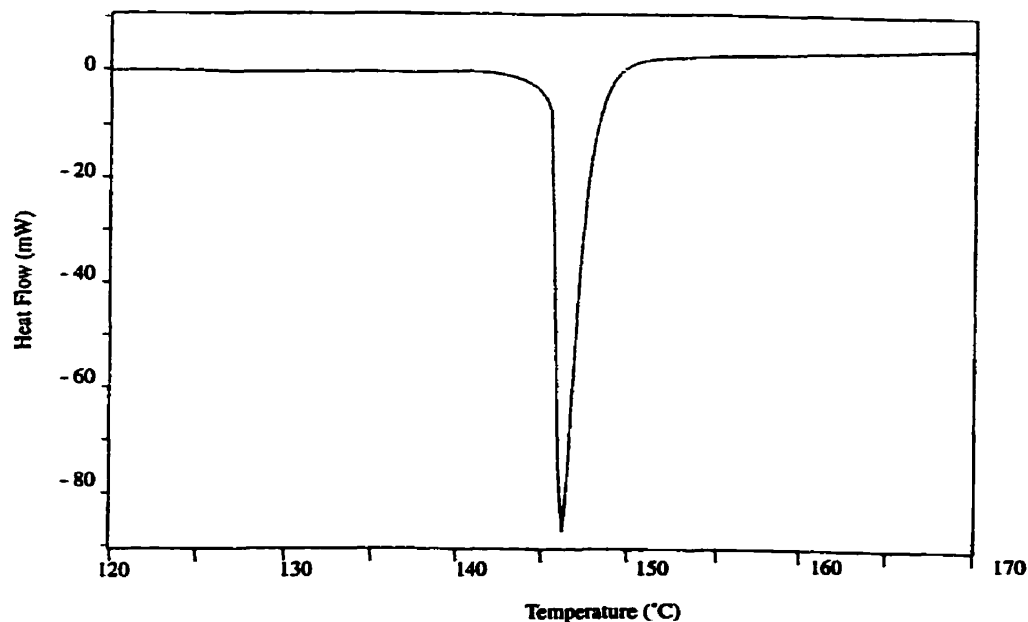


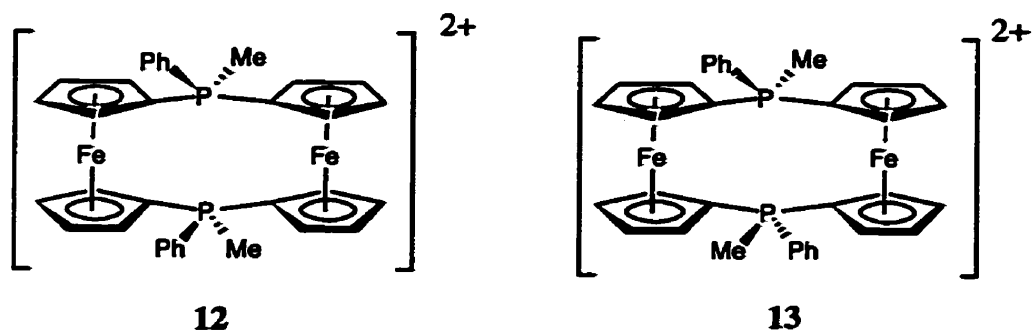
Figure 4.3 DSC Thermogram of **10b**

This ROP experiment was conducted on a preparative scale by heating **10b** in a sealed, evacuated Pyrex tube at 145 °C for 30 min. This led to the formation of a product which was insoluble in ethanol, water and organic solvents such as CH<sub>2</sub>Cl<sub>2</sub>, THF and hexanes but that was soluble in the highly polar solvents DMF, DMSO and acetone (the product was found to be unstable in all the solvents but more so in DMSO, acetone and methanol). Analysis of the product by NMR was consistent with a ring-opened structure. In particular, the <sup>31</sup>P NMR spectrum in DMSO-d<sub>6</sub> showed only one resonance at 23.8 ppm with no sign of any residual monomer ( $\delta = 37.5$  ppm). The <sup>1</sup>H NMR spectrum contained only broad resonances with none of the definition that had been seen for the monomer but which were nonetheless consistent with the assigned structure. For example, the four resonances in the Cp region of **10b** were reduced to three broad resonances. Similarly, the coupling between the methyl

protons and phosphorus could no longer be resolved for **11**. In the case of the  $^{13}\text{C}$  NMR spectrum, the ipso carbon had shifted downfield to 66.5 ppm in comparison to **10b** and was in the region normally associated with Cp carbons in an unstrained system.

#### 4.3.6 Transition Metal-Catalyzed ROP Behaviour of **10b**

It has been previously noted by other research groups that by coordination to the lone pair of the P(III) site or oxidation to P(V) permits facile cleavage of P-C bonds.<sup>20,28-31</sup> With this in mind, we attempted the transition metal-catalyzed ROP of **10b**. In the presence of approx. 10 mol %  $\text{PtCl}_2$ , **10b** was indeed found to undergo ROP and the polymer formed possessed the same NMR characteristics as that formed via thermal ROP. To our knowledge, this represents the first example of a phosphorus-containing ring that undergoes transition metal-catalyzed ROP. However, the yields (ca. 56 %) were significantly lower than those obtainable via thermal ROP (ca. 70 %). We have observed the formation of other products in this reaction which are as of yet unidentified ( $^{31}\text{P}$  NMR spectrum: 25.8 and 25.5 ppm in  $\text{DMSO-d}_6$ ) and appear to be formed in greater amounts with increasing dilution of the reaction solution. In the transition metal-catalyzed ROP of **1** ( $\text{ER}_x = \text{SiMe}_2$ ), cyclic dimers analogous to **1** have been isolated from the reaction mixtures.<sup>32</sup> A similar situation may also occur with the thermal and transition metal-catalyzed ROP of **10b**. The presence of two resonances for the potential dimer may arise from the possibility of *cis* and *trans* isomers, **12** and **13**. Significantly, in the case of the transition metal-catalyzed ROP of **1** ( $\text{E} = \text{SiMeCl}$ ), a cyclic dimer was proposed as a byproduct of the reaction and the two resonances for this dimer observed in the  $^{29}\text{Si}$  NMR spectrum were attributed to *cis* and *trans* isomers.<sup>13</sup>

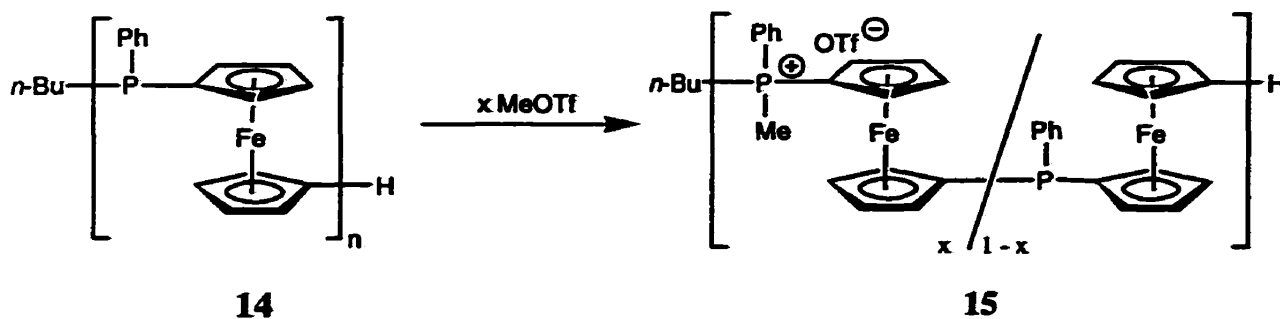


#### 4.3.7 Attempted Copolymerizations of 10b with 1

In an attempt to synthesize a generally more soluble product, we attempted copolymerizations of **10b** with silicon-bridged, [1]ferrocenophanes (**1**,  $ER_x = SiMe_2$ ) using both thermal and transition metal-catalyzed routes. In the case of attempted thermal copolymerization, only the homopolymer **2** ( $ER_x = SiMe_2$ ) and **11** were isolated. For the transition metal-catalyzed polymerizations, only **2** ( $ER_x = SiMe_2$ ) and unreacted **10b** were observed. In each case, absence of copolymerization was proven by the lack of cross-over peaks were observed in the  $^{31}P$  and  $^1H$  NMR spectra of the isolated products.

#### 4.3.8 Methylation of poly(ferrocenylphenylphosphine) **14** as an Alternative Route to **11**

In order to explore an alternative route to **11**, we studied the partial to complete methylation (yielding copolymer **15**) of well-defined, poly(ferrocenylphosphine) (**14**) synthesized via anionic ROP of **3a** using  $n$ -BuLi as an initiator and  $H_2O$  as a termination reagent:



### Reaction 4.3 Methylation of Polymer 14

Partial methylations ranging from 17 % to 50 % methylation of phosphorus sites in the polymer were easily achieved by addition of the appropriate amount of MeOTf to a  $\text{CH}_2\text{Cl}_2$  solution of **14**. At methylations higher than 50 %, it was found that the polymer would precipitate from solution and not undergo further methylations readily. In order to achieve 100 % methylation, it was necessary to first suspend **14** in MeOTf and then add  $\text{CH}_2\text{Cl}_2$ . This resulted in complete methylation for both the high ( $n = 100$ ) and low ( $n = 11$ ) molecular weight samples of **14**.

Figure 4.4 illustrates the effect of increasing methylation of **12** on the  $^{31}\text{P}$  NMR spectrum of the polymer. Even at a low degree of methylations, the presence of the methyl groups at presumably random phosphorus sites along the polymer main chain leads to different environments that were readily distinguishable by NMR. Thus, unmethylated phosphorus nuclei (at ca. -33 ppm) with i) no Me groups on adjacent P sites (-P-fc-P-fc-P-) (where fc =  $(\eta\text{-C}_5\text{H}_4)_2\text{Fe}$  and P = PPh,) ii) one Me group on one adjacent P site on either side (-P<sup>+</sup>-fc-P-fc-P-) (where P<sup>+</sup> = PMePh<sup>+</sup>) and iii) Me groups on both of the adjacent P sites (-P<sup>+</sup>-fc-P-fc-P<sup>+</sup>-) were detected. Analogous resonances were observed for the methylated P sites at ca. 24 ppm. At 0 % methylation, as expected, only one resonance was detected. At 17 % methylation, there is one resonance for the methylated P sites as well as three resonances for the free P sites corresponding to situations i) - iii) with i) being the most

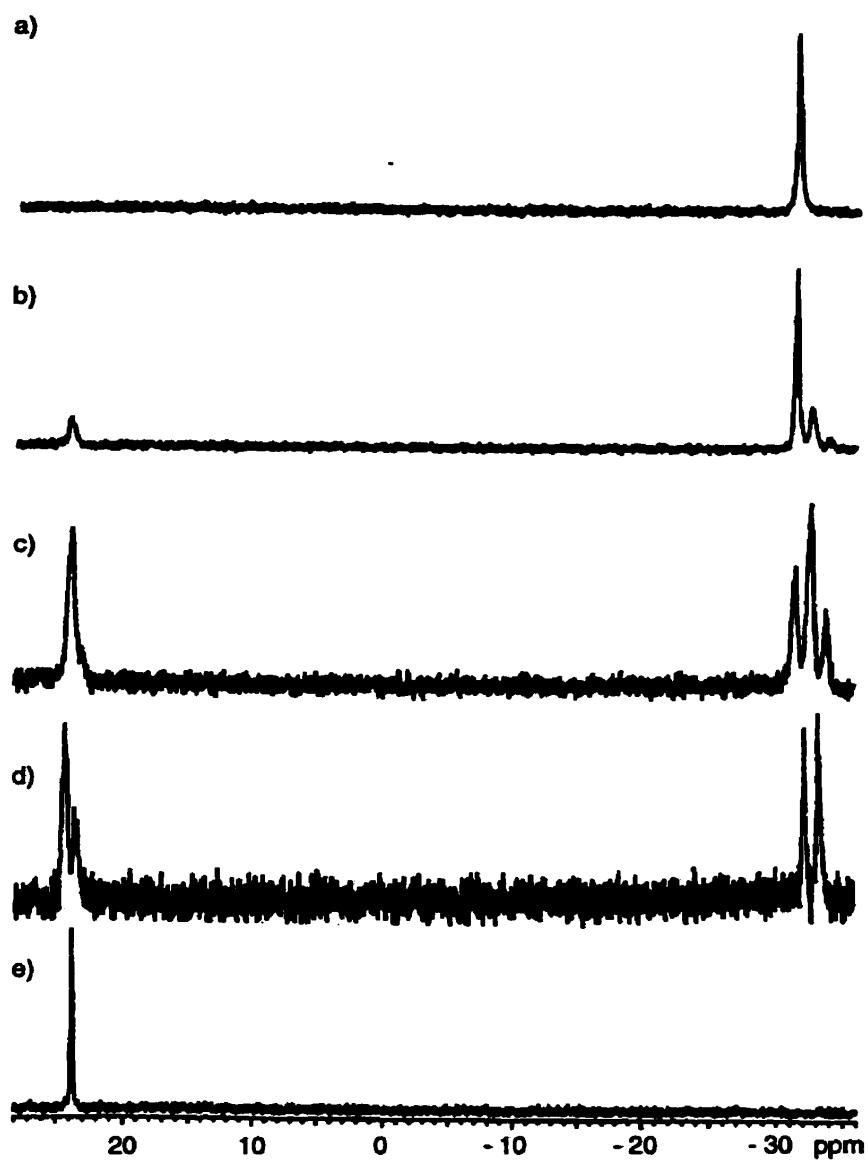


Figure 4.4  $^{31}\text{P}$  NMR Spectra (in  $\text{CD}_2\text{Cl}_2$  for a - d and  $\text{DMSO-d}_6$  for e) of the Methylation of Polymer 14: a) 0%, b) 17%, c) 33%, d) 50% and e) 100 % methylation.

prevalent and iii) being the least. However, as the degree of methylation increased, the resonance for (-P-fc-P-fc-P-) sites decreased in intensity until, at 50 % methylation, only two resonances, due to (-P<sup>+</sup>-fc-P-fc-P-) and (-P<sup>+</sup>-fc-P-fc-P<sup>+</sup>-) sites were observed. Also, two resonances due to methylated phosphorus sites can be seen in the spectrum. At 100 % methylation, only one resonance is visible with a shift of 23.8 ppm, the same shift found for both the thermal and transition metal-catalyzed polymerizations of **10b** and, therefore, fully supports our conclusion that **11** can be obtained from **10b** via ROP.

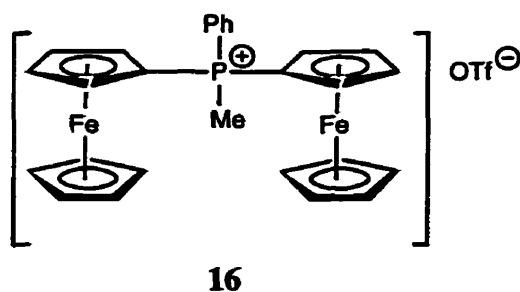
In the case of the complete methylation of the lower ( $n = 11$ ) molecular weight sample of **14**, end groups can also be seen at 26.9 and 24.1 ppm corresponding to the initiated and terminated ends of the polymer chain. End groups can also be detected by <sup>1</sup>H NMR. For all cases, however, no sample would elute from a GPC running on THF for any partially or fully methylated polymers, even after sulfurization of the remaining unreacted P sites<sup>10,17</sup> and with only 17 % methylation. It is unclear at this point in time why this is the case. The reason may involve the presence of interactions between the polymer and the column packing material or simply the decrease in solubility of the methylated polymer in comparison to the unmethylated polymer. It should be noted that polymers **4a - b** also do not elute from a GPC column until all the phosphorus sites have been sulfurized.<sup>10,17</sup>

#### 4.3.9 Electronic and Electrochemical Properties of **11**

The  $\lambda_{\text{max}}$  value obtained for polymer **11** is 452 nm (in DMF), considerably blue-shifted in comparison to the [1]ferrocenophane **10b** ( $\lambda_{\text{max}} = 484$  nm in THF and DMF). This is not unusual for these systems and has also been observed for poly(ferrocenylsilanes) and poly(ferrocenylgermanes) relative to their respective monomers. The  $\lambda_{\text{max}}$  value of 444 nm (in CH<sub>2</sub>Cl<sub>2</sub>) for polymer **4a** is also blue-shifted relative to **11**. Certainly, in this situation, it is unlikely that this effect is due to a difference in tilt angles for the Cp rings; the rings are probably close to being parallel in the polymer. More likely, it is an example of the effect

that the bridging element has upon the HOMO-LUMO gap. In this case, it appears that the presence of phosphonium centres in close proximity to iron leads to a red shift.

Cyclic voltammetry of **11** in DMF revealed the presence of only one redox wave at -0.16 V which is irreversible at low scan rates ( $I_{\text{red}}/I_{\text{ox}} = 0.91$  and  $0.82$  at  $250$  and  $100 \text{ mV s}^{-1}$  respectively) but reversible at higher scan rates. The reduction wave is split into two components which may be a consequence of absorption to the electrode. The presence of only one wave is unusual and contrasts with the two waves normally detected for poly(ferrocenes) with bridging elements such as silicon, germanium and phosphorus. However, it is possible that the presence of a cationic phosphonium site as the spacer unit between iron sites decreases the interaction between the metal atoms. Even more unusual is the observation that the  $E_{1/2}$  value is at a *lower* oxidation potential than ferrocene. To provide a simple model for **11**, we synthesized compound **16** by reaction of bis(ferrocenyl)phenylphosphine with methyl triflate.



The dimer **16** was found to be soluble in both  $\text{CH}_2\text{Cl}_2$  and DMF and thus the electrochemical behaviour of this species was examined in each solvent. In  $\text{CH}_2\text{Cl}_2$ , there were two oxidation waves at  $+0.65$  and  $+0.97$  V and a single reduction wave at  $+0.39$  V (vs. ferrocene at  $250 \text{ mV s}^{-1}$ ) with the shape of the reduction wave possibly due to a two electron reduction as well as absorption. Similar behaviour has been reported for the analogous species with an  $\text{I}^-$  counterion.<sup>33</sup> The high oxidation potentials observed for **16** in  $\text{CH}_2\text{Cl}_2$  are consistent with the high value that was detected for the monomer **10b** in the same solvent.

In DMF, the cyclic voltammogram of **16** revealed only one irreversible oxidation wave at  $-0.14$  V (vs ferrocene at  $250$   $\text{mV s}^{-1}$ ). This is at lower potential than for the monomer **10b** for which the oxidation wave was found at  $+0.26$  V but is at a similar value for polymer **11** in the same solvent ( $-0.16$  V vs. ferrocene at  $250$   $\text{mV s}^{-1}$ ). The unusually low oxidation potentials for dimer **16** and polymer **11** in DMF may be the result of strong solvation of the cationic main chain by the donor solvent. Indeed, based on the solubility properties of polymer **11**, such interactions are probably vital to effect dissolution of the material.

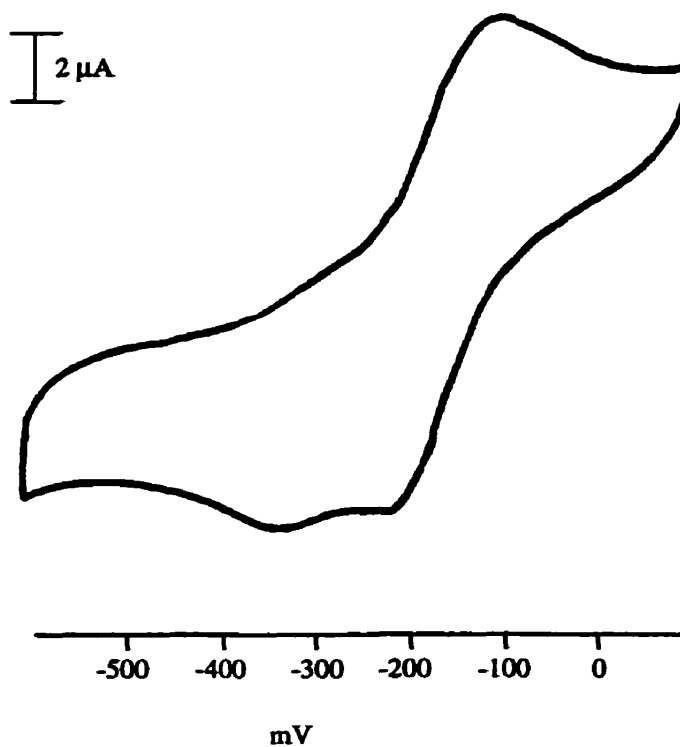


Figure 4.5 Cyclic Voltammogram of Polymer **11** in DMF at a scan rate of  $250$   $\text{mV s}^{-1}$  (referenced vs. ferrocene)



#### 4.3.10 Thermal Transition Behaviour, Thermal Stability and Morphology of 11

The thermal transition behaviour and the thermal stability of **11** (produced via TROP and transition metal-catalyzed ROP) were studied by differential scanning calorimetry (DSC) and thermal gravimetric analysis (TGA) and compared to that of the unmethylated polymer **14**. The morphologies of the two polymers were examined using wide-angle X-ray scattering (WAXS). By DSC, both **11** and **14** were found to be amorphous with no evidence for melt transitions for either polymer. However, glass transitions were observed in both cases at 176 °C and 126 °C, for **11** (via thermal ROP) (Figure 4.6) and **14**<sup>18</sup> respectively. The higher value for **11** is reasonable considering that the addition of a methyl group to the backbone of **14** probably reduces the flexibility of the polymer main chain. For comparison, there is an increase in the  $T_g$  from 9 °C to 33 °C for **2** ( $ER_x = SiHMe$ ) and **2** ( $ER_x = SiMe_2$ ) respectively. Also, the  $T_g$  for **11** is significantly higher than the value of 54 °C for the analogous poly(ferrocenylsilane) **2** ( $R = Me, R' = Ph$ ) although the value for **14** is also higher (to date, no analogous silicon-bridged species **2** has been synthesized where  $R = Ph, R' = H$ ). However, the triflate counterion no doubt plays a role in the thermal transition behaviour of this polymer as well and may also contribute to its fairly high  $T_g$  value. Interestingly, the  $T_g$  for the transition metal-catalyzed ROP of **10b** was found to be 164 °C (see Section 4.3.11). WAXS analysis of these polymers is also consistent with a generally amorphous nature (one broad amorphous halo was detected at 5.5 Å and 5.2 Å for **11** and **14** respectively).

TGA results reveal similar thermal stabilities for **11** and **14** and the polymers started to lose weight at 385 °C and 410 °C respectively. However, the weight loss for **11** is significantly higher than that for **14** with weight losses of 50 % and 30 %, respectively, by 600 °C. This may possibly coincide with the loss of all groups leaving behind an unsubstituted poly(ferrocenylphosphine) backbone; i.e. loss of phenyl, methyl and triflate groups from **11** while **14** only loses phenyl groups.

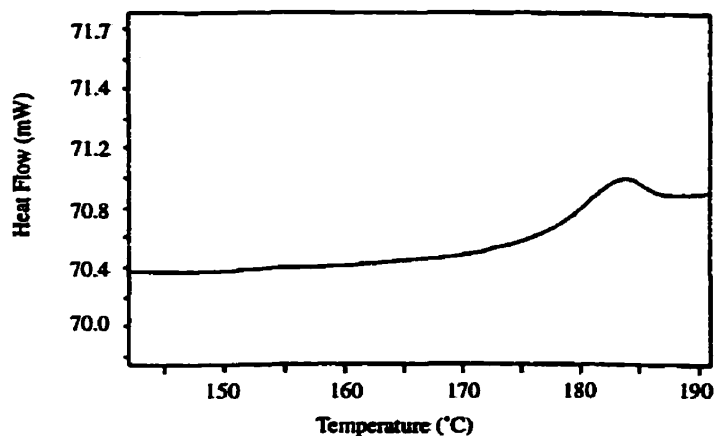


Figure 4.6 DSC Thermogram of Polymer 11 (produced via TROP)

#### 4.3.11 Molecular Weight Determination for 11

We have attempted to determine the molecular weight for **11** by a number of methods with limited success. In the case of GPC, no polymer was detected using polystyrene sulfonate columns and either N-methylpyrrolidinone (NMP) or 0.2 M sodium nitrate methanol/water (75/25) as an elution solvent. As the polymer backbone of **11** is cationic whereas the column possessed surface negative charges, this is not particularly surprising. In the case of viscometry, the polymer was not found to be stable in DMF or methanol long enough for measurements to be completed. Analysis by electrospray mass spectrometry of **11** produced both thermally and via transition metal-catalyzed ROP detected only oligomers (dimer, trimer and tetramer).

With the problems of polymer-stability in mind, dynamic light scattering analyses were conducted on samples of **11** obtained via both thermal ROP and transition metal-catalyzed ROP in methanol. The hydrodynamic radii were in the range of 30 - 45 nm which suggested the compound was polymeric rather than oligomeric in nature. However, due to

the instability of the polymer in the solvent as well as the possibility for aggregation, it was not possible to get an accurate value.

As solution methods were hindered by polymer instability in solvents in which the material was soluble, we determined the glass transition temperatures by DSC for a range of samples of polymer 11 of known molecular weight ( $n = 20, 55, 70$  and  $100$ ) that had been prepared via the 100 % methylation of samples of 14 prepared via anionic ROP. The results are shown in Table 4.6 and the  $T_g$  values were plotted as a function of  $(M_n)^{-2/3}$  (Figure 4.7).

Table 4.6 Thermal Data for Polymer 11 (where  $n =$  number of repeat units)

$n$	$M_n$	$T_g$ ( $^{\circ}\text{C}$ )	$\Delta C_p$ (J/gK)
20	$9.1 \times 10^3$	135	0.18
55	$2.5 \times 10^4$	154	0.18
70	$3.2 \times 10^4$	158	0.19
100	$4.6 \times 10^4$	162	0.19

It has been previously found for polymer 2 (where  $\text{ER}_x = \text{SiMe}_2$ ) that the  $T_g$  value reached a maximum of  $33^{\circ}\text{C}$  at a length of approximately 90 repeat units<sup>15,34</sup> and the data fitted well to the O'Driscoll equation where  $T_{g,\infty}$  is the glass transition temperature of the polymer with infinite molar mass:<sup>34</sup>

$$T_g = T_{g,\infty} - K(M_n)^{-2/3} \quad (1)^{35}$$

Similarly, we found that the data for 11 over the range of 20 to 100 repeat units fits well to the O'Driscoll equation with a regression coefficient of 0.998. The predicted  $T_{g,\infty}$  value is  $175.5^{\circ}\text{C}$ . Based on these results, this would suggest the  $M_n$  value for 11 derived by transition metal-catalyzed ROP ( $T_g = 164^{\circ}\text{C}$ ) is ca.  $4.6 \times 10^4$ . It is more difficult to

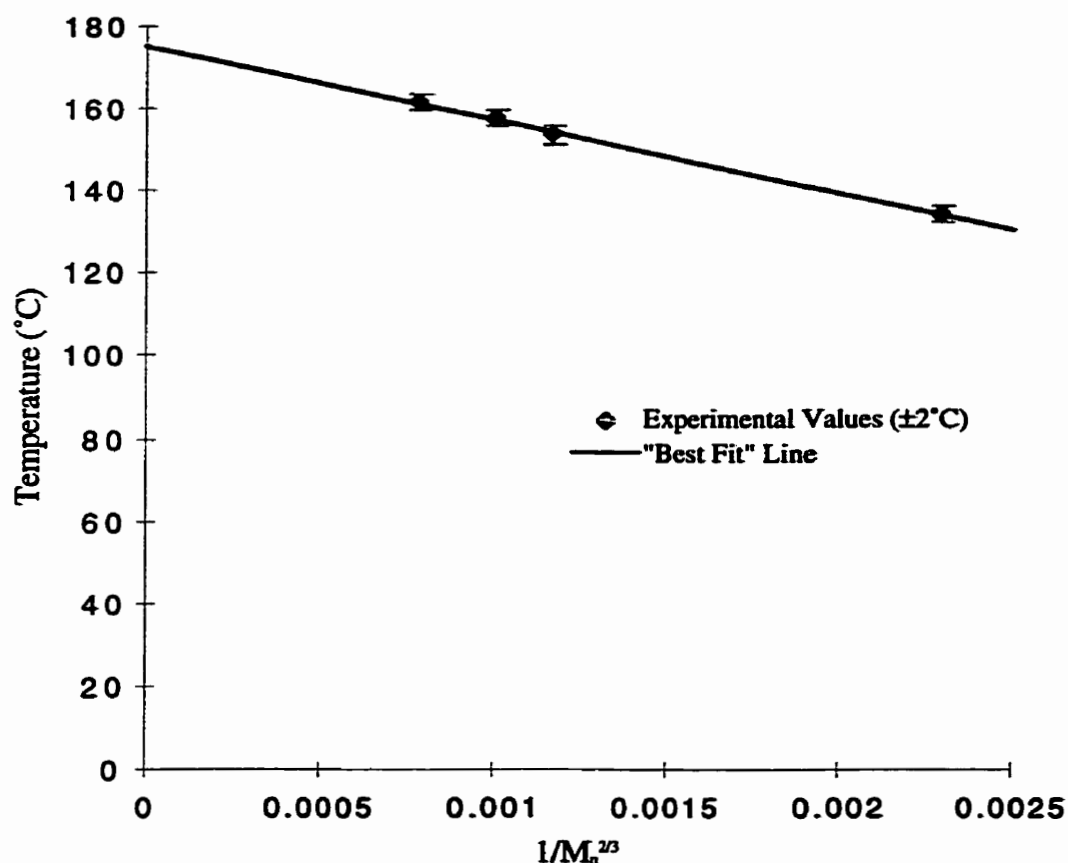


Figure 4.7  $T_g$  as a Function of  $M_n^{-2/3}$  for Polymer 11 ( $n = 20$  to 100)  
(Temperature:  $\pm 2$  °C)

determine an approximate molecular weight for the thermal ROP-derived polymer as the experimental  $T_g$  (176 °C) is close to the theoretical  $T_{g,\infty}$ . The higher  $T_g$  value for the thermal ROP-derived product in comparison to the value for the transition metal-catalyzed product does suggest, however, that the former possesses significantly higher molecular weight than the latter. This is not surprising as the latter precipitates from solution during the polymerization and thus probably cannot reach such a long chain length before becoming completely insoluble in the reaction solvent.

#### 4.4 Summary

The synthesis of a stable, phosphonium-bridged [1]ferrocenophane (**10b**) has been achieved. The compound was characterized by a variety of spectroscopic techniques as well as by single crystal X-ray diffraction. In contrast to compounds **5 - 7**, compound **10b** was found to undergo both thermal and transition metal-catalyzed ROP. Although a number of phosphonium-containing linear<sup>36-41</sup> and cyclopolymers<sup>42</sup> have been synthesized in the past, the results represent the first synthesis of a phosphonium-containing polymer via ROP as well as the first transition metal-catalyzed ROP of a phosphorus (III)-containing monomer. The resultant polymer **11** was found to be amorphous and displayed similar thermal stability to poly(ferrocenylphosphine) **14**. Based on glass transition temperature measurements for a series of samples of polymer **11** of known molecular weight, the number average molecular weight of **11** produced via transition metal-catalyzed ROP was ca. 46 000 (ca. 100 repeat units) and the thermally ring-opened polymer was of even higher molecular weight. In contrast to **10b**, a series of tetra-coordinate, phosphorus-bridged [1]ferrocenophanes (**5 - 7**) were found to be resistant to undergo transition metal-catalyzed ROP in the presence of either Pt(II) or Pt(0) catalysts.

## 4.5 Experimental Section

**Materials.** All chemicals, unless otherwise noted, were purchased from Aldrich. Compounds **5**, **6**, **7** and bis(ferrocenyl)phenylphosphine were synthesized according to the literature.<sup>19 20,43</sup> Samples of polymer **14** were prepared by living anionic polymerization as described previously by our group.<sup>17,18</sup>

**Equipment.** All reactions and manipulations were carried out under an atmosphere of prepurified nitrogen using either Schlenk techniques or an inert-atmosphere glovebox (Vacuum Atmospheres). Solvents were dried by standard methods, distilled, and stored under nitrogen over activated molecular sieves. 300 MHz <sup>1</sup>H NMR spectra, 75.5 MHz <sup>13</sup>C NMR spectra, 282.3 MHz <sup>19</sup>F NMR spectra and 121.4 MHz <sup>31</sup>P NMR spectra were recorded on a Varian Gemini 300 spectrometer. 400 MHz <sup>1</sup>H NMR spectra were also recorded on a Varian Unity 400 Spectrometer. Chemical shifts are reported relative to residual protonated solvent (<sup>1</sup>H or <sup>13</sup>C), external H<sub>3</sub>PO<sub>4</sub> (<sup>31</sup>P) and external CFCl<sub>3</sub> (<sup>19</sup>F). Melting points and enthalpies of polymerization were obtained with a Perkin-Elmer DSC 7 differential scanning calorimeter operating at a heating rate of 10 °C per minute under N<sub>2</sub>. TGA were carried out with a Perkin-Elmer TGA-7 thermogravimetric analyzer under nitrogen at a heating rate of 10 °C per minute. UV/vis spectra were recorded on a Perkin-Elmer UV/vis/NIR Lambda 900 Spectrometer in either anhydrous THF or DMF. Elemental analyses were performed by Quantitative Technologies, Inc., Whitehouse, NJ.

Dynamic light scattering experiments were carried out on a wide angle laser light scattering photometer from Brookhaven Instruments Corporation. A 5 mW vertically polarized He-Ne laser from Spectra physics was the light source. The solutions were filtered through disposable 0.2 μm filters from Millipore into glass scattering cells with a diameter of 12.3 mm. The cells were placed into the BI-200SM goniometer and sat in a vat of thermostated toluene which matched the index of refraction of the glass cells. The angle of

measurement for the goniometer was 90°. The scattered light was detected by a photomultiplier interfaced to the BI-2030AT digital correlator with 136 channels and measured the correlation function in real time. The instrument was controlled by a 486AT computer. The data was analyzed by software supplied by Brookhaven.

Electrochemical experiments were carried out using a PAR model 273 potentiostat with a Pt working electrode, a W secondary electrode, and an Ag wire reference electrode in a Luggin capillary. Polymer solutions were  $1 \times 10^{-3}$  M in  $\text{CH}_2\text{Cl}_2$  with 0.1 M  $[\text{Bu}_4\text{N}][\text{PF}_6]$  as a supporting electrolyte.

Powder diffraction data were obtained on a Siemens D5000 diffractometer using Ni filtered  $\text{CuK}\alpha$  ( $\lambda = 1.54178 \text{ \AA}$ ) radiation. The samples were scanned at step widths of  $0.02^\circ$  with 1.0 s per step in the range of 3 to  $40^\circ 2\theta$ . Samples were prepared by spreading the finely ground polymer on grooved glass slides.

**Synthesis of the methylated phosphorus-bridged [1]ferrocenophane 10b.** 1.88 g (6.44 mmol) of **3a**<sup>17,44</sup> was dissolved in 50 mL of toluene, giving a dark red solution. 1.03 g (6.30 mmol) of MeOTf was added to this solution dropwise with stirring. A bright red powder was immediately observed to precipitate during the addition. The reaction mixture was allowed to stir for a further 30 min after the addition was complete. The bright orange-red powder was then isolated under  $\text{N}_2$  on a filtration frit or under air using a water aspirator and washed with toluene until the washings were colourless. Dark red microcrystals of **10b** could be grown via recrystallization from THF. Yield: 2.54 g (88 %)  $^{31}\text{P}\{^1\text{H}\}$  NMR ( $\text{CDCl}_3$ ):  $\delta = 37.5$  ppm.  $^{19}\text{F}$  NMR ( $\text{CDCl}_3$ ):  $\delta = -78.6$  ppm.  $^{13}\text{C}$  NMR (in  $\text{CDCl}_3$ ):  $\delta = 136.3$  (s, para-Ph), 131.2 (d, meta-Ph,  $^3J_{\text{PC}} = 13$  Hz), 130.8 (d, ortho-Ph,  $^2J_{\text{PC}} = 14$  Hz), 118.9 (d, ipso-Ph,  $^1J_{\text{PC}} = 90$  Hz), 84.5 (d, Cp,  $^3J_{\text{PC}} = 11$  Hz), 83.5 (d, Cp,  $^3J_{\text{PC}} = 10.4$  Hz), 76.4 (d, Cp,  $^2J_{\text{PC}} = 11.7$  Hz), 75.2 (d, Cp,  $^2J_{\text{PC}} = 14.9$  Hz), 11.3 (d, Me,  $^1J_{\text{PC}} = 55$  Hz), 4.2 (d, ipso Cp,  $^1J_{\text{PC}} = 71.9$  Hz) ppm.  $^1\text{H}$  NMR (400 MHz, in  $\text{CDCl}_3$ ):  $\delta = 8.80$  (m, 2 H, Ph), 7.89 (m, 1 H, Ph), 7.79 (m, 2 H, Ph), 5.45 (m, Cp), 5.02 (m, Cp), 4.93 (m, Cp), 4.41 (m, Cp), 2.66 (d, Me,  $^2J_{\text{PH}}$

= 13.9 Hz) ppm. UV-visible (THF):  $\lambda_{\text{max}}$ (band II) = 484 nm ( $\epsilon = 307 \text{ M}^{-1} \text{ cm}^{-1}$ ).  $\text{C}_{18}\text{H}_{16}\text{F}_3\text{Fe}_1\text{O}_3\text{P}_1\text{S}_1$ : Calculated: C 47.39, H 3.54; Found: C 47.11, H 3.36.

**Thermal ROP of 10b.** 0.75 g (1.64 mmol) of **10b** were sealed in an evacuated Pyrex tube and heated at 145 °C for 30 min. During this time, the contents were observed to undergo a change to a dark red-orange colour. After this time, the tube was broken and the polymer washed with  $\text{CH}_2\text{Cl}_2$ . The product (**11**) was then dried under vacuum and isolated as an orange powder. Yield: 0.65 g (87 %).  $^{31}\text{P}$  NMR ( $\text{DMSO-d}^6$ ):  $\delta = 23.8$  ppm.  $^{19}\text{F}$  NMR ( $\text{DMSO-d}^6$ ):  $\delta = -78.2$  ppm.  $^{13}\text{C}$  NMR ( $\text{DMSO-d}^6$ ):  $\delta = 134.8$  (s, para-Ph), 131.6 (d, meta-Ph,  $^3J_{\text{PC}} = 10$  Hz), 130.0 (d, ortho-Ph,  $^2J_{\text{PC}} = 13$  Hz), 121.7 (d, ipso-Ph,  $^1J_{\text{PC}} = 94$  Hz), 76.3 - 72.8 (Cp, multiplet, broad), 66.5 (ipso-Cp,  $^1J_{\text{PC}} = 102$  Hz), 5.2 (d, Me,  $^1J_{\text{PC}} = 62$  Hz).  $^1\text{H}$  NMR (300 MHz, in  $\text{DMSO-d}^6$ ):  $\delta = 7.85$  (broad, 3 H, phenyl), 7.68 (broad, 2 H, Ph), 4.88 (broad, 2 H, Cp), 4.65 (broad, 4 H, Cp), 3.97 (broad, 2 H, Cp), 2.93 (broad, 3H, Me) ppm. UV-visible (DMF):  $\lambda_{\text{max}}$ (band II) = 452 nm ( $\epsilon = 137 \text{ M}^{-1} \text{ cm}^{-1}$ ).  $\text{C}_{18}\text{H}_{16}\text{F}_3\text{Fe}_1\text{O}_3\text{P}_1\text{S}_1$ : Calculated: C 47.39, H 3.54; Found: C 46.65, H 3.55. Electrospray MS: 1676 ( $[\text{fcPPhMe}]_4[\text{OTf}]_3$ , 10 %), 1219 ( $[\text{fcPPhMe}]_3[\text{OTf}]_2$ , 100 %), 763 ( $[\text{fcPPhMe}]_2[\text{OTf}]$ , 10 %), 307 ( $[\text{fcPPhMe}]^+$ , 50 %).

**Transition Metal-Catalyzed ROP of 10b.** 0.196 g (0.430 mmol) of **10b** were dissolved in 5 mL of  $\text{CH}_2\text{Cl}_2$ . To this solution was added 9 mg (7.9 mol %) of  $\text{PtCl}_2$ . The solution was then allowed to stir overnight. A fine light orange powder precipitated out of solution during this time. The precipitate was allowed to settle and then the solvent was removed via cannulation. The product (**11**) was washed with  $\text{CH}_2\text{Cl}_2$  and then dried under vacuum.  $^1\text{H}$ ,  $^{13}\text{C}$ ,  $^{19}\text{F}$  and  $^{31}\text{P}$  NMR data were consistent with the same product obtained via thermal ROP. Yield: 0.105 g (54 %). Electrospray MS: 1676 ( $[\text{fcPPhMe}]_4[\text{OTf}]_3$ , 10 %), 1219 ( $[\text{fcPPhMe}]_3[\text{OTf}]_2$ , 100 %), 763 ( $[\text{fcPPhMe}]_2[\text{OTf}]$ , 65 %), 307 ( $[\text{fcPPhMe}]^+$ , 100 %).



**Partial Methylation of Poly(ferrocenylphenylphosphine) 14 (n = 100).** The procedure for various per cent methylations of **14** was the same for all samples. a) 124 mg, b) 107 mg or c) 105 mg of **14** (n = 100) ( $M_w$  of sulfurized **14** = 38 000,  $M_w/M_n$  = 1.30) were dissolved in  $CD_2Cl_2$  in a 5mm NMR tube. To this solution was added, via a microsyringe: a) 7  $\mu$ L, b) 14  $\mu$ L or c) 21  $\mu$ L of MeOTf.  $^{31}P$  NMR data were run. Samples of the solution were then treated with  $S_8$  in an attempt to produce a GPC-analyzable polymer. However, no polymer was found to elute from the Ultrastyrigel column using THF as eluent even for the polymer sample treated with only 7  $\mu$ L of MeOTf. Similarly, a 112 mg sample of **14** (n = 100) was treated sequentially with the same amounts of MeOTf and a  $^{31}P$  NMR spectrum obtained after each addition. The spectra were essentially the same.

**Complete Methylation of Poly(ferrocenylphenylphosphine) 14 (n = 100).** 65 mg of **14** (n = 100) ( $M_w$  of sulfurized **14** = 38 000,  $M_w/M_n$  = 1.30) were suspended in an excess of MeOTf. 2 mL of  $CH_2Cl_2$  were added and the solution stirred for 10 min. The solution was removed and the remaining insoluble material dried under vacuum. The product was analyzed by NMR and the data were consistent with the structure proposed for the products of thermal and transition metal-catalyzed ROP of **10b**.

**Complete Methylation of Poly(ferrocenylphenylphosphine) 14 (n = 11).** 60 mg of **14** (n = 11) ( $M_w$  of sulfurized **14** = 2 600,  $M_w/M_n$  = 1.08) were suspended in an excess of MeOTf. 2 mL of  $CH_2Cl_2$  were added and the solution stirred for 10 min. The mother liquors were removed and the remaining insoluble material dried under vacuum. The product was analyzed by  $^1H$  and  $^{31}P$  NMR and the data were consistent with the structure proposed for the products of thermal and transition metal-catalyzed ROP of **10b**. Additionally, end groups were observed by  $^{31}P$  NMR (in  $DMSO-d_6$ ) at 26.9 ppm and 24.1 ppm

**Attempted Thermal Copolymerization of 1 ( $ER_x = SiMe_2$ ) and 10b.** 100 mg (0.413 mmol) of 1 ( $ER_x = SiMe_2$ ) and 53 mg (0.116 mmol) of 10b were sealed in an evacuated Pyrex tube at 140 °C for 15 minutes. The THF soluble fraction of the contents of the tube was dissolved in THF and then precipitated into hexanes. The insoluble and soluble fractions were then dissolved in DMSO- $d_6$  and  $C_6D_6$  respectively and analyzed by  $^1H$  and  $^{31}P$  NMR. This analysis revealed only the presence of the respective homopolymers 11 and 2 ( $ER_x = SiMe_2$ ) with no evidence for switching groups.

**Attempted Transition Metal-Catalyzed Copolymerization of 1 ( $ER_x = SiMe_2$ ) and 10b.** 193 mg (0.798 mmol) of 1 ( $ER_x = SiMe_2$ ) and 109 mg (0.239 mmol) of 10b were dissolved in 25 mL of  $CH_2Cl_2$ . To this were added 4 mg (6.3 mol %) of  $PtCl_2$ . The reaction mixture was allowed to stir overnight. Analysis as described above revealed only the presence of homopolymers 2 ( $ER_x = SiMe_2$ ) and 11.

**Attempted Thermal Copolymerization of 1 ( $ER_x = SiMePh$ ) and 10b.** 151 mg (0.497 mmol) of 1 ( $ER_x = SiMePh$ ) and 45 mg (0.099 mmol) of 10b were sealed in an evacuated Pyrex tube at 140 °C for 15 minutes. Analysis as described above revealed only the presence of homopolymers 2 ( $ER_x = SiMePh$ ) and 11.

**Attempted Transition Metal-Catalyzed Copolymerization of 1 ( $ER_x = SiMePh$ ) and 10b.** 160 mg (0.526 mmol) of 1 ( $ER_x = SiMePh$ ) and 50 mg (0.110 mmol) of 10b were dissolved in 25 mL of  $CH_2Cl_2$ . To this were added 4 mg (13.6 mol %) of  $PtCl_2$ . The reaction mixture was allowed to stir overnight. Examination of the products by  $^1H$  and  $^{31}P$  NMR showed evidence only for homopolymer 1 ( $ER_x = SiMePh$ ) and unreacted 10b.

**Attempted Transition Metal-Catalyzed ROP of 5a.** 60 mg (0.19 mmol) of 5a were dissolved in 0.7 mL of  $C_6D_6$  in a 5 mm NMR tube. To this solution was added 8 mol % of

PtCl<sub>2</sub>. The contents of the tube were shaken at intermittent intervals over 24 h. No change in the <sup>31</sup>P NMR spectrum was observed during this time. The contents were also heated at 60 °C overnight. No changes were observed by <sup>31</sup>P NMR.

**Attempted Transition Metal-Catalyzed ROP of 6.** 60 mg (0.13 mmol) of **6** were dissolved in 0.7 mL of C<sub>6</sub>D<sub>6</sub> in a 5 mm NMR tube. To this solution were added 8 mol % of PtCl<sub>2</sub>. The contents of the tube were shaken at intermittent intervals over 24 h. No change in the <sup>31</sup>P NMR spectrum was observed during this time. The contents were also heated at 60 °C overnight. No changes were observed by <sup>31</sup>P NMR.

**Synthesis of Model Compound 16.** 0.362 g (0.757 mmol) of bis(ferrocenyl)phenylphosphine was dissolved in 5 mL of toluene. To this stirred solution was added 0.128 g (0.780 mmol) of MeOTf. A reddish-orange oil was immediately observed to precipitate from solution. The solution was removed by decantation. The oil was dissolved in CH<sub>2</sub>Cl<sub>2</sub> and precipitated into hexanes. The solution was removed by decantation. The product was dried overnight under vacuum and isolated as a reddish-orange semi-solid. Yield: 0.406 g (84 %). <sup>31</sup>P{<sup>1</sup>H} NMR (CDCl<sub>3</sub>): δ = 24.8 ppm. <sup>19</sup>F NMR (CDCl<sub>3</sub>): δ = - 78.5 ppm. <sup>13</sup>C NMR (in CDCl<sub>3</sub>): δ = 134.4 (s, para-Ph), 131.6 (d, meta-Ph, <sup>3</sup>J<sub>PC</sub> = 9 Hz), 129.9 (d, ortho-Ph, <sup>2</sup>J<sub>PC</sub> = 12 Hz), 122.9 (d, ipso-Ph, <sup>1</sup>J<sub>PC</sub> = 92 Hz), 74.3 (d, Cp, <sup>3</sup>J<sub>PC</sub> = 9.9 Hz), 73.9 (d, Cp, <sup>3</sup>J<sub>PC</sub> = 9.7 Hz), 72.6 (d, Cp, <sup>2</sup>J<sub>PC</sub> = 12.6 Hz), 71.8 (d, Cp, <sup>2</sup>J<sub>PC</sub> = 13.5 Hz), 70.8 (s, Cp), 63.6 (d, ipso Cp, <sup>1</sup>J<sub>PC</sub> = 105 Hz), 10.8 (d, Me, <sup>1</sup>J<sub>PC</sub> = 64 Hz) ppm. <sup>1</sup>H NMR (400 MHz, in CDCl<sub>3</sub>): δ = 7.5 - 7.9 (m, 5 H, Ph), 4.79 (m, 2H, Cp), 4.73 (m, 2H, Cp), 4.63 (m, 2 H, Cp), 4.41 (m, 2 H, Cp), 4.20 (s, 10 H, Cp), 2.93 (d, 3 H, Me, <sup>2</sup>J<sub>PH</sub> = 13.9 Hz) ppm. C<sub>28</sub>H<sub>26</sub>F<sub>3</sub>Fe<sub>2</sub>O<sub>3</sub>P<sub>1</sub>S<sub>1</sub>: Calculated: C 52.37, H 4.08; Found: C 52.62, H 4.20.

## 4.6 References

- (1) (a) Pittman, C. U.; Carraher, C. E.; Reynolds, J. R. in *Encyclopedia of Polymer Science and Engineering*; Eds. Mark, H. F.; Bikales, N. M.; Overberger, C. G.; Menges, G.; Wiley: New York, 1989; Vol. 10; p. 541. (b) Sheats J. E.; Carraher, C. E.; Pittman, C. U.; Zeldin M., Currell B.; *Inorganic and Metal-Containing Polymeric Materials*; Plenum: New York, 1989. (c) Gonsalves K. E.; Rausch M. D. in *Inorganic and Organometallic Polymers. ACS Symposium Series 360*; Eds. Zeldin, M.; Wynne, K.; Allcock, H. R. American Chemical Society: Washington, DC. 1988. (d) Allcock, H. R. *Adv. Mater.* **1994**, *6*, 106. (e) Manners, I. *Chem. Br.* **1996**, *32*, 46.
- (2) a) Wright, M. E.; Sigman, M. S. *Macromolecules* **1992**, *25*, 6055. (b) Davies, S. J.; Johnson, B. F. G.; Khan, M. S.; Lewis, J.; *J. Chem. Soc., Chem. Commun.* **1991**, 187. (c) Tenhaeff, S. C.; Tyler, D. R. *J. Chem. Soc., Chem. Commun.* **1989**, 1459. (d) Neuse, E. W.; Bednarik, L. *Macromolecules* **1979**, *12*, 187. (e) Brandt, P. F.; Rauchfuss, T. B. *J. Am. Chem. Soc.* **1992**, *114*, 1926. (f) Sturge, K. C.; Hunter, A. D.; McDonald, R.; Santarsiero, B. D. *Organometallics* **1992**, *11*, 3056. (g) Gonsalves, K.; Zhan-ru, L.; Rausch, M. D. *J. Am. Chem. Soc.* **1984**, *106*, 3862. (h) Katz, T. J.; Sudhakar, A.; Teasley, M. F.; Gilbert, A. M.; Geiger, W. E.; Robben, M. P.; Wuensch, M.; Ward, M. D. *J. Am. Chem. Soc.* **1993**, *115*, 3182. (i) Nugent, H. M.; Rosenblum, M. *J. Am. Chem. Soc.* **1993**, *115*, 3848. (j) Patterson, W. J.; McManus, S. P.; Pittman, C. U. *J. Polym. Sci.: Poly. Chem. Ed.* **1974**, *12*, 837. (k) Burtea, M. A.; Tilley, T. D. *Organometallics* **1997**, *16*, 1507. (l) Stanton, C. E.; Lee, T. R.; Grubbs, R. H.; Lewis, N. S.; Pudelski, J. K.; Callstrom, M. R.; Erickson, M. S.; McLaughlin, M. L.; *Macromolecules* **1995**, *28*, 8713. (m) Heo, R. W.; Somoza, F. B.; Lee, T. R. *J. Am. Chem. Soc.* **1998**, *120*, 1621.
- (3) Manners, I. *Angew. Chem. Int. Ed. Engl.* **1996**, *35*, 1602.
- (4) Manners, I. *Can. J. Chem.* **1998**, *76*, 731.

- (5) Foucher, D. A.; Ziembinski, R.; Petersen, R.; Pudelski, J.; Edwards, M.; Ni, Y.; Massey, J.; Jaeger, C. R.; Vancso, G. J.; Manners, I. *Macromolecules* **1994**, *27*, 3992.
- (6) Peckham, T. J.; Massey, J. A.; Edwards, M.; Manners, I.; Foucher, D. A. *Macromolecules* **1996**, *17*, 2396.
- (7) Rulkens, R.; Lough, A. J.; Manners, I. *Angew. Chem., Int. Ed. Engl.* **1996**, *35*, 1805.
- (8) Pudelski, J. K.; Gates, D. P.; Rulkens, R.; Lough, A. J.; Manners, I. *Angew. Chem., Int. Ed. Engl.* **1995**, *34*, 1506.
- (9) Braunschweig, H.; Dirk, R.; Müller, M.; Nguyen, P.; Resendes, R.; Gates, D. P.; Manners, I. *Angew. Chem. Int. Ed. Engl.* **1997**, *36*, 2338.
- (10) Honeyman, C. H.; Foucher, D. A.; Dahmen, F. Y.; Rulkens, R.; Lough, A. J.; Manners, I. *Organometallics* **1995**, *14*, 5503.
- (11) For the work of other groups on poly(ferrocenylsilanes) see: (a) Nguyen, M. T.; Diaz, A. F.; Dement'ev, V. V.; Pannell, K. H. *Chem. Mater.* **1993**, *5*, 1389. (b) Hmyene, M.; Yasser, A.; Escorne, M.; Percheron-Guegan, A.; Garnier, F. *Adv. Mater.* **1994**, *6*, 564 (c) Reddy, N. P.; Yamashita, H.; Tanaka, M. *J. Chem. Soc., Chem. Commun.* **1995**, 2263. (d) Barlow, S.; Rohl, A. L.; Shi, S.; Freeman, C. M.; O'Hare, D. *J. Am. Chem. Soc.* **1996**, *118*, 7578. (e) J. Park, Y. Seo, S. Cho, D. Whang, K. Kim, and T. Chang, *J. Organomet. Chem.*, **1995**, *489*, 23.
- (12) Foucher, D. A.; Ziembinski, R.; Tang, B.-Z.; Macdonald, P. M.; Massey, J.; Jaeger, C. R.; Vancso, G. J.; Manners, I. *Macromolecules* **1993**, *26*, 2878.
- (13) Zechel, D. L.; Hultsch, K. C.; Rulkens, R.; Balaishis, D.; Ni, Y.; Pudelski, J. P.; Lough, A. J.; Manners, I. *Organometallics* **1996**, *15*, 1972.
- (14) Nguyen, P.; Lough, A. J.; Manners, I. *Macromol. Rapid Commun.* **1997**, *18*, 953.
- (15) Ni, Y. Z.; Rulkens, R.; Manners, I. *J. Am. Chem. Soc.* **1996**, *118*, 4102.
- (16) Ni, Y. Z.; Rulkens, R.; Pudelski, J. K.; Manners, I. *Makromol. Chem. Rapid Communications* **1995**, *16*, 637.

- (17) Honeyman, C. H.; Peckham, T. J.; Massey, J. A.; Manners, I. *J. Chem. Soc., Chem. Commun.* **1996**, 2589.
- (18) Peckham, T. J.; Massey, J. A.; Power, K. N.; Manners, I. Manuscript in preparation.
- (19) Seyferth, D.; Withers, H. P. *Organometallics* **1982**, *1*, 1275.
- (20) Mizuta, T.; Yamasaki, T.; Nakazawa, H.; Miyoshi, K. *Organometallics* **1996**, *15*, 1093.
- (21) Cullen, W. R.; Retting, S. J.; Zheng, T. C. *J. Organomet. Chem.* **1993**, *452*, 97.
- (22) DENZO-SMN, Nonius Company, Delft, Holland. (1997).
- (23) Sheldrick, G. M., SHELXTL\PC, Siemens Analytical X-ray Instruments Inc., Madison, Wisconsin, U.S.A. (1994)
- (24) Stoeckli-Evans, H.; Osborne, A. G.; Whiteley, R. H. *J. Organomet. Chem.* **1980**, *134*, 91.
- (25) Cristau, H. J.; Plénat, F. In *The Chemistry of Organophosphorus Compounds*; F. R. Hartley, Ed.; John Wiley & Sons: Toronto, 1994; Vol. 3; pp 45.
- (26) Rulkens, R.; Gates, D. P.; Balaishis, D.; Pudelski, J. K.; McIntosh, D. F.; Lough, A. J.; Manners, I. *J. Am. Chem. Soc.* **1997**, *119*, 10976.
- (27) Green, J. C. *Chem. Soc. Rev.* **1998**, 263.
- (28) Nakazawa, H.; Matsuoka, Y.; Nakagawa, I.; Miyoshi, K. *Organometallics* **1992**, *11*, 1385.
- (29) Arce, A. J.; De Sanctis, Y.; Machado, R.; Capparelli, M. V.; Manzur, J.; Deeming, A. *J. Organometallics* **1995**, *14*, 3592.
- (30) Wicht, D. K.; Kourkine, I. V.; Lew, B. M.; Nthenge, J. M.; Glueck, D. S. *J. Am. Chem. Soc.* **1997**, *119*, 5039.
- (31) Carmichael, D.; Hitchcock, P. B.; Nixon, J. F.; Mathey, F.; Pidcock, A. *J. Chem. Soc., Chem. Commun.* **1986**, 762.

- (32) a) Ni, Y.; Rulkens, R.; Pudelski, J. K.; Manners, I. *Makromol. Chem. Rapid Commun.* **1995**, *16*, 637. b) Gomez-Elipe, P.; Resendes, R.; Macdonald, P. M.; Manners, I. *J. Am. Chem. Soc.* **1998**, in press.
- (33) Kotz, J. C.; Nivert, C. L.; Lieber, J. M.; Reed, R. C. *J. Organomet. Chem.* **1975**, *91*, 87.
- (34) Lammertink, R. G. H.; Hempenius, M. A.; Manners, I.; Vancso, G. J. *Macromolecules* **1998**, *31*, 795.
- (35) O'Driscoll, K.; Sanayei, A. R. *Macromolecules* **1991**, *24*, 4479.
- (36) Kanazawa, A.; Ikeda, T.; Endo, T. *J. Appl. Polym. Sci.* **1994**, *52*, 641.
- (37) Kanazawa, A.; Ikeda, T.; Endo, T. *J. Appl. Polym. Sci.* **1994**, *52*, 1237.
- (38) Kanazawa, A.; Ikeda, T.; Endo, T. *J. Appl. Polym. Sci.* **1994**, *52*, 1305.
- (39) Kanazawa, A.; Ikeda, T.; Endo, T. *J. Appl. Polym. Sci.* **1994**, *53*, 1245.
- (40) Izawa, T.; Yamada, Y.; Ogura, Y.; Sato, Y. *J. Polym. Sci. Polym. Chem.* **1994**, *32*, 2057.
- (41) Hughes, I. *Tetrahedron Lett.* **1996**, *37*, 7595.
- (42) Seyferth, D.; Masterman, T. C. *Macromolecules* **1995**, *28*, 3055.
- (43) Sollott, G. P.; Mertwoy, H. E.; Portnoy, S.; Snead, J. L. *J. Organomet. Chem.* **1963**, *28*, 1090.
- (44) The synthesis of **3a** has been previously described. See: (a) Osborne, A. G.; Whiteley, R. H.; Meads, R. E.; *J. Organomet. Chem.* **1980**, *193*, 345. (b) Seyferth, D.; Withers, H. P. Jr. *J. Organomet. Chem.* **1980**, *185*, C1.

## **Chapter 5 Living Anionic Polymerization of Phosphorus-Bridged, [1]Ferrocenophanes: A Route to Well-Defined Poly(ferrocenylphosphine) Homopolymers and Block Copolymers**

### **5.1 Abstract**

The living anionic ring-opening polymerization (ROP) of the phenylated phosphorus-bridged [1]ferrocenophane  $\text{Fe}(\eta\text{-C}_5\text{H}_4)_2\text{PPh}$  **1** initiated by *n*-BuLi in THF at 20 °C has allowed the preparation of well-defined poly(ferrocenylphenylphosphines)  $[\text{Fe}(\eta\text{-C}_5\text{H}_4)_2\text{PPh}]_n$  **5** with control of molecular weight, narrow polydispersities and controlled end-group structures. Reaction of polymers **5** (runs 1 - 5) with sulfur allowed the synthesis of the analogous poly(ferrocenylphenylphosphine sulfides)  $[\text{Fe}(\eta\text{-C}_5\text{H}_4)_2\text{P(S)Ph}]_n$  **6**. Analysis of the high molecular weight polymers **5** and **6** (where  $n = 100$ ) by DSC showed glass transition temperatures of 126 °C and 206 °C respectively but no melting transitions. These polymers were found to be amorphous by WAXS. The living nature of the polymerization has also permitted the synthesis of well-defined block copolymers, poly(ferrocenylphenylphosphine)-*b*-poly(dimethylsiloxane) (PFP-*b*-PDMS) (**7a** and **7b**) and poly(ferrocenylphenylphosphine)-*b*-poly(ferrocenyldimethylsilane) (**8**). Analysis of the block copolymer **7b** by DSC showed the presence of individual thermal transitions for each block which indicated that they were incompatible. Copolymer **7b** was also found to form spherical micelles in hexane solution as confirmed by dynamic (DLS) and static (SLS) light scattering studies. These studies also showed that the average aggregation number was ca. 320 polymer molecules. When the solvent is evaporated, transmission electron microscopy (TEM) and atomic force microscopy (AFM) showed that the iron-rich, organometallic PFP core is encased in a corona of PDMS. Metal coordination studies on copolymer **7b** showed



that it could coordinate  $\text{PdCl}_2$  (yielding insoluble **11**) as well as  $\text{Fe}(\text{CO})_4$  resulting in the formation of **12** which remained soluble in hexane. Analysis of **12** after solvent evaporation by TEM and AFM showed that spherical micelles had still been formed although generally larger than those found for **7b**.

## 5.2 Introduction

Anchoring metal catalysts to a support material has long been one favoured way of immobilizing a catalytic species and which also facilitates both catalyst-product separation and increases the lifetime of the catalyst.<sup>1</sup> The material used for immobilization may be an inorganic solid (e.g. silica,  $\text{MgCl}_2$ ) or an organic polymer (e.g. polystyrene).<sup>2</sup> A number of different catalysts have been attached to polymers including those for hydroformylation, olefin hydrogenation, oligomerization, polymerization, carbonylation, oxidation and hydrosilylation.<sup>3</sup> In general, however, inorganic materials are favoured over organic polymers as they often possess much greater mechanical and thermal stability. However, the possibility for inorganic materials to participate in metal bonding<sup>4</sup> may influence the catalyst. Both inorganic and organic supports tend to suffer from leaching of the catalyst, thus decreasing the advantages of a supported catalyst that were mentioned earlier.

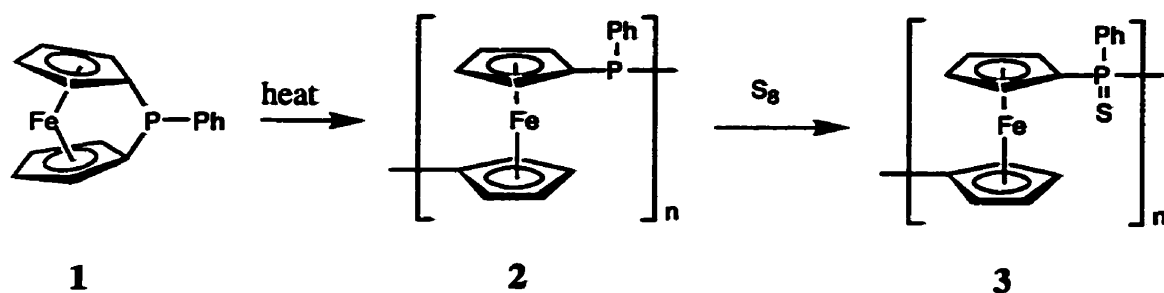
Some interesting strategies to overcome catalyst leaching have been studied. One such approach is to immobilize catalysts in the channels of zeolites. This allows for the possibility of not only firmly attaching the catalyst but also adding new opportunities for size and shape selectivity.<sup>1</sup> The use of polyoxymetalates in which the metal species is incorporated into the framework of the material is another possibility.<sup>1</sup>

Polymeric supports may be used in other ways such that the catalyst does not easily leach from the material. Attaching the catalyst by means of strong, non-labile covalent bonds virtually removes the possibility of leaching but synthesizing such polymer systems is often

difficult. Another method involves surrounding the catalyst particle(s) with the polymer in such a way that there are a large number of coordinative sites to prevent catalyst leaching and yet still allow for the relatively free movement of reactants and products. Microencapsulation is one such method and a preliminary report of one such recent example, based on microencapsulation of a Lewis acid catalyst within polystyrene, illustrated that the catalyst could be recycled a number of times without any apparent loss of catalytic activity.<sup>5</sup>

Polymeric micelles provide another variation on this method of immobilization. In this case, the metal catalyst is stabilized within the core of the micelle which makes leaching in the appropriate solvent an unlikely possibility. A recent report by Antonietti *et al.* involved using polystyrene-*b*-poly-4-vinylpyridine and forming micelles around Pd colloids in a non-solvent for the poly-4-vinylpyridine block (e.g. toluene).<sup>6</sup> The catalytic activity for the Heck reaction of these colloids was then tested and found to be comparable to low molecular weight Pd complexes but the stability of the micellized catalysts was found to be much higher with catalytic activity remaining even after 50 000 turn over cycles.

Over the past few years, our group has used ring-opening polymerization (ROP) of a number of different [1]- and [2]ferrocenophanes as a route to soluble, high molecular weight poly(ferrocenes) which have been shown to possess a number of interesting properties.<sup>7-14</sup> Poly(ferrocenylphosphines) such as **2** are a particularly interesting target as they are possible polymeric supports for catalysts. Materials of structure **2** were first reported via condensation routes and coordination studies of these compounds with  $\text{Co}_2(\text{CO})_8$  and their subsequent use as a hydroformylation catalysts were also described.<sup>15,16</sup> In 1995, we first reported that high molecular poly(ferrocenylphosphines) (e.g. **2**) may be obtained via thermal ROP of strained, phosphorus-bridged [1]ferrocenophanes (**1**).<sup>17</sup> They may be subsequently functionalized by the reaction with elemental sulfur to obtain the analogous poly(ferrocenylphosphine sulfides) (**3**).



**Reaction 5.1** Synthesis of Poly(ferrocenylphenylphosphine) and Subsequent Sulfurization via Thermal ROP of **1**

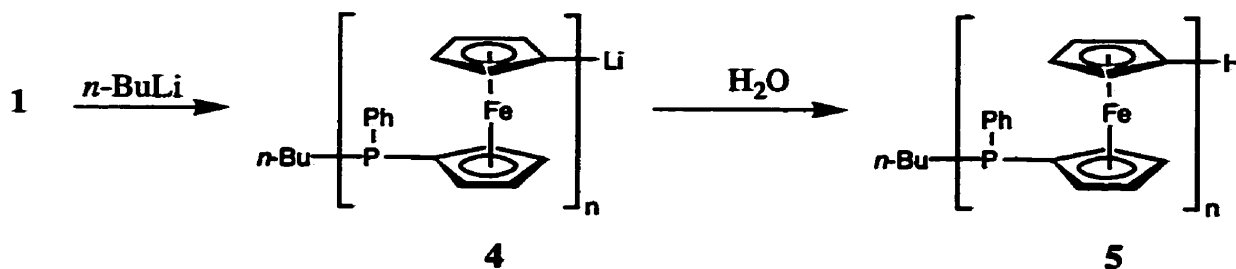
More recently, we have made a preliminary report of the living anionic ROP of the phosphorus-bridged [1]ferrocenophane **1** which has allowed us access to poly(ferrocenylphosphines) with controlled molecular weights as well as poly(ferrocenylphosphine)-*b*-poly(dimethylsiloxane) and poly(ferrocenylphosphine)-*b*-poly(ferrocenylsilane) copolymers.<sup>18</sup> In this chapter, we report full details of our work in this area, including the aggregation behaviour of poly(ferrocenylphosphine)-*b*-poly(dimethylsiloxane) in solution<sup>19</sup> and metal coordination studies on this copolymer.

## 5.3 Results and Discussion

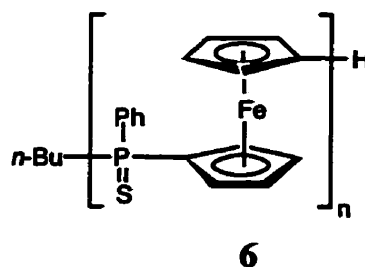
### 5.3.1 Anionic ROP of Phosphorus-Bridged, [1]Ferrocenophane **1** with *n*-BuLi

Reaction of **1** with *n*-BuLi in THF at 25 °C for 30 min was followed by quenching of the living polymer **4** by the addition of H<sub>2</sub>O to yield polymer **5**. As has been noted by Seyferth and by us,<sup>17,20</sup> poly(ferrocenylphosphine) homopolymers do not elute from a gel permeation chromatograph using THF as the elution solvent. However, these polymers will elute once the phosphorus (III) sites have been sulfurized to phosphorus (V).<sup>17,18</sup> Thus,

samples of all the homopolymers were sulfurized to give poly(ferrocenylphosphine sulfides) (6).



**Reaction 5.2 Synthesis of Poly(ferrocenylphosphine) via Living Anionic ROP of 1**



The molecular weights of the polymers could be controlled from  $M_n = 2.4 \times 10^3$  to  $3.6 \times 10^4$  with narrow polydispersities ( $M_w/M_n = 1.08$  to  $1.25$ ) by varying the  $n\text{-BuLi} : 1$  ratio from 1:11 to 1:100 and this is graphically represented in Figure 5.1. These results are summarized in Table 5.1. The polymer products 5 and 6 gave  $^{31}\text{P}$ ,  $^{13}\text{C}$  and  $^1\text{H}$  NMR spectra which were consistent with those previously reported for 2 formed by thermal ROP. The  $^{31}\text{P}$  NMR for the unsulfurized homopolymers (5, runs 1 - 3, 5) are shown in Figure 5.2. For run 1, the three major resonances can be clearly seen. The resonance at  $-31.7$  ppm was attributed to the P(III) centres in the polymer main chain and is consistent with the literature value.<sup>20</sup> The  $n\text{-BuP(Ph)Cp}$  end group can be observed at  $-28.8$  ppm while we have attributed the resonance at  $-31.1$  ppm to the crossover P(III) centre between the terminal phosphorus and

the phosphorus centres in the main chain. The integration for these resonances in runs 1 - 5 is consistent with the original monomer:initiator ratio in each case. The integrations of the resonances for the end groups and the main polymer chain in the  $^1\text{H}$  NMR spectra are also consistent the original monomer:initiator ratio. Similar results were observed in the NMR spectra of the sulfurized derivatives **6**.

Table 5.1 Synthesis of Poly(ferrocenylphosphines) and Related Copolymers via the Living Anionic ROP of **1**.<sup>a</sup>

product	mole ratio <i>n</i> -BuLi:1: <i>x</i>	$M_n$		$M_w/M_n$
		calcd <sup>a</sup>	found	
<b>5</b>	1:11:-	$3.6 \times 10^3$	$2.4 \times 10^3$	1.08
<b>5</b>	1:20:-	$6.5 \times 10^3$	$3.9 \times 10^3$	1.08
<b>5</b>	1:55:-	$1.8 \times 10^4$	$1.3 \times 10^4$	1.11
<b>5</b>	1:70:-	$2.3 \times 10^4$	$2.7 \times 10^4$	1.17
<b>5</b>	1:100:-	$3.2 \times 10^4$	$3.6 \times 10^4$	1.25
<b>7a<sup>b</sup></b>	1:11:27 <sup>c</sup>	$9.2 \times 10^3$	$8.7 \times 10^3$	1.10
<b>7b<sup>b</sup></b>	1:50:47 <sup>c</sup>	$2.5 \times 10^4$	$2.4 \times 10^4$	1.30
<b>8<sup>c</sup></b>	1:11:11 <sup>d</sup>	$5.9 \times 10^3$	$3.2 \times 10^3$	1.08
<b>10<sup>e</sup></b>	1:11:11 <sup>d</sup>	$6.2 \times 10^3$	$4.4 \times 10^3$	1.11

<sup>a</sup> based on calculated weight for the analogous sulfurized polymer (**6**) except where noted

<sup>b</sup> molecular weights determined (by GPC in THF vs polystyrene standards) and calculated for unsulfurized copolymer (calculated based on integration of the  $^1\text{H}$  NMR and assuming full conversion of monomer **1** into living polymer **4**)

<sup>c</sup>  $x = [\text{Me}_2\text{SiO}]_3$

<sup>d</sup>  $x = [1]\text{dimethylsiliferrocenophane}$

<sup>e</sup> molecular weights determined and calculated for sulfurized copolymer

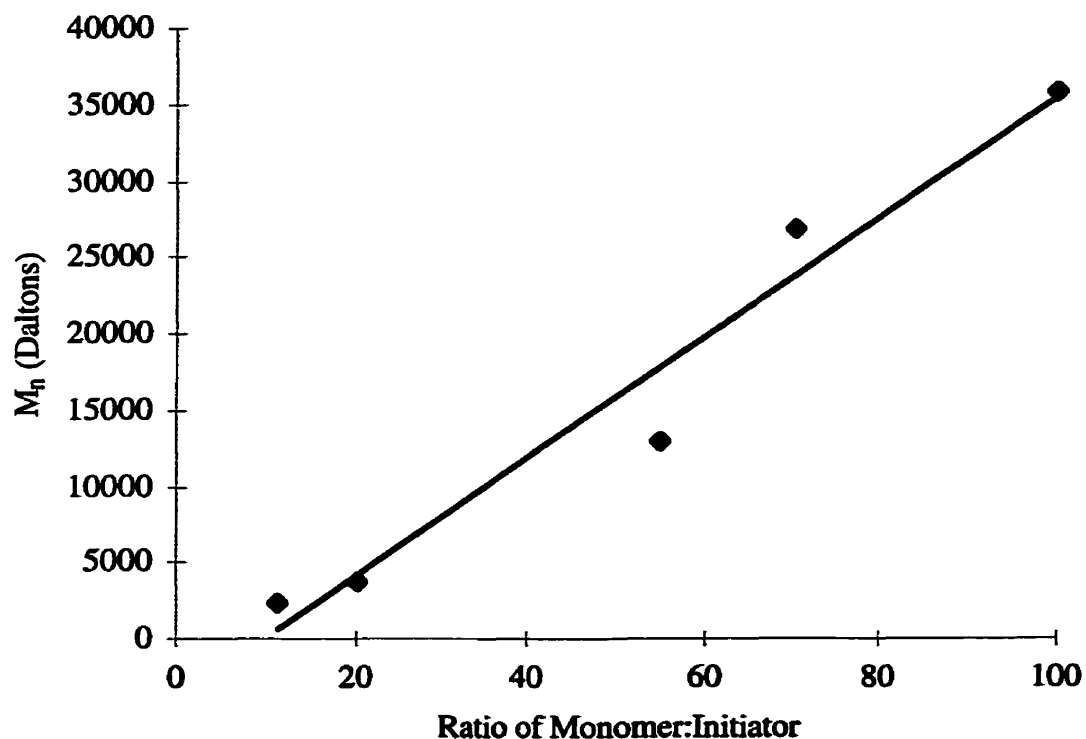


Figure 5.1 Graph of Number Average Molecular Weight ( $M_n$ ) versus the Ratio of Monomer:Initiator for **5** (runs 1 - 5) with "Best-Fit" Line

### 5.3.2 Thermal Transition Behaviour, Thermal Stability and Morphology of **5** and **6** (where $n = 100$ ).

As no characterization data on the thermal properties of polymers **5** and **6** had been reported, the thermal transition behaviour and thermal stabilities were analyzed by differential scanning calorimetry (DSC) and thermal gravimetric analysis (TGA) respectively. The morphology of these polymers was also studied using wide-angle X-ray scattering (WAXS).

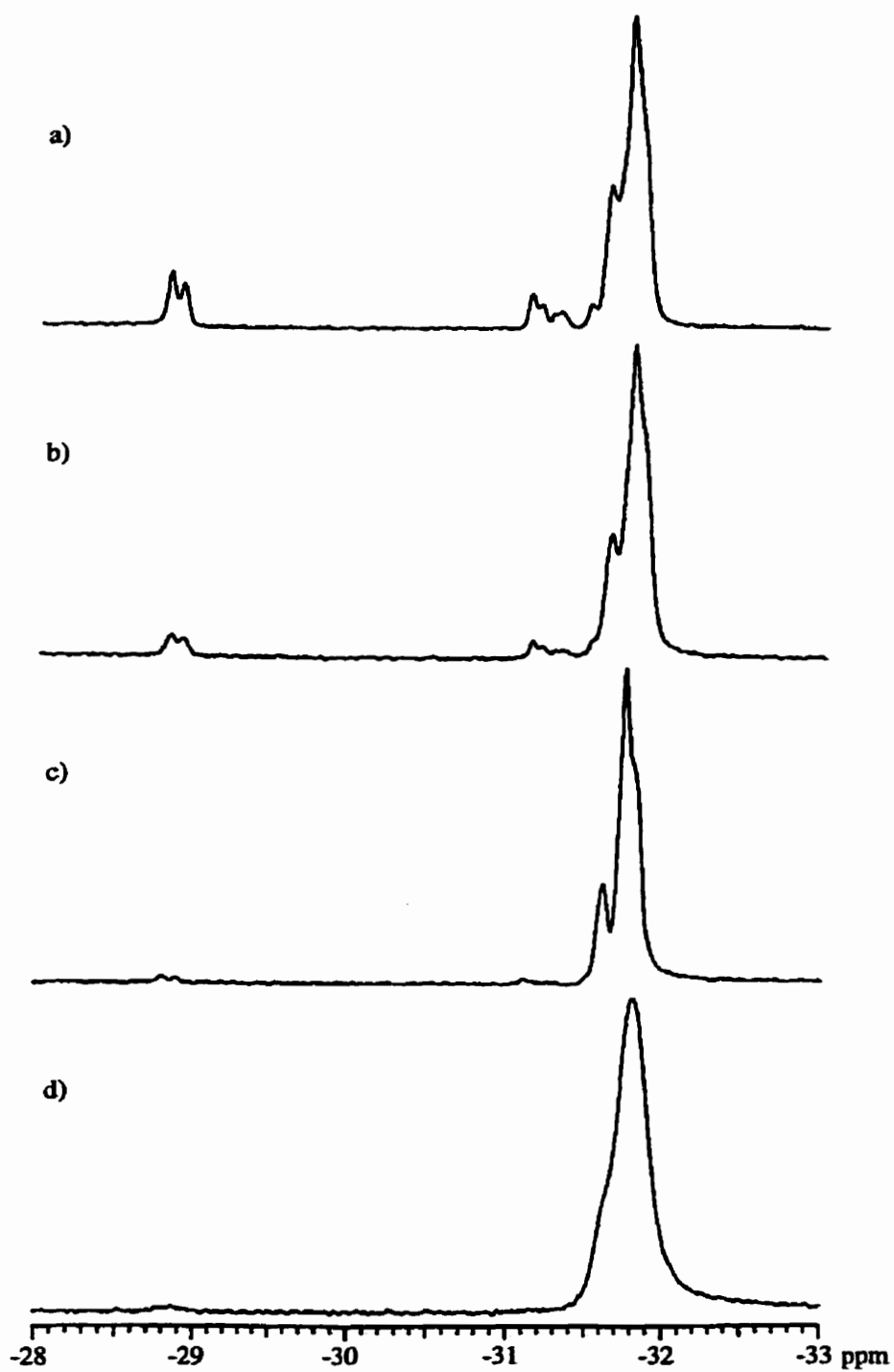


Figure 5.2  $^{31}\text{P}$  NMR Spectra (in  $\text{C}_6\text{D}_6$ ) of **5** (runs 1 - 3, 5) where 1:*n*-BuLi = a) 11:1; b) 20:1; c) 55:1; d) 100:1

Analysis by DSC (Figures 5.3a) and b) ) showed that both **5** and **6** were amorphous with no evidence for any melting transitions. Glass transitions were found, however, at 126 °C and 206 °C respectively. These values suggest that the addition of a sulfur group to phosphorus in the backbone of **5** leads to a less flexible backbone in the case of **6**. It was similarly found that an addition of a methyl group to the phosphorus centres of **5**, giving the polymer  $\{[(\eta\text{-C}_5\text{H}_4)_2\text{FePPhMe}][\text{OTf}]\}_n$  also lead to an increase in the  $T_g$  value (176 °C ) although it was noted that the presence of triflate counterions could have also played a role in the thermal transition behaviour of this polymer.<sup>21</sup> The amorphous nature of the two polymers was corroborated by the results from WAXS studies which afforded diffractograms with only one broad and featureless amorphous halo at 5.2 Å and 7.4 Å for **5** and **6**, respectively.

Polymers **5** and **6** were found to be thermally stable up to 385 °C and 410 °C respectively by TGA analysis, with 10 % weight losses having occurred by 440 °C and 430 °C for **5** and **6** respectively. By 800 °C, polymer **6** had lost 50 % of its weight whereas **5** still retained 56% of its weight even at 900 °C. The weight losses by 600 °C of 30 % and 33 % respectively were consistent with the loss of substituents from phosphorus and leaving behind an unsubstituted poly(ferrocenylphosphine) backbone.

### 5.3.3 Synthesis and Characterization of the Diblock Copolymers PFP<sub>11</sub>-*b*-PDMS<sub>81</sub> (**7a**), PFP<sub>50</sub>-*b*-PDMS<sub>141</sub> (**7b**) and PFP<sub>11</sub>-*b*-PFS<sub>11</sub> (**8**)

It was also possible to utilize the active end group of the living polymer **4** to synthesize block copolymers with either poly(siloxane) (**7a** and **7b**) or poly(ferrocenylsilane) (**8**) segments, producing polymers which were soluble and insoluble in hexanes, respectively. As the non-poly(ferrocene) segments of these copolymers are GPC-analyzable, a comparison was made between the molecular weights obtained for both the sulfurized and unsulfurized copolymers. It might be expected that the unsulfurized copolymer would give a lower



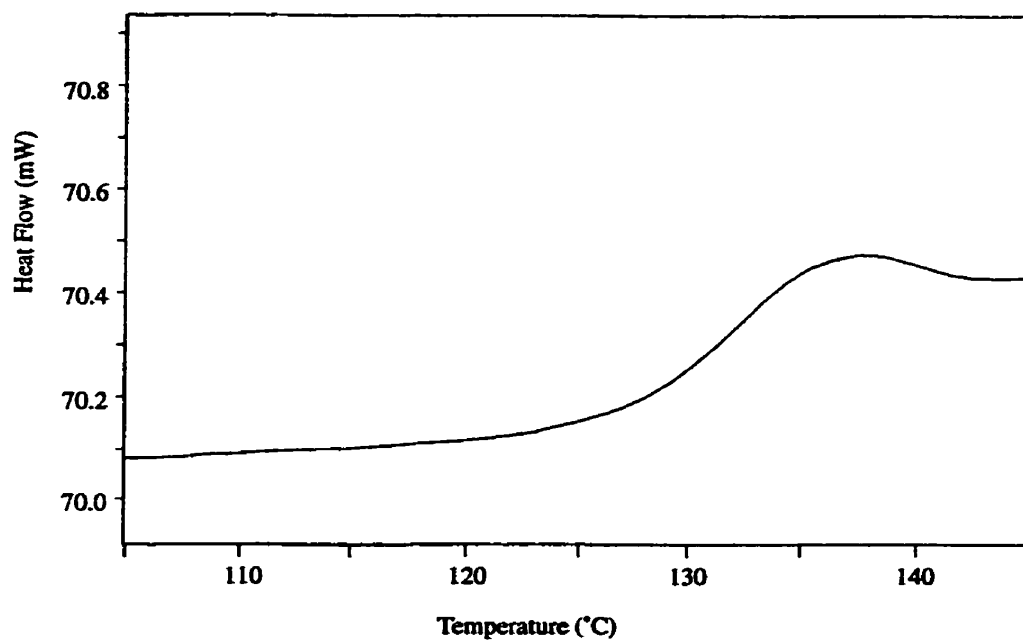


Figure 5.3a) DSC Thermogram of **5** (where  $n = 100$ )

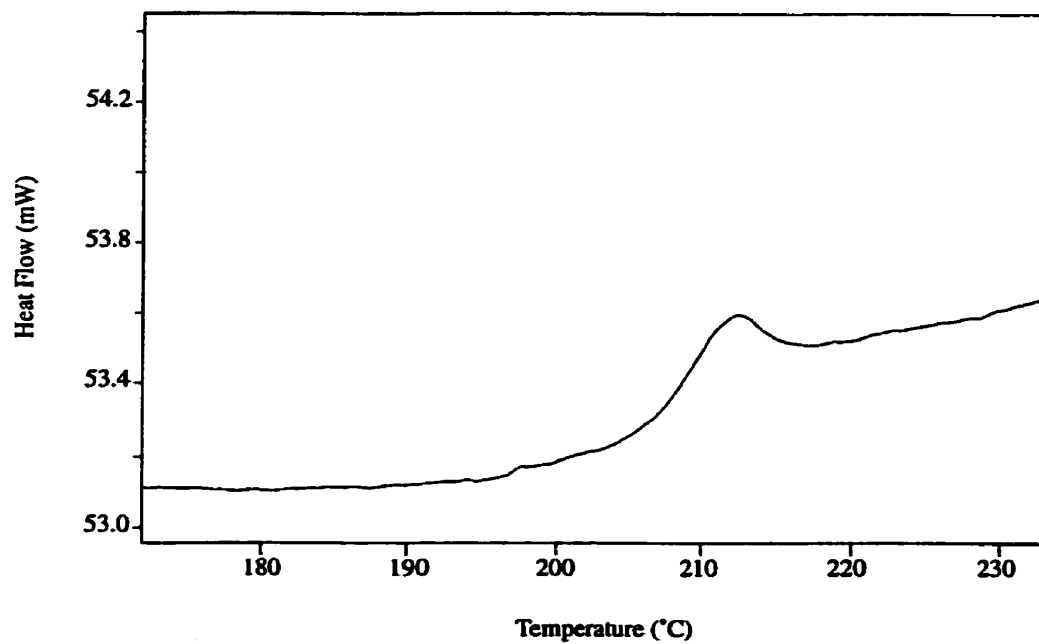


Figure 5.3b) DSC Thermogram of **6** (where  $n = 100$ )

apparent molecular weight value than the sulfurized analogue due to attractive interactions between the column material and the poly(ferrocenylphosphine) segment. This was seen for the case of the poly(ferrocenylphosphine)-poly(ferrocenylsilane) **8** (run 7 in Table 5.1) with no indication of a lower molecular fraction of any kind (i.e. the molecular weight distribution was monomodal). In the case of copolymer **7b**, there is also a tailing effect observed for the GPC trace of this polymer (Figure 5.4) which might be expected due to the presence of the poly(ferrocenylphosphine) segment of the copolymer.<sup>22</sup>

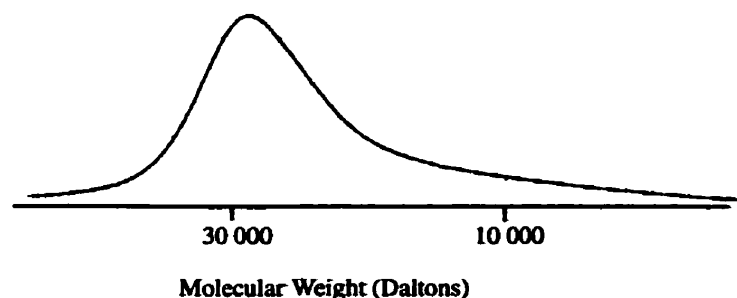
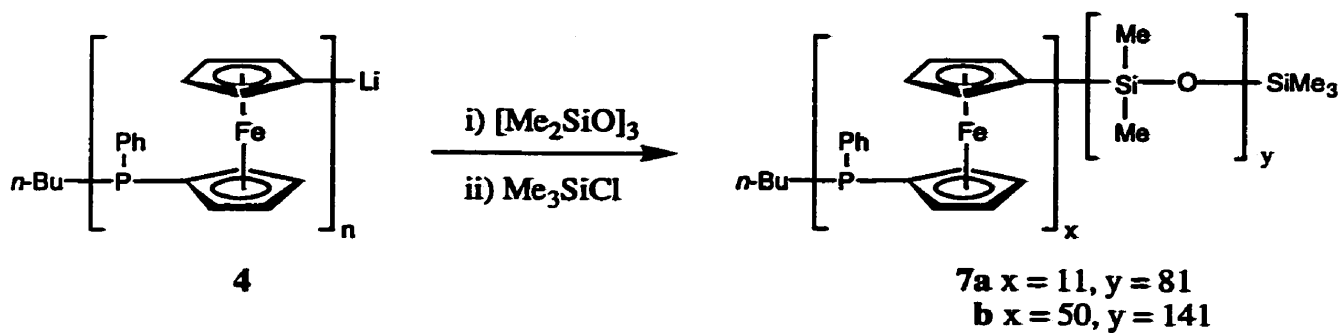
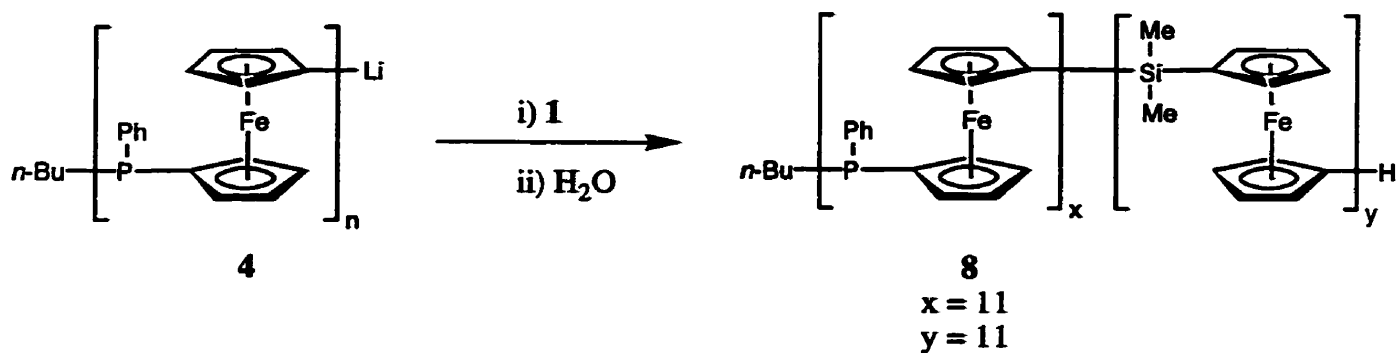


Figure 5.4 GPC Chromatogram of **7b**

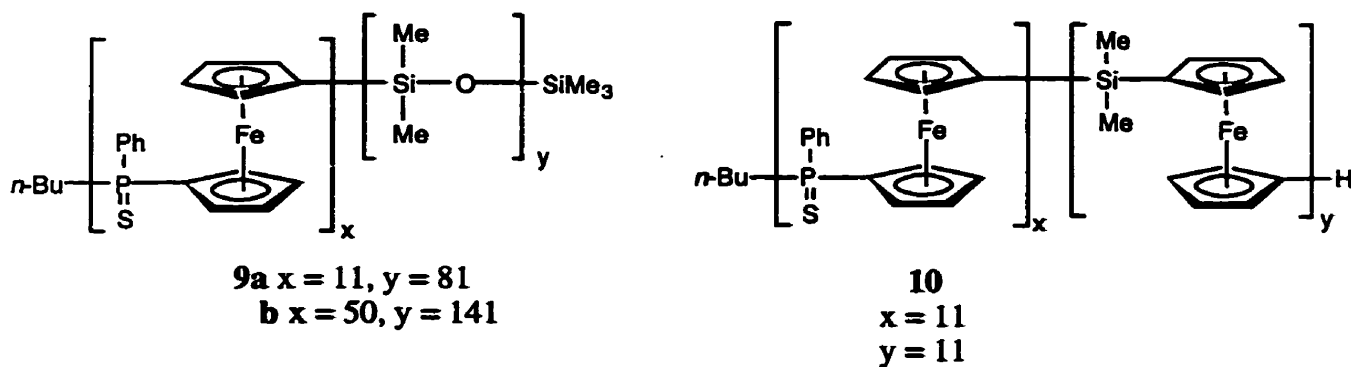
$^1\text{H}$ ,  $^{13}\text{C}$ ,  $^{29}\text{Si}$  and  $^{31}\text{P}$  NMR were run on copolymers **7a** and **7b**. For the  $^1\text{H}$  NMR of both copolymers, resonances were found for the phenyl (7.0 - 7.6 ppm) and cyclopentadienyl (3.9 - 4.4 ppm) protons of the poly(ferrocenylphosphine) segment as well as a silicon methyl resonance (0.28 ppm) assigned to the dimethylsiloxane block. The integrations for the  $^1\text{H}$  NMR spectra were consistent with the assigned ratios. In the  $^{29}\text{Si}$  NMR spectra, there was an intense resonance at -21.4 ppm due to the poly(siloxane) segment as well as small peaks due to the crossover group ( $\text{fcSiMe}_2\text{O}$ ) and the end groups ( $\text{OSiMe}_3$ ). The  $^{31}\text{P}$  NMR spectrum



**Reaction 5.3** Synthesis of Poly(ferrocenylphosphine)-Poly(siloxane) Block Copolymers



**Reaction 5.4** Synthesis of Poly(ferrocenylphosphine)-Poly(ferrocenylsilane) Block Copolymers



was consistent with a poly(ferrocenylphosphine) block consisting of 11 repeat units in the case of **7a**. Similarly, the NMR spectra for **8** were consistent with the assigned structure as were the spectra for the sulfurized analogues for **7** and **8** (**9** and **10** respectively).

#### 5.3.4 Thermal Behaviour of Block Copolymers **7b** and **8**

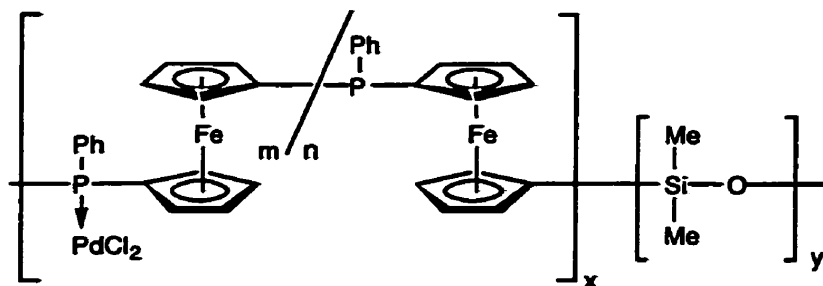
Similar to polymers **5** and **6**, copolymers **7b** and **8** were analyzed by DSC. In the case of **7b**, glass transitions were detected for both the poly(dimethylsiloxane) block ( $T_g = -126$  °C) and also the poly(ferrocenylphosphine) block ( $T_g = 126$  °C) as well as a crystallization transition ( $T_c = -107$  °C) and melting transition ( $T_m = -60$  °C) for the poly(dimethylsiloxane) block. Separate thermal transitions were also observed for the poly(ferrocenyldimethylsilane)-poly(dimethylsiloxane) copolymer.<sup>23</sup> No transitions were seen for copolymer **8**, possibly due to the shortness of both blocks.

The thermal stability of the block copolymers was examined by TGA. Copolymer **7b** was stable up to 300 °C while **8** did not begin to experience weight loss until 400 °C, with 10 % weight losses having occurred at 430 °C and 450 °C for **7b** and **8** respectively. On the other hand, **7a** only experienced 50 % weight loss by 790 °C while **8** had already lost 50 % of its weight by 660 °C.

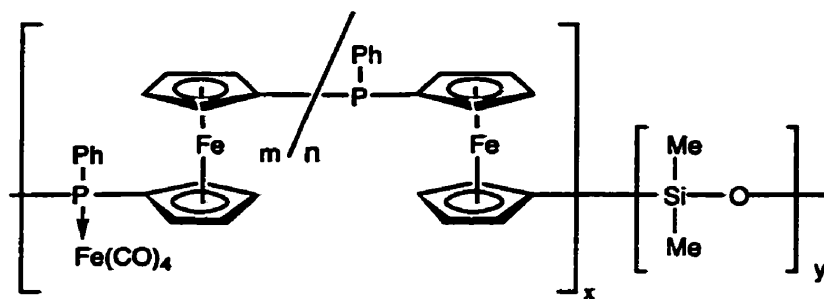
#### 5.3.5 Metal Coordination Behaviour of Block Copolymer **7b** with PdCl<sub>2</sub> and Fe(CO)<sub>4</sub>

In order to test the metal coordination behaviour of copolymer **7b**, we reacted this material with Pd(1,5-cod)Cl<sub>2</sub> and Fe(CO)<sub>4</sub>(THF) resulting in polymers **11** and **12** respectively. In both cases, the amount of coordination that occurred was estimated to be 20 - 22 % (based on the integration of the <sup>31</sup>P NMR spectra). Different behaviours, however, were observed in solution. Copolymer **11** was initially soluble in THF. However, after

removal of the THF, the material was no longer found to be appreciably soluble in either THF or chloroform. Subsequent analysis by CP-MAS  $^{31}\text{P}$  NMR spectroscopy (Figure 5.5) of the insoluble material revealed two resonances (at 29.6 and -33.9 ppm for phosphorus sites with coordinated and no coordinated  $\text{PdCl}_2$  respectively). The value for the phosphorus sites



$$\mathbf{11} \quad x = 50, y = 141 \\ m = 10, n = 40$$



$$\mathbf{12} \quad x = 50, y = 141 \\ m = 11, n = 39$$

with coordinated  $\text{PdCl}_2$  corresponds reasonably well with the value for the initial solution  $^{31}\text{P}$  NMR as well as for the model compound  $\text{fc}(\text{PPh}_2)_2\text{PdCl}_2$  (33.0 ppm).<sup>24</sup> An additional resonance at 6.6 ppm was also detected. We have attributed the resonances at 29.6 ppm and 6.6 ppm to different coordination modes for phosphorus; i.e. *cis* and *trans* coordination in which the polymer chain acts as a bidentate ligand for each Pd centre. As in general the higher field resonance is due to phosphorus ligands in a *trans* conformation,<sup>25</sup> we have assigned the resonances at 29.6 and 6.6 ppm to *cis* and *trans* conformations respectively. The

insolubility of the block copolymer may be due to crosslinking that results from coordination of Pd centres by two polymer chains rather than one. Evaporation of the reaction solvent would have led to the polymer chains being closer to one another and thus increasing the

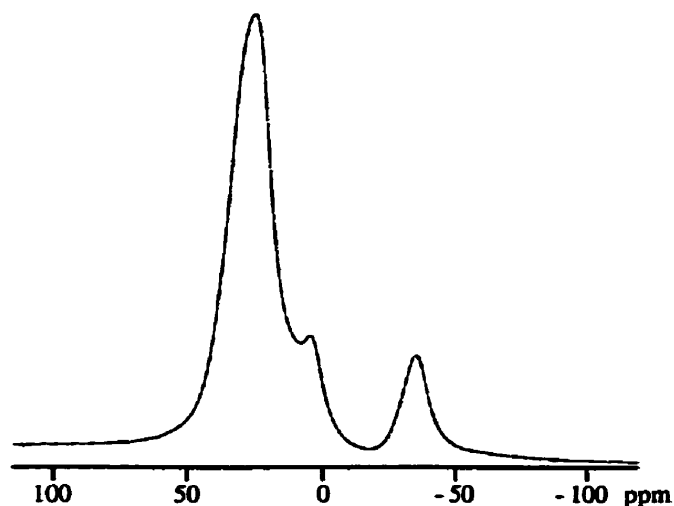


Figure 5.5 CP-MAS  $^{31}\text{P}$  NMR spectrum of **11** (spinning rate = 15 kHz)

likeliness that Pd centres on one polymer chain could also be coordinated by phosphorus sites on a neighbouring chain. It is interesting to note that the *trans* conformation is only observed in the insoluble fraction. Such a conformation is likely the preferred mode for crosslinking by the block copolymer as interchain linkage via coordination would be sterically less favourable. Also, a *cis* conformation for coordination is more likely to promote solubility which probably explains why only one conformation (presumably *cis*) is observed in the solution  $^{31}\text{P}$  NMR spectrum.

In an attempt to prevent crosslinking, we also studied the metal coordination behaviour of  $\text{Fe}(\text{CO})_4$  which would be less likely to coordinate to more than one phosphorus site. Copolymer **12**, in contrast to **11**, was found to be very soluble in THF, chloroform and benzene. It was even found to be soluble in hexane and its behaviour in this solvent is

discussed in Section 5.3.6. The solution  $^{31}\text{P}$  NMR spectrum of **12** (Figure 5.6) was found to be similar to that of **11** with resonances for coordinated and uncoordinated phosphorus sites.

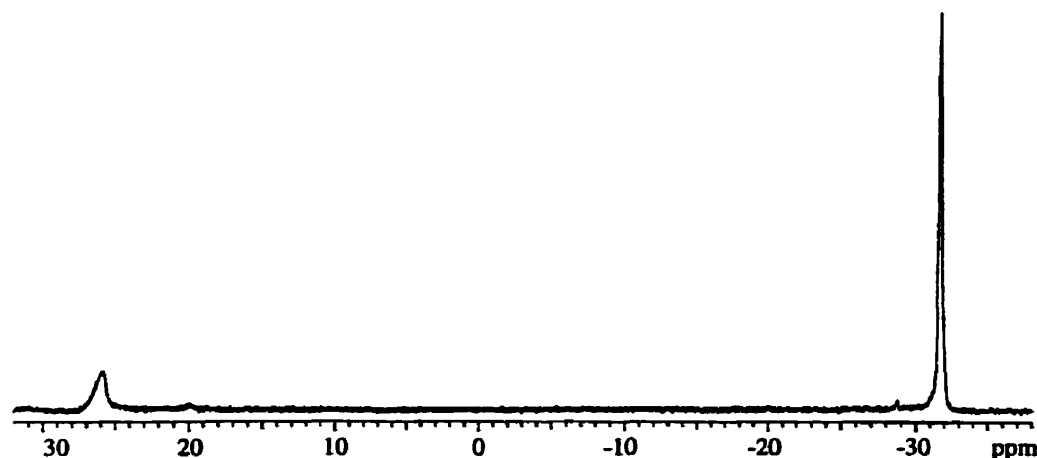


Figure 5.6  $^{31}\text{P}$  NMR spectrum (in THF) of Polymer **12**

The resonance at 25.8 ppm was attributed to monocoordination while a very small resonance at 19.9 ppm was probably due to bidentate coordination of the polymer chain. Additional evidence for coordination of  $\text{Fe}(\text{CO})_x$  moieties to the polymer were provided by IR spectroscopy. The region of for the CO stretching region is expanded and shown in Figure 5.7. The intense absorbances for **12** at 2049, 1975 and 1940  $\text{cm}^{-1}$  have been attributed to the presence of  $\text{Fe}(\text{CO})_4\text{L}$  sites (i.e. monocoordination at an axial site) where L represents coordinating phosphorus sites. The absorbance at 1884  $\text{cm}^{-1}$  has been attributed to *trans* bidentate coordination. In both cases, these results correspond well to the IR spectra of model compounds,  $\text{Fe}(\text{CO})_4(\text{PPh}_3)$  (2049, 1973 and 1939  $\text{cm}^{-1}$  in benzene) and *trans*- $\text{Fe}(\text{CO})_3(\text{PPh}_3)_2$  (1885  $\text{cm}^{-1}$  in benzene) respectively.<sup>26</sup> Other low intensity absorbances were also found at 2065, 1987 and 1917  $\text{cm}^{-1}$ . We have tentatively assigned these to an equatorial coordination of the phosphine ligand to  $\text{Fe}(\text{CO})_4$ . Corresponding resonances were not observed in the  $^{31}\text{P}$  NMR spectrum which is not particularly surprising as the amount of this form present (as judged by IR) is quite small and NMR in this situation is less sensitive.

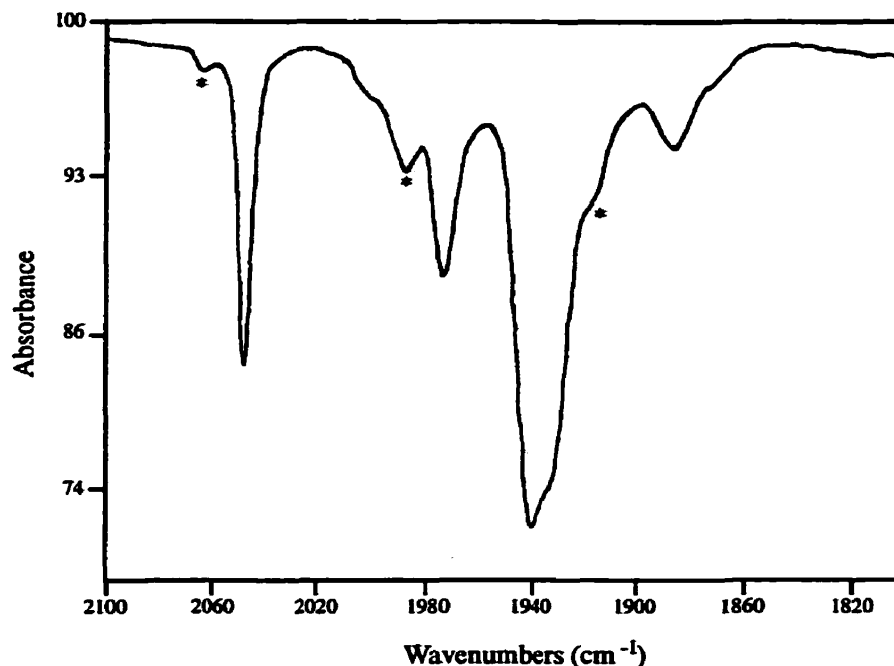


Figure 5.7 IR Spectrum (in  $\text{CCl}_4$ ) of **12**, CO Stretching Region  
 (\* unassigned peaks)

### 5.3.6. Solution Aggregation Behaviour of Block Copolymers **7b** and **12** in Hexane and Film Morphology of **7b**

As was mentioned earlier, PFS-*b*-PDMS block copolymers had been found to form "worm-like", cylindrical micelle structures in solution.<sup>19</sup> We have also examined the aggregation behaviour of **7b** and **12** in a non-solvent for the PFP block (hexane) by dynamic and static light scattering, and by transmission electron microscopy (TEM) and atomic force microscopy (AFM) after solvent evaporation. The morphology of a film of **7b** cast from THF was also examined by TEM and AFM.

Copolymer **7b** was not appreciably soluble in hexane at room temperature. However, by dissolving it in the minimum amount of THF, it was found to go into boiling hexane and remain in solution even after cooling to room temperature. The solution was dialyzed against



hexane to remove the THF. In the case of copolymer **12**, the sample was prepared by dissolution of the copolymer in boiling hexanes but no dialysis was carried out.

TEM images of **7b** after solvent evaporation are shown in Figures 5.8 and 5.9. As was found for the PFS-*b*-PDMS block copolymer,<sup>19</sup> no staining was required to obtain contrast. The most commonly observed morphology was spherical. There were, however, a range of sizes with the most common being ca. 22 nm (for example, **a** in Figure 5.8) or ca. 30 nm (e.g. **b** in Figure 5.8). In addition to these smaller spheres, larger aggregates are also visible which range from spheres (diameters up to 44 nm, **c** in Figure 5.8) to elliptical (**d** in Figure 5.9) and even more distorted shapes (**e** in Figure 5.8 and **f** in Figure 5.9). These larger shapes appear to be aggregates of the smaller spheres. Indeed, two smaller spheres in Figure 5.8 (**g**) appear to be in the process of merging and a larger and smaller sphere merging in the case of **h** (Figure 5.8). The aggregation of the smaller spheres may have resulted during sample preparation.

Similar shapes were also observed after solvent evaporation from **12** and for a film of **7b** (Figures 5.10 and 5.11 respectively). In the case of the film, the sizes of the spheres had the same range as in the samples prepared by dialysis. There was no apparent order to the distribution of the spheres, even after annealing at 150 °C for 24 h. Copolymer **12**, however, formed a greater proportion of spheres (Figure 5.10) with average diameters of 30 nm (**a**) than had been found for **7b**. Even larger spheres were also visible (e.g. **b**, diameter = 80 nm) as well as what appear to be smaller spheres in the process of merging (**c**).

Samples of **7b** prepared by dialysis and **12** were also analyzed by AFM. The results for **7b** are shown in Figure 5.12a) and b) in which the images correspond to 5 μm x 5 μm scans. Basically spherical aggregates were observed as had been seen by

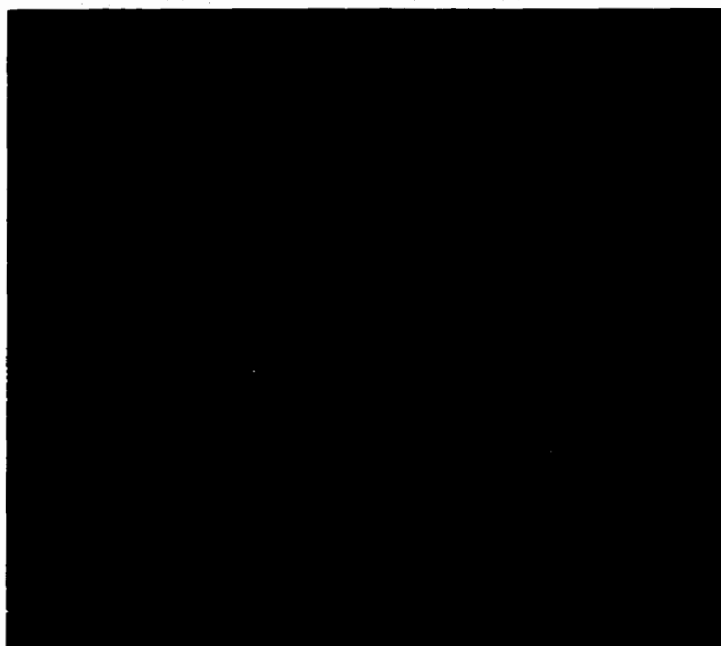


**Figure 5.8** TEM Image of **7b** after Solvent Evaporation



**Figure 5.9** More Magnified TEM Image of **7b** after Solvent Evaporation



**Figure 5.10** TEM Image of **12** after Solvent Evaporation

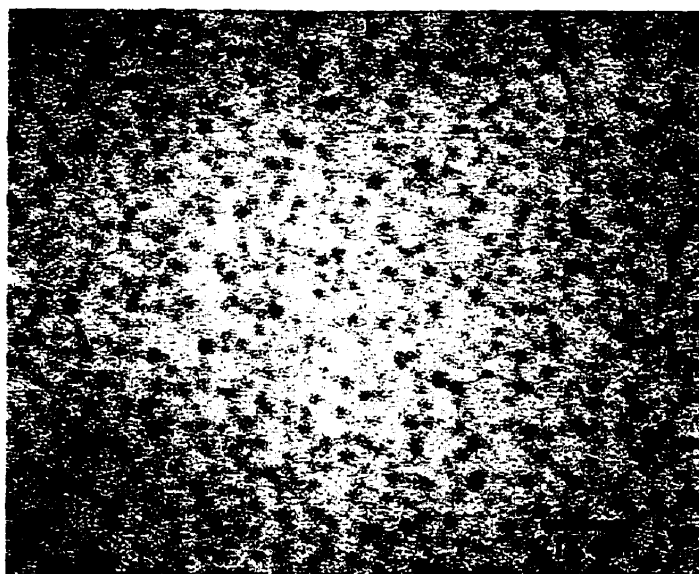


**Figure 5.11** TEM Image of Film of **7b**



**Figure 5.12a) AFM (Height) Image of 7b After Solvent Evaporation (5µm x 5µm)**



**Figure 5.12b) AFM (Phase) Image of 7b After Solvent Evaporation (5µm x 5µm)**

TEM. However, the width of the aggregates was significantly larger with an average value of 112 nm. A larger size for the aggregates as observed by AFM versus TEM would be expected as the former technique would image the corona and core rather than just the core. On the other hand, DLS studies (see later in this section) suggested an average diameter of 58.4 nm. This discrepancy may be due to flattening of the spheres on the mica support used in the AFM study. Unfortunately, in the case of **7b**, a number of layers had formed, making height measurements difficult to achieve. In the case of **12**, however, the aggregates were dispersed enough to allow both height and width measurements. The sizes varied considerably (heights ranged from 3 nm to 68 nm; widths ranged from 109 nm to 197 nm) but the flattening was apparent as the height and width values were never equal (e.g. width 122 nm, height 68 nm).

The PFP-*b*-PDMS solutions used to obtain the TEM images in Figures 5.8 and 5.9 were also examined by static (SLS) and dynamic (DLS) light scattering.<sup>27,28</sup> Micelle-like aggregates were observed even at very low concentrations ( $10^{-3}$  g/L), indicating that the critical micelle concentration (CMC) of the polymer is sufficiently low that the onset of association can be neglected in the interpretation of the scattering data. As we demonstrate below, the aggregates examined here are in fact “frozen micelles,” whose structure depends upon the method of sample preparation. These aggregates do not equilibrate on an experimentally accessible time scale.

DLS results gave a  $D_{z,0}$  value for the micelles of  $2.37 \cdot 10^{-7}$  cm<sup>2</sup>/s. This corresponds to an effective hydrodynamic radius  $R_H$ , of 29.2 nm calculated from the Stokes-Einstein relationship. This is larger than what was seen in the TEM results although this would be expected based on the TEM only resolving the core rather than the corona of the micelle. As mentioned above, due to distortion effects, AFM results were larger than would have been expected based on the DLS studies.

The ratio  $\Gamma_2/\Gamma_1^2$  is a useful measure of size polydispersity for unimodal distributions. For monodisperse spheres  $\Gamma_2/\Gamma_1^2$  has a value of ca. 0.01, and star-like spherical micelles of

narrow size distribution are typically characterized by  $\Gamma_2/\Gamma_1^2$  values of 0.4 to 0.7. We find  $\Gamma_2/\Gamma_1^2 = 0.105$ , which indicates a fairly narrow distribution of size, but not as narrow as expected for spherical micelles. This is in agreement with TEM results in which a distribution of sphere sizes was seen.

SLS experiments gave an apparent molecular weight of the micelles ( $M_w$ ) to be  $8.74 \times 10^6$  g/mol (with  $A_2 = 1.8 \times 10^{-5}$  cm<sup>3</sup> mol/g<sup>2</sup>, where  $A_2$  is the second virial coefficient) and the rms. radius of gyration,  $R_G$  was 29.8 nm. When compared to the molecular weight of the block copolymer itself, we estimate a mean aggregation number of about 320. This is slightly larger than the 50 to 150 polymer molecules per micelle found typically for spherical block copolymer micelles. The  $R_G/R_H$  value of 1.02, however, is within the range expected for spherical micelles.

## 5.4 Summary

The living anionic ROP of a phosphorus-bridged [1]ferrocenophane has been achieved and has allowed access to well-defined poly(ferrocenylphosphine) homopolymers and novel block copolymers with coordinating phosphorus atoms. Glass transition temperatures were found by DSC for high molecular weight ( $n = 100$ ) samples of polymers **5** and **6** at 126 °C and 206 °C respectively and these materials were found to be amorphous by WAXS. Analysis of the poly(ferrocenylphenylphosphine)-*b*-poly(dimethylsiloxane) copolymer **7b** by DSC showed separate thermal transitions for each block which indicated that they were incompatible. Both dynamic and static light scattering established that copolymer **7b** forms spherical micelles in hexane (a non-solvent for the poly(ferrocenylphosphine) block) and that the micelles possessed an aggregation number of ca. 320 polymer molecules. TEM and AFM after solvent evaporation also showed a spherical morphology for the aggregates with spheres ranging in size from 22 to 44 nm.

Copolymer **7b** was also found to coordinate  $\text{PdCl}_2$  (to yield insoluble copolymer) **11** as well as  $\text{Fe}(\text{CO})_4$  resulting in the formation of **12** which was still soluble in hexane. TEM and AFM after solvent evaporation showed that spherical aggregates had still been formed although they were generally larger than those found for **7b**.

Future studies will encompass investigations of the influence of block lengths on the morphologies observed for poly(ferrocenylphenylphosphine)-*b*-poly(dimethylsiloxane) in hexane as well as the synthesis of new poly(ferrocenylphosphine) block copolymers with other blocks (e.g. poly(ethylene oxide) ). In addition, we will continue studies on the metal coordination behaviour of these block copolymers and investigate applications in catalysis.

## 5.5 Experimental Section

**Equipment and Materials.** All reactions were carried out under an atmosphere of prepurified nitrogen using either Schlenk techniques or an inert-atmosphere glovebox (Vacuum Atmospheres). All of the living anionic polymerization reactions were performed in an Innovative Technologies glovebox purged with prepurified nitrogen. Hexanes and THF were dried over Na/benzophenone and distilled immediately prior to use.  $\text{CH}_2\text{Cl}_2$  was dried over  $\text{CaH}_2$  and distilled immediately prior to use. All chemicals were purchased from Aldrich unless otherwise noted.  $\text{Me}_3\text{SiCl}$  was distilled immediately prior to use. Distilled  $\text{H}_2\text{O}$  was degassed prior to use. Hexamethylcyclotrisiloxane,  $[\text{Me}_2\text{SiO}]_3$ , was dried over  $\text{CaH}_2$  and sublimed prior to use. 12-Crown-4 was distilled from  $\text{CaH}_2$  and then stored in a glovebox. The monomeric [1]ferrocenophane **1** was prepared by a modification of a previously reported procedure.<sup>29</sup> *n*-BuLi (1.6 M in hexanes ) was titrated immediately prior by addition from a 100  $\mu\text{L}$  syringe to menthol with 1,10-phenanthroline as an indicator. 1,1'-dilithioferrocene,  $\text{fcLi}_2 \cdot 2/3\text{TMEDA}$ , was prepared by a literature method.<sup>30</sup>

200 or 400 MHz  $^1\text{H}$  NMR spectra and 50.3 or 100.5 MHz  $^{13}\text{C}$  NMR spectra were recorded either on a Varian Gemini 200 or Varian Unity 400 spectrometer. 79.5 MHz  $^{29}\text{Si}$

and 121.5 MHz  $^{31}\text{P}$  NMR spectra were recorded on a Varian Unity 400 spectrometer and a Varian Gemini 300 spectrometer respectively. Solid-state 81.0 MHz  $^{31}\text{P}$  CP/MAS NMR spectra were obtained on a Bruker DSX200 spectrometer using a spinning rate of 15 kHz, a recycle delay of 10 s and a contact time of 5 ms. Molecular weights were estimated by gel permeation chromatography (GPC) using a Waters Associates liquid chromatograph equipped with a Model 510 HPLC pump, a Model U6K injector, Ultrastyrigel columns with pore sizes of  $10^3$  to  $10^5$  Å and a differential refractometer. A flow rate of 1.0 mL/min was used, and the eluent was a solution of 0.1 % tetra-*n*-butylammonium bromide in THF. Polystyrene standards were used for calibration purposes.

A Perkin-Elmer DSSC-7/Unix Differential Scanning Calorimeter equipped with a TAC 7 instrument controller was used to study the thermal behaviour. The thermograms were calibrated with the melting transitions of decane, cyclohexane and indium and were obtained at a heating rate of 10 °C/min from - 145 °C to 150 °C. A Perkin-Elmer TGA-7/Unix Thermal Gravimetric Analyzer equipped with a TAC 7 instrument controller was used to study the polymer thermal stability. Thermograms were calibrated with the magnetic transitions of Nicoseal and Perkalloy and were obtained at a heating rate of 10 °C/min under  $\text{N}_2$ .

Dynamic light scattering experiments were carried out on a wide angle laser light scattering photometer from Brookhaven Instruments Corporation. A 5 mW vertically polarized He-Ne laser from Spectra physics was the light source. The solutions were filtered through disposable 0.5 µm filters from Millipore into glass scattering cells with a diameter of 12.3 mm. The cells were placed into the BI-200SM goniometer and sat in a vat of thermostated toluene which matched the index of refraction of the glass cells. The angular range of the goniometer was 7° - 162°. The scattered light was detected by a photomultiplier interfaced to the BI-2030AT digital correlator with 136 channels and measured the correlation function in real time. The instrument was controlled by a 486AT computer. The data was analyzed by software supplied by Brookhaven.



Static light scattering experiments were also carried out on the same instrument as that used for the dynamic light scattering measurements. A larger quartz cell was used with a diameter of 22 nm. Toluene was used as a reference for the Rayleigh ratio ( $R_{\theta} = 14 \times 10^{-6} \text{ cm}^{-1}$ ).

Transmission electron micrographs were obtained on a Hitachi Model 600 electron microscope. Atomic force images were obtained using a NanoScope III (Digital Instruments) in tapping mode with a silicon cantilever with a resonance frequency of 300 - 380 KHz.

**Synthesis of Phosphorus-Bridged [1]Ferrocenophane 1.** Over a period of 15 min, 15.9 mL (117 mmol) of  $\text{PhPCl}_2$  were added dropwise to a stirred suspension of 30.0 g (109 mmol)  $\text{fcLi}_2 \cdot 2/3\text{TMEDA}$  in 250 mL of hexanes cooled to  $-30^\circ\text{C}$ . The reaction mixture was then allowed to warm to room temperature at which point it was filtered. Solvent and excess  $\text{PhPCl}_2$  were removed under vacuum. The solid was also dried under vacuum. Both fractions were then recombined and **1** was extracted using hexanes and recrystallized at  $-55^\circ\text{C}$ . The monomer was purified by two further recrystallizations resulting in 12.7 g (40 %) of dark red crystalline **1**. This purified product was found to be suitable for living anionic polymerizations as no resonances in the  $^1\text{H}$  NMR spectrum other than those for **1** and benzene were observed on 20x expansion of the vertical scale of a  $^1\text{H}$  spectrum of a solution containing 30 mg of **1** in 0.5 mL of  $\text{C}_6\text{D}_6$ .  $^1\text{H}$ -NMR (200 MHz,  $\text{C}_6\text{D}_6$ ) is included for comparison: 7.7 - 7.5 (m, *o*-Ph, 2H), 7.2 - 7.0 (m, *p,m*-Ph, 3H), 4.6 - 4.5 (m, Cp, 2H), 4.4 - 4.3 (m, Cp, 2H), 4.3 - 4.1 (m, Cp, 4H).

Examples of standard procedures for the anionic polymerization experiments are provided in the following sections:

**Anionic ROP of 1 Initiated by *n*-BuLi.** The reactions were carried out by the addition of *n*-BuLi (1.6 M in hexanes) to a solution of **1** in 2 mL of THF. The reaction was stirred at room

temperature for 10 minutes before termination by the addition of a few drops of H<sub>2</sub>O. The yellow polymer product **5** was isolated by precipitation into hexanes and filtration, and was dried under high vacuum for 12 h (Table 1).

For **5** (where  $n = 11, 20$  or  $55$ ): <sup>31</sup>P NMR (C<sub>6</sub>D<sub>6</sub>):  $\delta = -28.8$  [PhP(*n*-Bu)fc-],  $-31.1$  (-fcPPhFc),  $-31.7$  (-fcPPhfc-) ppm. <sup>13</sup>C NMR (C<sub>6</sub>D<sub>6</sub>):  $\delta = 139.9$  (Ph, *ipso*-C),  $134.5$  (Ph),  $129.0$  (Ph),  $79.3$  (Cp, *ipso*-C),  $72.0 - 74.8$  (Cp),  $69.5$  [( $\eta$ -C<sub>5</sub>H<sub>4</sub>)Fe( $\eta$ -C<sub>5</sub>H<sub>5</sub>)] ppm. <sup>1</sup>H NMR (C<sub>6</sub>D<sub>6</sub>):  $\delta = 7.6 - 7.7$  (Ph),  $7.0 - 7.2$  (Ph),  $3.9 - 4.4$  (Cp)  $1.95$  (CH<sub>2</sub>CH<sub>2</sub>CH<sub>2</sub>CH<sub>3</sub>),  $1.23 - 1.60$  (CH<sub>2</sub>CH<sub>2</sub>CH<sub>2</sub>CH<sub>3</sub>)  $0.86$  (CH<sub>2</sub>CH<sub>2</sub>CH<sub>2</sub>CH<sub>3</sub>) ppm.

For **5** (where  $n = 70$  or  $100$ ), the NMR data was the same as per above but there were no detectable resonances associated with either the *n*-Bu or PPhFc end groups.

#### Synthesis of the Poly(ferrocenylphosphine)-*b*-Poly(dimethylsiloxane) Copolymer **7a**.

A solution (50  $\mu$ L, 0.08 mmol) of 1.6 M *n*-BuLi in hexanes was injected into a dark red solution of 260 mg (0.89 mmol) of **1** in 2 mL of THF cooled down to 0 °C. The solution gradually changed from dark red to dark orange over 5 min. After 30 min, 219 mg (0.90 mmol) of hexamethylcyclotrisiloxane were added and the solution stirred for overnight. The reaction was then quenched by the addition of a few drops of Me<sub>3</sub>SiCl and copolymer **7a** was isolated by precipitation into a 1 % solution of triethylamine in methanol, filtration, and then drying under high vacuum for 12 h. The polymer was found to be a sticky yellow solid. Yield: 400 mg (83 %);  $M_w = 9.6 \times 10^3$ ,  $M_n = 8.7 \times 10^3$ , PDI = 1.10, (calculated  $M_n = 9.2 \times 10^3$ ).

For **7a**: <sup>31</sup>P NMR (C<sub>6</sub>D<sub>6</sub>):  $\delta = -28.8$  [PhP(*n*-Bu)fc-],  $-31.7$  (-fcPPhfc-) ppm. <sup>29</sup>Si NMR (C<sub>6</sub>D<sub>6</sub>):  $\delta = 7.6$  (-OSiMe<sub>3</sub>),  $0.5$  (-fcMe<sub>2</sub>SiO-),  $-21.4$  (-Me<sub>2</sub>SiO-) ppm. <sup>13</sup>C NMR (C<sub>6</sub>D<sub>6</sub>):  $\delta = 139.9$  (Ph, *ipso*-C),  $134.5$  (Ph),  $129.0$  (Ph),  $79.3$  (Cp, *ipso*-C),  $72.0 - 74.8$  (Cp),  $69.5$  [( $\eta$ -C<sub>5</sub>H<sub>4</sub>)Fe( $\eta$ -C<sub>5</sub>H<sub>5</sub>)-Me<sub>2</sub>SiO-],  $1.4$  (-Me<sub>2</sub>SiO-) ppm. <sup>1</sup>H NMR (C<sub>6</sub>D<sub>6</sub>):  $\delta = 7.6 - 7.7$  (Ph),  $7.0 - 7.2$  (Ph),  $3.9 - 4.4$  (Cp),  $1.95$  (CH<sub>2</sub>CH<sub>2</sub>CH<sub>2</sub>CH<sub>3</sub>),  $1.23 - 1.60$  (CH<sub>2</sub>CH<sub>2</sub>CH<sub>2</sub>CH<sub>3</sub>)  $0.86$  (CH<sub>2</sub>CH<sub>2</sub>CH<sub>2</sub>CH<sub>3</sub>)  $0.28$  (-Me<sub>2</sub>SiO-) ppm. <sup>1</sup>H NMR integration gave for **7a**  $x = 11$  and  $y = 27$ ; for **7b**  $x = 50$  and  $y = 141$ .

**Synthesis of the Poly(ferrocenylphosphine)-*b*-Poly(ferrocenylsilane) Copolymer 8.** A solution (50  $\mu\text{L}$ ) of 1.6 M *n*-BuLi in hexanes was injected into a dark red solution of 260 mg (0.89 mmol) of **1** in 2 mL of THF. The solution gradually changed from dark red to dark orange over 5 min. At this point, 219 mg (0.90 mmol) of [1]dimethylsilaferrocenophane were added and the solution stirred for a further 20 min. The reaction was then quenched by the addition of a few drops of H<sub>2</sub>O and polymer **8** was isolated by precipitation into hexanes and filtration, and was then dried under high vacuum for 12 h. The polymer was found to be an orange-yellow powder. Yield: 470 mg (98 %);  $M_w = 9.6 \times 10^3$ ,  $M_n = 3.5 \times 10^3$ , PDI = 1.08, (calculated  $M_n = 5.9 \times 10^3$ ).

For **8**: <sup>31</sup>P NMR (C<sub>6</sub>D<sub>6</sub>):  $\delta = -28.8$  [PhP(*n*-Bu)fc-],  $-31.1$  (-fcPPhfcSiMe<sub>2</sub>-),  $-31.7$  (-fcPPhfc-) ppm. <sup>29</sup>Si NMR (C<sub>6</sub>D<sub>6</sub>):  $\delta = -6.4$  (-fcSiMe<sub>2</sub>fc-) ppm. <sup>13</sup>C NMR (C<sub>6</sub>D<sub>6</sub>):  $\delta = 139.9$  (Ph, *ipso*-C), 134.5 (Ph), 129.0 (Ph), 79.3 (Cp<sub>2</sub>FePPh, *ipso*-C), 72.0 - 74.8 (Cp), 69.5 [( $\eta$ -C<sub>5</sub>H<sub>4</sub>)Fe( $\eta$ -C<sub>5</sub>H<sub>5</sub>)],  $-0.5$  (-fcSiMe<sub>2</sub>fc-) ppm. <sup>1</sup>H NMR (C<sub>6</sub>D<sub>6</sub>):  $\delta = 7.6 - 7.7$  (Ph), 7.0 - 7.2 (Ph), 3.9 - 4.4 (Cp), 1.95 (CH<sub>2</sub>CH<sub>2</sub>CH<sub>2</sub>CH<sub>3</sub>), 1.23 - 1.60 (CH<sub>2</sub>CH<sub>2</sub>CH<sub>2</sub>CH<sub>3</sub>), 0.86 (CH<sub>2</sub>CH<sub>2</sub>CH<sub>2</sub>CH<sub>3</sub>) 0.54 (-fcMe<sub>2</sub>Sifc-) ppm. <sup>1</sup>H NMR integration gave for **8**,  $x = 11$  and  $y = 11$ .

**Reaction of the Poly(ferrocenylphosphine) Homopolymers and Block Copolymers with Elemental Sulfur: Synthesis of the Analogous Poly(ferrocenylphosphine sulfide)s 6, 9, 10.** All reactions were carried out in a similar fashion, and that for **5** is detailed as a representative example.

Polymer **5** (50 mg, 0.171 mmol) was dissolved in 2 mL of dry dichloromethane with stirring. To this solution was added elemental sulfur (5.5 mg, 0.021 mmol of S<sub>8</sub>). The reaction mixture was allowed to stir overnight. This solution was then filtered and the solvent removed under vacuum. GPC analysis was then carried out and the results are listed in Table 1. The NMR data for polymers **5** were essentially identical and the full data for **6** (n

= 11, 20 or 55) is only reported here. The NMR data for the block copolymers **9a** and **10** are also given.

For **6** (where  $n = 11, 20$  or  $55$ ):  $^{31}\text{P}$  NMR ( $\text{C}_6\text{D}_6$ ):  $\delta = 41.4$  [ $\text{PhP}(\text{S})(n\text{-Bu})\text{fc-}$ ],  $37.1$  ( $-\text{fcP}(\text{S})\text{PhFc}$ ),  $37.2$  ( $-\text{fcPPhfc-}$ ) ppm.  $^{13}\text{C}$  NMR ( $\text{C}_6\text{D}_6$ ):  $\delta = 135.0$  (Ph, *ipso-C*),  $131.3$  (Ph),  $129.0$  (Ph),  $79.5$  (Cp, *ipso-C*),  $72.5 - 75.8$  (Cp),  $70.3$  [ $(\eta\text{-C}_5\text{H}_4)\text{Fe}(\eta\text{-C}_5\text{H}_5)$ ] ppm.  $^1\text{H}$  NMR ( $\text{C}_6\text{D}_6$ ):  $\delta = 7.9 - 8.1$  (Ph),  $7.0 - 7.2$  (Ph),  $4.0 - 5.0$  (Cp),  $2.15$  ( $\text{CH}_2\text{CH}_2\text{CH}_2\text{CH}_3$ ),  $1.10 - 1.50$  ( $\text{CH}_2\text{CH}_2\text{CH}_2\text{CH}_3$ ),  $0.75$  ( $\text{CH}_2\text{CH}_2\text{CH}_2\text{CH}_3$ ) ppm.

For **6** (where  $n = 70$  or  $100$ ), the NMR data was the same as per above but there were no detectable resonances for the terminal *n*-Bu group.

For **9a**:  $^{31}\text{P}$  NMR ( $\text{C}_6\text{D}_6$ ):  $\delta = 41.4$  [ $\text{PhP}(\text{S})(n\text{-Bu})\text{fc-}$ ],  $37.2$  ( $-\text{fcP}(\text{S})\text{Phfc-}$ ) ppm.  $^{29}\text{Si}$  NMR ( $\text{C}_6\text{D}_6$ ):  $\delta = 7.6$  ( $-\text{OSiMe}_3$ ),  $0.5$  ( $-\text{fcMe}_2\text{SiO-}$ ),  $-21.4$  ( $-\text{Me}_2\text{SiO-}$ ) ppm.  $^{13}\text{C}$  NMR ( $\text{C}_6\text{D}_6$ ):  $\delta = 135.0$  (Ph, *ipso-C*),  $131.3$  (Ph),  $129.0$  (Ph),  $79.5$  (Cp, *ipso-C*),  $72.5 - 75.8$  (Cp),  $70.3$  [ $(\eta\text{-C}_5\text{H}_4)\text{Fe}(\eta\text{-C}_5\text{H}_5)$ ],  $1.4$  ( $-\text{Me}_2\text{SiO-}$ ) ppm.  $^1\text{H}$  NMR ( $\text{C}_6\text{D}_6$ ):  $\delta = 7.9 - 8.1$  (Ph),  $7.0 - 7.2$  (Ph),  $4.0 - 5.0$  (Cp),  $2.15$  ( $\text{CH}_2\text{CH}_2\text{CH}_2\text{CH}_3$ ),  $1.10 - 1.50$  ( $\text{CH}_2\text{CH}_2\text{CH}_2\text{CH}_3$ ),  $0.75$  ( $\text{CH}_2\text{CH}_2\text{CH}_2\text{CH}_3$ ),  $0.28$  ( $-\text{Me}_2\text{SiO-}$ ) ppm.

For **10**:  $^{31}\text{P}$  NMR ( $\text{C}_6\text{D}_6$ ):  $\delta = 41.4$  [ $\text{PhP}(\text{S})(n\text{-Bu})\text{fc-}$ ],  $37.1$  ( $-\text{fcP}(\text{S})\text{PhfcSiMe}_2\text{-}$ ),  $37.2$  ( $-\text{fcPPhfc-}$ ) ppm.  $^{29}\text{Si}$  NMR ( $\text{C}_6\text{D}_6$ ):  $\delta = -6.4$  ( $-\text{fcSiMe}_2\text{fc-}$ ) ppm.  $^{13}\text{C}$  NMR ( $\text{C}_6\text{D}_6$ ):  $\delta = 135.0$  (Ph, *ipso-C*),  $131.3$  (Ph),  $129.0$  (Ph),  $79.5$  (Cp, *ipso-C*),  $72.5 - 75.8$  (Cp),  $70.3$  [ $(\eta\text{-C}_5\text{H}_4)\text{Fe}(\eta\text{-C}_5\text{H}_5)$ ]  $-0.5$  ( $-\text{fcSiMe}_2\text{fc-}$ ) ppm.  $^1\text{H}$  NMR ( $\text{C}_6\text{D}_6$ ):  $\delta = 7.9 - 8.1$  (Ph),  $7.0 - 7.2$  (Ph),  $4.0 - 5.0$  (Cp),  $2.15$  ( $\text{CH}_2\text{CH}_2\text{CH}_2\text{CH}_3$ ),  $1.10 - 1.50$  ( $\text{CH}_2\text{CH}_2\text{CH}_2\text{CH}_3$ ),  $0.75$  ( $\text{CH}_2\text{CH}_2\text{CH}_2\text{CH}_3$ ),  $0.54$  ( $-\text{fcMe}_2\text{Sifc-}$ ) ppm.

**Reaction of Block Copolymer 7b with Pd(1,5-cod)Cl<sub>2</sub>.** 0.113 g (0.226 mmol of available P sites) of **7b** were dissolved in 2 mL of THF under air. To this stirred orange solution were added 0.019 g (0.067 mmol) of Pd(1,5-cod)Cl<sub>2</sub>. The solution immediately turned red-purple

and the evolution of 1,5-cod was noted based on the characteristic odour of the material. The solution was allowed to stir for 1 h. An aliquot of this solution was analyzed by solution NMR, the results of which are described below. The solution was filtered and the solvent removed under high vacuum yielding **11** as a glossy, dark red film. The compound was no longer appreciably soluble in either THF or  $\text{CDCl}_3$ . The sample was then analyzed by CP-MAS  $^{31}\text{P}$  NMR and the results are described below. Yield: 0.090 g (74 % based on 20 % coordinated P sites).

For **11**:  $^{31}\text{P}$  NMR (THF):  $\delta = 25.2$  (with coordinated  $\text{PdCl}_2$ ) and  $-31.7$  (uncoordinated PPh sites) ppm. Based on integration of the NMR spectrum, the amount of phosphorus sites with coordinated  $\text{PdCl}_2$  was estimated to be 20 %. CP-MAS  $^{31}\text{P}$  NMR: 29.6 (with coordinated  $\text{PdCl}_2$  in a *cis* conformation), 6.6 (with coordinated  $\text{PdCl}_2$  in a *trans* conformation) and  $-33.9$  (uncoordinated PPh sites) ppm.

**Reaction of Block Copolymer 7b with  $\text{Fe}(\text{CO})_4(\text{THF})$ .** 0.090 g (0.247 mmol) of  $\text{Fe}_2(\text{CO})_9$  were dissolved in 10 mL of THF. This solution was then added dropwise with stirring to 0.515 g (1.03 mmol of P sites) of **7b** dissolved in 5 mL of THF. The solution was then allowed to stir for a further 2 h and filtered. Polymer **12** was isolated by precipitation into methanol and dried under high vacuum, yielding a sticky orange-yellow material. After isolation, **12** was stored under nitrogen. Based on the  $^{31}\text{P}$  NMR analysis, the amount of phosphorus sites with coordinated  $\text{Fe}(\text{CO})_4$  was estimated to be 22 %. In contrast to **11**, **12** remained soluble in the same solvents as the parent polymer **7b**. Yield: 0.489 g (88 % based on 22 % coordinated P sites)

For **12**:  $^{31}\text{P}$  NMR ( $\text{C}_6\text{D}_6$ ):  $\delta = 25.8$  (with coordinated  $\text{Fe}(\text{CO})_4$ ) and  $-31.7$  (no coordinated  $\text{Fe}(\text{CO})_4$ ) ppm. There are additionally very small resonances at 19.9 (with coordinated  $\text{Fe}(\text{CO})_3$ ) and  $-28.8$  (*n*-BuP(Ph)Cp end group) ppm.  $^1\text{H}$  NMR spectrum was consistent with retention of the structure described for **7b**. IR spectrum (in  $\text{CCl}_4$ , terminal carbonyl region): 2049 (s), 1975 (s) and 1940 (vs)  $\text{cm}^{-1}$  which are due to the CO groups of  $\text{Fe}(\text{CO})_4(\text{L})$ ; 1884

(s)  $\text{cm}^{-1}$  due to the CO groups of  $\text{Fe}(\text{CO})_3\text{L}_2$  where L represents P(III) sites within the polymer backbone.

**Static Light Scattering.** SLS experiments were carried out to determine the weight averaged molecular weight,  $M_w$ , radius of gyration,  $R_G$ , and the second virial coefficient,  $A_2$ . The values were obtained by the Rayleigh-Debye relationship

$$K_c/R_\theta = [(1/M_w) + 2A_2c + 3A_3c^2 + \dots](1 + (16\pi^2/3\lambda^2)R_G^2\sin^2(\theta/2)) \quad (5.1)$$

where  $c$  is the concentration,  $R_\theta$  is the measured Rayleigh ratio, and  $K$  is an optical constant defined as

$$K = [4\pi^2n^2/N_A\lambda_0^4](dn/dc)^2 \quad (5.2)$$

where  $n$  is the refractive index of the solvent,  $\lambda_0$  is the wavelength of the laser light in vacuum  $N_A$  is Avogadro's number and  $dn/dc$  is the refractive index increment of the solution. Refractive index increment measurements were performed at five different concentrations in hexane at 21°C. A value of  $dn/dc$  at 632.8 nm of 0.2024 ml/g was obtained.

**Dynamic Light Scattering.** In dynamic light scattering the experimentally determined intensity auto-correlation function  $G^{(2)}(\tau)$  is related to the auto-correlation function representative of the motions of the particles  $G^{(1)}(\tau)$

$$G^{(2)}(\tau) = I_\theta^2[1 + \geq[G^{(1)}(\tau)/G^{(1)}(0)\geq^2] = I_\theta^2[1 + \exp(-2Dq^2\tau)] \quad (5.3)$$

where the normalized intensity auto-correlation function which is determined experimentally can be expressed as an exponential with a decay of  $\Gamma$ ,

$$g^{(1)}(\tau) = [G^{(1)}(\tau)/G^{(1)}(0)] = A\exp(-\Gamma\tau) \quad (5.4)$$

Real systems can rarely be described by a single decay, and often a cumulant expansion is used, where the logarithm of  $g^{(1)}(\tau)$  is expanded in a power series in terms of the delay time  $\tau$ ,

$$\ln g^{(1)}(\tau) = -\Gamma_1\tau + (\Gamma_2/2!)\tau^2 - (\Gamma_3/3!)\tau^3 + \dots \quad (5.5)$$

where  $\Gamma_1$  is the first cumulant,  $\Gamma_2$  the second cumulant and so forth. Finally once  $\Gamma_1$  is determined the concentration and angular dependence can be expressed as

$$\Gamma_2/q^2 = D_{z0}(1 + k_D C + \dots)(1 + C(R_G)^2 q^2 + \dots) \quad (5.6)$$

where  $D_{z0}$  is the diffusion coefficient,  $C$  is a parameter that is characteristic of the molecular architecture,  $k_D$  is the effective interaction parameter,  $R_G$  is the average radius of gyration and  $q$  is the magnitude of the scattering vector,  $q = (4\pi n/\lambda_0)\sin(\theta/2)$ .

From the diffusion coefficient the effective hydrodynamic radius,  $R_H$  can be determined from the Stokes-Einstein relation,

$$R_H = (kT)/(6\pi\eta D_z) \quad (5.7)$$

where  $\eta$  is the solvent viscosity.

**Preparation of Samples for TEM and AFM.** Thin carbon films (ca. 5 Å) were grown on mica as a support, then 25  $\mu$ L of a dilute solution of the block copolymer in hexane (ca. 0.2 %) was aerosol sprayed onto the carbon film. Each carbon film was floated off the mica support in water and deposited onto a 300 mesh Gilder copper grid. The sample was air dried before introduction into the electron microscope. No staining of the samples was necessary. Samples for AFM were prepared in an analogous manner, except that the solution was aerosol sprayed directly on a freshly cleaved mica surface which was then mounted for imaging.

## 5.6 References

- (1) Herrmann, W. A.; Cornils, B. *Angew. Chem. Int. Ed. Engl.* **1997**, *36*, 1048.
- (2) Hartley, F. R. *Supported Metal Complexes. A New Generation of Catalysts.*; Reidel: Dordrecht, 1985, .
- (3) Pittman jr., C. U. In *Comprehensive Organometallic Chemistry*; G. Wilkinson, Ed.; Pergamon Press: Toronto, 1982; Vol. 9; pp 553.
- (4) Herrmann, W. A.; Anwander, R.; Dufaud, V.; Scherer, W. *Angew. Chem. Int. Ed. Engl.* **1994**, *33*, 1285.
- (5) Kobayashi, S.; Nagayama, S. *J. Am. Chem. Soc.* **1998**, *120*, 2985.
- (6) Klingelhöfer, S.; Heitz, W.; Greiner, A.; Oestreich, S.; Förster, S.; Antonietti, M. *J. Am. Chem. Soc.* **1997**, *119*, 10116.
- (7) Manners, I. *Polyhedron* **1996**, *15*, 4311.
- (8) Manners, I. *Can. J. Chem.* **1998**, *76*, 731.
- (9) Foucher, D. A.; Honeyman, C. H.; Nelson, J. M.; Tang, B.-Z.; Manners, I. *Angew. Chem.* **1993**, *105*, 1843.
- (10) Petersen, R.; Foucher, D. A.; Tang, B.-Z.; Lough, A. J.; Raju, N. P.; Greedan, J. E.; Manners, I. *Chem. Mater.* **1995**, *7*, 2045.
- (11) Nelson, J. M.; Rengel, H.; Petersen, R.; Nguyen, P.; Manners, I.; Raju, N. P.; Greedan, J. E.; Barlow, S.; O'Hare, D. *Chem. Eur. J.* **1997**, *3*, 573.
- (12) Rulkens, R.; Lough, A. J.; Manners, I. *Angew. Chem., Int. Ed. Engl.* **1996**, *35*, 1805.
- (13) Rulkens, R.; Gates, D. P.; Balaishis, D.; Pudelski, J. K.; McIntosh, D. F.; Lough, A. J.; Manners, I. *J. Am. Chem. Soc.* **1997**, *119*, 10976.
- (14) Braunschweig, H.; Dirk, R.; Müller, M.; Nguyen, P.; Resendes, R.; Gates, D. P.; Manners, I. *Angew. Chem. Int. Ed. Engl.* **1997**, *36*, 2338.
- (15) Seyferth, D.; Withers, H. P. *Organometallics* **1982**, *1*, 1275.



- (16) Fellman, J. D.; Garrou, P. E.; Withers, H. P.; Seyferth, D.; Traficante, D. D. *Organometallics* **1983**, *2*, 818.
- (17) Honeyman, C. H.; Foucher, D. A.; Dahmen, F. Y.; Rulkens, R.; Lough, A. J.; Manners, I. *Organometallics* **1995**, *14*, 5503.
- (18) Honeyman, C. H.; Peckham, T. J.; Massey, J. A.; Manners, I. *J. Chem. Soc., Chem. Commun.* **1996**, 2589.
- (19) We have recently reported the formation of worm-like micelles by poly(ferrocenyldimethylsilane)-*b*-poly(dimethylsiloxane) in solution: Massey, J. A.; Power, K. N.; Winnik, M.; Manners, I. *J. Am. Chem. Soc.* Manuscript accepted for publication.
- (20) Withers, H. P.; Seyferth, D.; Fellman, J. D.; Garrou, P. E.; Martin, S. *Organometallics* **1982**, *1*, 1283.
- (21) Peckham, T. J.; Lough, A. J.; Manners, I. Manuscript in preparation.
- (22) It was observed that the GPC traces for **9** were multimodal whereas those of **10** were monomodal. The integration of the  $^1\text{H}$  NMR spectra remained consistent with the lengths of the blocks calculated for **7**. Initial tests have suggested that sulfurization of **9** results in cleavage of the polysiloxane backbone via a mechanism that requires the presence of P(III) sites in the polymer backbone.
- (23) Ni, Y. Z.; Rulkens, R.; Manners, I. *J. Am. Chem. Soc.* **1996**, *118*, 4012.
- (24) We ran the  $^{31}\text{P}$  NMR spectrum ourselves in THF. The material was kindly provided by Digital Specialty Chemicals Ltd.
- (25) Pregosiu, P. S.; Kunz, R. W.  *$^{31}\text{P}$  and  $^{13}\text{C}$  NMR of Transition Metal Phosphine Complexes*; Springer-Verlag: New York, 1979, .
- (26) Graff, J. L.; Sanner, R. D.; Wrighton, M. S. *Organometallics* **1982**, *1*, 837.
- (27) Berne, B. J.; Pecora, R. J. *Dynamic Light Scattering*; John Wiley & Sons: Toronto, 1976, .
- (28) Chu, B. *Laser Light Scattering: Basic Principles and Practice*; 2nd ed.; Academic Press: Boston, 1991, .

- (29) The synthesis of **3** has been previously described. See: (a) Osborne, A. G.; Whiteley, R. H.; Meads, R. E.; *J. Organomet. Chem.* **1980**, *193*, 345. (b) Seyferth, D.; Withers, H. P. Jr. *J. Organomet. Chem.* **1980**, *185*, C1.
- (30) Bishop, J. J.; Davison, A.; Katcher, M. L.; Lichtenberg, D. W.; Merrill, R. E.; Smart, J. C. *J. Organomet. Chem.* **1971**, *27*, 241.

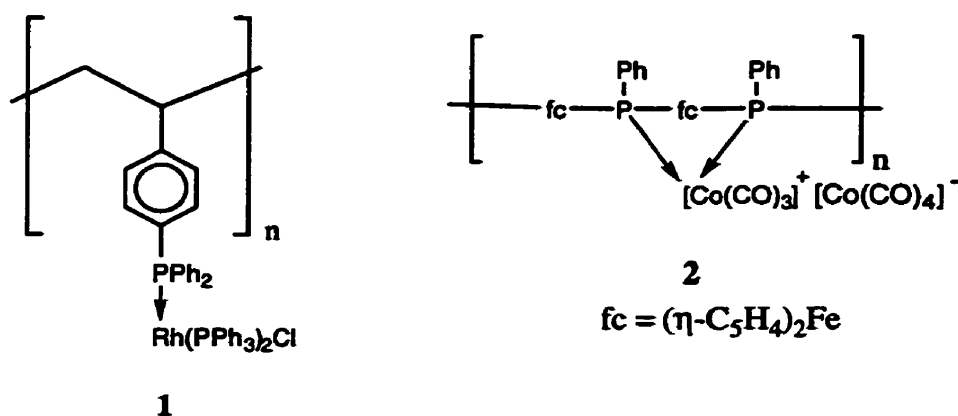
# Chapter 6 The Synthesis, Characterization and Polymerization Behaviour of Silicon-Bridged, Group 4 [1][1]- and Spirocyclic Metallocenophanes: Ring-Opening Polymerization as a Prospective Route to Polymer-Supported Ziegler-Natta Catalysts

## 6.1 Abstract

A new silicon-bridged [1][1]zirconocenophane,  $\text{Zr}(\eta\text{-C}_5\text{H}_3)_2(\text{SiMe}_2)_2(\text{NEt}_2)_2$  (**7a**) was synthesized by the reaction of  $\text{Zr}(\text{NEt}_2)_4$  with  $(\text{C}_5\text{H}_4)_2(\text{SiMe}_2)_2$  (**10**). Single crystal X-ray diffraction revealed a highly tilted structure with a tilt angle of  $73.1(4)^\circ$ . However, this and related compounds  $\text{M}(\eta\text{-C}_5\text{H}_4)_2(\text{SiMe}_2)\text{Cl}_2$  (**4a**,  $\text{M} = \text{Ti}$ ; **4b**,  $\text{M} = \text{Zr}$ ) and  $\text{Zr}(\eta\text{-C}_5\text{H}_3)_2(\text{SiMe}_2)_2\text{Cl}_2$  (**7b**) were not observed to undergo ring-opening polymerization (ROP) either thermally or in the presence of a transition metal catalyst. Two new silicon-bridged, spirocyclic [1]zirconocenophanes,  $\text{Zr}(\eta\text{-C}_5\text{H}_4)_2(\text{Si}(\text{CH}_2)_3)_2\text{X}_2$  (**9a**,  $\text{X} = \text{NMe}_2$ ; **9b**,  $\text{X} = \text{Cl}$ ; **9c**,  $\text{X} = \text{O-}n\text{-C}_{12}\text{H}_{25}$ ) were also synthesized. Single crystal X-ray diffraction of **9a** and **9b** revealed moderate tilt angles ( $61.7(2)^\circ$  and  $59.69(7)^\circ$  respectively) as well as highly strained silacyclobutane rings with C-Si-C bond angles of  $82.4(4)^\circ$  and  $80.64(10)^\circ$  respectively. Compound **9b** was found to undergo ROP in THF at room temperature in the presence of  $\text{PtCl}_2$  leading to the formation of an insoluble white solid. Characterization by EA and CP-MAS  $^{29}\text{Si}$  and  $^{13}\text{C}$  NMR supported the formation of polymer **11b**. Attempts to synthesize the analogous polymer **11c** by  $\text{Pt}^0$ - or  $\text{Pt}^{\text{II}}$ -catalyzed ROP of **9c** resulted in the formation of an insoluble solid. Characterization of the material by EA and CP-MAS  $^{29}\text{Si}$  and  $^{13}\text{C}$  NMR and of the soluble fraction by  $^1\text{H}$  NMR and GC/MS showed the loss of *n*-dodecyloxy groups and suggested the possibility of Cp-Si bond cleavage and Si-O-*n*- $\text{C}_{12}\text{H}_{25}$  bond formation.

## 6.2 Introduction

The synthesis of transition-metal containing polymers is an area of active research due to the possibility of combining the processability commonly found for organic polymers with the potentially interesting properties that are characteristic of transition metals (e.g. optical, electronic, electrical and magnetic).<sup>1,2</sup> Of particular interest is the inclusion of transition metal species which are known to be catalytically active. Polymer-supported transition metal-based catalysts have been known for a considerable period of time. Two such examples are Wilkinson's catalyst supported on a polystyrene backbone (1)<sup>3</sup> and a Co-based, hydroformylation catalyst supported on a poly(ferrocenylphosphine) backbone (2)<sup>4</sup>:

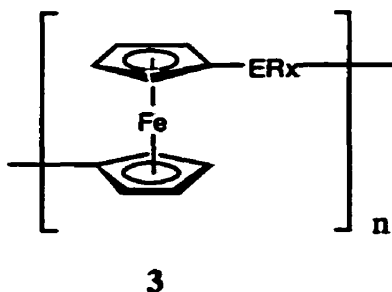


In the area of homogeneous Ziegler-Natta catalysis, the number of metallocene-based catalyst systems has grown prodigiously over the last eighteen years since the first effective system was synthesized by Kaminsky and coworkers in 1980.<sup>5,6</sup> This has been largely due to the potential for controlling the stereochemistry of the resultant polyolefins as well as accessing novel copolymers (e.g. poly(ethylene)-poly(1-hexene)) that cannot be obtained with conventional heterogeneous catalysts.<sup>7-10</sup> One goal, however, has to been to make supported versions of these metallocene catalysts. Such systems would, at least in theory, offer the possibility of combining the well-defined, homogeneous metallocene catalysts with

the ease of catalyst-product separation and robustness offered by a heterogeneous catalyst. Supported "classical" Ziegler-Natta catalysts have long been employed in industry using materials such as  $\text{SiO}_2$ ,  $\text{Al}_2\text{O}_3$  and  $\text{MgCl}_2$ .<sup>11</sup> Similarly, attempts have been made to attach metallocene catalysts via modification of the surface with cyclopentadienyl ligands. When these ligands were attached directly to the surface, the activities were found to be quite low. Attaching the cyclopentadienyl ligands to the surface via a siloxane linkage increased the activities dramatically by comparison.<sup>12,13</sup>

Another method that has been investigated is the attachment of the metallocene to a polymer backbone. One system that has been investigated involves polysiloxane-supported metallocene catalysts.<sup>14</sup> In this case, the polymer was modified by attaching suitable ligands (e.g. cyclopentadienyl, indenyl), lithiating and then reacting with a suitable metal halide. The molecular weight distributions of the products suggested that the active catalytic species formed by these supported zirconocenes were not uniform.

Our group has successfully used ROP of strained, [1]ferrocenophanes as a route to high molecular weight poly(ferrocenes) (**3**) in which the spacer unit ( $\text{ER}_x$ ) can be  $\text{SiR}_2$ ,  $\text{GeR}_2$ ,  $\text{SnR}_2$ ,  $\text{PR}$ ,  $\text{B}(\text{NR}_2)$ ,  $\text{S}$  or  $\text{Se}$ .<sup>15-26</sup> These polymers have displayed a wide range of interesting properties (e.g. redox, magnetic, electronic) and several potential applications are under investigation.



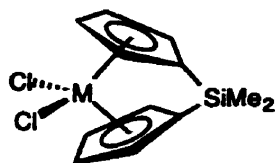
In order to broaden the scope of ROP to include metallocenophanes based on metals outside of group 8, we have begun to investigate the ROP behaviour silicon-bridged, [1]-

and [1][1]metallocenophanes of the Group 4 elements as a route to potential, polymer-based Ziegler-Natta catalysts. We now wish to report our progress in this area.

## 6.3 Results and Discussion

### 6.3.1 ROP Behaviour of the Silicon-Bridged [1]Metallocenophanes 4a and 4b

Our first attempt to obtain our desired Ziegler-Natta catalyst-containing polymer was to investigate the ROP behaviour of 4a and 4b:

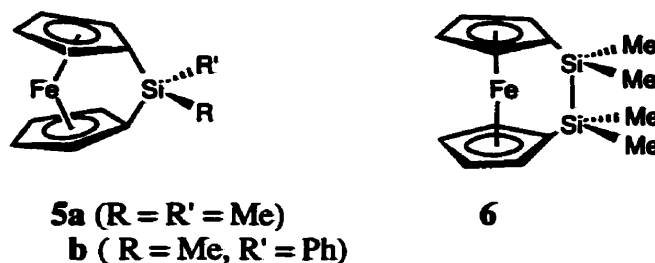


4a (M = Ti)  
b (M = Zr)

These compounds proved to be thermally stable up to 300 °C but were found to decompose rather than polymerize (no evidence for polymer by GPC and only broad resonances attributed to unidentified decomposition products) at higher temperatures. Attempts to polymerize these compounds in solution (benzene) using catalytic amounts of PtCl<sub>2</sub> at either room temperature or under reflux conditions also proved unsuccessful and only unreacted monomer was detected by <sup>1</sup>H NMR.

In light of our studies on the ROP behaviour of silicon-bridged ferrocenophanes, the results are not surprising. In the case of the Group 8 [n]metallocenophanes, we have found that ROP only occurs if there is significant tilting of the cyclopentadienyl rings (tilt angle =  $\alpha$ ) which induces strain into the molecule. Therefore, the highly-strained 5a ( $\alpha = 20.8^\circ$ ) will

readily undergo ROP whereas the relatively unstrained **6** ( $\alpha = \text{ca. } 4^\circ$ ) has remained, to date, resistant to all attempts to induce ROP.



In the case of  $(\eta\text{-C}_5\text{H}_4\text{CH}_3)_2\text{TiCl}_2$  and  $(\eta\text{-C}_5\text{H}_4\text{CH}_3)_2\text{ZrCl}_2$ , the cyclopentadienyl rings are already tilted with respect to one another with values of  $53.3^\circ$  and  $54.2^\circ$  respectively. In attempting to discern which bridged compounds might be strained, it would therefore seem more appropriate to determine the effective tilt angle for these species; that is, the difference between the tilt angle of the bridged compound and the tilt angle of the corresponding metallocene dichloride. Using this measure, it appears that, if based on effective tilt angle, neither **4a** or **4b** (effective tilt angles ( $\alpha'$ ) of  $-2.1^\circ$  and  $2.6^\circ$  respectively) are strained molecules and thus are unlikely to undergo ROP.

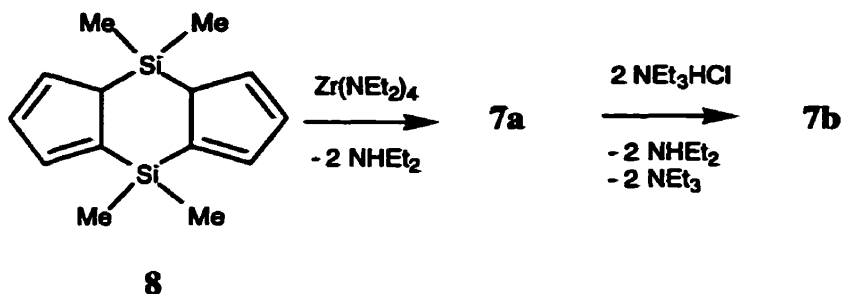
### 6.3.2 Synthesis of [1][1]Zirconacenophanes **7a** and **7b**

By increasing the tilt angle of these compounds, we sought to introduce more strain. Thus, we synthesized doubly-strapped **7a** in which the addition of another bridging silicon atom increased  $\alpha'$  to  $18.9^\circ$  (see Table 6.1).



**7a** (X = NEt<sub>2</sub>)  
**b** (X = Cl)

Compound **7b** ( $\alpha' = 17.9^\circ$ ) has been synthesized previously by Royo *et al.* using dilithiated cyclopentadienide ligands and zirconocene tetrachloride. The yields using this route tend to be moderate at best so we chose to synthesize both **7a** and **b** via an amine elimination method which has gained prominence as a very high yield route to many ansa titanocenes and zirconocenes. The syntheses of these compounds are outlined in Reaction 6.1:



### Reaction 6.1 Synthesis of Compounds **7a** and **7b**

Both compounds were synthesized in greater than 90 % yields with only a minimal amount of purification being necessary to obtain pure product. All the data (multinuclear NMR, MS and EA) collected for **7a** were consistent with the structure shown as was a single crystal X-ray crystallographic analysis. NMR data for **7b** were consistent with literature values.



### 6.3.3 Thermal ROP Behaviour of 7a and 7b

Similar to compounds 4a and 4b, 7a and 7b were found to be thermally stable up to 250 °C but decomposed at higher temperatures. No evidence was found for the formation of any polymers, only unidentified decomposition products (based on GPC and <sup>1</sup>H NMR).

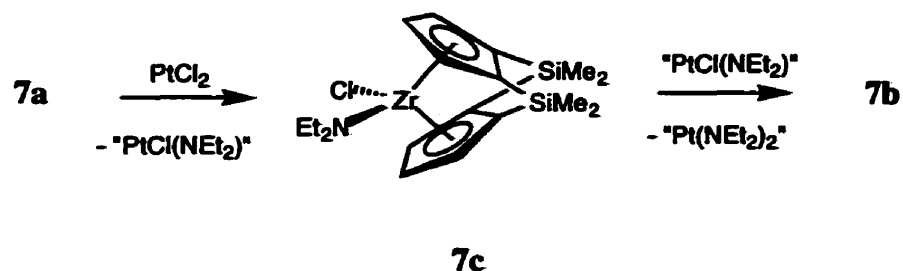
### 6.3.4 Transition Metal-Catalyzed ROP Behaviour of 7a and 7b in the Presence of PtCl<sub>2</sub>

Two different amounts of catalyst (4 mol % and 40 mol %) were used in attempts to polymerize 7a with PtCl<sub>2</sub>. Only resonances due to unreacted 7a were observed in the <sup>1</sup>H NMR spectrum when 4 mol % catalyst were observed even after 16 h.

Use of 40 mol % catalysts, however, resulted in a very different spectrum. New resonances in both the Cp and ethylamido regions were seen to increase until the reaction appeared to be complete after 16 h. Based on the number of resonances in the ethylamido region, we were able to determine that there were at least two products in addition to unreacted monomer present in the reaction mixture. Our first idea was that polymer had been formed. However, upon closer inspection, it became apparent that one set of the unknown resonances was due to 7b which had formed during the reaction between 7a and PtCl<sub>2</sub>. The values obtained were exactly consistent with those found in the literature. Therefore, it seemed likely that the second unknown product was an unsymmetrically substituted species with one chloride and one diethylamido group bonded to zirconium. This product, unfortunately, could not be isolated from the reaction mixture.

Based on these observations, we reacted 7a and PtCl<sub>2</sub> in a 1:1 ratio over 16 h. We observed peaks consistent with 7a, the presumed 7c and 7b with both 7a and 7c disappearing at the end of the reaction and only 7b being present. No soluble Pt-containing compound could be detected or isolated from the reaction mixture. The reaction appears to involve a

metathesis between **7a** and  $\text{PtCl}_2$ , with the eventual formation of **7b** through the intermediate **7c** (Equation 2) and perhaps the formation of an unstable Pt amido compound which rapidly decomposes in solution. Insoluble black material was observed to form throughout the reaction. A white precipitate that was insoluble in  $\text{C}_6\text{D}_6$  was identified as  $[\text{NEt}_2\text{H}_2]\text{Cl}$  by  $^1\text{H}$  NMR. The origin of the hydrogen is currently unknown.

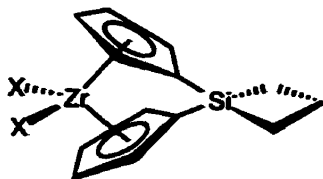


#### Reaction 6.2 Metathesis Reaction Between **7a** and $\text{PtCl}_2$

Attempts to ROP **7b** in the presence of catalytic amounts of  $\text{PtCl}_2$  proved unsuccessful. Only unreacted **7b** was observed by  $^1\text{H}$  NMR and this species could be re-isolated quantitatively from the reaction mixture. No reaction was observed to occur for either **7a** or **7b** in the presence of a  $\text{Pt}(0)$  catalyst, Karstedt's catalyst.

#### 6.3.5 Synthesis and Characterization of the Spirocyclic-Bridged [1]Zirconocenophanes **9a** and **9b**

Due to our lack of success in synthesizing group 4 poly(metallocenes) in which the metal forms part of the polymer backbone via ROP, we decided to investigate other potential monomers which would lead to the metallocene in the polymer side chain. The first two species we have examined are **9a** and **9b**.



- 9a** (X = NMe<sub>2</sub>)  
**b** (X = Cl)  
**c** (X = *n*-C<sub>12</sub>O<sub>25</sub>O)

These compounds were synthesized (starting with ligand **10**, (CH<sub>2</sub>)<sub>3</sub>Si(C<sub>5</sub>H<sub>5</sub>)<sub>2</sub>) in a similar way (cf. Reaction 6.1) to compounds **9a** and **9b**. It was found, however, that the formation of **9a** occurred at a much lower temperature than was utilized in the synthesis of **7a**; that is, the mixing of **10** and Zr(NMe<sub>2</sub>)<sub>4</sub> was conducted at - 78 °C whereas reflux conditions were necessary in order to form **7a**. Yields for the formation of **9a** were found to be much lower than for **7a**. Attempts to improve the yield by initiating reflux conditions resulted in the formation of unknown products and no remaining evidence for **9a**. The substitution chemistry of the NMe<sub>2</sub> groups on **9a** for other ligands, however, was found to be quite facile and the yields for such products were quite high (> 80 %).

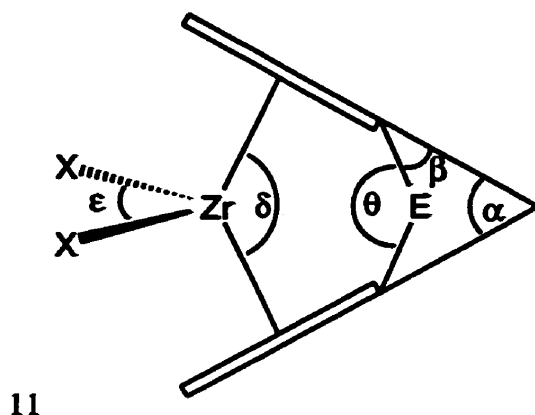
The NMR spectra for both **9a** and **9b** were found to be consistent with the predicted structures. The separation of 0.83 and 0.94 ppm respectively between the two pseudo triplets of the cyclopentadienyl resonances in the <sup>1</sup>H NMR spectra are typical values for silicon-bridged, ansa-zirconocenes. The resonances for the cyclopentadienyl carbons in the region of 110 to 130 ppm in the <sup>13</sup>C NMR spectra are also to analogous species such as **4b**. The <sup>29</sup>Si NMR values are shifted downfield in comparison to the double silyl-bridged species **7a** and **7b** by approximately 6 ppm. No value was reported for **4b**.

### 6.3.6 A Comparative Study of the Single Crystal X-ray Structures for **9a** and **9b**

Crystals of **7a**, **9a** and **9b** suitable for single crystal X-ray diffraction were all obtained from hexanes at - 30 °C. A view of the molecular structures of **7a**, **9a** and **9b** are shown in Figures 6.21, 6.3 and 6.4 respectively. Table 6.1 gives selected structural data for these and related compounds. The angles  $\alpha$ ,  $\alpha'$ ,  $\beta$ ,  $\theta$ ,  $\delta$  and  $\epsilon$  are defined in Figure 6.1. Summaries of the crystal data and collection parameters are found in Tables 6.2 - 6.4. Tables of the fractional coordinates, bond lengths and selected angles are found in Tables 6.5 - 6.13.

In most respects, the structural features of **7a**, **9a** and **9b** are similar to those of the other compounds listed in Table 6.2. As would be expected, the additional bridge between the cyclopentadienyl rings increases the effective tilt angle,  $\alpha'$ , of **7a** over that of the mono-bridged analogue **4b** by an additional 16.3° and, not surprisingly,  $\alpha'$  is similar for all the mono-bridged compounds **4b**, **9a** and **9b**. The Zr-midpoint distance and the Zr-Si distance appear to be somewhat related to tilt angle with the former increasing with increasing tilt angle except in the case of **9a** and the latter increasing as well except in the case of **9b**. These factors, though, are also probably related to the electronic environment of the Zr atom and hence the nature of the X ligand.

Angle  $\beta$  and the Si-C(Cp<sub>ispo</sub>) bond length are often structural features used in addition to  $\alpha$  as indicators of strain in [1]ferrocenophanes. However, in the case of these [1]zirconocenophanes, it is interesting to note that these features hardly vary significantly even as the effective angle is increased. It would appear then that the structural features that are indicative of strain in [1]ferrocenophanes cannot be so used in the case of [1]zirconocenophanes. Based on the lack of ROP behaviour so far found for even quite tilted structures such as **7a** and **7b**, it does not appear that increasing tilt angle leads to increasing strain in these molecules. A recent theoretical study on bent metallocenes by Green *et al.* suggests that whereas increasing the tilt angle of ferrocene significantly increases the total energy of the molecule (and hence the strain in a bridged analogue), this does not lead to any



11

Figure 6.1 Distortions in Ansa-Zirconocenes Defining Angles  $\alpha$ ,  $\beta$ ,  $\theta$ ,  $\delta$  and  $\epsilon$   
 $(\alpha' = \alpha - 54.2)$

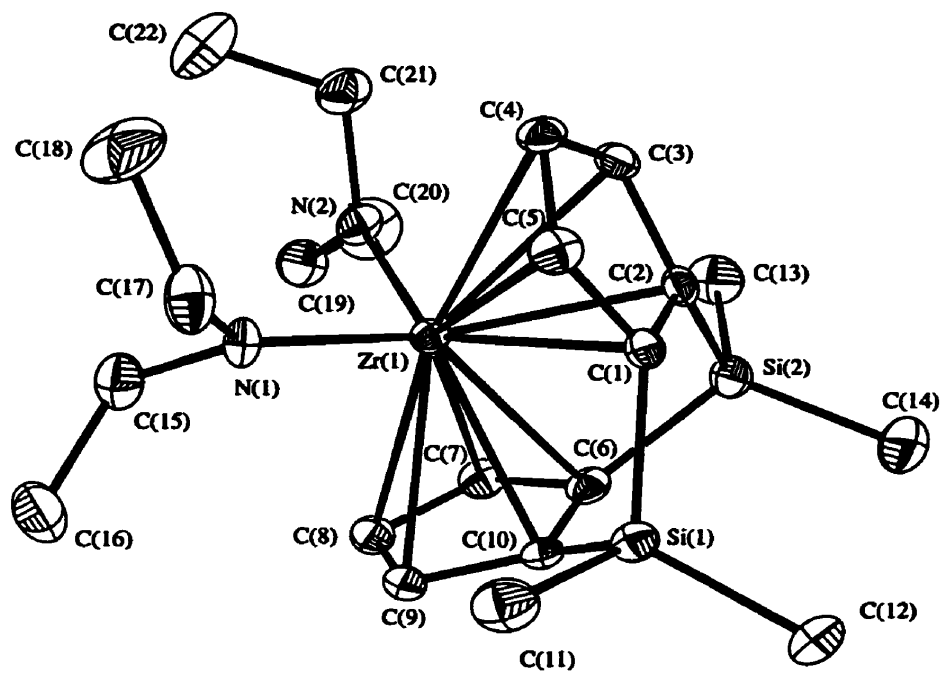


Figure 6.2 Molecular Structure of **7a** (vibrational ellipsoids at 25 % probability level)

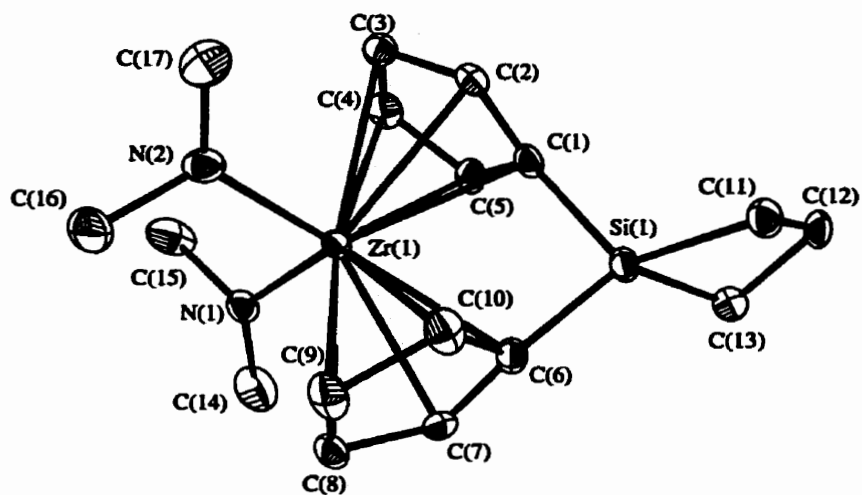


Figure 6.3 Molecular Structure of **9a** (vibrational ellipsoids at 25 % probability level)

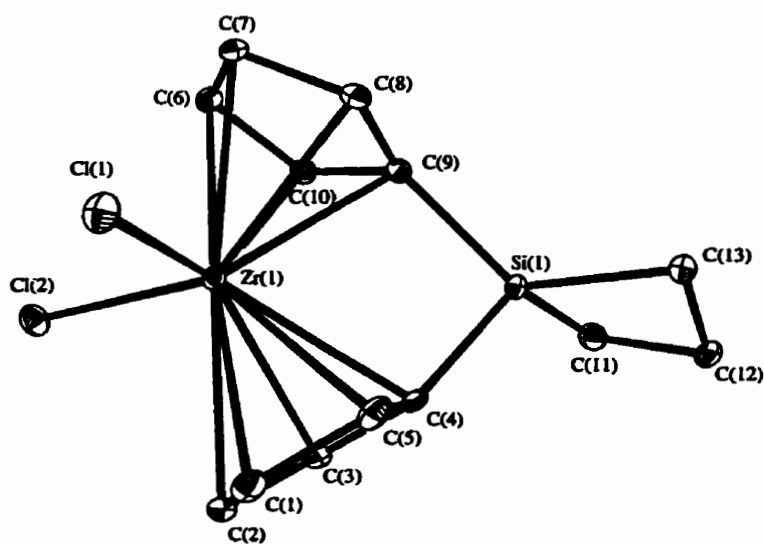


Figure 6.3 Molecular Structure of **9b** (vibrational ellipsoids at 25 % probability level)

Table 6.1. Selected Structural Parameters for **7a**, **9a** and **9b** and Related Zirconocenes, With Esd's in Parentheses (Where Available)  
**[11: ( $\eta$ -C<sub>5</sub>H<sub>4</sub>CH<sub>3</sub>)<sub>2</sub>ZrCl<sub>2</sub>]**

	<b>11</b>	<b>4b</b>	<b>7a</b>	<b>7c</b>	<b>9a</b>	<b>9b</b>
Zr-Si dist (Å)	-	3.3493(4)	3.286(4)	3.233(3)	3.445(4)	3.330(4)
Zr-X (av) (Å)	2.443(1)	2.435(1)	2.096(4)	2.428(1)	2.1065(3)	2.4380(8)
Zr-midpoint (Å)	0.952(2)	1.007(4)	1.217(4)	1.090	1.108(4)	0.998(4)
Si-C (C <sub>ipso</sub> ) (av) (Å)	-	1.866(4)	1.874(4)	1.884	1.899(3)	1.865(2)
$\alpha$ (deg)	54.2	56.8	73.1(4)	69.6(1)	61.7(2)	59.69(7)
$\alpha'$ (deg)	0	2.6	18.9(4)	15.4(1)	7.5(2)	5.49(7)
$\beta$ (av) (deg)	-	17.2	19.7(3)	19.6	18.2(2)	18.2(2)
$\theta$ (av) (deg)	-	93.2(2)	93.3(2)	91.5	96.52(14)	94.68(9)
$\delta$ (av) (deg)	128.8(2)	125.4(3)	116.0(3)	120.6(3)	123.0(2)	126.2(2)
$\varepsilon$ (av) (deg)	95.10(5)	97.98(4)	98.3(2)	99.64(4)	98.56(13)	100.01(3)
ref.	27	28	this work	29	this work	this work

Table 6.2 Summary of Crystal Data and Collection Parameters for 7a

empirical formula	$C_{22}H_{38}N_2Si_2Zr$
formula weight	477.94
wavelength (Å)	0.71073
crystal system	monoclinic
space group	P21/c
a (Å)	8.0131(8)
b (Å)	9.2651(8)
c (Å)	32.692(5)
$\alpha$ (deg)	90
$\beta$ (deg)	94.95(1)
$\gamma$ (deg)	90
V (Å <sup>3</sup> )	2418.1(4)
Z	4
$\rho$ (calculated) (g/cm <sup>3</sup> )	1.313
absorption coefficient (mm <sup>-1</sup> )	0.563
F(000)	1008
crystal size (mm)	0.40 x 0.30 x 0.20
$\theta$ range for data collection (deg)	2.29 to 21.49
reflections collected	4057
independent reflections	2781 ( $R_{int} = 0.0401$ )
data / restraints / parameters	2780 / 0 / 245
goodness-of-fit on $F^2$	1.269
final R indices [ $I > 2\sigma(I)$ ]	$R1 = 0.0390$ , $wR2 = 0.0870$
R indices (all data)	$R1 = 0.0486$ , $wR2 = 0.0893$
extinction coefficient	0.0077(5)
largest diff. peak and hole (eÅ <sup>-3</sup> )	0.378 and -0.428



Table 6.3 Summary of Crystal Data and Collection Parameters for **9a**

empirical formula	$C_{17}H_{26}N_2SiZr$
formula weight	377.71
wavelength (Å)	0.71073
crystal system	triclinic
space group	P-1
a (Å)	8.2103(2)
b (Å)	8.53240(10)
c (Å)	14.7223(3)
$\alpha$ (deg)	94.6170(10)
$\beta$ (deg)	99.0970(10)
$\gamma$ (deg)	113.1860(10)
$V(\text{Å}^3)$	924.48(3)
Z	2
$\rho$ (calculated) ( $\text{g}/\text{cm}^3$ )	1.357
absorption coefficient ( $\text{mm}^{-1}$ )	0.656
F(000)	392
crystal size (mm)	0.40 x 0.40 x 0.15
crystal color	yellow plate
$\theta$ range for data collection (deg)	1.42 to 27.92
reflections collected	6107
independent reflections	3834 ( $R_{\text{int}} = 0.0221$ )
data / restraints / parameters	3813 / 0 / 190
goodness-of-fit	1.082
final R indices [ $I > 2\sigma(I)$ ]	$R1 = 0.0359$ , $wR2 = 0.1226$
R indices (all data)	$R1 = 0.0460$ , $wR2 = 0.1776$
largest diff. peak and hole ( $e\text{Å}^{-3}$ )	0.747 and -0.845

Table 6.4 Summary of Crystal Data and Collection Parameters for 9b

empirical formula	$C_{13}H_{14}Cl_2SiZr$
formula weight	360.45
wavelength (Å)	0.71073
crystal system	triclinic
space group	$P_1$
a (Å)	7.3911(2)
b (Å)	8.7010(2)
c (Å)	10.8001(4)
$\alpha$ (deg)	86.89(1)
$\beta$ (deg)	82.13(1)
$\gamma$ (deg)	88.32(1)
V (Å <sup>3</sup> )	686.8(1)
Z	2
$\rho$ (calculated) (g cm <sup>-3</sup> )	1.743
absorption coefficient (mm <sup>-1</sup> )	1.250
F(000)	360
crystal size (mm)	0.25 x 0.20 x 0.10
$\theta$ range for data collection (deg)	2.78 to 26.37
reflections collected	6885
independent reflections	2778 ( $R_{int} = 0.024$ )
data/restraints/parameters	2778/0/155
goodness-of-fit on $F^2$	1.060
final R indices [ $I > 2\sigma(I)$ ]	$R1 = 0.0228$ , $wR2 = 0.0598$
R indices (all data)	$R1 = 0.0255$ , $wR2 = 0.0604$
extinction coefficient	0.019(2)
largest diff. peak and hole (eÅ <sup>-3</sup> )	0.414 and -0.670

**Table 6.5** Atomic Coordinates ( $\times 10^4$ ) and Equivalent Isotropic Displacement Coefficients ( $\text{\AA}^2 \times 10^3$ ) for the Non-Hydrogen Atoms of **7a** with Esd's in Parentheses

Zr(1)	1085.6(5)	1774.5(4)	8837.7(1)	27(1)
Si(1)	-1487(2)	4199(1)	8414.9(4)	37(1)
Si(2)	-1162(2)	771(2)	7993.0(4)	41(1)
N(1)	2031(4)	2975(4)	9350(1)	35(1)
N(2)	2529(4)	-93(4)	8948(1)	39(1)
C(1)	-1975(5)	2498(5)	8694(1)	30(1)
C(2)	-1770(5)	1086(5)	8527(1)	31(1)
C(3)	-1481(5)	111(5)	8862(1)	36(1)
C(4)	-1525(5)	879(5)	9227(1)	39(1)
C(5)	-1819(6)	2327(5)	9125(1)	39(1)
C(6)	639(6)	2057(5)	8061(1)	37(1)
C(7)	2354(6)	1662(5)	8121(1)	40(1)
C(8)	3270(6)	2770(6)	8330(1)	42(1)
C(9)	2153(6)	3871(5)	8401(1)	39(1)
C(10)	517(6)	3473(5)	8243(1)	32(1)
C(11)	-1038(7)	5714(5)	8781(2)	55(2)
C(12)	-3069(6)	4826(6)	7997(2)	56(2)
C(13)	-2840(7)	1163(6)	7572(2)	68(2)
C(14)	-428(7)	-1130(6)	7939(2)	63(2)
C(15)	1334(7)	3614(6)	9711(2)	57(2)
C(16)	1426(9)	2660(8)	10081(2)	88(2)
C(17)	3856(6)	3081(5)	9393(2)	52(1)
C(18)	4566(7)	4604(6)	9367(2)	68(2)
C(19)	2137(6)	-1124(6)	9270(2)	57(2)
C(20)	3308(9)	-1112(8)	9651(2)	94(2)
C(21)	4155(6)	-463(6)	8799(2)	56(2)
C(22)	4199(8)	-1798(6)	8548(2)	88(2)

Table 6.6. Bond Lengths (Å) for **7a** with Esd's in Parentheses

Zr(1)-N(2)	2.095(4)	Si(2)-C(2)	1.874(4)
Zr(1)-N(1)	2.097(4)	N(1)-C(17)	1.460(6)
Zr(1)-C(2)	2.505(4)	N(1)-C(15)	1.474(6)
Zr(1)-C(10)	2.513(4)	N(2)-C(21)	1.471(5)
Zr(1)-C(1)	2.547(4)	N(2)-C(19)	1.474(6)
Zr(1)-C(6)	2.547(4)	C(1)-C(5)	1.412(6)
Zr(1)-C(3)	2.577(4)	C(1)-C(2)	1.433(6)
Zr(1)-C(9)	2.599(4)	C(2)-C(3)	1.424(6)
Zr(1)-C(5)	2.634(4)	C(3)-C(4)	1.391(6)
Zr(1)-C(7)	2.634(4)	C(4)-C(5)	1.398(6)
Zr(1)-C(4)	2.672(4)	C(6)-C(7)	1.419(6)
Zr(1)-C(8)	2.679(4)	C(6)-C(10)	1.447(6)
Si(1)-C(11)	1.860(5)	C(7)-C(8)	1.403(7)
Si(1)-C(10)	1.872(4)	C(8)-C(9)	1.390(6)
Si(1)-C(12)	1.874(5)	C(9)-C(10)	1.416(6)
Si(1)-C(1)	1.879(4)	C(15)-C(16)	1.494(7)
Si(2)-C(14)	1.870(5)	C(17)-C(18)	1.527(7)
Si(2)-C(6)	1.870(5)	C(19)-C(20)	1.494(8)
Si(2)-C(13)	1.874(6)	C(21)-C(22)	1.485(7)

Table 6.7. Selected Bond Angles for **7a** with Esd's in Parentheses

N(2)-Zr(1)-N(1)	98.3(2)	C(1)-C(2)-Si(2)	123.0(3)
C(11)-Si(1)-C(10)	110.0(2)	C(4)-C(3)-C(2)	108.7(4)
C(11)-Si(1)-C(12)	108.4(2)	C(4)-C(3)-Zr(1)	78.5(3)
C(10)-Si(1)-C(12)	115.8(2)	C(2)-C(3)-Zr(1)	71.0(2)
C(11)-Si(1)-C(1)	110.9(2)	C(3)-C(4)-C(5)	107.7(4)
C(10)-Si(1)-C(1)	93.7(2)	C(3)-C(4)-Zr(1)	70.9(2)
C(12)-Si(1)-C(1)	117.2(2)	C(5)-C(4)-Zr(1)	73.2(2)
C(14)-Si(2)-C(6)	111.4(2)	C(4)-C(5)-C(1)	110.1(4)
C(14)-Si(2)-C(13)	109.0(3)	C(4)-C(5)-Zr(1)	76.3(2)
C(6)-Si(2)-C(13)	117.5(2)	C(1)-C(5)-Zr(1)	70.8(2)
C(14)-Si(2)-C(2)	110.1(2)	C(7)-C(6)-C(10)	106.0(4)
C(6)-Si(2)-C(2)	92.9(2)	C(7)-C(6)-Si(2)	125.5(4)

C(13)-Si(2)-C(2)	115.2(2)	C(10)-C(6)-Si(2)	123.2(3)
C(17)-N(1)-C(15)	110.0(4)	C(8)-C(7)-C(6)	109.8(4)
C(17)-N(1)-Zr(1)	113.7(3)	C(9)-C(8)-C(7)	107.5(4)
C(15)-N(1)-Zr(1)	135.8(3)	C(8)-C(9)-C(10)	109.7(4)
C(21)-N(2)-C(19)	109.6(4)	C(9)-C(10)-C(6)	107.0(4)
C(21)-N(2)-Zr(1)	128.8(3)	C(9)-C(10)-Si(1)	126.0(3)
C(19)-N(2)-Zr(1)	120.6(3)	C(6)-C(10)-Si(1)	122.7(3)
C(5)-C(1)-C(2)	106.0(4)	N(1)-C(15)-C(16)	114.5(5)
C(5)-C(1)-Si(1)	125.0(4)	N(1)-C(17)-C(18)	115.6(4)
C(2)-C(1)-Si(1)	123.0(3)	N(2)-C(19)-C(20)	115.7(5)
C(3)-C(2)-C(1)	107.5(4)	N(2)-C(21)-C(22)	116.1(5)
C(3)-C(2)-Si(2)	125.5(3)		

Table 6.8 Atomic Coordinates ( $\times 10^4$ ) and Equivalent Isotropic Displacement Coefficients ( $\text{\AA}^2 \times 10^3$ ) for the Non-Hydrogen Atoms of **9a** with Esd's in Parentheses

Zr(1)	4315.7(3)	-2014.3(3)	2114.6(2)	25(1)
Si(1)	6571(1)	-3000(1)	4006(1)	37(1)
N(1)	2964(4)	-3599(4)	811(2)	38(1)
N(2)	3826(4)	159(4)	1849(2)	44(1)
C(1)	2748(4)	-4684(5)	2894(2)	39(1)
C(2)	1324(4)	-4143(5)	2590(2)	43(1)
C(3)	1772(5)	-2510(6)	3116(2)	49(1)
C(4)	3498(5)	-2017(6)	3740(2)	45(1)
C(5)	4103(4)	-3393(5)	3628(2)	38(1)
C(6)	7145(4)	-2651(5)	2084(2)	37(1)
C(7)	7320(4)	-1440(5)	1461(2)	41(1)
C(8)	7624(4)	162(5)	1981(2)	41(1)
C(9)	7666(4)	-48(5)	2946(2)	37(1)
C(10)	7402(4)	-1803(5)	3023(2)	36(1)
C(11)	7937(5)	-2032(5)	5239(2)	43(1)
C(12)	8906(5)	-3279(5)	5091(2)	42(1)
C(13)	7466(5)	-4685(5)	4271(3)	43(1)
C(14)	2067(6)	-5452(6)	523(3)	60(1)

C(15)	3403(6)	-2752(7)	-23(3)	70(2)
C(16)	1959(6)	-150(7)	1402(5)	75(2)
C(17)	4818(7)	1976(5)	2295(3)	56(1)

Table 6.9. Bond Lengths (Å) for **9a** with Esd's in Parentheses

Zr(1)-N(2)	2.099(3)	N(1)-C(14)	1.449(5)
Zr(1)-N(1)	2.114(3)	N(1)-C(15)	1.495(5)
Zr(1)-C(4)	2.586(3)	N(2)-C(17)	1.474(5)
Zr(1)-C(6)	2.591(3)	N(2)-C(16)	1.479(5)
Zr(1)-C(1)	2.596(3)	C(1)-C(2)	1.439(5)
Zr(1)-C(5)	2.600(3)	C(1)-C(5)	1.443(5)
Zr(1)-C(10)	2.602(3)	C(2)-C(3)	1.417(6)
Zr(1)-C(9)	2.618(3)	C(3)-C(4)	1.445(5)
Zr(1)-C(2)	2.657(3)	C(4)-C(5)	1.451(6)
Zr(1)-C(3)	2.663(3)	C(6)-C(7)	1.416(5)
Zr(1)-C(8)	2.669(3)	C(6)-C(10)	1.451(5)
Zr(1)-C(7)	2.669(3)	C(7)-C(8)	1.421(6)
Si(1)-C(13)	1.895(4)	C(8)-C(9)	1.444(5)
Si(1)-C(10)	1.899(3)	C(9)-C(10)	1.443(5)
Si(1)-C(5)	1.899(3)	C(11)-C(12)	1.579(6)
Si(1)-C(11)	1.902(3)	C(12)-C(13)	1.580(5)
Si(1)-C(12)	2.395(3)		

Table 6.10. Selected Bond Angles for **9a** with Esd's in Parentheses

N(2)-Zr(1)-N(1)	98.56(13)	C(2)-C(3)-C(4)	107.7(3)
C(13)-Si(1)-C(10)	114.9(2)	C(3)-C(4)-C(5)	109.2(3)
C(13)-Si(1)-C(5)	126.5(2)	C(1)-C(5)-C(4)	105.5(3)
C(10)-Si(1)-C(5)	96.52(14)	C(1)-C(5)-Si(1)	127.8(3)
C(13)-Si(1)-C(11)	79.7(2)	C(4)-C(5)-Si(1)	121.9(3)
C(10)-Si(1)-C(11)	117.8(2)	C(1)-C(5)-Zr(1)	73.7(2)
C(5)-Si(1)-C(11)	123.4(2)	C(7)-C(6)-C(10)	109.3(3)
C(13)-Si(1)-C(12)	41.19(14)	C(6)-C(7)-C(8)	108.0(3)
C(10)-Si(1)-C(12)	113.98(13)	C(7)-C(8)-C(9)	108.3(3)

C(5)-Si(1)-C(12)	149.49(13)	C(8)-C(9)-C(10)	108.1(3)
C(11)-Si(1)-C(12)	41.2(2)	C(9)-C(10)-C(6)	106.1(3)
C(14)-N(1)-C(15)	108.9(3)	C(9)-C(10)-Si(1)	125.7(3)
C(14)-N(1)-Zr(1)	133.3(3)	C(6)-C(10)-Si(1)	123.7(3)
C(15)-N(1)-Zr(1)	115.4(2)	C(12)-C(11)-Si(1)	86.4(2)
C(17)-N(2)-C(16)	109.6(3)	C(13)-C(12)-C(11)	100.8(3)
C(17)-N(2)-Zr(1)	129.9(3)	C(13)-C(12)-Si(1)	52.2(2)
C(16)-N(2)-Zr(1)	117.1(3)	C(11)-C(12)-Si(1)	52.5(2)
C(2)-C(1)-C(5)	109.5(3)	C(12)-C(13)-Si(1)	86.6(2)
C(3)-C(2)-C(1)	108.1(3)	C(11)-Si(1)-C(13)	82.4(2)

Table 6.11 Atomic Coordinates ( $\times 10^4$ ) and Equivalent Isotropic Displacement Coefficients ( $\text{\AA}^2 \times 10^3$ ) for the Non-Hydrogen Atoms of **9b** with Esd's in Parentheses

	x	y	z	U(eq)
Zr(1)	3361(1)	7623(1)	3388(1)	13(1)
Si(1)	1451(1)	7800(1)	762(1)	15(1)
Cl(1)	6620(1)	7650(1)	3574(1)	25(1)
Cl(2)	2094(1)	7439(1)	5588(1)	22(1)
C(1)	3951(3)	10500(2)	2970(2)	21(1)
C(2)	2213(3)	10416(2)	3657(2)	19(1)
C(3)	1063(3)	9661(2)	2952(2)	17(1)
C(4)	2090(3)	9305(2)	1778(2)	16(1)
C(5)	3893(3)	9799(2)	1820(2)	19(1)
C(6)	4249(3)	4831(2)	2914(2)	27(1)
C(7)	2516(3)	4786(2)	3602(2)	25(1)
C(8)	1294(3)	5618(2)	2898(2)	19(1)
C(9)	2274(3)	6156(2)	1733(2)	16(1)
C(10)	4122(3)	5690(2)	1771(2)	21(1)
C(11)	-846(3)	7567(2)	282(2)	21(1)
C(12)	217(3)	7053(2)	-985(2)	23(1)
C(13)	2106(3)	7805(2)	-970(2)	21(1)

Table 6.12. Bond Lengths (Å) for **9b** with Esd's in Parentheses

Zr(1)-Cl(2)	2.4305(8)	Zr(1)-Cl(1)	2.4455(7)
Zr(1)-C(5)	2.474(2)	Zr(1)-C(8)	2.477(2)
Zr(1)-C(4)	2.477(2)	Zr(1)-C(9)	2.483(2)
Zr(1)-C(10)	2.487(2)	Zr(1)-C(3)	2.490(2)
Zr(1)-C(7)	2.554(2)	Zr(1)-C(6)	2.558(2)
Zr(1)-C(1)	2.559(2)	Zr(1)-C(2)	2.569(2)
Si(1)-C(11)	1.862(2)	Si(1)-C(9)	1.864(2)
Si(1)-C(4)	1.865(2)	Si(1)-C(13)	1.867(2)
Si(1)-C(12)	2.336(2)	C(1)-C(2)	1.394(3)
C(1)-C(5)	1.419(3)	C(2)-C(3)	1.414(3)
C(3)-C(4)	1.430(3)	C(4)-C(5)	1.420(3)
C(6)-C(7)	1.390(3)	C(6)-C(10)	1.421(3)
C(7)-C(8)	1.417(3)	C(8)-C(9)	1.426(3)
C(9)-C(10)	1.419(3)	C(11)-C(12)	1.563(3)
C(12)-C(13)	1.562(3)		

Table 6.13. Selected Bond Angles for **9b** with Esd's in Parentheses

Cl(2)Zr(1)-Cl(1)	100.01(3)	C(7)-C(6)-C(10)	108.1(2)
C(11)-Si(1)-C(9)	115.20(10)	C(7)-C(8)-C(9)	108.2(2)
C(9)-Si(1)-C(4)	94.68(9)	C(10)-C(9)-Si(1)	126.2(2)
C(9)-Si(1)-C(13)	118.02(9)	C(12)-C(11)-Si(1)	85.54(13)
C(2)-C(1)-C(5)	107.8(2)	C(12)-C(13)-Si(1)	85.37(12)
C(11)-Si(1)-C(4)	126.03(9)	C(3)-C(4)-Si(1)	124.0(2)
C(11)-Si(1)-C(13)	80.64(10)	C(1)-C(5)-C(4)	109.0(2)
C(4)-Si(1)-C(13)	124.66(9)	C(6)-C(7)-C(8)	108.1(2)
C(9)-C(3)-C(4)	108.6(2)	C(10)-C(9)-C(8)	105.9(2)
C(1)-C(2)-C(3)	108.5(2)	C(8)-C(9)-Si(1)	122.95(14)
C(5)-C(4)-C(3)	106.0(2)	C(9)-C(10)-C(6)	108.9(2)
C(5)-C(4)-Si(1)	125.35(14)	C(13)-C(12)-C(11)	101.1(2)



significant change in the total energy of zirconocene.<sup>30</sup> Therefore, it would seem unlikely that any significant strain (that would possibly lead to ROP) could ever be introduced into [1]zirconocenes by increasing the angle between the cyclopentadienyl ligands.

Compounds **9a** and **9b** do, however, possess structural features which suggest the possibility for ROP. These are due to the strained nature not of the silicon bridging the cyclopentadienyl ligands but rather the silacyclobutane ring, most notably the small C-Si-C bond angle of 82.4(4)° and 80.64(10)° for **9a** and **9b** respectively in comparison with a tetrahedral angle of 109.5°. The C-C-C bond angles of the silacyclobutane rings are also significantly smaller than the normal tetrahedral angle of 109.5° with angles of 100.8(3)° and 101.1(2)° for **9a** and **9b** respectively. The ring puckers (the angle between the plane defined by Si, C(11) and C(13) and the plane defined by C(11), C(12) and C(13) ) are 21.0(4)° and 22.4(1)° for **9a** and **9b** respectively and represent intermediary values to the ferrocenophane analogue (angle 20.6(2)°)<sup>31</sup> and cyclotrimethylene-1,1-dimethylsilane, (CH<sub>2</sub>)<sub>3</sub>Si(CH<sub>3</sub>)<sub>2</sub> (30(2)° as determined by electron diffraction<sup>32</sup>). A large number of silacyclobutanes and disilacyclobutanes have been found to undergo ROP by a variety of different routes.<sup>33-36</sup> We thus felt that **9a** and **9b** would also undergo ROP in contrast to **4b**, **7a** and **7b** although the zirconocene moiety would then function more as a substituent on a carbosilane polymer backbone rather than being integrated within the polymer main chain itself.

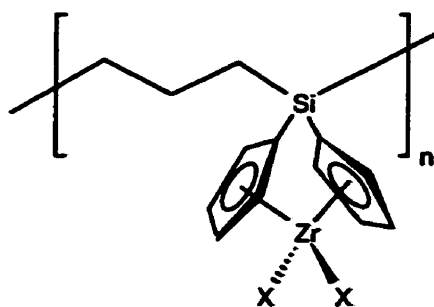
### 6.3.7 Attempted Thermal and Transition Metal-Catalyzed ROP of **9a**

As was found for the doubly-strapped compounds **7a** and **7b**, heating of **9a** resulted in formation of unknown decomposition products at temperatures in excess of 275 °C with no evidence for the formation of polymer. In a manner analogous to the reaction between **7a** and PtCl<sub>2</sub>, attempts to ROP **9a** with PtCl<sub>2</sub> to form polymer **10a** merely resulted in NMe<sub>2</sub>/Cl

exchange and no formation of polymer. With Karstedt's catalyst, only unreacted **9a** was observed in the  $^1\text{H}$  NMR spectrum of the reaction mixture.

### 6.3.8 Transition Metal-Catalyzed ROP Behaviour of **9b**; Attempted Synthesis of **11b**

In the presence of catalytic amounts of  $\text{PtCl}_2$ , **9b** was found to undergo facile ROP in solution at room temperature. Small amounts of catalyst ( $< 4$  mol %) were found to result in low yields ( $< 40$  %). However, using larger amounts of catalyst (12 mol %) resulted in good yields ( $> 80$  %). The resulting compound was an insoluble, off-white solid. The compound



**11a** ( $\text{X} = \text{NMe}_2$ )  
**b** ( $\text{X} = \text{Cl}$ )  
**c** ( $\text{X} = n\text{-C}_{12}\text{O}_{25}\text{O}$ )

was characterized by elemental analysis (EA) and solid state CP-MAS  $^{29}\text{Si}$  and  $^{13}\text{C}$  NMR as shown in Figures 6.5 and 6.6.

Elemental analysis of the product was slightly low (1.6 %) on carbon but provided support for the assigned structure (**11b**), bearing in mind that purification was difficult due to insolubility. The  $^{29}\text{Si}$  NMR spectrum showed one major resonance at -13.5 ppm which is at a similar chemical shift to that observed in both the solution and CP-MAS  $^{29}\text{Si}$  NMR spectra of  $[(\text{CH}_2)_3\text{SiPh}_2]_n$  (**12**) for which the resonance is found at -8.0 ppm and corresponds to

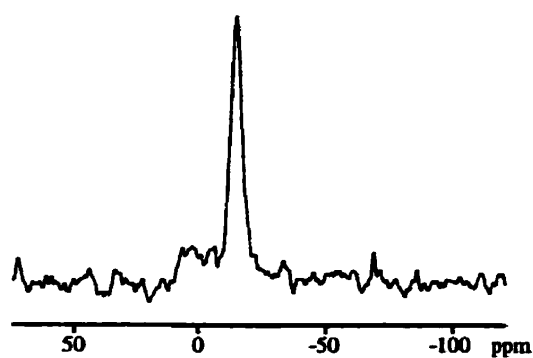


**Figure 6.5** CP-MAS  $^{29}\text{Si}$  NMR Spectrum of Insoluble Polymer **11b**  
(spinning rate = 6 kHz)

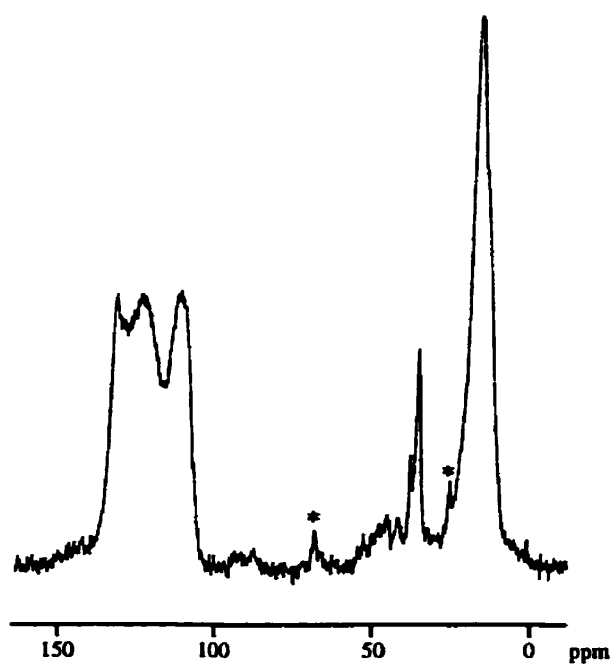


**Figure 6.6** CP-MAS  $^{13}\text{C}$  NMR Spectrum of Insoluble Polymer **11b**  
(\* residual THF) (spinning rate = 11 kHz)

an upfield shift from 7.1 ppm from the monomer, cyclotrimethylene-1,1-diphenylsilane. Unlike **11b**, however, poly(carbosilane) **12** can be dissolved in many common organic solvents (e.g. THF, benzene, CHCl<sub>3</sub>). The difference in chemical shifts is likely due to the more donating nature of the cyclopentadienyl versus the phenyl rings.

The <sup>13</sup>C NMR spectrum for **11b**, while broadly consistent with the structure, also showed some additional resonances. In addition to the resonances in the region of 106 to 138 ppm assigned to the cyclopentadienyl groups and a resonance centred at 16 ppm assigned to methylene of the carbosilane backbone, there is one small but sharp resonance at 36 ppm and even smaller, broader resonances in the region of 46 to 50 ppm. At present, the chemical explanation for these unexpected, small resonances is unclear. It should be noted that the presence of chlorine substituents on Zr would be expected to lead to the formation of an insoluble polymer. For example, the analogous poly(ferrocenylsilane) **3** (ER<sub>x</sub> = SiCl<sub>2</sub>) was found to be insoluble and also resulted in EA results that were low (1.6 %) for carbon.<sup>37</sup>

### 6.3.9 Synthesis and Attempted Transition Metal-Catalyzed ROP Behaviour of **9c**.

As our attempts to polymerize **9b** led to an insoluble product, we decided to utilize the facile substitution chemistry of **9a** to prepare a precursor to a potentially more soluble ring-opened polymer. To this effect, we reacted **9a** with a small excess of *n*-dodecanol which resulted in the formation of **9c** in high yields (>80 %). This species was characterized by <sup>1</sup>H, <sup>13</sup>C and <sup>29</sup>Si NMR as well as EA.

Since **9c** was a liquid, it was found to be easier to perform the polymerizations neat. Both H<sub>2</sub>PtCl<sub>6</sub> and Karstedt's catalyst were explored as catalysts for the polymerizations in order to obtain the desired product **11c**. Significantly, no change was detected by NMR when **9c** was heated at 120 °C overnight in the absence of catalyst. Surprisingly, however, as was found for the ROP product of **9b**, the polymers were insoluble in both cases. In the case of the product resulting from the H<sub>2</sub>PtCl<sub>6</sub>-catalyzed reaction, the EA for carbon was

extremely low (24 %) in comparison with the expected value. The  $\text{CH}_2\text{Cl}_2$ -soluble fraction contained *n*-dodecanol based on both  $^1\text{H}$  NMR and GC/MS. No polymeric material was found by GPC. As we noted earlier, there is ligand exchange between  $\text{PtCl}_2$  and **7a**. However, the large amount of carbon loss and *n*-dodecanol detected suggests that the reaction is catalytic rather than stoichiometric. This is also emphasized by the small amount of catalyst (0.9 mol %) present and that the reaction does not occur in the absence of catalyst. In the CP-MAS  $^{29}\text{Si}$  NMR spectrum for the insoluble product (Figure 6.7), there are multiple resonances. It is highly unlikely that these are due to changes in the substituents on zirconium as, in the case of the monomers **9a - c**, this had little effect upon the chemical shift (< 1 ppm). A tentative possible explanation is that the distinct environments are due to different substituents at silicon that have resulted from a partial exchange process. The resonance at -17.7 ppm is consistent with silicon environments of the type expected in product **11c**. Based on the loss of *n*-dodecanol from the Zr centre, the additional resonances at 2.2 and -8.8 ppm may be due to

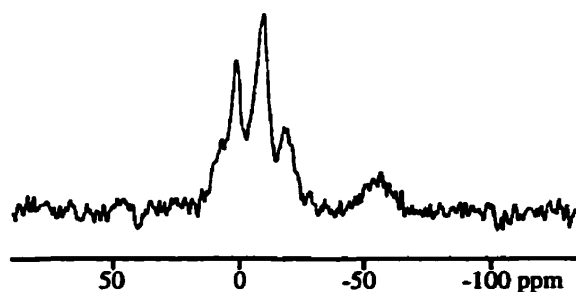


Figure 6.7 CP-MAS  $^{29}\text{Si}$  NMR Spectrum of the Insoluble Product:  
 $\text{H}_2\text{PtCl}_6$ -Catalyzed ROP of **9c** (spinning rate = 6 kHz)

$\text{Si}(\text{O}-\text{C}_{12}\text{H}_{25})$  and  $\text{Si}(\text{O}-\text{C}_{12}\text{H}_{25})_2$  environments, respectively, within the polymer resulting from Cp-Si bond cleavage. That this bond is broken rather than the Si- $\text{CH}_2$  bond is not

surprising as the former is more labile than the latter. These chemical shifts are comparable to those found for analogous compounds,  $\text{Me}_2\text{Si}(\text{OEt})\text{Ph}$  (5 ppm) and  $\text{Me}_2\text{Si}(\text{OEt})_2$  (-6 ppm).<sup>38</sup>

As with the  $\text{H}_2\text{PtCl}_6$ -catalyzed reaction, the product obtained using Karstedt's catalyst was mainly insoluble with a  $\text{CH}_2\text{Cl}_2$ -soluble fraction that contained a large amount of *n*-dodecanol that was detected by  $^1\text{H}$  NMR and GC/MS. There were, however, some very small resonances in the  $^1\text{H}$  NMR in the cyclopentadienyl region and, additionally, polymeric material was detected by GPC ( $M_w = 5.9 \times 10^4$ ;  $M_w/M_n = 1.5$ ). However, after precipitation, the soluble material no longer contained any detectable polymer (by  $^1\text{H}$  NMR or GPC). The EA carbon result was lower (by 6.9 %) than expected but not by as much as was found for the  $\text{H}_2\text{PtCl}_6$ -route. The CP-MAS  $^{29}\text{Si}$  NMR spectrum (Figure 6.8) is similar to that in Figure 6.7. The resonance at -18.0 ppm, again, is probably due to the expected product **11c** and the additional resonances at 2.1 and -9.3 ppm due to  $\text{Si}(\text{O}-\text{C}_{12}\text{H}_{25})$  and  $\text{Si}(\text{O}-\text{C}_{12}\text{H}_{25})_2$

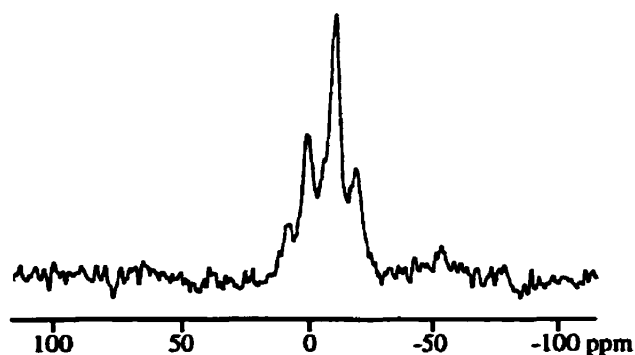


Figure 6.8 CP-MAS  $^{29}\text{Si}$  NMR Spectrum of the Insoluble Product:  
Karstedt's-catalyzed ROP of **9c**  
(spinning rate = 6 kHz)

environments. The CP-MAS  $^{13}\text{C}$  NMR spectrum is shown in Figure 6.9. Expected resonances are in the cyclopentadienyl region (111 to 143 ppm), the methylene region of the carbosilane backbone (18 ppm), the Zr-O-CH<sub>2</sub> resonance (70 ppm) and the remaining n-dodecyloxy resonance (20 - 33 ppm). The additional resonances in the region of 35 - 50 ppm may be due to n-dodecyloxy groups attached to silicon and the resonance at 60 ppm resulting from Si-O-CH<sub>2</sub> environments.

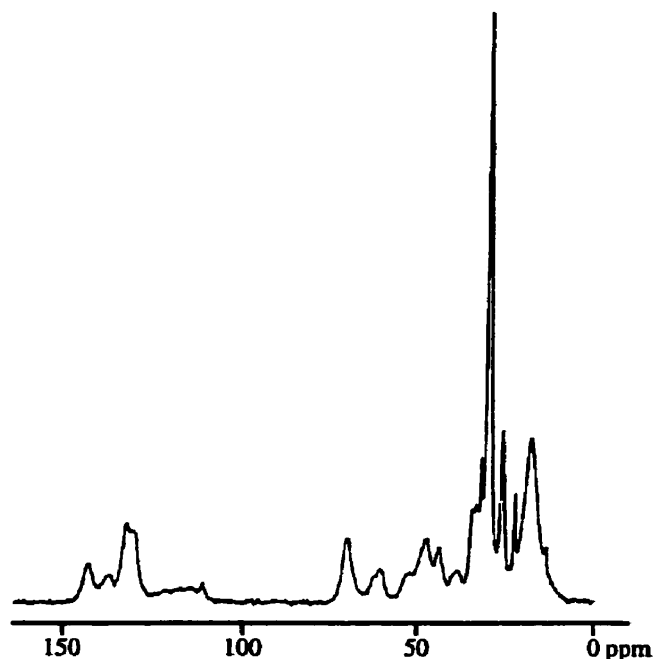


Figure 6.9 CP-MAS  $^{13}\text{C}$  NMR Spectrum of the Insoluble Product: Karstedt's-Catalyzed ROP of **9c** (spinning rate = 11 kHz)

## 6.4 Summary

A series of dimethylsilyl-bridged, Group 4 [1]- and [1][1]metallocenophanes **4a,b** and **7a, b** were synthesized. An examination of the single crystal X-ray structures for these

compounds revealed increased tilting of the cyclopentadienyl rings in comparison to an unbridged zirconocene analogue. However, no polymer was detected after attempted thermal and transition metal-catalyzed ROP. Strained, spirocyclic [1]zirconocenophanes **9a** - **c** were synthesized and characterized by both multinuclear NMR and, in the case of **9a** and **9b**, by single crystal X-ray diffraction. Compound **9a** was found not to undergo ROP either thermally or in the presence of a transition metal catalyst. Compound **9b** underwent ROP in the presence of  $\text{PtCl}_2$  leading to the formation of an insoluble white solid. Characterization by EA and CP-MAS  $^{29}\text{Si}$  and  $^{13}\text{C}$  NMR supported the formation of polymer **11b**. The transition metal-catalyzed ROP (with either  $\text{H}_2\text{PtCl}_6$  or Karstedt's catalyst) of **9c**, however, also gave an insoluble product. Characterization of the material by EA and CP-MAS  $^{29}\text{Si}$  and  $^{13}\text{C}$  NMR and of the soluble fraction by  $^1\text{H}$  NMR and GC/MS showed the loss of *n*-dodecyloxy groups and suggested the possibility of Cp-Si bond cleavage and Si-O-*n*- $\text{C}_{12}\text{H}_{25}$  bond formation.

Future work will concentrate on the synthesis of potential precursors to soluble polymers via substitution on the cyclopentadienyl rings and less labile substituents at zirconium. We will also investigate the use of more active transition metal catalysts which would allow ROP to take place at lower temperatures and thus hopefully avoid the Zr-O and Si-Cp bond cleavage that appears to occur with **9c**.

## 6.5 Experimental Section

**Materials.** Unless otherwise noted, all chemicals were purchased from Aldrich. Cyclotrimethylenedichlorosilane was purchased from Gelest Inc. Triethylammonium chloride was synthesized by the reaction of triethylamine and HCl in  $\text{Et}_2\text{O}$ . Zirconium tetrakis(diethylamide), zirconium tetrakis(dimethylamide), bis(cyclopentadienyl)-dimethylsilane, **4a**, **4b** and **8** were synthesized according to literature procedures.<sup>28,29,39</sup>



Tetrahydrofuran, hexanes and toluene were dried over Na and stored under nitrogen prior to use. Methylene chloride was dried over  $\text{CaH}_2$  and stored nitrogen prior to use. *n*-Dodecanol was distilled over magnesium and stored under nitrogen prior to use.

**Equipment.** All reactions and manipulations were carried out under an atmosphere of prepurified nitrogen using either Schlenk techniques or an inert-atmosphere glovebox (Vacuum Atmospheres). Solvents were dried by standard methods, distilled, and stored under nitrogen over activated molecular sieves. 300 MHz  $^1\text{H}$  NMR spectra and 75.5  $^{13}\text{C}$  NMR spectra were recorded on a Varian Gemini 300 spectrometer.  $^1\text{H}$  NMR spectra were recorded on a Varian Unity 400 Spectrometer. Solid-state 39.75 MHz  $^{29}\text{Si}$  CP/MAS NMR spectra were obtained on a Bruker DSX200 spectrometer using a spinning rate of 6 kHz, a recycle delay of 10 s and a contact time of 3 ms. Solid-state 100.62 MHz  $^{13}\text{C}$  NMR spectra were obtained on a Bruker DSX400 spectrometer using a spinning rate of 11 kHz, a recycle delay of 5s and a contact time of 1 ms.

Mass spectra were obtained with the use of a VG 70-250S mass spectrometer operating in an Electron Impact (EI) mode. Melting points and decomposition temperatures were obtained with a Perkin-Elmer DSC 7 differential scanning calorimeter operating at a heating rate of 10  $^\circ\text{C}$  per minute under  $\text{N}_2$ .

Single crystal X-ray data were collected on a Siemens P4 diffractometer with a SMART CCD detector (for **7a** and **9a**) or a Nonius Kappa-CCD (for **9b**) using graphite monochromated MoK $\alpha$  radiation ( $\lambda = 0.71073 \text{ \AA}$ ). 180 frames, of  $1^\circ$  rotations of phi, were exposed for 90 seconds each. There were no measureable data higher than  $21^\circ$  in  $\theta$ . The data were integrated and scaled using the DENZO package.<sup>40</sup> The structures were solved and refined using the SHELXTLPC package.<sup>41</sup> Refinement was by full-matrix least-squares on  $F^2$  using all data (negative intensities included). The weighing scheme was  $w = 1/[s^2(F_o^2) +$

$(0.0699)^2 + 25.07P]$  where  $P = (F_o^2 + 2F_c^2)/3$ . Hydrogen atoms were included in calculated positions.

**Synthesis of the [1][1]Zirconocenophane 7a.** Zirconium tetrakis(diethylamide) (4.00 g, 10.6 mmol) and **8** (2.55 g, 10.6 mmol) were combined in a flask with a reflux condenser in the drybox. To the flask were added 50 mL of toluene. The apparatus was then removed from the drybox and the reaction mixture was refluxed overnight. The solution was observed to change from a light orange to a dark red colour during this time. The solvent was removed under high vacuum leaving behind an orange-yellow powder. The product was then recrystallized from hexanes at -30 °C resulting in pale orange-yellow crystals. Yield: 4.65 g (92 %). For **7a**:  $Zr(NEt_2)_2(\eta-C_5H_3)_2(SiMe_2)_2$  Pale orange-yellow crystals:  $^{29}Si$  NMR (in  $C_6D_6$ )  $\delta = -18.5$  (s,  $SiMe_2$ ) ppm;  $^{13}C$  NMR (in  $C_6D_6$ )  $\delta = 130.6$  (Cp), 116.7 ( $C_{p_{ipso}}$ ), 110.1 (Cp), 50.3 ( $NCH_2CH_3$ ), 15.4 ( $NCH_2CH_3$ ), 2.7 ( $SiMe_2$ ), -3.8 ( $SiMe_2$ ) ppm.  $^1H$  NMR (in  $C_6D_6$ )  $\delta = 6.75$  (d, 4H, Cp), 6.03 (t, 2H, Cp), 3.28 (q, 8H,  $NCH_2CH_3$ ), 1.06 (t, 12H,  $NCH_2CH_3$ ), 0.75 (s, 6H,  $SiMe_2$ ), 0.43 (s, 6H,  $SiMe_2$ ) ppm. DSC: mp = 130 °C;  $T_{dec} = 225$  °C. Elemental analysis for  $C_{22}H_{40}N_2SiZr$ : Calcd. C 55.05, H 8.40 %; Found C 53.89, H 7.58 %.

**Synthesis of the [1][1]Zirconocenophane 7b.** To a stirred 0 °C solution of compound **7a** (1.50 g, 3.15 mmol) in 50 mL of  $CH_2Cl_2$  was added a solution of  $NEt_3HCl$  (0.43 g, 3.15 mmol) in 10 mL of  $CH_2Cl_2$ . The reaction mixture was allowed to stir and warm up to room temperature overnight. The solution was concentrated and the product recrystallized by cooling down to -30 °C. The  $^1H$  NMR spectrum of the white crystalline product was consistent with the literature values.<sup>29</sup> Yield: 1.16 g (91 %).

**Reaction of the [1][1]Zirconocenophane 7a with 4 mol %  $PtCl_2$ .** In a 5 mm NMR tube, **7a** (250 mg, 0.53 mmol) was dissolved in  $C_6D_6$ . To this solution was added a catalytic

amount of PtCl<sub>2</sub> (4 mg, 0.02 mmol). The NMR tube was then placed in a sonicating water bath and sonicated for 16 h. <sup>1</sup>H NMR spectra were run approximately every 4 h. No resonances in addition to those of **7a** were discernable.

**Reaction of the [1][1]Zirconocenophane **7a** with 40 mol % PtCl<sub>2</sub>.** In a 5 mm NMR tube, **7a** (250 mg, 0.53 mmol) was dissolved in C<sub>6</sub>D<sub>6</sub>. To this solution was added 38 mol % of PtCl<sub>2</sub> (40 mg, 0.20 mmol). The NMR tube was then placed in a sonicating water bath and sonicated for 16 hours. <sup>1</sup>H NMR spectra were run approximately every four hours. In addition to the resonances due to **7a**, new resonances were observed to appear and increase in intensity in the cyclopentadienyl, ethylamido and methyl regions. At least two other products (based on the number of resonances observed in the ethylamido region) were present in the reaction mixture. One of the new products was determined to be **7b** based on the resonances in the cyclopentadienyl region.<sup>29</sup> The other product could not be isolated. However, as amido-chloro exchange appears to have occurred during this reaction, it is logical that this product is the presumed intermediate between **7a** and **7b** (i.e. **7c**). For **7c**: <sup>29</sup>Si NMR (in C<sub>6</sub>D<sub>6</sub>) δ = -17.1 (s, SiMe<sub>2</sub>) - 18.5 (s, SiMe<sub>2</sub>) ppm; <sup>13</sup>C NMR (in C<sub>6</sub>D<sub>6</sub>) δ = 138.7 (Cp), 130.5 (Cp), 125.6 (Cp<sub>ipso</sub>), 113.8 (Cp<sub>ipso</sub>), 112.1 (Cp), 51.2 (NCH<sub>2</sub>CH<sub>3</sub>), 14.7 (NCH<sub>2</sub>CH<sub>3</sub>), 2.2 (SiMe<sub>2</sub>), 1.4 (SiMe<sub>2</sub>), -4.0 (SiMe<sub>2</sub>), -4.5 (SiMe<sub>2</sub>) ppm. <sup>1</sup>H NMR (in C<sub>6</sub>D<sub>6</sub>) δ = 6.87 (m, 2H, Cp), 6.46 (m, 2H, Cp), 6.02 (m, 2H, Cp), 3.38 (q, 4H, NCH<sub>2</sub>CH<sub>3</sub>), 0.96 (t, 6H, NCH<sub>2</sub>CH<sub>3</sub>), 0.60 (s, 3H, SiMe<sub>2</sub>), 0.54 (s, 3H, SiMe<sub>2</sub>), 0.26 (s, 3H, SiMe<sub>2</sub>), 0.22 (s, 3H, SiMe<sub>2</sub>) ppm.

**1: 1 Reaction of the [1][1]Zirconocenophane **7a** with PtCl<sub>2</sub>.** In a 5 mm NMR tube, **7a** (50 mg, 0.11 mmol) was dissolved in C<sub>6</sub>D<sub>6</sub>. To this solution was added PtCl<sub>2</sub> (28 mg, 0.11 mmol). The NMR tube was then placed in a sonicating water bath and sonicated for 16 h. Resonances due to **7b** were observed to increase in intensity in the <sup>1</sup>H NMR during this time until there was no sign of either **7a** or **7c**. A white precipitate was found at the bottom of the

NMR tube. This precipitate was isolated by filtration of the reaction mixture under  $N_2$ . The precipitate was found to dissolve in  $CDCl_3$  and was determined to be diethylammonium chloride  $[NEt_2H_2]Cl$  based on the  $^1H$  NMR spectrum.  $^1H$  NMR (in  $CDCl_3$ )  $\delta = 9.48$  (broad, 2H,  $NH_2$ ), 3.10 (q, 4H,  $NCH_2$ ), 1.52 (t, 6H,  $CH_3$ ) ppm.

**Synthesis of cyclotrimethylenedicyclopentadienylsilane 10.** To a stirred solution of cyclotrimethylenedichlorosilane (10 g, 71 mmol) in 50 mL of THF at  $-78\text{ }^\circ C$  was added a solution on NaCp (13 g, 148 mmol) in the same solvent (150 mL) dropwise via cannula over 1 h. The reaction mixture was allowed to stir while warming up to room temperature. The solvent was removed in vacuo, the product was taken up in hexanes (200 mL) and filtered through celite to give a clear faint yellow solution. Upon removal of hexanes, a viscous yellow liquid was obtained (10 g, 70 %). Compound **10** was used subsequently without further purification (purity was estimated to be 90 % by GC/MS). For **10**:  $^{29}Si$  NMR (in  $C_6D_6$ )  $\delta = 14.6$  ppm.  $^1H$  NMR (in  $C_6D_6$ )  $\delta = 6.0 - 6.8$  (broad, 10 H, Cp), 1.86 (quintet, 2H,  $CH_2$ ), 0.82 (t, 4H,  $SiCH_2$ ) ppm. GC/MS: 200 (10,  $M^+$ ), 135 (100,  $M^+ - Cp$ ).

**Synthesis of the Spirocyclic [1]Zirconocenophane 9a:** A solution of  $Zr(NMe_2)_4$  (8.09 g, 30.3 mmol) in 150 ml of toluene was cooled to  $-78\text{ }^\circ C$ . To this solution was added a solution of **10** (6.06 g, 30.3 mmol) in the same solvent (150 ml) was added dropwise via a cannula over 1 h. The reaction mixture was allowed to stir while warming up slowly to room temperature overnight. The solvent was then removed under high vacuum and crude **9a** was obtained by recrystallization from hexanes at  $-70\text{ }^\circ C$ . Purified **9a** could be obtained as yellow crystals by sublimation at  $80\text{ }^\circ C$ ,  $5 \times 10^{-3}$  mm Hg. Yield: 6.35 g (56 %). For **9a**:  $^1H$  NMR (400 MHz,  $C_6D_6$ )  $\delta$  1.49 (t,  $^3J_{HH} = 8.4$  Hz, 4H,  $SiCH_2$ ), 2.27 (quintet,  $^3J_{HH} = 8.4$  Hz, 2H,  $CH_2$ ), 2.75 (s, 12H,  $NMe_2$ ), 5.70 (m, 4H, CpH), 6.53 (m, 4H, CpH) ppm;  $^{13}C$  NMR (100.5 MHz,  $C_6D_6$ )  $\delta$  14.0 ( $SiCH_2$ ), 18.7 ( $CH_2$ ), 48.8 ( $NMe_2$ ), 109.7 (Cp), 112.2 (*ipso* Cp), 117.3 (Cp) ppm;  $^{29}Si$  NMR (79.4 MHz,  $C_6D_6$ )  $\delta$  -0.99 (s) ppm. MS (EI, 70 eV): 376 (26,

M<sup>+</sup>), 330 (100, M<sup>+</sup> - N(CH<sub>3</sub>)<sub>2</sub>, - H<sub>2</sub>). Elemental analysis for C<sub>17</sub>H<sub>26</sub>N<sub>2</sub>SiZr : Calcd. C 54.06, H 6.94 %; Found C 51.95, H 6.27%.

**Synthesis of the Spirocyclic [1]Zirconacenophane 9b:** To the solution of 9a (1.55 g, 4.11 mmol) in toluene cooled to - 78 °C was added excess chlorotrimethylsilane (2.0 mL, 15.8 mmol) via slow addition with a syringe. The reaction mixture was allowed to warm up to room temperature and stirred overnight. Solvent and excess chlorotrimethylsilane were removed in vacuo. The crude product was dissolved in CH<sub>2</sub>Cl<sub>2</sub> and filtered through celite to give a yellow solution. Removal of the solvent under vacuum and recrystallization from toluene gave colourless crystals of 9b. Yield: 1.05 g (71 %). For 9b: <sup>1</sup>H NMR (400 MHz, CDCl<sub>3</sub>) δ 1.72 (t, <sup>3</sup>J<sub>HH</sub> = 8.4 Hz, 4H, SiCH<sub>2</sub>), 2.47 (quintet, <sup>3</sup>J<sub>HH</sub> = 8.4 Hz, 2H, CH<sub>2</sub>), 6.03 (m, 4H, CpH), 6.98 (m, 4H, CpH) ppm; <sup>13</sup>C NMR (100.5 MHz, CDCl<sub>3</sub>) δ 14.03 (SiCH<sub>2</sub>), 18.25 (CH<sub>2</sub>), 108.4 (*ipso* Cp), 113.80 (Cp), 128.3 (Cp) ppm; <sup>29</sup>Si NMR (79.4 MHz, CDCl<sub>3</sub>) δ -0.36 (s) ppm. MS (EI, 70 eV): 360 (45, M<sup>+</sup>), 322 (100, M<sup>+</sup> - Cl, H<sub>2</sub>, H). Elemental analysis for C<sub>13</sub>H<sub>14</sub>Cl<sub>2</sub>SiZr : Calcd. C 43.32, H 3.91 %; Found C 42.76, H 3.85 %.

**Transition Metal-Catalyzed ROP of 9b; Synthesis of 11b.** To a solution of 9b (1.00 g, 2.78 mmol) in THF at 25 °C was added a catalytic amount of PtCl<sub>2</sub> (0.089 g, 12 mol %). A white precipitate began to form within ten minutes after the addition of the catalyst. The reaction mixture was allowed to stir for two weeks. The insoluble polymer was isolated on a frit and washed with THF. Yield: 0.80 g (80 %). Elemental analysis for C<sub>13</sub>H<sub>14</sub>Cl<sub>2</sub>SiZr : Calcd. C 43.32, H 3.91 %; Found C 41.73, H 4.20 %. CP-MAS <sup>29</sup>Si NMR: 13.5 ppm; CP-MAS <sup>13</sup>C NMR: 106 - 138 (cyclopentadienyl), 16 (methylene of carbosilane backbone) ppm.

**Synthesis of Spirocyclic [1]Zirconocenophane 9c.** To a solution of 9a (1.20 g, 3.18 mmol) in 30 mL of Et<sub>2</sub>O at - 78 °C was added *n*-dodecanol (1.39 g, 7.47 mmol) dissolved in 5 mL of

Et<sub>2</sub>O via syringe over 15 min. The mixture was allowed to stir and warm up to room temperature overnight. Solvent was removed under high vacuum. Excess alcohol was removed by sublimation at 90 °C, 5 x 10<sup>-3</sup> mm Hg. At room temperature, **9c** was an orange-yellow liquid. Yield: 1.72 g (82 %). <sup>1</sup>H NMR (400 MHz, C<sub>6</sub>D<sub>6</sub>) δ 0.95 (d, 6 H, -O-CH<sub>2</sub>-(CH<sub>2</sub>)<sub>10</sub>-CH<sub>3</sub>), 1.35 (broad m, 40 H, -O-CH<sub>2</sub>-(CH<sub>2</sub>)<sub>10</sub>-CH<sub>3</sub>), 1.57 (t, 4 H, SiCH<sub>2</sub>), 2.41 (quintet, 2H, CH<sub>2</sub>), 3.92 (t, 4 H, -O-CH<sub>2</sub>-(CH<sub>2</sub>)<sub>10</sub>-CH<sub>3</sub>), 5.91 (m, 4H, Cp), 6.54 (m, 4H, Cp) ppm; <sup>13</sup>C NMR (100.5 MHz, C<sub>6</sub>D<sub>6</sub>) δ 14.1 (-O-CH<sub>2</sub>-(CH<sub>2</sub>)<sub>10</sub>-CH<sub>3</sub>) 14.4 (SiCH<sub>2</sub>), 18.7 (CH<sub>2</sub>), 23.1 (-O-CH<sub>2</sub>-(CH<sub>2</sub>)<sub>9</sub>-CH<sub>2</sub>-CH<sub>3</sub>), 26.5 (-O-CH<sub>2</sub>-(CH<sub>2</sub>)<sub>8</sub>-CH<sub>2</sub>-CH<sub>2</sub>-CH<sub>3</sub>), 29.8 (-O-CH<sub>2</sub>-(CH<sub>2</sub>)<sub>7</sub>-CH<sub>2</sub>-(CH<sub>2</sub>)<sub>2</sub>-CH<sub>3</sub>), 30.1 (-O-CH<sub>2</sub>-(CH<sub>2</sub>)<sub>7</sub>-(CH<sub>2</sub>)<sub>2</sub>-(CH<sub>2</sub>)<sub>3</sub>-CH<sub>3</sub>), 30.2 (-O-CH<sub>2</sub>-(CH<sub>2</sub>)<sub>3</sub>-(CH<sub>2</sub>)<sub>2</sub>-(CH<sub>2</sub>)<sub>5</sub>-CH<sub>3</sub>), 30.3 (-O-CH<sub>2</sub>-(CH<sub>2</sub>)<sub>2</sub>-CH<sub>2</sub>-(CH<sub>2</sub>)<sub>7</sub>-CH<sub>3</sub>), 32.3 (-O-CH<sub>2</sub>-CH<sub>2</sub>-CH<sub>2</sub>-(CH<sub>2</sub>)<sub>7</sub>-CH<sub>3</sub>), 34.7 (-O-CH<sub>2</sub>-CH<sub>2</sub>-(CH<sub>2</sub>)<sub>9</sub>-CH<sub>3</sub>), 73.7 (-O-CH<sub>2</sub>-(CH<sub>2</sub>)<sub>10</sub>-CH<sub>3</sub>), 110.8 (Cp), 114.0 (*ipso*, Cp), 119.9 (Cp) ppm; <sup>29</sup>Si NMR (79.4 MHz, C<sub>6</sub>D<sub>6</sub>) δ -0.96 (s) ppm. Elemental analysis for C<sub>37</sub>H<sub>64</sub>O<sub>2</sub>SiZr : Calcd. C 67.31, H 9.77 %; Found C 67.25, H 9.97 %.

**Heating **9c** in the Absence of any Catalysts.** **9c** (1.00 g, 2.78 mmol) was heated at 120 °C for 24 h. There was no observable increase in viscosity and examination by <sup>1</sup>H NMR revealed only unreacted **9c**.

**Attempted Transition Metal-Catalyzed ROP of **9c** in the Presence of H<sub>2</sub>PtCl<sub>6</sub>.** To **9c** (1.00 g, 2.78 mmol) was added a catalytic amount of H<sub>2</sub>PtCl<sub>6</sub> (0.010 g, 0.9 mol %). The mixture was then stirred while heating at 120 °C for 24 h. During this time, the mixture darkened and became increasingly viscous. Upon cooling, the mixture solidified. The mixture was washed overnight with CH<sub>2</sub>Cl<sub>2</sub>. The solid was filtered off and isolated as a pale yellow to white powder. Analysis by <sup>1</sup>H and <sup>13</sup>C NMR in CDCl<sub>3</sub>, and by GC/MS of the compound contained within the soluble fraction revealed it to be mainly *n*-dodecanol. No evidence in the solution NMR spectra was found for the presence of the expected polymer

**11c.** Yield of insoluble solid: 0.27 g (27 %) Elemental analysis for  $C_{37}H_{64}O_2SiZr$  : Calcd. C 67.31, H 9.77 %; Found C 42.96, H 7.13 %.

**Transition Metal-Catalyzed ROP of 9c in the Presence of Karstedt's Catalyst.** To **9c** (1.00 g, 2.78 mmol) was added a catalytic amount of the platinum-divinyltetramethyldisiloxane complex in xylenes (2.1 - 2.4 wt % platinum concentration) (20  $\mu$ L, 0.08 mol %). The mixture was then stirred while heating at 120 °C for 24 h. During this time, the mixture darkened and became increasingly viscous. Upon cooling, the mixture solidified. The mixture was washed overnight with  $CH_2Cl_2$ . The insoluble material was filtered off and isolated as a yellow fibrous solid. Analysis by  $^1H$  and  $^{13}C$  NMR in  $CDCl_3$ , and by GC/MS of the compound contained within the soluble fraction revealed it to be mainly *n*-dodecanol. No evidence in the solution NMR spectra was found for the presence of expected polymer **11c**. A THF fraction, however, did suggest the presence of what was at least a temporarily soluble polymer (see Section 6.3.9);  $M_w = 5.9 \times 10^4$ ;  $M_w/M_n = 1.5$ . Yield of insoluble solid: 0.40 g (40 %) Elemental analysis for  $C_{37}H_{64}O_2SiZr$  : Calcd. C 67.31, H 9.77 %; Found C 60.46, H 9.11 %.

**Synthesis of Cyclotrimethylene-1,1-diphenylsilane.** 11.58 g (82.1 mmol) of cyclotrimethylene-1,1-dichlorosilane were dissolved in 200 mL of THF. 83 mL (166 mmol) of 2.0 M phenylmagnesium chloride in THF was added dropwise to the above solution at 0 °C. The reaction was allowed to warm up to room temperature and stir overnight. The THF was removed under high vacuum and purified monomer was obtained by distillation at 80 °C,  $8 \times 10^{-3}$  mmHg. Yield: 15.5 g (84 %).  $^{29}Si$  NMR ( $CDCl_3$ ): 7.1 ppm;  $^{13}C$  NMR ( $CDCl_3$ ): 136.4 (ipso-Ph), 134.5 (Ph), 129.7 (Ph), 128.0 (Ph), 18.3 ( $CH_2$ ), 13.8 (Si- $CH_2$ ) ppm;  $^1H$  NMR ( $CDCl_3$ ): 7.64 (m, Ph, 4H), 7.41 (m, Ph, 6H), 2.29 (quintet,  $CH_2$ , 2H), 1.52 (t, Si- $CH_2$ , 4H).

**Synthesis of Polymer 12.** 2.00 g (8.92 mmol) of cyclotrimethylene-1,1-diphenylsilane were dissolved in 5 mL of toluene. To this solution were added 5 mg of PtCl<sub>2</sub> (0.3 mol %). The reaction mixture was allowed to stir at room temperature for 5 h. The solution was filtered and the polymer was isolated by precipitation into methanol. The solution was decanted off and the polymer washed several times with methanol. The polymer was then dried under vacuum overnight and found to be a gray, fibrous solid. Yield: 1.56 g (78 %). <sup>29</sup>Si NMR (CDCl<sub>3</sub>): -7.7 ppm; <sup>13</sup>C NMR (CDCl<sub>3</sub>): 134.7 (Ph), 128.8 (Ph), 127.6 (Ph), 126.0 (Ph), 18.1 (CH<sub>2</sub>), 17.0 (Si-CH<sub>2</sub>) ppm; <sup>1</sup>H NMR (CDCl<sub>3</sub>): 7.22 (m, Ph, 6H), 7.18 (m, Ph, 4H), 1.25 (quintet, CH<sub>2</sub>, 2H), 0.88 (t, Si-CH<sub>2</sub>, 4H). CP-MAS <sup>29</sup>Si NMR: -8.0 ppm; CP-MAS <sup>13</sup>C NMR: 134.5 (Ph), 128.0 (Ph), 18.1 (methylene) ppm. Elemental analysis for C<sub>15</sub>H<sub>16</sub>Si : Calcd. C 80.30, H 7.19 %; Found C 77.99, H 7.15 %.



## 6.6 References

- (1) (a) Pittman, C. U.; Carraher, C. E.; Reynolds, J. R. in *Encyclopedia of Polymer Science and Engineering*; Eds. Mark, H. F.; Bikales, N. M.; Overberger, C. G.; Menges, G.; Wiley: New York, 1989; Vol. 10; p. 541. (b) Sheats J. E.; Carraher, C. E.; Pittman, C. U.; Zeldin M., Currell B.; *Inorganic and Metal-Containing Polymeric Materials*; Plenum: New York, 1989. (c) Gonsalves K. E.; Rausch M. D. in *Inorganic and Organometallic Polymers. ACS Symposium Series 360*; Eds. Zeldin, M.; Wynne, K.; Allcock, H. R. American Chemical Society: Washington, DC. 1988. (d) Allcock, H. R. *Adv. Mater.* **1994**, *6*, 106. (e) Manners, I. *Chem. Br.* **1996**, *32*, 46.
- (2) a) Fyfe, H. B.; Melkuz, M.; Zargarian, D.; Taylor, N. J.; Marder, T. B. *J. Chem. Soc., Chem. Commun.* **1991**, 188. b) Wright, M. E.; Sigman, M. S. *Macromolecules* **1992**, *25*, 6055. (c) Davies, S. J.; Johnson, B. F. G.; Khan, M. S.; Lewis, J.; *J. Chem. Soc., Chem. Commun.* **1991**, 187. (d) Manners, I. *J. Chem. Soc., Ann. Rep. Prog. Chem. A.* **1991**, *77*. (e) Sturge, K. C.; Hunter, A. D.; McDonald, R.; Santarsiero, B. D. *Organometallics* **1992**, *11*, 3056. (f) Katz, T. J.; Sudhakar, A.; Teasley, M. F.; Gilbert, A. M.; Geiger, W. E.; Robben, M. P.; Wuensch, M.; Ward, M. D. *J. Am. Chem. Soc.* **1993**, *115*, 3182. (g) Nugent, H. M.; Rosenblum, M. *J. Am. Chem. Soc.* **1993**, *115*, 3848.
- (3) Pittman jr., C. U. In *Comprehensive Organometallic Chemistry*; G. Wilkinson, Ed.; Pergamon Press: Toronto, 1982; Vol. 9; pp 553.
- (4) Fellman, J. D.; Garrou, P. E.; Withers, H. P.; Seyferth, D.; Traficante, D. D. *Organometallics* **1983**, *2*, 818.
- (5) Sinn, H.; Kaminsky, W.; Vollmer, H. J.; Woldt, R. *Angew. Chem., Int. Ed. Engl.* **1980**, *29*, 390.
- (6) Sinn, H.; Kaminsky, W. *Adv. Organomet. Chem.* **1980**, *18*, 99.
- (7) Herrmann, W. A.; Cornils, B. *Angew. Chem. Int. Ed. Engl.* **1997**, *36*, 1048.
- (8) Thayer, A. M. In *Chem. Eng. News*; 1995; pp 15.

- (9) Hamielec, A. E.; Soares, J. P. *Prog. Polym. Sci.* **1996**, *21*, 651.
- (10) Kaminsky, W. *Macromol. Chem. Phys.* **1996**, *197*, 3907.
- (11) For a more recent example, see: Sun, L.; Hsu, C. C.; Bacon, D. W. *J. Polym. Sci. Polym. Chem.* **1994**, *32*, 2127.
- (12) Soga, K.; Shiono, T.; Kim, H. J. *Makromol. Chem.* **1993**, *194*, 3499.
- (13) Iiskola, E. I.; Timonen, S.; Pakkanen, T. T.; Härkki, O.; Lehmus, P.; Seppälä, J. V. *Macromolecules* **1997**, *30*, 2853.
- (14) Soga, K.; Arai, T.; Hoang, B. T.; Uozumi, T. *Macromol. Rapid Commun.* **1995**, *16*, 905.
- (15) Foucher, D. A.; Tang, B.-Z.; Manners, I. *J. Am. Chem. Soc.* **1992**, *114*, 6246.
- (16) Foucher, D. A.; Edwards, M.; Burrow, R. A.; Lough, A. J.; Manners, I. *Organometallics* **1994**, *13*, 4959.
- (17) Peckham, T. J.; Massey, J. A.; Edwards, M.; Manners, I.; Foucher, D. A. *Macromolecules* **1996**, *17*, 2396.
- (18) Rulkens, R.; Lough, A. J.; Manners, I. *Angew. Chem., Int. Ed. Engl.* **1996**, *35*, 1805.
- (19) Honeyman, C. H.; Foucher, D. A.; Dahmen, F. Y.; Rulkens, R.; Lough, A. J.; Manners, I. *Organometallics* **1995**, *14*, 5503.
- (20) Honeyman, C. H.; Peckham, T. J.; Massey, J. A.; Manners, I. *J. Chem. Soc., Chem. Commun.* **1996**, 2589.
- (21) Peckham, T. J.; Massey, J. A.; Power, K. N.; Manners, I. Manuscript in preparation.
- (22) Braunschweig, H.; Dirk, R.; Müller, M.; Nguyen, P.; Resendes, R.; Gates, D. P.; Manners, I. *Angew. Chem. Int. Ed. Engl.* **1997**, *36*, 2338.
- (23) Rulkens, R.; Gates, D. P.; Balaishis, D.; Pudelski, J. K.; McIntosh, D. F.; Lough, A. J.; Manners, I. *J. Am. Chem. Soc.* **1997**, *119*, 10976.
- (24) Nguyen, P.; Lough, A. J.; Manners, I. *Macromol. Rapid Commun.* **1997**, *18*, 953.
- (25) Manners, I. *Polyhedron* **1996**, *15*, 4311.
- (26) Manners, I. *Adv. Organomet. Chem.* **1995**, *37*, 131.

- (27) Petersen, J. L.; Egan, J. W., Jr. *Inorg. Chem.* **1983**, *22*, 3571.
- (28) Bajgur, C. S.; Tikkanen, W. R.; Petersen, J. L. *Inorg. Chem.* **1985**, *24*, 2539.
- (29) Cano, A.; Cuenca, T.; Gomez-Sal, P.; Royo, B.; Royo, P. *Organometallics* **1994**, *13*, 1688.
- (30) Green, J. C. *Chem. Soc. Rev.* **1998**, 263.
- (31) MacLachlan, M. J.; Lough, A. J.; Geiger, W. E.; Manners, I. *Organometallics* **1998**, *17*, 1873.
- (32) Mastryukov, V. S.; Dorefeeva, O. V.; Vilkov, L. V.; Cyvin, S. J.; Cyvin, B. N. *J. Struct. Chem. (Engl. Transl.)* **1975**, *16*, 438.
- (33) Ushakov, N. V.; Finkel'shtein, E. S.; Babich, E. D. *Poly. Sci. Ser. A* **1995**, *37*, 320.
- (34) Interrante, L. V.; Wu, H. J.; Apple, T.; Shen, Q.; Ziemann, B.; Narsavage, D. M.; Smith, K. *J. Am. Chem. Soc.* **1994**, *116*, 12085.
- (35) Interrante, L. V.; Liu, Q.; Rushkin, I.; Shen, Q. *J. Organomet. Chem.* **1996**, *521*, 1.
- (36) Shen, Q. H.; Interrante, L. V. *J. Poly. Sci., Poly. Chem.* **1997**, *35*, 3193.
- (37) Foucher, D. A.; Ziembinski, R.; Tang, B.-Z.; Macdonald, P. M.; Massey, J.; Jaeger, C. R.; Vancso, G. J.; Manners, I. *Macromolecules* **1993**, *26*, 2878.
- (38) Marsmann, H. In *NMR Basic Principles and Progress: Oxygen-17 and Silicon-29*; P. Diehl, E. Fluck and R. Kosfeld, Eds.; Springer-Verlag: New York, 1981.
- (39) Diamond, G. M.; Rodewald, S.; Jordan, R. F. *Organometallics* **1995**, *14*, 5.
- (40) DENZO-SMN, Nonius Company, Delft, Holland. (1997).
- (41) Sheldrick, G. M., SHELXTLPC, Siemens Analytical X-ray Instruments Inc., Madison, Wisconsin, U.S.A. (1994)

*Curriculum Vitae***Timothy James Peckham**

---

---

**Personal Information**

Date of Birth	November 3, 1970	Correspondence Address
Place of Birth	Toronto, Ontario, Canada	80 St. George Street
Citizenship	Canadian and UK	Toronto, Ontario
Marital Status	Single	Canada
Health	Excellent	M5S 3H6
		Telephone Numbers
		(416) 978 2450 (work)
		(416) 978 6157 (fax)
		(416) 767 0526 (home)
		e-mail
		tpeckham@alchemy.chem.utoronto.ca

**Present Position**

Doctoral Student, Department of Chemistry, University of Toronto with Professor Ian Manners

**Education**

1994 - present

Doctoral Research (Chemistry), University of Toronto

My research has involved the synthesis of small molecules and their use as precursors to new organometallic polymers via ring-opening polymerization using thermal, living anionic or transition metal-catalyzed routes. The polymerization behaviour and reactivity of these molecules were studied extensively. Both the physical and chemical behaviour of the resultant polymer systems were also examined. Much of this work involved manipulating

highly reactive and air-sensitive compounds using Schlenk techniques and inert atmosphere glove boxes. Characterization involved hands-on use of equipment such as multinuclear NMR ( $^1\text{H}$ ,  $^{13}\text{C}$ ,  $^{19}\text{F}$ ,  $^{29}\text{Si}$  and  $^{31}\text{P}$ ), GPC, UV/Vis, IR, GC/MS, DSC, TGA and cyclic voltammetry. I have also gained experience in writing scientific papers for publication and proposals for research grants.

1989 - 1994

Bachelor of Science (Honours, with High Distinction), University of Toronto

### Scholarships, Fellowship and Other Awards Received

Scholarship	Place of Tenure	Period Held
NSERC Postgraduate Scholarship (PGSB)	University of Toronto	1996 - 1998
Ontario Graduate Scholarship	University of Toronto	1995 - 1996
University of Toronto Open Fellowship (2 terms)	University of Toronto	1994 - 1995

### Research and Technical Experience

Within the research group of Prof. Ian Manners, I have gained experience relating not only to research but also management and organization of a large group (ca. 20 students). My experience in a large group has enabled me to not only work independently, but also in collaboration with other graduate and postdoctoral students with a wide range of expertise. In addition, I have been responsible for the supervision of several undergraduate, exchange and new graduate students. I have also had the opportunity to interact with other academic institutions [e.g. University of Delaware (Prof. A. L. Rheingold)] as well as industry [e.g. Xerox (Dr. D. A. Foucher) and Nova Chemicals Inc. (Dr. D. Harrison & Dr. Q. Wang)]. I have also had the opportunity to present my work in both oral and poster formats at local, national and international conferences.

My other responsibilities in the lab have included the maintenance of several pieces of equipment (e.g. GPC, DSC, TGA and an inert atmosphere glove box), providing thermal analyses (DSC & TGA) for customers within and external to the University of Toronto, general upkeep of the lab and organizing group attendance at conferences (duties such as registration, submission of abstracts and hotel reservations).

## **Teaching Experience**

1995 and 1997            **Advanced Inorganic Laboratory (fourth year)**

**Demonstration of a high level inorganic undergraduate laboratory, student evaluations, oral examinations of students on lab techniques and theory**

1996                    **Intermediate Inorganic Laboratory (third year)**

**Demonstration of an intermediate level inorganic undergraduate laboratory, student evaluations marking of quizzes and laboratory reports**

1996                    **General Chemistry Laboratory (first year)**

**Demonstration of basic level undergraduate chemistry laboratory, student evaluations, marking of quizzes and laboratory reports**

1995                    **Introductory Inorganic Laboratory (second year)**

**Demonstration of basic level undergraduate chemistry laboratory, student evaluations, marking of quizzes and laboratory reports**

## **Extra Curricular Activities**

I have participated in a number of activities within the University of Toronto. I served for one year as the Secretary of the Chemistry Graduate Students Union and the Chemistry Club. This involved the organization of social and sporting activities within the Chemistry department, as well as operating a store selling lab supplies for undergraduate chemistry students. I also helped to organize the 30th Inorganic Discussion Weekend which is was held at the University of Toronto, October 24 - 26, 1997.

I have also been active in participating and organizing softball teams for both regular season and tournament play here at the university. Other interests include badminton, hiking, camping, travel, music and writing.

## **Research Contributions**

### **Publications**

"The Synthesis and Polymerization Behaviour of Silicon-Bridged [1]- and [2]Ferrocenophanes with Sterically Demanding Trimethylsilyl Substituents Attached to the Cyclopentadienyl Rings." Peckham, T. J.; Foucher, D. A.; Lough A. J.; Manners I. *Can. J. Chem.* **1995**, *73*, 2069.

"Synthesis, Characterization and Properties of High Molecular Weight Poly(ferrocenylgermanes) and Poly(ferrocenylsilane)-Poly(ferrocenylgermane) Random Copolymers." Peckham, T. J.; Massey, J. A.; Edwards, M.; Manners, I.; Foucher, D. A. *Macromolecules* **1996**, *29*, 2396.

"Living Anionic Polymerization of Phosphorus-Bridged [1]Ferrocenophanes: Synthesis and Characterization of Poly(ferrocenylphosphine) Homopolymers and Block Copolymers." Honeyman, C. H.; Peckham, T. J.; Massey, J. A.; Manners, I. *Chem. Comm.* **1996**, 2589.

"Metallocene-Based Polymers," Chapter in "Metallocenes" book (ed. A. Togni) Elipse, P. G.; Peckham, T. J.; Manners, I. in press (1998 expected release), 73 pages in length.

"Living Anionic Polymerization of Phosphorus-Bridged, [1]Ferrocenophanes " Peckham, T. J.; Massey, J. A.; Power, K. N.; Manners, I. full paper, manuscript in preparation.

"Synthesis and Polymerization Behaviour of Ansa-Titanocenes and Zirconocenes." Peckham, T. J.; Nguyen, P.; Manners, I.; Wang, Q.; Harrison, D. manuscript in preparation.

"Synthesis and Polymerization Behaviour of Some Tetra-Coordinate, Phosphorus-Bridged, [1]Ferrocenophanes." Peckham, T. J.; Lough, A. J.; Manners, I. manuscript in preparation.

### **Presentations**

"Ring-Opening Polymerization Behaviour of Tri- and Tetra-coordinate Phosphorus-Bridged, [1]Ferrocenophanes" Peckham, T. J., Manners, I. invited lecture, Melville Laboratory for Polymer Synthesis, University of Cambridge, February 1998 - **oral presentation**

"Living Anionic Polymerization of Phosphorus-Bridged [1]Ferrocenophanes: Synthesis and Solution Characterization of Poly(ferrocenylphosphine) Homopolymers and Block Copolymers." Peckham, T. J.; Massey, J. A.; Honeyman, C. H.; Manners, I. 5th Chemical Congress of North America, Cancun, Mexico, November 1997 - **oral presentation**

"Living Anionic Polymerization of Phosphorus-Bridged [1]Ferrocenophanes: Synthesis and Solution Characterization of Poly(ferrocenylphosphine) Homopolymers and Block Copolymers." Peckham, T. J.; Massey, J. A.; Honeyman, C. H.; Manners, I. 30th Inorganic Discussion Weekend, Toronto, Ontario, Canada, 1997 - **oral presentation**

"Living Anionic Polymerization of Phosphorus-Bridged [1]Ferrocenophanes: Synthesis and Characterization of Poly(ferrocenylphosphine) Homopolymers and Block Copolymers." Peckham, T. J.; Massey, J. A.; Honeyman, C. H.; Manners, I. 80th Canadian Society for Chemistry Conference and Exhibition, Windsor, Ontario, Canada, June 1997 - **oral presentation**

"Silicon-Containing Poly(ferrocene) Block Copolymers." Peckham, T. J.; Balaishis, D.; Manners, I. 30th Organosilicon Symposium, University of Western Ontario, London, Ontario, Canada, May 1997 - **poster presentation**

"Living Anionic Polymerization of Phosphorus-Bridged [1]Ferrocenophanes: Synthesis and Characterization of Poly(ferrocenylphosphine) Homopolymers and Poly(ferrocenylphosphine)-Poly(ferrocenylsilane) and Poly(ferrocenylphosphine)-Poly(siloxane) Block Copolymers." Peckham, T. J.; Massey, J. A.; Honeyman, C. H.; Manners, I. 29th Inorganic Discussion Weekend, Montreal, Quebec, Canada, November 1996 - **poster presentation**

"Synthesis of High Molecular Weight Poly(ferrocene) Homopolymers and Block Copolymers via Ring-Opening Polymerization." Ni, Y.; Peckham, T. J.; Manners, I. Environmental Sciences and Technology Alliance Canada, Mississauga, Ontario, Canada, November 1995 - **poster presentation**

"The Enthalpies of Polymerization for Symmetrically-Substituted, Silicon-Bridged [1]Ferrocenophanes: Strain Energies of Organometallic Rings." Peckham, T. J.; Foucher, D. A.; Pudelski, J. K.; Manners, I. 27th Inorganic Discussion Weekend, Hamilton, Ontario, Canada, November 1994 - **poster presentation**



## References

Personal and professional references will be supplied on requests. References can also be sought from the following individuals.

**Professor Ian Manners**            80 St. George Street            ph. (416) 978 6157  
Dept. of Chemistry            fx. (416) 978 6157  
University of Toronto  
Toronto, Ontario  
CANADA  
M5S 3H6  
e-mail: [imanners@alchemy.chem.utoronto.ca](mailto:imanners@alchemy.chem.utoronto.ca)

**Professor Geoff Ozin**            80 St. George Street            ph. (416) 978 2082  
Dept. of Chemistry            fx. (416) 971 2011  
University of Toronto  
Toronto, Ontario  
CANADA  
M5S 3H6  
e-mail: [gozin@alchemy.chem.utoronto.ca](mailto:gozin@alchemy.chem.utoronto.ca)

**Professor Robert Morris**            80 St. George Street            ph. (416) 978 6962  
Dept. of Chemistry            fx. (416) 978 8775  
University of Toronto  
Toronto, Ontario  
CANADA  
M5S 3H6  
e-mail: [rmorris@alchemy.chem.utoronto.ca](mailto:rmorris@alchemy.chem.utoronto.ca)